EFFECTS OF WASTE DISPOSAL ON SOIL AND WATER CHEMISTRY AT AN INDUSTRIAL COMPLEX NEAR SOMERSET WEST, SOUTH AFRICA

Sean Doel
B.Sc(Hons) (UCT)

Submitted in partial fulfilment of the requirements of the degree of
MASTER OF SCIENCE
in the
Department of Geological Sciences
Faculty of Science
University of Cape Town

January, 1997

I declare that this research is my own and that it was conducted under the supervision of Assoc. Prof. J.P. Willis and Dr. M.V. Fey. No part of this research has been submitted in the past, or is being submitted, for a degree at another university.

S. Doel

ACKNOWLEDGEMENTS

I would like to sincerely thank and acknowledge the help and support of the following people and organisations:

Associate Professor James Willis and Dr. Martin Fey for their continual support, advice and constructive criticism throughout this project, and for an extremely valuable and memorable year.

Dave Griffiths, Project Manager Site Remediation, AECI, for making this project possible.

Richie Morris, John Murray and Anne-Carol Simpson, SRK, for making their reports, data files and other valuable information so readily available.

Isaac Rosseau, AECI, for arranging all the neccessary permits, passes and access keys required during the study.

Michael Chetty, Institute for Commercial Forestry Research, University of Natal, Pietermaritzburg, for performing the foliar analyses.

The Computing Centre for Water Research (CCWR) at the University of Natal, Pietermaritzburg, for access to MINTEQA2 software.

Darren Handforth, Department of Chemistry, University of Cape Town, for performing the ICP-AES analyses so timeously.

Patrick Sieas, Department of Geology, University of Cape Town, for help with HPIC analyses.

Neville Eden, Department of Geology, University of Cape Town, for always being prepared to 'drop everything' and make 'urgent' copies of documents five minutes before a dead-line, no matter what!

James Lake, partner in crime, for all the help with sampling.

The "env. geochem" rabble, Mieke, Ruth, Justin, Torsten, Glen, Johann, Vusi, James, John and Bruce, for a most enjoyable and 'not soon to be forgotten' year.

And most importantly, my family, relatives and friends for always being there.

ABSTRACT

The estimated total annual production of waste in South Africa is 318 million metric tons. Of this waste, 3.8%, approximately 12 million metric tons, arises from the chemical manufacturing industry. Although increasing attention is being given to methods of land treatment for waste disposal waste is still disposed of by dumping/stockpiling. This study focuses on the effects of such waste disposal on soil and water chemistry at an industrial complex near Somerset West, South Africa. Since 1903 a multitude of industrial activitities have occurred on the site including manufacture of explosives, chemicals, fertilizers and vinyl-coated products. Decommissioning of the industrial complex is presently in progress.

The overall objective of this study was to conduct an investigation of the water and soils in an area termed the Dead Tree Area. The area was considered of particular interest due to the presence of a sulphur stockpile, gypsum waste dumps and fertilizer wastewater evaporation site located immediately adjacent to the area. Four key objectives were addressed in the study, namely: (i) to chemically characterise the water and soils in the Dead Tree Area, (ii) to assess the degree of contamination of the water and soils in the area, (iii) to question whether tree mortality in the area could have resulted from toxicy or deficiency effects, and (iv) to determine the potential of gypsum application as a means of remediating dispersed, sodic soils.

Analyses of subsurface water in the Dead Tree Area revealed marked spatial variability in water charactertistics, with some samples being strongly acidic (pH<2.5; acidity 5.9 to 17.1 mmol/l) and others being close to neutral (pH >6; alkalinity 100 - 520 mg $CaCO_3$/l). The range in EC for these waters was extreme (1.6 to 90.3 mS/cm), with the most saline being 60% more saline than sea water. Heavy metal concentrations were generally low. High concentrations of Al (max. 108 mg/l), Fe (max. 10.6 mg/l), and Mn (max. 17.8 mg/l) were, however, found in some samples.

The ratios of Na^+ to Cl^- and Ca^{2+} to Mg^{2+} in all samples were found to be the same as those of sea water indicating that these ions were of marine origin. The ratios of Cl^- to SO_4^{2-} and Na^+ to K^+ were not, however, found to be the same as those of sea water for all samples, indicating anthropogenic contamination.

Samples that had pH values <3.4 were suspected to have been affected by contamination from one or more of the surrounding industrial activities. These samples were found to have elevated SO_4^{2-} concentrations, and this was considered to indicate that the samples had been impacted by a low pH contaminant plume evolving from the sulphur stockpile. To assess whether contamination from the gypsum dumps or fertilizer evaporation ponds had also affected the water in the Dead Tree Area, the concentrations of F^-, PO_4^{2-}, NO_3^- and NH_4^+ were

investigated. Elevated concentrations of these ions were found in some water samples. Based on considerations of groundwater flow direction, it was concluded that contamination from the gypsum dumps had impacted on these waters.

The soils in the Dead Tree Area were characterised by being slightly acidic to neutral in pH, having generally low organic carbon and a clay mineralogy dominated by kaolinite. The salinity of the soils in the Dead Tree Area, ranged from 0.5 to 47.1 mS/cm. Some samples were classified as being saline (EC >4 mS/cm). The calculated osmotic pressure of these samples was up to 33 atmospheres, sufficient pressure to significantly impeed water uptake by plants.

The ESP values of the soils from the Dead Tree Area were found to range from between 4.81 and 45.3%, indicating that sodicity was potentially a problem in these soils. Two samples were classified as saline-sodic and two samples as sodic. The dispersible clay content of selected samples showed that dispersion occurred at ESP values as low as 4.81%. This finding is consistent with reports in recent literature. The sodicity hazard of these waters, as defined on the basis of SAR values, was found to range from low to very high (1.6 to 42.1 $mol^{1/2}m^{-3/2}$*). Based on interpretation of the subsurface water chemistry of the Dead Tree Area, it was concluded that the salinity and sodicity of the soils in the area was largely a natural phenomenon that would have persisted in the abscence of industrial activities.*

Eucalyptus foliar analyses were inconclusive in proving tree mortality in the Dead Tree Area to be a consequence of osmotic stress (salinity effect) or sodium toxicity (sodicity effect).

Gypsum application was found to be an effective means to increase soil hydraulic conductivity. Application, at an equivalent rate of 10 tons/ha, stabalised the hydraulic conductivity of a soil composite at conductivities between 3.71×10^{-3} *and* 5.89×10^{-4} *cm/s. In contrast, the hydraulic conductivities of two untreated samples decreased to* 3.23×10^{-5} *and* 5.22×10^{-6} *cm/s, respectively.*

On the basis of the findings of this study, a three part remediation strategy for the Dead Tree Area was proposed, involving (i) application of gypsum to the soil surface to increase hydraulic conductivity; (ii) installation of subsurface drains to stabalise and maintain the water table at a minimum of at least two metres; and (iii) if neccesary, irrigation to flush salts from the soil profile.

TABLE OF CONTENTS

LIST OF FIGURES

LIST OF TABLES

1. INTRODUCTION

Situated in the Hottentots Holland Basin approximately 40 km southeast of Cape Town, and adjacent to the Strand and Somerset West municipal areas is the AECI Somerset West Factory (Figures 1.1 and 1.2). The site is 1230 ha and falls within the Cape Metropolitan Area and the local authority of the Cape Rural Council. The site is bounded to the north and northeast by the N2 freeway and R44 arterial roads, respectively. North of the N2 freeway are the higher income residential areas of Somerset West. To the east, development consists mainly of higher income areas of Strand, as well as the lower-middle income area Helderzicht, Somerset Mall, a golf course and soccer field. The site is bounded to the west by the Somchem factory, and state-owned land leased to AECI along the beachfront of False Bay forms the southern boundary.

The site has an extensive history, having first been purchased by De Beers in 1899. Prior to this the site was believed to have been used primarily for farming activities, although the earliest known industrial use was by limeburners. The present factory was established by De Beers in 1903 to make explosives for the Kimberley diamond mines. Since 1903 a multitude of industrial activites have occurred on the site including manufacture of explosives, chemicals, fertilizers and vinyl-coated products. Current operations at the site are linked to several operating companies, the non-production areas falling under AECI Operating Services (Pty) Ltd. The operating companies include:

- AECI Explosives Limited;
- Kynoch Agrochemicals (Pty) Ltd;
- Kynoch Fertilizer Limited;
- Vynide (Pty) Ltd;
- Polykay (Pty) Ltd.

The site layout is shown in Figure 1.3.

AECI is presently considering potential alternative land uses for the site. Decommissioning and closure of several operations has and is occurring and a structure plan has been prepared to ensure optimal future development of the site. To date two major contamination studies have been completed by Steffen, Robertson and Kirsten (SRK) consulting engineers. A preliminary site rehabilitation study was submitted in June 1992 by SRK (SRK Report

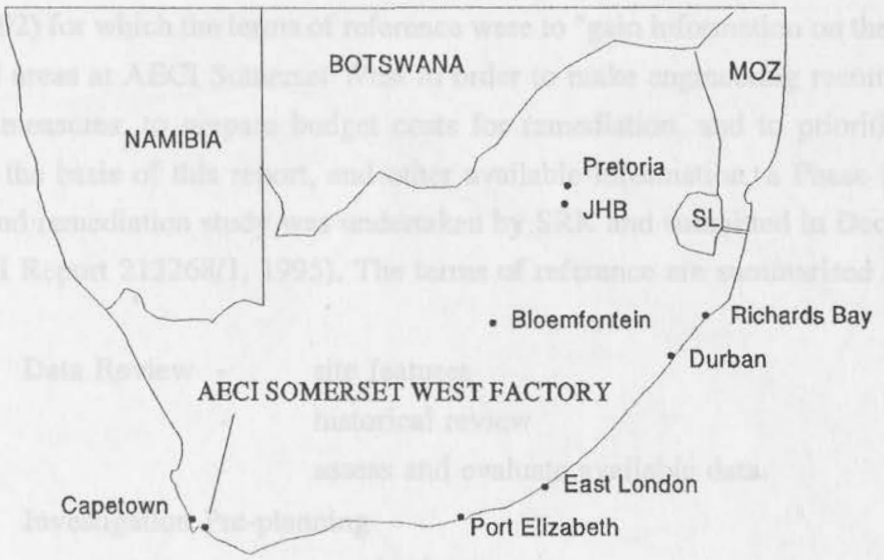

Figure 1.1 Map of Southern Africa showing the approximate location of the AECI Somerset West Factory.

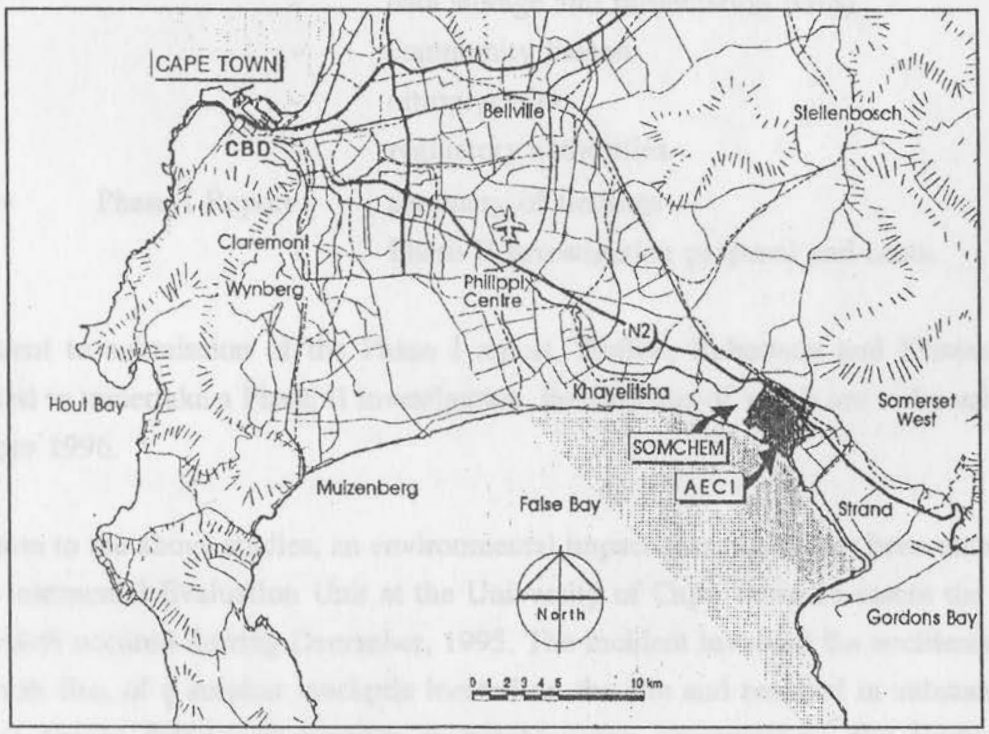

Figure 1.2 Enlarged map of the greater Cape Town area showing the position of the AECI Factory in relation to Somerset West, Stellenbosh and Cape Town (from MLH Architect and Planners Report 96 904: 'AECI Helderberg Conceptual Development Framework Draft Report', November 1996, pg. 2).

180429/1, 1992) for which the terms of reference were to "gain information on the chemically contaminated areas at AECI Somerset West in order to make engineering recommendations on remedial measures, to prepare budget costs for remediation, and to prioritise remedial actions". On the basis of this report, and other available information, a Phase I subsurface assessment and remediation study was undertaken by SRK and submitted in December 1995 (SRK Phase I Report 213268/1, 1995). The terms of reference are summarised below:

- Data Review - site features
  - historical review
  - assess and evaluate available data.
- Investigation Pre-planning
  - geophysics
  - site safety plan
  - monitoring protocol
  - chemical and laboratory analysis
  - data storage and presentation (GIS)
  - community liaison
  - nitroglycerine
  - regulatory authorities.
- Phase I Report - summary of findings
  - Phase II investigation proposal and costs.

Subsequent to submission of the Phase I report, Steffen, Robertson and Kirsten were re-contracted to undertake a Phase II investigation, the findings of which are to be submitted by December 1996.

In addition to the above studies, an environmental impact assessment has been undertaken by the Environmental Evaluation Unit at the University of Cape Town to assess the impact of a fire which occured durring December, 1995. The incident involved the accidental ignition, by a brush fire, of a sulphur stockpile located on the site and resulted in substantial media coverage due to deletarious impacts on neighbouring communities. The findings of this assessment are not as yet in the public domain.

Following a site visit during February of this year (1996) a proposal was submitted to AECI to undertake this masters thesis. An investigation of the impacts of industrial activities, occurring on the northern section of the site, on soil and water quality of an area known as the 'Dead Tree Area' was proposed. The area has received this name due to the fact that a

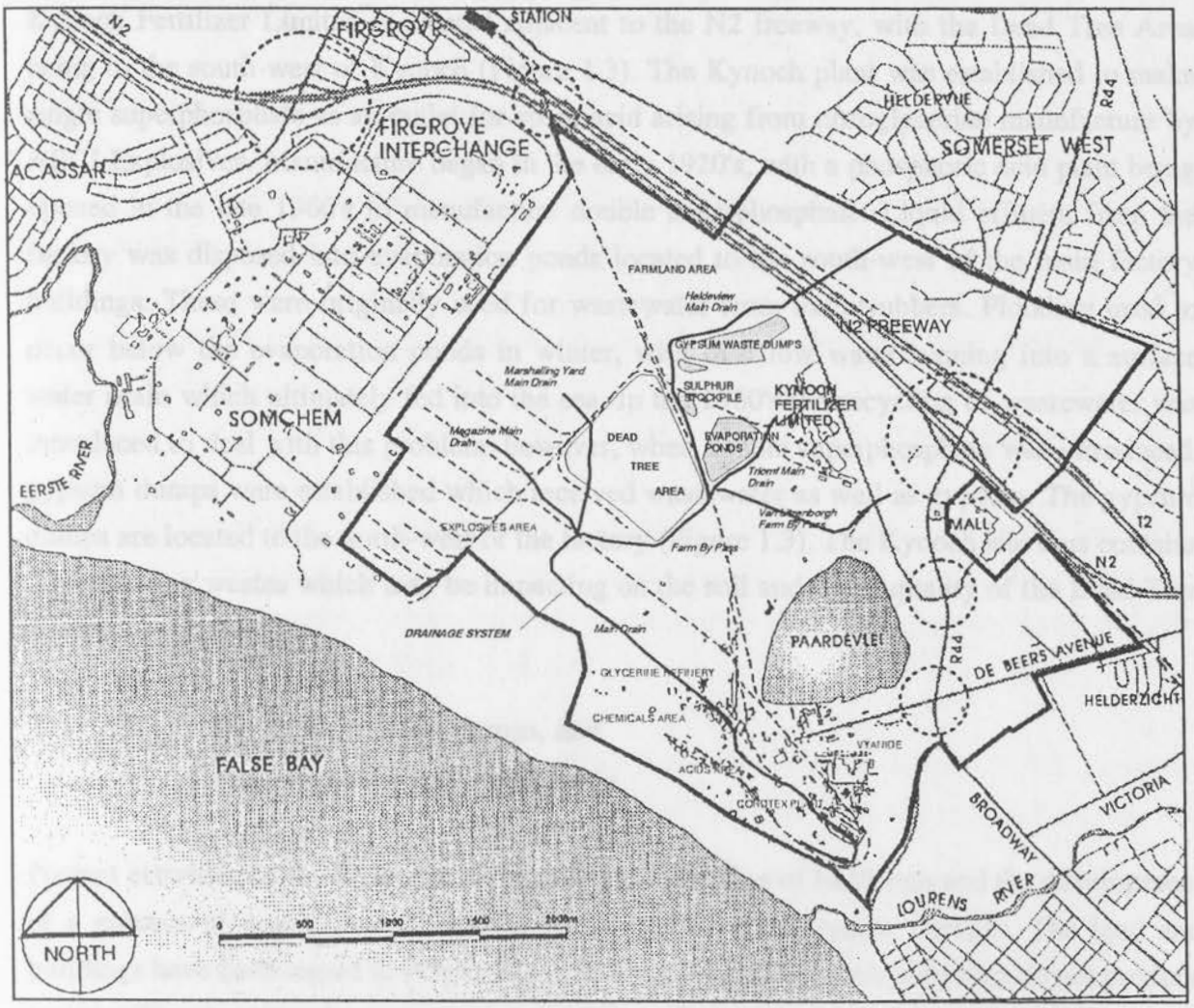

Figure 1.3 Layout of the AECI Somerset West Factory Site (modified from MLH Architect and Planners Report 96 904: 'AECI Helderberg Conceptual Development Framework Draft Report', November 1996, pg. 37).

large number of eucalyptus trees which occur in the area are dead, giving the area the appearance of a 'waste land'. The objectives and key questions of this study are discussed in section 1.1.

The industrial activities of interest to the study, and which occur on the northern section of the site, include:

- the manufacture of single and double superphosphate by Kynoch Fertilzer Limited, and
- the storage of elemental sulphur.

Kynoch Fertilizer Limited is located adjacent to the N2 freeway, with the Dead Tree Area being to the south-west of Kynoch (Figure 1.3). The Kynoch plant was established to make single superphosphate as an outlet for spent acid arising from nitroglycerine manufacture by AECI Explosives. Manufacture began in the early 1920's, with a phosphoric acid plant being opened in the late 1960's to manufacture double superphosphate. Liquid effluent from the factory was disposed into evaporation ponds located to the south-west of the main factory buildings. These were originally used for wastewater from the scrubbers. Flooding used to occur below the evaporation ponds in winter, with overflow water running into a surface water drain which ultimately fed into the sea. In the 1960's the recycling of wastewater was introduced to deal with this problem, however, when double superphosphate was introduced, gypsum dumps were established which received wastewater as well as gypsum. The gypsum dumps are located to the north-west of the factory (Figure 1.3). The Kynoch site thus contains the following wastes which may be impacting on the soil and water quality of the Dead Tree Area:

- the gypsum waste dumps, and
- the fertilizer evaporation ponds.

Present activities on the Kynoch area include bulk blending of fertilizers and the development of a process of granulation of chicken manure to produce organic fertilzer. The land and buildings have been leased to Polykay for rotational moulding. These activities do not produce any significant wastes, however, and are thus not of any concern to this project. The gypsum from the dumps is presently being sold.

In addition to the wastes associated with the Kynoch site, the presence of an elemental sulphur stockpile located north of the Dead Tree Area and south of the gypsum dumps represents a further source of contamination that may be impacting on soil and water quality in the Dead Tree Area. The sulphur is a strategic stockpile owned by the South African Government (Department of Trade and Industry), and stored by AECI on their behalf. Tenders are presently being sought for its removal.

The ground and surface water flow direction in the areas described above is approximately south-west and hence any contamination resulting from past industrial activities and present waste dumps/stockpiles may be anticipated to migrate toward the Dead Tree Area. It is the effects of such contamination on soil and water quality in the Dead Tree Area that form the focus of this project.

1.1 Objectives of the Study

The objectives of this study are:

1) to review the pertinent literature on some of the environmental impacts of salinity and sodicity, and

2) to conduct an investigation of the water and soils of the Dead Tree Area by;

   (i) chemically characterising the water and soils in the Dead Tree Area,

   (ii) assessing the degree of contamination of the water and soils in the Dead Tree Area and questioning whether contamination from the gypsum dumps, fertilizer evaporation ponds and/or sulphur stockpile has impacted on the water and soils quality in the Dead Tree Area.

   (iii) determining whether the concentration of various elements in foliar samples from eucalyptus trees in the Dead Tree Area exceed reported values, and investigate the question:

   Could tree mortality in the Dead Tree Area have resulted from toxicity or deficiency effects?

   iv) determining the potential of gypsum application as a means of remmediating dispersed, sodic soils, and suggesting what remmediation strategy may be indicated for the Dead Tree Area on the basis of these findings.

To meet the above objectives - in particular to assess the degree of contamination of the water and soils in the Dead Tree Area and to determine the impact of the gypsum dumps, fertilizer evaporation ponds and/or sulphur stockpile on the area - the following additional questions had to be considered:

3) What are the 'background levels' for water and soils quality in the study area?

4) Three key potential sources of contamination may be identified on the site, namely the sulphur stockpile, the gypsum dumps and the fertilizer evaporation ponds. What are the chemical characteristics of these three potential sources of contamination?

1.2 The Study Area

1.2.1 Physiography and Hydrogeology

The AECI property lies between 3 and 21 metres above sea level and generally slopes in a southerly and southwesterly direction with slopes of 1:10 and less. The Dead Tree Area and Kynoch area lack any marked natural phsyiographic features. A number of anthropogenically created features are, however, found on the site including a phosphogypsum dump, fertilizer evaporation ponds and a sulphur stockpile.

A number of drains pass through the Kynoch area and/or the Dead Tree Area. These include the Heldeview Main Drain and Van Litzenborgh Farm By Pass which are storm water drains, and the Triomf Main Drain which is the main aqueous effluent discharge drain for the Kynoch fertilizer factory. These three drains merge to form the Farm By Pass drain which flows along the eastern border of the Dead Tree Area. Flow rates for the Helderview Drain during 1991 varied from 700 m^3/day in December to 5200 m^3/day in August (SRK Report 180429/1, 1992). Flow rates for the other drains were not available. The surface drainage network is illustrated in Figure 1.3.

A discontinuous groundwater upper seepage horizon at 3 to 4 m below ground surface is present in the Kynoch area (SRK Report 180429/1, 1992). The piezometric surface in this area was between 1 to 1.5 m below ground surface at the end of April/beginning of May 1991. During winter, however, water levels are at the ground surface both in the Kynoch area and the Dead Tree area. Large portions of the Dead Tree Area in particular are covered by standing water during the winter months. The groundwater flow direction is estimated to be south-westerly with the haudraulic gradient decreasing from 1 in 70 in the Kynoch area to approximately 1 in 400 toward the coast (SRK Report 180429/1, 1992).

1.2.2 Regional and Site Geology

The area can be divided into three distinct physiographic zones which reflect the underlying geological formations (Figure. 1.4) (SRK Report 180429/1, 1992). Extending from inland to False Bay these zones comprise the Helderberg Mountains and foothills, Coastal Plain and Coastal Dune Belt. The Helderberg Mountains are formed from Table Mountain Sandstone with the foothills and Coastal Plain zone being composed of the underlying Malmesbury Group rocks. The Malmesbury Group rocks, which comprise shales, sandstones and hornfels, form a peneplain which slopes gently seaward. Located to the west of the Helderberg

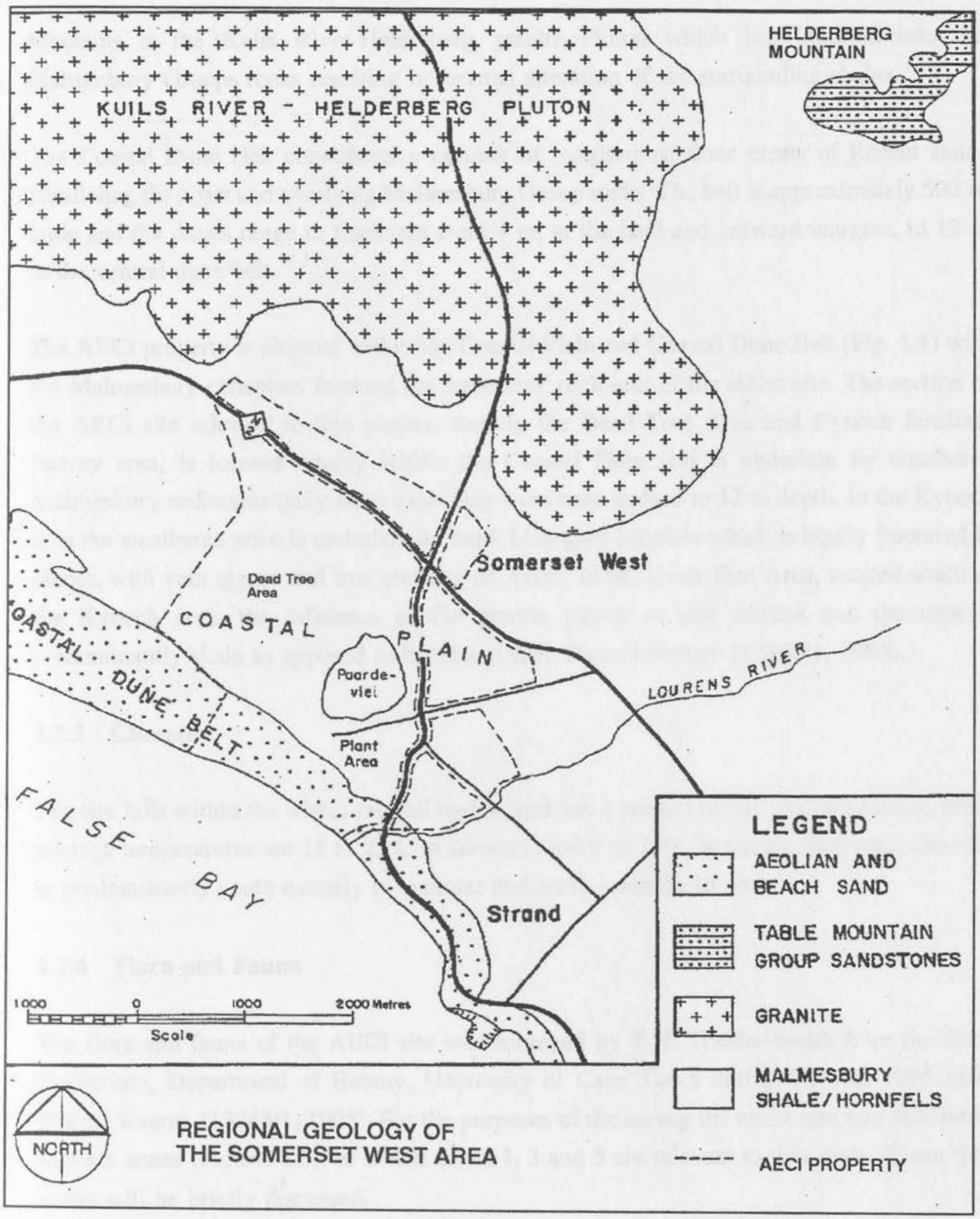

Figure 1.4 Regional Geology of the Somerset West Area (modified from SRK Report 180429/1, June 1992, pg 2.).

Moutains is the Kuils River-Helderberg granite Pluton which has intruded into the Malmesbury Groups rocks resulting in thermal alteration of the surrounding shales.

The Coastal Dune Belt consists of a number of longitudinal dune crests of Recent sands paralleling the coast and overlying Malmesbury Group rocks. The belt is approximately 500 m wide and the dunes range in thickness from 4 m, at the land and seaward margins, to 12 m in the central dune belt.

The AECI property is situated within the Coastal Plain and Coastal Dune Belt (Fig. 1.4) with the Malmesbury peneplain forming the 'basement' rock unit of the entire site. The section of the AECI site relevant to this project, namely the Dead Tree Area and Kynoch fertilizer factory area, is located wholly within the Coastal Plain and is underlain by weathered Malmesbury sediments (silty clay) extending from near surface to 12 m depth. In the Kynoch area the weathered zone is underlain by hard, blue-grey hornfels which is highly fractured in places, with vein quartz and iron staining on joints. In the Dead Tree Area, located south of the Kynoch area, the influence of the granite pluton is less marked and the rock is predominantly shale as apposed to hornfels (SRK Phase I Report 213268/1, 1995).

1.2.3 Climate

The site falls within the winter rainfall region, and has a rainfall of 570 mm per annum. Mean average temperatures are 15 to 25°C in summer, and 9 to 20°C in winter. The wind direction is predominantly south-easterly in summer and north-westerly in winter.

1.2.4 Flora and Fauna

The flora and fauna of the AECI site was surveyed by T.H. Trinder-Smith from the Bolus Herbarium, Department of Botany, University of Cape Town during October 1995 (SRK Phase I Report 213268/1, 1995). For the purposes of the survey the entire site was subdivided into six zones (Figure. 1.5), of which zones 1, 3 and 5 are relevant to this study. These three zones will be briefly discussed.

Zone 1

This zone encompasses cultivated fields, which are grazed by cattle on a rotational basis, and *Eucalyptus* plantations located to the N and NW of the Kynoch fertilizer plant. The area is

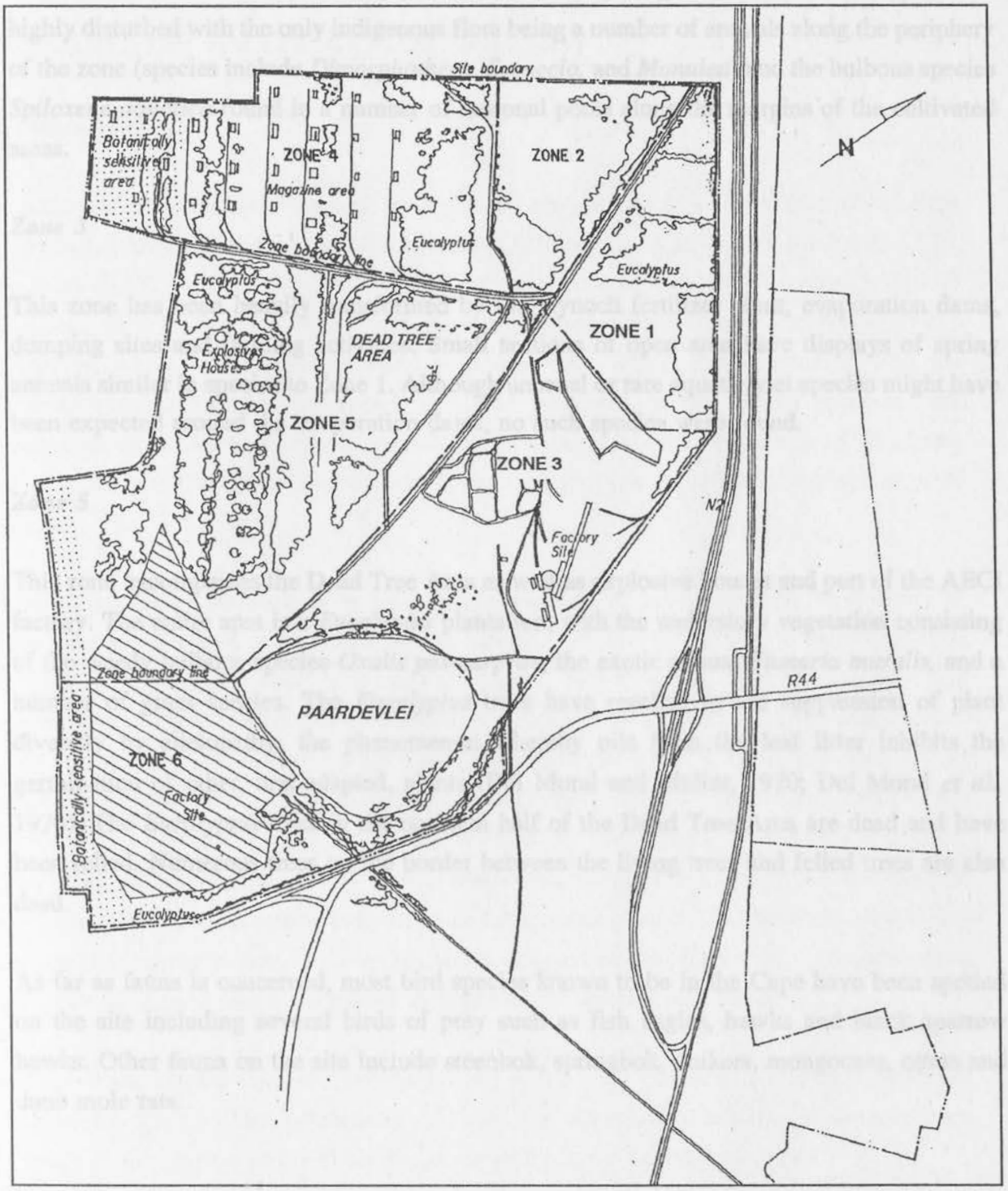

Figure 1.5 Flora and Fauna survey zones within the AECI Somerset West Factory site (from SRK Report 213268/1, December 1995, Appendix H).

highly disturbed with the only indigenous flora being a number of annuals along the periphery of the zone (species include *Dimorphotheca, Scenecio,* and *Manulea*) and the bulbous species *Spiloxene aquatica* found in a number of seasonal pools along the margins of the cultivated areas.

Zone 3

This zone has been heavily transformed by the Kynoch fertilizer plant, evaporation dams, dumping sites and farming activities. Small sections of open area have displays of spring annuals similar in species to Zone 1. Although unusual or rare aquatic/vlei species might have been expected around the evaporation dams, no such species were found.

Zone 5

This zone encompasses the Dead Tree Area as well as explosive houses and part of the AECI factory. The entire area is a *Eucalyptus* plantation, with the understory vegetation consisting of the weedy bulbous species *Oxalis pes-carprae*, the exotic annual *Fumaria muralis,* and a number of grass species. The *Eucalyptus* trees have resulted in the suppression of plant diversity by allelopathy, the phenomenon whereby oils from the leaf litter inhibits the germination of other, non-adapted, plants (Del Moral and Muller, 1970; Del Moral *et al.,* 1970). The *Eucalyptus* trees in the northern half of the Dead Tree Area are dead and have been felled. Numerous trees on the border between the living trees and felled trees are also dead.

As far as fauna is concerned, most bird species known to be in the Cape have been spotted on the site including several birds of prey such as fish eagles, hawks and black sparrow hawks. Other fauna on the site include steenbok, springbok, duikers, mongooses, otters and dune mole rats.

2. SOME ENVIRONMENTAL EFFECTS OF SALINITY AND SODICITY: A LITERATURE REVIEW

2.1 Introduction

The estimated total annual production of waste in South Africa is ±318 million metric tons (Korentajer, 1992), and arises mainly from mining (75% of total), electricity generation (7%), agriculture (6.3%), municipalities (4.7%) and the chemical manufacturing industry (3.8%). Of this waste, 75% is disposed of by land disposal methods (Bredenhann and Airey, 1991). Landfilling, where wastes are confined to areas from which their migration into the surrounding environment is prevented, and land treatment, where natural processes are exploited so as to detoxify, dilute, immobilize and degrade all or a portion of the waste applied to the land (Simon & Tedesco, 1987), are the two most important land-based disposal methods.

Although increasing attention is being given to methods of land treatment, most waste in South Africa is disposed of by means of some form or another of landfill. In many instances the waste is simply disposed of by dumping/stock piling on an open site without any consideration or investigation into the suitability of the site for attenuation and or confinement of any contaminant(s) that may evolve from the waste in the form of leachate. Depending on the characteristics of the site, such as soil properties, climatic conditions, topography, hydrology and vegetation cover, all of which affect the attenuation or assimilative capacity of the site, and the nature of the waste, which determines the character of the leachate evolved ie. pH, electrical conductivity, organic compounds present, phosphorous, sulphur and heavy metal concentrations etc., groundwater contamination, food chain contamination, production of odours and/or permanent degradation of the soil may result.

In many instances the leachate evolving from waste sites contains a high inorganic salt concentration and may thus be considered saline. The effects of such saline wastes will form the focus of this review and will be discussed with respect to two key issues;

(1) the effect of salts on soil hydraulic conductivity, and

(2) plant responses to salinity and sodicity.

A brief overview of the key measures for characterising salt solutions will be presented first as an introduction and foundation for the ensuing discussion of these topics.

2.2 Measures for Characterising Salt Solutions

2.2.1 Salinity

Salinity, or the concentration of dissolved salts, is most easily measured by electrical conductivity (EC). Electrical conductivity is based on the principle that the conductivity, or ease with which an electric current is carried through a solution, is proportional to the quantity of ionic charge in solution (McBride, 1994). Aside from H^+ and OH^-, which have anomalously high conductances, most cations and anions contribute approximately equally per mole of ionic charge to the conductivity of solutions, which allows for the following empirical relationships to be established between the concentration of electrolyte solutions and the conductivity, irrespective of ionic composition (McBride, 1994):

$$\text{Total cations (mmoles(+)/liter)} \approx \text{EC (mS/cm)} \times 10 \quad (1)$$
$$\text{Total anions (mmoles(+)/liter)} \approx \text{EC (mS/cm)} \times 10$$

$$\text{TDS (mg/liter)} \approx \text{EC (mS/cm)} \times 640 \quad (2)$$

where TDS = "total dissolved solids" in the form of soluble salts.

These equations are applicable unless the pH indicates the solution to be very acid or very alkaline. Sposito (1989) defines a soil as saline if the electrical conductivity of a saturated paste extraction is >4 mS/cm.

2.2.2 Sodicity

The sodium status of soils is characterised by the proportion of Na on the soil exchange sites, termed ESP (exchangeable sodium percentage), and the proportion of Na to divalent cations, termed SAR (sodium adsorption ratio). Sodic soils are those which have higher than normal levels of exchangeable Na^+. From mass-action principles of cation exchange, the important ionic concentrations in soil solutions that affect the level of exchangeable Na^+ are $[Na^+]$, $[Ca^{2+}]$ and $[Mg^{2+}]$. Because of its low solubility in most soils, K^+ rarely occupies a significant fraction of the exchange sites and thus has little effect on the level of exchangeable Na^+. The relative cation composition of exchange sites for sodic soils as compared with nonsodic ("normal" and acid) soil is shown in Figure 2.1. Although this plot suggests that soils are either sodic and alkaline or nonsodic and acid, it is possible in certain instances for sodic soils to develop which are also acidic.

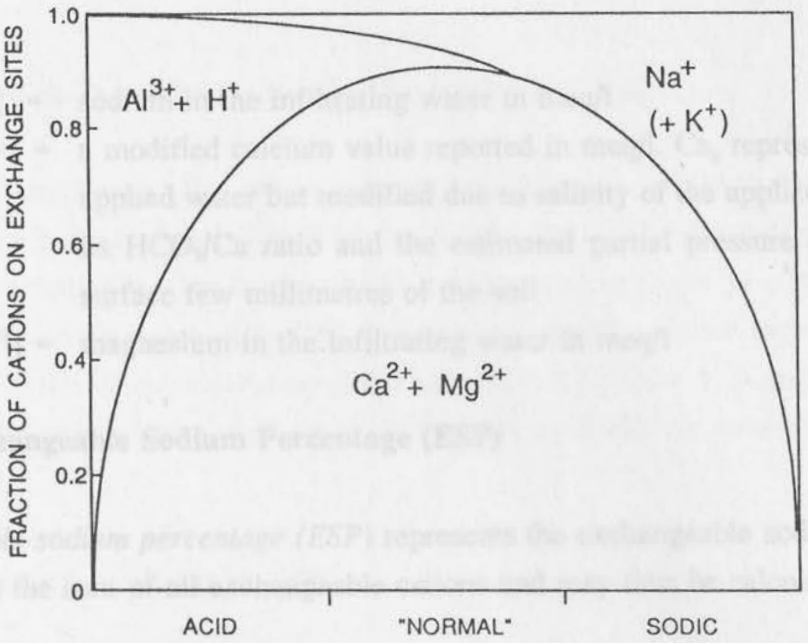

Figure 2.1 Relative cation composition of exchange sites for sodic soils compared with nonsodic ("normal" and acid) soils (McBride, 1994, pg. 281).

Such soils may develop where there is a high input of salts from the sea, as occurs at coastal areas, as well as acidity arising from the soil parent material.

2.2.2.1 Sodium Adsorption Ration (SAR)

The *sodium adsorption ratio (SAR)*, is a solution property defined by the equation (McBride, 1994):

$$SAR = [Na^+] / \{ ([Ca^{2+}] + [Mg^{2+}])/2 \}^{1/2} \quad (3)$$

where all solution concentrations are expressed in units of millimoles of cationic charge (or milliequivalents) per liter.

2.2.2.2 Adjusted SAR

Ayers & Westcot (1985) propose an adjusted SAR value (adj SAR) due to the fact that soon after infiltration of saline waters, dissolution or precipitation of $CaCO_3$ and $CaSO_4$ may occur which is not accounted for in the standard SAR. The *adjusted SAR* may be calculated from the equation:

$$\text{adj SAR} = [Na^+] / \{ ([Ca_x^{2+}] + [Mg^{2+}])/2 \}^{1/2} \quad (4)$$

where: $[Na^+]$ = sodium in the infiltrating water in meq/l

$[Ca_x^{2+}]$ = a modified calcium value reported in meq/l. Ca_x represents Ca in the applied water but modified due to salinity of the applied water (EC_w), its HCO_3/Ca ratio and the estimated partial pressure of CO_2 in the surface few millimetres of the soil

$[Mg^{2+}]$ = magnesium in the infiltrating water in meq/l

2.2.2.3 Exchangeable Sodium Percentage (ESP)

The *exchangeable sodium percentage (ESP)* represents the exchangeable sodium content of a soil relative to the sum of all exchangeable cations and may thus be calculated as:

$$ESP = \{\text{Exchangeable } Na^+ \text{ ions}\} / \{\sum \text{Exchangeable cations}\} \times 100\% \quad (5)$$

The composition of the exchange sites of the soil (ESP) may also be calculated based on knowledge of the soil solution composition (SAR) from the empirically derived equation (McBride, 1994):

$$ESP / (100 - ESP) = 0.015\ SAR \quad (6)$$

Saline soils ordinarily have a pH of less than 8.5 and an ESP = 15%. Tan (1992) considers soils with an ESP > 15% to be saline and soils with an ESP > > 15% to be sodic.

2.2.2.4 Residual Sodium Carbonate (RSC) Value

The *residual sodium carbonate (RSC)* value is a property of solutions, and has been used to quantify the alkalinity hazard of irrigation water applied to soils. It is defined by the equation (McBride, 1994):

$$RSC = [HCO_3^- + CO_3^{2-}] - [Ca^{2+} + Mg^{2+}] \quad (7)$$

where all concentrations are expressed in millimoles of charge per litre.

Typically, an RSC > 2.5 is considered hazardous and an RSC < 1.25 generally safe, with intermediate values being potentially hazardous.

2.3 The Effect of Salts on the Hydraulic Conductivity of Soils

Physiochemical interactions taking place between soil particles and pore fluid may cause significant changes in the hydraulic conductivity of soils. The swelling and dispersion of soil clay minerals may markedly alter the structural stability and permeability of the soil and is a key physiochemical interaction controlled predominantly by the salt concentration and type of the pore-fluid. In this discussion the fundamental concepts of water movement in soils will be briefly reviewed after which the effect of salts on the hydraulic conductivity of soils will then be reviewed.

2.3.1 Movement of Water in Soils

Hydraulic conductivity and water retention are the two key soil properties which determine the behaviour of soil water flow systems. These properties determine the response of a soil water system to imposed boundary conditions, and are measures of the soil's ability to transmit water, in the case of *hydraulic conductivity*, and its ability to store water in the case of *water retention*. These properties are typically termed the hydraulic properties of the soil, and may be used to analyze the behaviour of a soil water system (Klute & Dirksen, 1986).

Darcy's Law is the fundamental and well established equation governing fluid flow through a saturated porous medium (Hillel, 1982; Klute & Dirksen, 1986). In the case of highly contaminated water, the density and viscosity of the fluids will be different from that of water and would be expected to significantly affect transport of the fluid. The *intrinsic permeability* of a soil, which is a function of the pore-space geometry, takes into account such changes in density and viscosity. The intrinsic permeability does not take into account, however, changes in concentration and kinds of cationic species in the soil solution. Both electrolyte concentration and electrolyte type may have a marked effect on the hydraulic conductivity of soils, especially those containing a significant amount of clay, and will be discussed in section 3.3.

2.3.1.1 Saturated versus unsaturated flow

Although the study of unsaturated flow has become one of the most important and active topics of research in soil physics in the last few decades (Hillel, 1982), unsaturated flow conditions are typically complicated and difficult to describe quantitatively, involving changes in both the state and content of soil water during flow.

The distinction between saturated and unsaturated flow conditions is important in the understanding of contaminant transport because of resulting differences in hydraulic conductivity between saturated and unsaturated flow. Under saturated conditions all pores are filled and conducting with the consequence that continuity and conductivity are maximal. With desaturation, there is a decrease in the cross-sectional area of the soil's conducting portion, some of the pores become air filled, and there is a resultant increase in tortuosity because of the circumvention of empty pores. Hence hydraulic conductivity will tend to decrease with desaturation.

There is also a marked distinction between the hydraulic conductivity of sandy versus clay rich soils depending on the saturation state. A saturated sandy soil will conduct water more rapidly than a clay rich soil, however, the opposite is usually true for unsaturated conditions. In a soil with large pores, these pores will empty quickly and become nonconducting, and as suction develops the initially high conductivity will decrease. In contrast, a soil with small pores will retain and conduct water even at an appreciable suction, with the result that hydraulic conductivity does not decrease as markedly and may actually be greater than that of a soil with large pores and subjected to the same degree of suction.

2.3.2 Effect of Salts on the Hydraulic Conductivity of Soils

2.3.2.1. Clay Swelling and Dispersion

Clay minerals, especially the 2:1 smectite minerals, are affected in a number of ways by changes in the solution environment. There are three key processes whereby changes in electrolyte concentration affect clay minerals and which result in changes in soil permeability (Quirk & Schofield, 1955):

(i) *Swelling* results from complete or partial blocking of the larger conducting pores, resulting in appreciable decreases in permeability even when swelling effects are relatively small. This is due to the fact that flow of water through a pore is proportional to the fourth power of the pore radius.

(ii) *Failure* of soil aggregates occurring due to stress resulting from unequal swelling throughout the soil mass.

(iii) *Deflocculation* and flocculation - two opposing colloidal processes involving clay particles which may influence physical or chemical properties such as hydraulic conductivity or contaminant transport adsorbed by migrating particles. Deflocculation, or dispersion, occurs when swelling of particles occurs past the critical distance which allows the interparticle repulsive forces to dominate over the van der Waals attractive forces (Tan, 1992).

2.3.2.1.1 Diffuse Double-layer Theory

Diffuse double-layer theory provides an explanation for the influence of the solution environment on swelling, and hence may be of use in predicting the effect of high electrolyte concentrations resulting from contamination of soil-water. The following brief explanation of the electric double layer has been drawn from Tan (1992).

The diffuse electric double-layer is a term applied to the aggregation of cations at a clay surface as a result of electrostatic attraction of the cations to the negatively charged clay surface. The diffuse electric double-layer forms as a result of the fact that although clays carry a negative charge which is ordinarily balanced by cations adsorbed to their surfaces, in suspension these cations diffuse away from the clay surface in response to the concentration gradient between the clay surface and the bulk of the solution. A large portion of these cations, however, cannot move far away from the clay surface because of its strong electrostatic attraction, and therefore form aggregates at the interface. Typically the diffuse electric double-layer ranges in thickness from 50 to 300 Å.

Such particles experience mutual repulsion because of the positively charged outer region of the double layers, and are considered in this situation to be dispersed and form a stable suspension. When two such particles approach each other, their diffuse counterion atmospheres interfere with one another leading to a rearrangement of the ion distribution in double layers of both particles. To bring about these changes, work in the form of the *repulsive energy* or *repulsive potential*, V_r, must be done on the system. The repulsive potential increases exponentially with decreasing interparticle distance. At interparticle distances of around 20 Å and less, however, attractive or *van der Waals* forces, V_a, also become significant. The double-layer repulsive forces and van der Waals forces are additive and give rise to the resultant force acting between the particles as shown in Figure 2.2. At interparticle distances of about 20 Å or less, the clay particles undergo flocculation as a result of the dominance of the attractive van der Waals forces, whereas at interparticle distances of greater than 20 Å, dispersion occurs and a stable suspension forms as a result of the dominance of the double-layer repulsive forces.

Both electrolyte concentration and type, play a role in this process. At low electrolyte concentrations dispersion is favoured due to the dominance of repulsive forces. Repulsive forces dominate at low electrolyte concentrations because clay particles are shielded by relatively thick double layers decreasing the possibility of mutual approach. At high electrolyte concentrations, however, reduced diffusion away from the double layer results in

compression of the double layer, with the consequence that mutual approach is much more likely to occur resulting in the dominance of V_a over V_r and coagulation or flocculation of the clay particles.

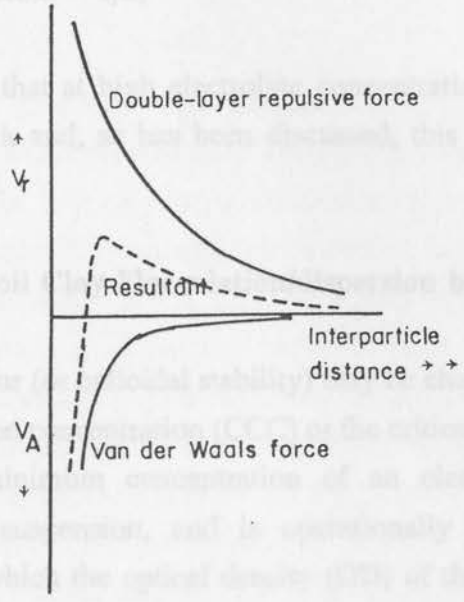

Figure 2.2 Double-layer repulsive and van der Waals interparticle atractive forces and the resultant force as a function of interparticle distance (Tan, 1992, pg. 204).

Two key properties of cations effect the dispersive properties of clay: firstly, the higher the charge of the cation the greater its attraction to the particle surface, and secondly, the greater the hydration, the weaker its attraction to the particle surface. As a consequence of these differences Ca, for instance, results in the formation of a more compact double layer than Na because Ca is divalent and has a lower degree of hydration than Na which is monovalent.

The effect of both electrolyte concentration and type on the thickness of the double layer, and hence the dispersion or flocculation potential of the clay fraction, is treated theoretically by the Gouy-Chapman theory of diffuse double-layer formation, and may be predicted from the approximate quantitative expression:

$$H = f\left[\left(DT / h_o^2 v^2 \right)^n \right] \quad (8)$$

where H = relative thickness of the double layer

D = dielectric constant of the medium
T = temperature
h_o = electrolyte concentration
v = cation valence
n = constant (approx. = 1/2)

The above expression shows that at high electrolyte concentrations and cation valence the double layer is relatively thick and, as has been discussed, this means that aggregation or flocculation will be promoted.

2.3.2.1.2 Characterising Soil Clay Flocculation/dispersion behaviour

Soil clay flocculation behaviour (or colloidal stability) may be characterised by determination of either the critical coagulation concentration (CCC) or the critical flocculation concentration (CFC). The CCC is the minimum concentration of an electrolyte required to cause flocculation of a colloidal suspension, and is operationally defined as the Ca or K concentration in solution at which the optical density (OD) of the supernatant suspension is reduced to 50% after a 24-hour flocculation period (Kretzschmar *et al.*, 1993). The CFC is defined as the minimum concentration of an electrolyte solution necessary to flocculate a suspension of clay under specified conditions of exchangeable cation composition, pH, and suspension concentration.

2.3.2.1.3 Sodicity

As has already been discussed in section 3.3.1.1, selective cation adsorption is greater for divalent than for monovalent cations, and for larger cations than for smaller ones because of the greater degree of hydration of the smaller cations. The typical selective adsorption affinity series can be represented as follows:

$$Al^{3+} > Ba^{2+} > Sr^{2+} > Ca^{2+} > Mg^{2+} = Cs^{+} > K^{+} = NH_{4+} > Na^{+}$$

Saline soils ordinarily have a pH of less than 8.5 and an ESP of = 15%. Because of their high electrolyte concentration these soils are usually flocculated. In the case of saline and sodic soils, however, where the ESP values are typically >15% and >>15%, respectively (Tan, 1992), marked clay swelling and dispersion is likely to occur (Oster *et al.*, 1980). This is due to the fact that at increasing ESP values, the CCC increases. The resulting clay

dispersion and soil aggregate structure deterioration may in turn cause reduced permeability and drainage of the soil, poor aeration, and enhanced surface crusting and shrink-swell behaviour under cycles of wetting and drying. The reduced permeability may also lead to a reduction in water supply to plants and hence a reduction in yield because crop water demand is not met.

Although the ESP value has long been used as a measure of the dispersibility of a soil, it does not provide a complete description of clay dispersibility (McBride, 1994). Soils with a high ESP under conditions of low electrolyte concentration will show severe degradation compared to a soil with the same ESP but a higher electrolyte concentration. Hence, soils will generally have the capacity to receive much larger Na inputs before exhibiting dispersion and reduced permeability in instances where the influent water contains a high electrolyte concentration in addition to high SAR. This would be expected to be the typical scenario for wastewaters evolving from saline wastes. It has also been noted (Thompson, 1983) that Na rich effluents that contain ammonium salts cause markedly lower ESP and soil pH values than would be expected taking into account the SAR of the effluent. Thompson (1983) concluded that the NH_4 ion kept an appreciable amount of Na off the exchange complex. Levy, Fine & Feigin (1986) showed that the Na hazard of wastewater on soil sodicity was reduced by the presence of NH_4 and by the higher apparent solubility of $CaCO_3$ precipitated from wastewaters containing soluble organic residues.

The pH of the soil must also be taken into account when considering ESP values because the CCC of clays is affected by pH. This is due the fact that clay mineral surface charge is pH-dependent. In general, the CCC values of clays increase with increasing pH (Kretzschmar *et al.*, 1993) with the consequence that for a given ESP clays are more dispersible at high pH than at low pH. This pH tendency is more pronounced in kaolinitic and illitic clays than smectitic clays which have a predominantly permanent charge. A graphic representation of the effects of pH, ESP, salt concentration, and exchangeable Ca or Al on the structural stability of soil clay is shown Figure 2.3.

Amelioration of problems resulting from sodicity is most commonly achieved through the application of gypsum ($CaSO_4.2H_2O$). It may either be applied to the land or added directly to applied water to provide for a relatively soluble source of Ca. This will reduce the SAR of the soil and ESP of the exchange sites, thereby reducing the sodicity hazard (Fey, 1986). A comprehensive review of the use of gypsum in soils for improving soil physical characteristics is provided by Shainberg *et al.* (1989).

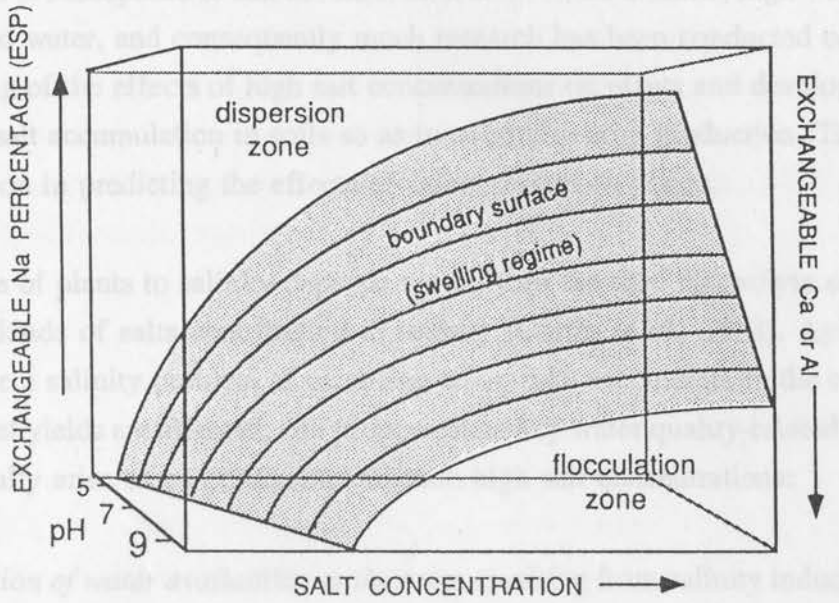

Figure 2.3 Graphic representation of the effects of ESP, salt concentration, exchangeable Ca or Al, and pH on the structural stability (flocculation zone) and instability (dispersion zone) of soil clay, and the position of the boundary surface (swelling regime) between these two zones (McBride, 1994, pg. 288).

2.4 Plant Responses to Salinity and Sodicity

Problems arising from high salt concentrations in soils occur in many parts of the world. Irrigated land is susceptible to salt accumulation from either a saline, high water table or salts in the applied water, and consequently much research has been conducted on developing an understanding of the effects of high salt concentrations on plants and developing methods of minimizing salt accumulation in soils so as to maximise crop production. This research will be drawn upon in predicting the effects of saline wastes on plants.

The response of plants to salinity depends not only on the total electrolyte concentration but also on the kinds of salts contributing to salinity (Curtin *et al.,* 1993). Ayers and Westcot (1985) define a salinity problem as occurring when salts accumulate in the crop root zone to the extent that yields are affected, and propose three key water quality-related problems which may potentially arise as a consequence of such high salt concentrations:

- *Reduction of water availability to the crop,* resulting from salinity induced osmotic stress;
- *Reduction in the rate at which water infiltrates the soil,* resulting from relatively high sodium or low calcium content of the soil or water;
- *Specific ion toxicity,* resulting from certain ions such as sodium, chloride, or fluoride, that accumulate in toxic concentrations.

2.4.1 Salinity induced Osmotic Stress

2.4.1.1 Build-up of Soil Salinity

A crop removes water from the soil to meet its evapotranspiration demand (ET) but leaves behind most of the salt which will become increasingly concentrated in the shrinking volume of soil-water. With each influx of water, more salt is added. A portion of this added salt must be leached from the root zone before the concentration affects the crop yield. Leaching occurs when the water influx is sufficient such that a portion percolates through and below the entire root zone carrying with it a portion of the accumulated salts. The fraction of the total water influx that passes through the entire rooting depth and percolates below is called the leaching fraction (LF). Leaching is only effective if drainage is sufficient to remove the required

amount of salts from the root zone to sustain plant growth. Low leaching rates will result in progressive salt accumulation which may eventually reach harmful levels. This is particularly a problem in arid and semi-arid regions in which accumulated salts are not flushed from soils by adequate rainfall (Kirkham, 1986).

If water salinity (EC_w) and the leaching fraction (LF) are known or can be estimated, both the salinity of the drainage water that percolates below the rooting depth and the average root zone salinity may be estimated (Ayers & Westcot, 1985). The salinity of the drainage water can be estimated from the equation:

$$EC_{dw} = EC_w / LF \quad (9)$$

where: EC_{dw} = salinity of the drainage water percolating below the root zone (equal to salinity of soil-water, EC_{sw})

EC_w = salinity of the applied irrigation water

LF = leaching fraction

By making certain assumptions concerning the percentage of water used by the crop from a particular rooting depth, the above equation may also be used to predict average soil-water salinity (EC_{sw}).

2.4.1.2 Response of Plants to Salinity induced Osmotic Stress

Salinity reduces the osmotic potential of the soil solution and thus imposes an osmotic stress on plants. When the osmotic stress in the root zone prevents the plant extracting sufficient water from the saline solution, yield losses will occur (Ayers & Westcot, 1985). The most common salinity effect is a general stunting of growth, with the decrease in growth occurring linearly as salinity increases above a critical threshold (Maas & Hofmann, 1977). Farooq *et al.* (1989) also include wilting and scorching of leaves as potential effects of salinity, and Shone & Gale (1983) suggest that even at water stress levels insufficient to cause visible damage plant growth may be slowed through a decrease in photosynthesis.

The response of plants to salinity is in most instances as a function of the total osmotic potential of soil water without regard to the specific salt species present. The response of some plants to salinity depends not only on the total electrolyte concentration, however, but also on the kinds of salts contributing to the salinity as is evidenced by the observation by

Maas & Hoffmann (1977) that in some cases salinity induces nutritional imbalances or deficiencies causing decreased growth and plant injury for which osmotic effects alone cannot account.

Plants differ greatly in their tolerance to saline conditions and Ayers & Westcot (1985) state that in agricultural crops, there is an 8 to 10-fold range in salt tolerance. Salt tolerance depends on a variety of plant traits and involves the mechanisms of uptake, transport and excretion of ions (Malkin & Waisel, 1986). Marcum & Murdoch (1990) have shown that for eleven cases of C_4 turfgrasses water stress was overcome by osmotic adjustment within the plant tissues achieved by both decreasing tissue water content and solute accumulation. Work on trees tolerant to saline conditions (Gupta & Abrol, 1989) may have potential use in that the higher salinity levels that can be tolerated and reduced necessity for drainage will in turn reduce the rate of contamination of groundwater with excessive amount of salts.

2.4.1.3 Management of Salinity induced Osmotic Stress Problems

2.4.1.3.1 Leaching

Leaching salts to beneath the root zone, thereby reducing the concentration of salts within the root zone is the key factor in controlling soluble salts, whether they are brought in by irrigation water or by leaching from saline wastes. Leaching is achieved by applying water to the affected area in excess of that required by the crop causing dissolved salts to be leached with the drainage water. The amount of water required for leaching is defined by the leaching requirement (LR).

The leaching requirement (LR) is defined as the fraction of the irrigation water that must be leached through the root zone to keep the salinity of the soil below a specified value (Ayers & Westcot, 1985). Rhoades & Merrill (1976) in Ayers & Westcot (1985) propose the following equation for calculating the leaching requirement (LR):

$$LR = \{ EC_w / (5.EC_e - EC_w) \} \qquad \textbf{(10)}$$

where LR = the minimum leaching requirement needed to control salts within the tolerance (EC_e) of the crop with ordinary surface methods of irrigation,

EC_w = salinity of the applied irrigation water in mS/cm,

EC_e = average soil salinity tolerated by the crop as measured on a soil saturation extract.

2.4.1.3.2 Drainage

Although the use of a leaching requirement may be potentially effective in reducing saline soils, in many instances salinity problems are in fact associated with an uncontrolled water table within one or two metres of the ground surface and leaching is not immediately possible. In such instances, water typically rises into the active root zone by capillarity and, if the water table contains salts, either natural or from waste contamination, it becomes a continual source of salts to the root zone as water is used by the crop or evaporates at the soil surface. The rate of soil salinity accumulation from an uncontrolled shallow water table will depend upon irrigation management, salt concentration and depth of the groundwater, soil type, and climatic conditions (Ayers & Westcot, 1985).

Salinity problems which arise from an uncontrolled shallow water table cannot be solved by the use of a leaching fraction, unless the water table is stabilized and maintained at a suitable depth of at least two metres. Installing sub-surface drains is the common means of improving internal drainage rate. Other alternatives include open or tile drains or drainage wells to remove a part of the salty subsurface water and transport it to an adequate salt-sink for safe disposal.

2.4.2 Toxicity Problems asociated with Particular Ions

Toxicity problems result from the accumulation of certain ions within the plant, normally the leaves, at concentrations which are toxic to that plant. Although toxicity problems are associated with the presence of high electrolyte concentrations in the soil and or groundwater, toxicity problems differ from salinity problems per se in the sense that they occur within the plant and are not caused by a salinity induced water shortage. Toxicity, however, often accompanies or complicates a salinity or infiltration problem. The effects of sodium, chloride, sulphate and fluoride on plants will be discussed in the following sections.

2.4.2.1 Chloride

Soils do not absorb chloride efficiently and it is usually freely bioavailable with the result that chloride toxicity is often cited as the most common toxicity under saline conditions. Chloride

taken up by a plant moves in the transpiration stream and accumulates in the leaves. If the concentration exceeds the tolerance of the plant, injury symptoms such as leaf burn or dying of the leaf tissue occurs. Plant injury typically begins at the leaf tips and progresses from the tip back along the edges as severity increases.

Due to the fact that chloride is essentially a physiologically neutral anion tolerated over a wide range of concentrations by most plants, Cerda & Martinex (1988) have suggested that processes such as chloride suppression of NO_3 uptake may in fact be the cause of apparent chloride toxicity.

2.4.2.2 Sodium

Sodium toxicity is not easily distinguished from chloride toxicity. Typical symptoms include leaf burn and scorch or dead tissue along the outside edge of leaves in contrast to chloride toxicity which is usually manifests at the extreme leaf tip. Sodium toxicity is often modified or reduced if sufficient calcium or potassium is available in the soil. Caution is required in diagnosing sodium toxicity with high SAR water because apparent toxic effects of sodium may be due to or complicated by poor water infiltration (Ayers & Westcot, 1985).

Although both sodium and chloride have the potential to affect plant growth adversely there is evidence that chloride may have a greater toxic effect than Na (Greub *et al.*, 1985). Chemical analysis of plant tissue is commonly used to diagnose either chloride or sodium toxicity.

2.4.2.3 Sulphate

Mills (1994) showed that sulphate in the soil solution has an inhibitory effect on ion uptake and growth of kikuyu (*Pennisetum clandestinum*), and that sulphate has a greater inhibitory effect than chloride (provided the plant is not susceptible to Cl toxicity) because Cl is particularly effective in osmotic adjustment as it can be rapidly accumulated in high concentrations. Tissue culture experiments with chinese cabbage (*Brassica campestris*) revealed that sulphate is twice as inhibitory on growth as the same concentration of chloride (Paek *et al.*, 1988).

High sulphate concentrations in either groundwater or irrigation water will result in gypsum precipitation. Consequently, leaching is largely ineffective in controlling salinity derived from SO_4 (Papadopoulos, 1986). Gypsum solubility in soils is greater than that predicted from pure

water due to the higher ionic strength of the soil solution. The formation of ion pairs in sulphate waters is not accounted for in EC values but increases osmotic pressure and therefore decreases water availability to plants. Hence, Papadopoulos (1986) suggests that the effects of sulphate salinity on plants may better be determined by the sum of cations or solute potential than electrical conductivity.

2.4.2.4 Fluoride

Primary fluoride containing minerals are fluorspar (CaF_2), cryolite (Na_3AlF_6) and fluorapatite ($Ca_{10}F_2(PO_4)_6$) (Lindsay, 1979). The greatest source of fluoride pollution is atmospheric, caused by Al smelters, coal combustion, steel works, brick yards etc. Contamination of groundwater by fluoride is often associated with leachate formation from phoshpogypsum waste stacks which are by-products of the phosphate fertilizer industry.

Fluoride is beneficial to mammals within the range 6 to 20 mg/kg. Toxic effects result, however, at concentrations of 30 to 50 mg/kg (Underwood, 1971). The major clinical signs of fluoride toxicity are found in the teeth and bone where mottling of the developing teeth is the first sign of fluorosis. Chronic fluorosis is endemic in sheep, cattle, goats, horses and humans in many parts of the world as a consequence of drinking water abnormally high in fluoride (Underwood, 1971). Fluoride is a cumulative poison and once bone tissue is saturated, continued intakes are deposited in soft tissues resulting in metabolic disturbances and ultimately death (McDowell, 1992).

Fluoride generally occurs in plant material in the range of 2 to 50 ppm in the dry matter, although some plant species are capable of accumulating much higher amounts (Mengel & Kirkby, 1978). Fluoride has a limited solubility, the amount available to the roots of plants depending not only on the concentrations in the soil solution but also on the rate at which the solution is replenished by release from the labile pool (Larson & Widdowson, 1971). Several authors have recorded higher leaf fluoride concentrations in plants grown on acid soils and lower concentrations on limed soils (Mengel & Kirkby, 1978), which points to the involvement of Al in fluoride uptake in plants.

2.5 Conclusions

The literature shows that physicochemical interactions taking place between soil particles and pore fluid may cause significant changes in the hydraulic conductivity of soils. The swelling and dispersion of soil clay minerals may markedly alter the structural stability and permeability of the soil and is a key physicochemical interaction controlled predominantly by the salt concentration and type of the pore-fluid. The effects of electrolyte type and concentration and pH are found to have the following effect on soil conductivity: soil clays readily disperse at low salt concentrations, high exchangeable sodium levels, and high pH, resulting in reduced soil conductivity; flocculation typically occurs at high salt concentrations, low exchangeable sodium levels and low pH, resulting in enhanced conductivity. The determination of critical coagulation or flocculation concentration (CCC or CFC, respectively) is the most common approach taken in study the dispersion-flocculation behaviour of soils.

Agricultural research shows that saline conditions may cause osmotic stress in plants, causing stunting of growth and wilting and scorching of leaves. Osmotic stress problems may be managed through the use of a leaching fraction. In cases of shallow groundwater levels, however, the establishment of effective drainage mechanisms is necessary before a leaching fraction can be effectively employed. Toxicity problems may arise from particular ions that may be concentrated under saline conditions. Chloride toxicity is cited as the most common toxicity problem in saline conditions. Plant responses to chloride toxicity include leaf burn or dying of the leaf tissue and are similar to the effects of sodium toxicity. Although chloride toxicity is considered most prevalent in saline conditions, the inhibitory effect of sulphate toxicity has been shown to be twice as great as that of chloride (eg. Paek *et al.*, 1988). Fluoride is found in higher concentrations in plants grown on acid soils and lower concentrations on limed soils, indicating that Al is involved in fluoride uptake by plants.

3. COLLECTION, PREPARATION AND ANALYSIS OF WATER, SOIL, SEDIMENT AND MATERIALS, AND FOLIAR SAMPLES

3.1 Introduction

The aim of this chapter is to describe the collection, preparation and analysis of water, soil, sediment and materials, and foliar samples. Analytical methods used are described only in brief in this chapter with the relevant details being contained in Appendix A.

3.2 Sample Collection

The number of samples collected was limited by the time available in which to complete the analytical work. The choice of sample number was based, therefore, on consideration of the time required for analysis of samples and subsequent interpretation and completion of the thesis. Comprehensive coverage of the Dead Tree Area was considered to be a priority in this study and consequently the rationale for the positioning of samples was that of maximizing the number of samples allocated to the Dead Tree Area, with the remaining samples being allocated to the ivestigation of background conditions and sources of contamination. To achieve suitable coverage of the Dead Tree Area a 'quasi-grid' system was used whereby a series of transect lines were placed across the area and samples equally spaced along these lines.

3.2.1 Water Sampling

A total of twenty-one water samples were collected from the site during the period August/September, 1996. Eight of these samples were collected from the surface drains and evaporation ponds located N and NE of the Dead Tree Area, with the remaining thirteen samples being from the Dead Tree Area.

3.2.1.1 Surface Drains and Evaporation Ponds

The positions of the water samples collected to the N and NE of the Dead Tree Area are shown on Figure 3.1. Samples K1 through K5 represent samples taken from the Kynoch wastewater evaporation site, with samples K1, K2, and K5 being from the evaporation ponds and K3 and K4 from two surface drains located adjacent to the ponds. The two drains

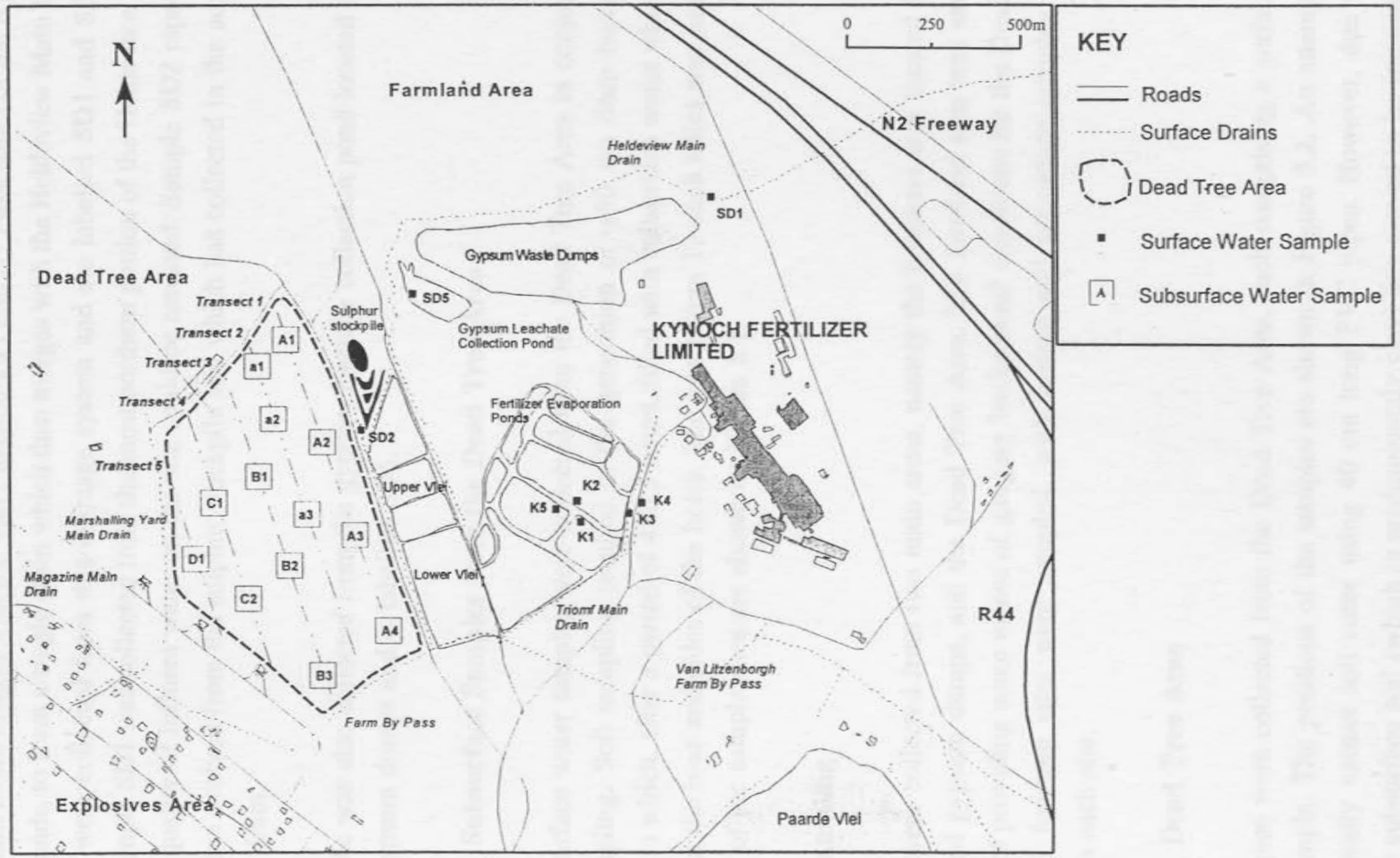

Figure 3.1 Map of the Dead Tree Area, Farmland Area and Kynoch Fertilizer Limited, showing the positions of the surface and subsurface water sampling points.

represent the main effluent outlet drains for Kynoch Fertilizer Limited and are labelled Triomf Main Drain on Figure 3.1. At the time of sampling (5 August 1996; 12:30 pm) there was no flow in either of these drains.

The Triomf Main Drain merges with the Van Litzenborgh Farm By Pass, south of the Kynoch evaporation ponds, to form a single drain which then merges with the Heldeview Main Drain. Two samples were collected from this drainage system and are labelled SD1 and SD2 on Figure 3.1. Sample SD1 was collected from the most northern portion of the Heldeview Main Drain so that quality of influent water on the site could be assessed. Sample SD2 represents leachate that has evolved from the sulphur stockpile and which has collected in the adjacent surface water drain.

A water sample was also collected from the gypsum leachate collection pond located south-west of the gypsum dumps and is labelled SD5.

3.2.1.2 Subsurface Samples from the Dead Tree Area

Thirteen subsurface water samples were collected from the Dead Tree Area in conjunction with soil sampling. Soil sampling resulted in the generation of ±50 cm deep holes (see Section 3.2.2.1) which, after a period of 4 to 5 hours, filled with subsurface water which had seeped in from the base and sides of the holes. The water from 13 such holes was sampled. The positions of the sample sites are shown on Figure 3.1.

3.2.2 Soil Sampling

Soil samples were collected from two main areas, namely the farmland area located NE of the sulphur and gypsum dumps, and the Dead Tree Area. The farmland area was sampled with the aim of providing some means of gauging 'background' conditions for the Dead Tree Area. In total fourteen sites were sampled, with surface and subsurface samples being collected from each site.

3.2.2.1 Dead Tree Area

Ten soil samples were collected from the Dead Tree Area, each comprising a surface and subsurface sample. The positions of the samples are shown in Figure 3.2. An attempt was made to manually extract soil cores using 40 cm long PVC pipes. However, due to the rigidity of the subsurface soil (which is predominantly clay) this proved to be impossible.

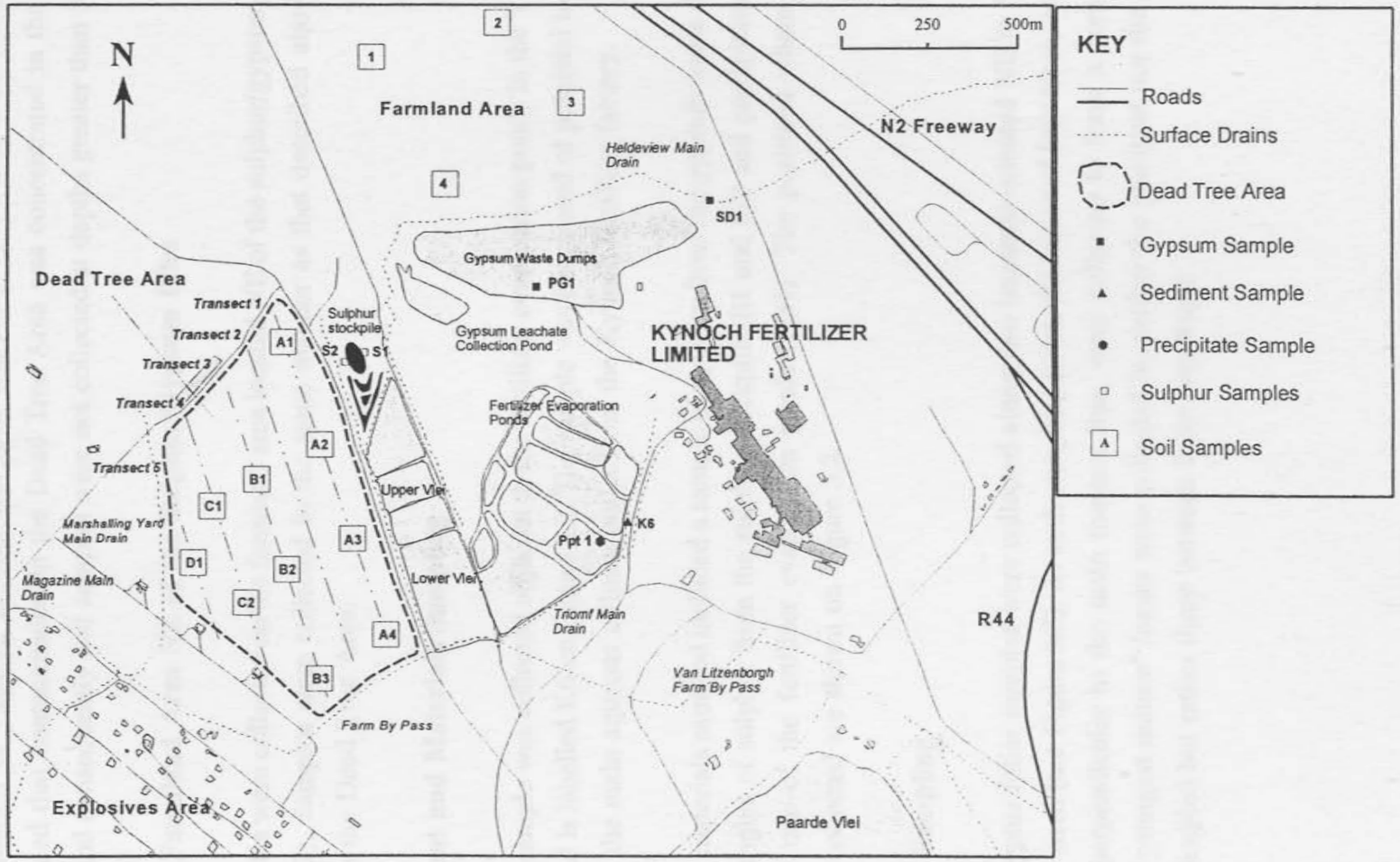

Figure 3.2 Map of the Dead Tree Area, Farmland Area and Kynoch Fertilizer Limited, showing the positions of the soil, sediment and materials sampling points.

Instead pits were dug to a depth of ±50 cm, removing the top layer from 0 to 6 cm as a surface sample and extracting a subsurface sample from about 40 to 50 cm. The sampling depths were chosen so that a comparison of the effect(s) of contamination on the more organic rich surface horizon (0 to 6cm) with that on the subsurface soils (40 to 50cm) could be made. Evaluation of existing geochemical data (supplied by Steffan, Robertson and Kirsten) indicated that contamination in the Dead Tree Area was concentrated in the near surface zone, and consequently soil samples were not collected at depths greater than 50cm.

3.2.2.2 Farmland Area NE of the Sulphur/Gypsum Piles

Four soil samples were collected on the farmland area located NE of the sulphur/gypsum piles (see Figure 3.2). Samples were collected in the same manner as that described above for samples within the Dead Tree Area.

3.2.3 Sediment and Materials Sampling

One sediment sample was collected adjacent to the fertilizer evaporation ponds in the Triomf Main Drain and is labelled K6 on Figure 3.2. The sample was considered of potential interest as the drain is the main aqueous effluent outlet from the Kynoch fertilizer factory.

Miscellaneous materials sampled included a sample of gypsum from the gypsum waste dumps (PG1), two samples of sulphur from the sulphur stockpile (S1 and S2) and precipitate from the bottom of one of the fertilizer evaporation ponds (Ppt1). The positions where these samples were collected are shown on Figure 3.2.

3.2.4 Foliar Sampling

Sixteen Eucalyptus foliar samples were collected along two transects oriented NE to SW in the Dead Tree Area (see Figure 3.3). At each sampling point, the leaves of four trees, oriented along a line perpendicular to the main transect line, were collected to form a composite sample. The "youngest mature" leaves were collected ie. neither the youngest nor the oldest leaves were sampled but rather those between these two stages.

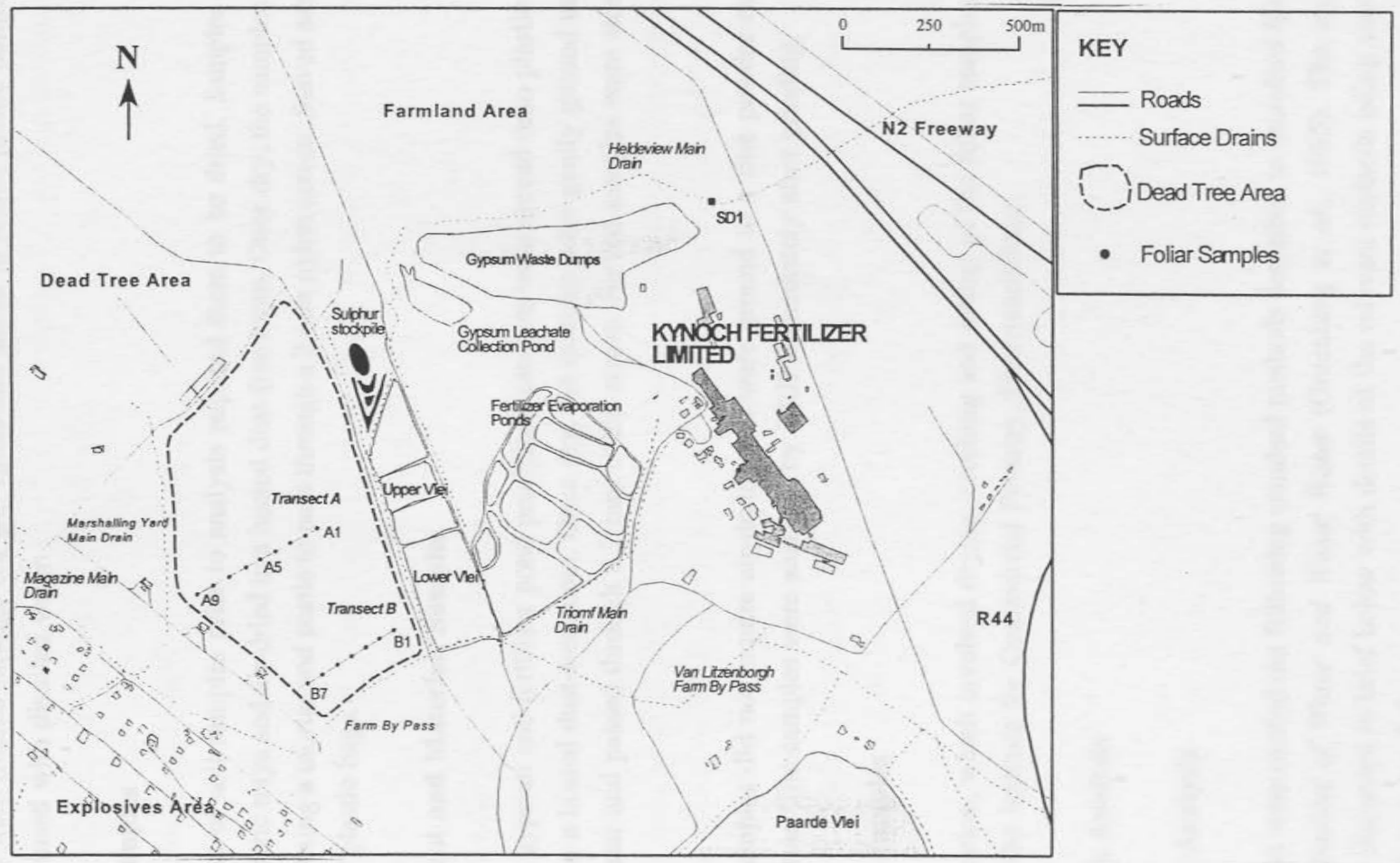

Figure 3.3 Map of the Dead Tree Area, Farmland Area and Kynoch Fertilizer Limited, showing the positions of the foliar sampling points.

3.3 Sample Preparation

3.3.1 Water Samples

Water samples were filtered through 0.2 µm filters and stored in sealed plastic bottles that had been pre-rinsed with distilled water.

3.3.2 Soil Samples

The preparation of soil samples prior to analysis required them to be dried. Samples were spread onto plastic trays and air-dried in a heated dust-free room. Once dry, the samples were gently ground using a mortar and pestle to pass through a 2 mm nylon screen. Sieved samples were stored in plastic bags.

3.3.3 Sediment and Materials Samples

The sediment, gypsum and fertilizer pond precipitate samples were spread onto plastic trays and air-dried in a heated dust-free room. Once dry, the samples were gently ground using a pestle and mortar and passed through a 2 mm nylon screen. Sieved samples were stored in plastic bags.

The sulphur samples did not require air-drying and were ground to a fine powder using a pestle and mortar. The samples were analysed by XRD immediately after grinding.

3.3.4 Foliar Samples

Sample preparation, which involved drying, crushing and ashing of the foliar samples, was performed by the Institute for Commercial Forestry, Pietermaritsburg.

3.4 Sample Analysis

3.4.1 Water Analysis

Water Analyses were carried out following standard methods described in *Standard Methods for the Examination of Water and Waste Water* (Greenberg *et al.,* 1985). The analyses performed are discussed in brief below with details of the relevant methods being contained in APPENDIX A:A.1 - A.6.

3.4.1.1 Electrical Conductivity (EC) and pH

Electrical Conductivity (EC) and pH were measured on unfiltered water samples using a *Crison microCM 2201* electrical conductivity meter and *Crison micropH 2001* microprocessor-controlled pH meter, respectively (see Appendix A:A.1 & A.2). The relative standard error of the EC measurements was ± 7%. The accuracy of the pH measurements was ± 0.1 pH unit and the precision was ± 0.05 pH units.

3.4.1.2 Alkalinity/Acidity

Alkalinity was determined on samples with pH values greater than 4.5 and acidity on samples with pH values less than 4.5. Alkalinity has been reported as mg $CaCO_3$/l and acidity as mmol/l (see Appendix A:A.3). Repeat analyses were within 1 mg $CaCO_3$/l and 0.5 mmol/l, respectively.

3.4.1.3 Major Cations and Anions

High Pressure Ion Chromatography (HPIC) was used to determine the major cation (Na^+, K^+, Ca^{2+}, Mg^{2+}, and NH_4^+) and anion (Cl^-, SO_4^{2-}, NO_2^-, NO_3^-, and PO_4^{3-}) concentrations of filtered (0.2 µm filter) water samples. Milli-Q de-ionised water was used to dilute the samples to an EC value of between 50 and 100 µS/cm, and the samples were filtered through On-Guard P filters to remove organics and particulates immediately prior to analysis. Analyses were carried out by means of a Dionex DX300 series suppressed IC system, which was coupled to an AI-450 chromatography software package (see Appendix A:A4). The precision of the anion analyses is shown in Table 3.1.

Table 3.1 Precision of HPIC anion analyses. All values in mg/l

Repeat No.	F^-	Cl^-	NO_3^-	SO_4^{2-}	Date (dd/mm)
1	0.25	0.90	0.43	0.84	01/09
2	0.25	0.93	0.49	0.85	01/09
3	0.23	0.94	0.46	1.19	03/09
4	0.23	0.49	0.48	0.96	03/09
5	0.22	0.90	0.47	0.95	09/09
6	0.24	0.93	0.49	0.96	04/09
7	0.23	0.90	0.58	0.93	04/09
8	0.22	0.91	0.57	0.97	04/09
9	0.23	0.91	0.48	0.96	04/09
10	0.24	0.94	0.50	0.96	04/09
Mean	0.235	0.920	0.493	0.956	
S.D.	0.010	0.017	0.044	0.091	
RSD (%)	4.1	1.8	8.9	9.5	

3.4.1.4 Phosphorus

Phosphorus was determined colorimetrically using the method of Murphy and Riley (1962). The results are reported as mg PO_4^{3-}/l. A *Turner 340 spectrophotometer* was used for the determinations (see Appendix A:A5). The relative standard deviation of the analyses was 2.4% and the relative error 2.3%.

3.4.1.5 Fluoride

Fluoride was determined using a *Corning pH/ion analyser 255* which was calibrated with a three point calibration curve using standards of 0.5, 1.0 and 10.0 mg F^-/l (see Appendix A:A6). The relative standard deviation of the analyses was 3.1% and the relative error 0.4%.

3.4.1.6 Total Elemental Concentrations

Inductively Coupled Plasma Atomic Emission Spectroscopy (ICP-AES) was used to determine the total concentrations of aluminum, iron, copper, nickel, lead, zinc, mercury, cadmium,

arsenic, manganese, chromium, and silicon. A *Jobin Yvon 70C (JY70C)* combined simultaneous/sequential ICP-AES spectrometer was used for the analyses. The instrumental conditions and parameters used were as follows:

Number of Scans:	simultaneous - 3; sequential - 3
Slits:	first - 25 µm; second - 50 µm
Flush Time:	10.00 seconds
Power:	1 kW
Pressure:	3.4 bar Ar gas
R.F.:	27.12 MHz
Sample Update:	2.0 ml/min
Observation Height:	14 mm above coil
Aerosol Gas Flow:	0.4 l/min [0.3 l/min - Na,K]
Plasma Gas Flow:	0.1 l/min
Coolant Gas Flow:	16 l/min

The analyses were performed by Darren Handsforth at the Department of Chemistry, University of Cape Town on 31 of October 1996. The lower limits of detection are shown in Table 3.2.

Table 3.2 Lower Limits of Detection (LLD) for ICP-AES analyses

Element	LLD (mg/l)	Element	LLD (mg/l)
Si	0.09	As	0.5
Al	0.5	Co	0.1
Cu	0.2	Mn	0.04
Ni	0.2	Cr	0.1
Zn	0.1	Fe	0.1
Cd	0.06	Pb	1.0

3.4.1.7 Prediction of Chemical Speciation and Saturation Indices (S.I.)

The mathematical model MINTEQA2 (Allison *et al.,* 1991), a geochemical equilibrium speciation model for dilute aqueous systems, was used to calculate the ionic speciation occurring in the water samples analysed, as well as to calculate saturation indices for minerals likely to be present under the prevailing conditions.

MINTEQA2 is based on the assumption of thermodynamic equilibrium between phases, with the thermodynamic equilibrium constant being defined as follows:

$$aA + bB \rightleftharpoons A_a B_b$$

$$K^0 = \frac{A_a B_b}{A^a B^b}$$

where A and B are chemical entities that react to form a reaction product A_aB_b, having a thermodynamic equilibrium constant K^0. MINTEQA2 uses the Davies equation to quantify the various chemical reactions modelled. The Davies equation is an extension of the Debye Huckel equation in which the ion-size-dependent parameters are the same for each charged ion (Lumsdon and Evans, 1995).

$$\log y_i = -Az^2 \left(\frac{\sqrt{I}}{1 + \sqrt{I}} - 0.24 \, . \, I \right)$$

where y_i = Activity Coefficient

$A = 1.82 \times 10^6 (\epsilon T)^{-3/2}$

z = valence of ion species

ϵ = Dielectric Constant (7.83 for water at 298 K)

T = Absolute Temperature (K)

I = Ionic Strength ($mol.dm^{-3}$)

3.4.2 Soil Analysis

Soil analyses were carried out following standard methods described in *Methods of Soil*

Analysis, Part 2: Chemical and Microbiological Properties (ASAA-SSSA 2nd edition, 1982). The analyses performed are discussed in brief below with details of the relevant methods being pesented in APPENDIX A:B.1 - B.7. Non standard methods included determination of dispersible clay percentage, and leaching tests to determine the effect of gypsum ammendment on the hydraulic conductivity of a composite soil sample from the Dead Tree Area. The desriptions of these methods appear in the chapter in which the respective results are discussed.

3.4.2.1 pH

The pH of soil samples was measured both in water and in $CaCl_2$, using a *Crison micropH 2001* microprocessor-controlled pH meter (see Appendix A:B.1). The accuracy of the pH measurements was ± 0.1 pH unit and the precision was ± 0.05 pH units.

3.4.2.2 Soluble Salts

In order to determine the concentrations of soluble salts within the soil samples, saturated paste extracts were prepared (See Appendix A:B.2). The extracts were analysed for pH, EC, Alkalinity/Acidity, Cations, Anions, and Fluoride following the same standard methods as those described for water samples in Appendix A:A.1 - A.6. The accuracy and precision of the pH measurements was as described above in section 3.4.2.1. The relative standard error of the EC measurements was ± 7%. Reapeat analyses for alkalinity and acidity were within 1 mg $CaCO_3$/l and 0.5 mmol/l, respectively. Cation and anion analyses were performed by HPIC as described in section 3.4.1.3. The relative standard deviation of the fluoride analyses was 3.0% and the relative error 0.5%.

3.4.2.3 Organic Carbon

Organic Carbon was determined by means of the Walkley-Black method (Walkley, 1935) (see Appendix A:B.3). Repeat analyses were found to be within 0.5% although Nelson and Sommers (1982) indicate that the results obtained cannot be considered strictly quantitative.

3.4.2.4 Exchangeable/Extractable Cations

Exchangeable/extractable cations (Na^+, K^+, Ca^{2+}, Mg^{2+}) were determined for samples A2a, A2b, A4a, A4b, B2a, B3a, C1b, D1b, 1b and 3b using the ammonium acetate method (see Appendix A:B.4). The analyses were performed by the Institute for Soil, Climate and Water,

Pretoria.

3.4.2.5 Clay Percentage

The percentage clay was determined for samples A2a, A2b, A4a, A4b, B2a, B3a, C1b, D1b, 1b and 3b using the pipette method (see Appendix A:B.5). The analyses were performed by the Institute for Soil, Climate and Water, Pretoria.

3.4.2.6 Dispersible Clay Percentage

Dispersible clay percentage was determined on samples A2a, A2b, A4a, A4b, B2a, B3a, C1b, D1b, 1b and 3b using the method of Levy and Torrento (1995). The method is described in chapter 6, section 6.2.1. Repeat analyses were within 1%.

3.4.2.7 Mineralogical Analysis of Clay Fraction

Mineralogical analysis of the clay fraction (<2 μm particles) of soil samples was performed using a method of (a) dispersion and fractionation to separate out the clay and (b) subsequent analysis of this fraction by means of X-ray diffractometry (XRD). A *Philips PW 1390* diffractometer fitted with a Cu X-ray tube operating at 40 kV and 25 mA was used for analysis. The samples were scanned through a range of 6 to 75° 2-theta, with a step-size of 0.1° 2-theta and a counting time of 1 second/step. (see Appendix A:B.6).

3.4.2.8 X-Ray Fluorescence Spectrometry (XRFS)

Sample powder briquettes were analysed for major and trace elements using a *Philips PW X'Unique II* X-ray spectrometer (see Appendix A:B.7). The trace elements determined quantitatively were Zn, Cu, Ni, Co, Mn, Cr, V, Mo, Nb, Zr, Y, Sr, U, Rb, Th and Pb. Details of sample preparation and analytical conditions are described in Appendix A:B.7 and Appendix B, respectively. Semi-quantitative analyses were performed on briquettes for the following majors (as oxides): Fe_2O_3, TiO_2, CaO, BaO, K_2O, P_2O_5, SiO_2, MgO, Na_2O, Cl and SO_4. Calibration was by means of international standard rock reference materials.

3.4.2.9 Leaching Trials

The effect of gypsum application on the hydraulic properties of a soil composite was studied using leaching columns following methods described by Smith and Fey (1996). The method

is described in chapter 6, section 6.2.2

3.4.3 Sediment and Materials Analysis

3.4.3.1 Sediment Analysis

Sediment analyses included pH (water and $CaCl_2$), soluble salts, organic carbon (Walkley-Black, 1935) and major and trace elements (XRFS). These analyses were performed in the same manner as described in the above section (section 3.4.2) on soil analysis.

3.4.3.2 Gypsum, Sulphur and Fertilizer Evaporation Pond Precipitate Analysis

3.4.3.2.1 Mineralogical Analysis

Mineralogical analysis of the sulphur and fertilizer pond precipitate samples was performed using an automatic *Philips PW 1390* X-ray diffractometer. The samples were ground in a pestle and mortar to a fine powder and loaded on plastic slides.

The diffractometer, which was fitted with a Cu X-ray tube, was operated at an accelerating voltage of 40 kV and a beam current of 20 mA. A step scan with a counting time of 1 second per step and step-size of 0.1° 2-theta was used and the scans were run from 6 to 75° 2-theta. Results were recorded by computer, and the intensity versus two theta plots interpreted manually to yield semi-quantitative estimates of sample mineralogy.

3.4.3.2.2 Major and Trace Element Analysis

The gypsum sample was analysed for major and trace elements using a *Philips PW X'Unique II* X-ray fluorescence spectrometer (XRFS). The trace elements determined quantitatively were Zn, Cu, Ni, Co, Mn, Cr, V, Mo, Nb, Zr, Y, Sr, U, Rb, Th and Pb. Semi-quantitative analyses for the following majors were performed (as oxides): Fe_2O_3, TiO_2, CaO, BaO, K_2O, P_2O_5, SiO_2, MgO, Na_2O, Cl and SO_4. Details of sample preparation and analytical conditions are described in Appendix A:B.7 and Appendix B, respectively. Calibration was by means of international standard rock reference materials.

3.4.4 Foliar Analysis

Foliar samples were analysed for N, P, K, Ca, Mg, Na, Mn, Fe, Zn and Cu by Michael Chetty

at the Institute for Commercial Forestry, Pietermaritzburg following standard methods described in Donkin *et al.,* (1993), Heffernan (1985), Kalra and Maynard (1991), and Nicholson (1984).

4. ENVIRONMENTAL CHEMISTRY OF THE FERTILIZER EVAPORATION PONDS, GYPSUM WASTE DUMPS, SULPHUR STOCKPILE AND HELDEVIEW MAIN DRAIN

4.1 Introduction

One of the objectives of this study is to assess the effects of contamination from the gypsum dumps, fertilizer evaporation ponds and sulphur stockpile on the quality of water and soils in the Dead Tree Area. In order to undertake such an assessment a chemical characterisation of the above potential sources of contamination is required. Consequently it is the aim of this chapter to characterise, chemically, the following potential sources of contamination that may be impacting on the Dead Tree Area:

- fertilizer evaporation ponds and associated Triomf Main Drain,
- gypsum waste dumps,
- sulphur stockpile, and
- water entering the site via the Heldeview Main Drain.

This has been done through the analysis and interpretation of selected water, sediment and material samples that are associated with the various waste/storage sites. In this chapter, the collection, preparation and analysis of the various samples is described and the results thereof discussed. Mineralogical (XRD) and bulk element (XRFS) analysis of selected materials has been used to determine what potential contaminants the various materials contain. In order to assess what ionic form these potential contaminants may take in aqueous media, MINTEQA2, a chemical speciation model, has been use to predict mineral solubility equilibria and the speciation of ionic components in water samples. The results of this modelling have been used to characterise the various sources of contamination evolving from the various waste/storage sites. The quality of water at the various waste/storage sites has also been assessed in terms of the draft water quality guidelines for industrial use (Department of Water Affairs and Forestry, 1995).

4.2 Water, Sediment and Materials Sampling and Analysis

The collection, preparation and analysis of water, sediment and materials samples from the area located to the N and NE of the Dead Tree Area has been described in chapter 3. Water analyses were carried out following standard methods described in *Standard Methods for the*

Examination of Water and Waste Water (Greenberg *et al.,* 1985), and include electrical conductivity (EC), pH, alkalinity/acidity, major cations and anions (HPIC), phosphorus (Murphy and Riley Method, 1962), fluoride (electrode method) and total elemental concentrations (ICP-AES). Sediment analyses were carried out following standard methods described in *Methods of Soil Analysis, Part 2: Chemical and Microbiological Properties* (ASAA-SSSA 2nd edition, 1982), and include pH (water & $CaCl_2$), soluble salts, organic carbon (Walkley, 1935) and major and trace elements (XRFS).

Mineralogical analysis of the sulphur and fertilizer pond precipitate samples was performed using an automatic *Phillips PW 1390* X-ray diffractometer, and the gypsum sample was analysed for major and trace elements using a *Philips PW X'Unique II* X-ray fluorescence spectrometer (XRFS). The trace elements determined quantitatively were Zn, Cu, Ni, Co, Mn, Cr, V, Mo, Nb, Zr, Y, Sr, U, Rb, Th and Pb. Semi-quantitative analyses for the following majors were performed (as oxides): Fe_2O_3, TiO_2, CaO, BaO, K_2O, P_2O_5, SiO_2, MgO, Na_2O, Cl and SO_4.

4.3 Results and Discussion of the Fertilizer Evaporation Ponds and Triomf Main Drain

4.3.1 Water Analyses

The results of analyses of water samples from the fertilizer evaporation ponds and Triomf Main Drain (located adjacent to the evaporation ponds) are tabulated in Table 4.1.

Both the evaporation pond and drain waters are characterised by very high salinity (6.3 to 11.7 mS/cm), low pH (≤4.5) and high acidity (12.9 to 34.5 mmol/l). The total dissolved solids (TDS) content of these waters may be estimated from the expression (McBride, 1994):

$$TDS\ (mg.dm^{-3}) \approx EC\ (mS.cm^{-1}) \times 640,$$

to range between 4.0 to 7.5 $g.dm^{-3}$. These waters may thus be described as saline.

The major cations and anions present in these waters are similar, with Na^+, Ca^{2+}, Mg^{2+}, K^+ and NH_4^+ being the dominant cations and Cl^-, SO_4^{2-}, PO_4^{3-}, NO_3^- and F^- being the dominant anions. Neither Br^- nor NO_2^- were detected. Although there is no general predominance of one cation over another in these waters, within the anion suite SO_4^{2-} and NO_3^- show markedly higher concentrations than the other anions. In general, the SO_4^{2-} and NO_3^-

Table 4.1 Analyses of water samples from Kynoch Fertilizer Limited evaporation ponds and Triomf Main Drain.

	Kynoch Fertilizer Limited Evaporation Ponds			Triomf Main Drain	
Sample No.	K1	K2	K5	K3	K4
pH	2.7	4.5	3.0	3.2	2.9
EC (mS/cm)	11.7	8.12	8.4	8.4	6.3
Acidity (mmol/l)	34.5	13.4	23.3	20.4	12.9
Cations (mg/l)					
Na^+	282	171	189	323	310
Ca^{2+}	589	468	574	545	477
Mg^{2+}	523	167	344	298	218
K^+	719	510	524	335	284
NH_4^+	781	459	486	351	159
Anions (mg/l)					
Cl^-	1030	651	655	788	561
SO_4^{2-}	3530	2880	2430	2380	1400
[1]$PO4^{3-}$	724	346	337	407	318
NO_3^-	1990	1530	1250	980	1060
[2]F^-	222	76.0	320	202	205
Total Elemental Concentrations (mg/l)					
Si	51.6	19.2	37.1	32.9	60.3
Al	60.2	18.9	55.7	130	76.2
Fe	1.64	0.14	1.28	0.50	3.55
Cu	0.86	0.24	0.48	2.11	0.31
Ni	0.57	0.24	0.46	0.71	0.46
Pb	BDL	BDL	BDL	BDL	BDL
Zn	2.07	1.13	1.69	10.7	3.94
Cd	0.09	0.08	0.10	0.11	0.09
As	0.91	BDL	BDL	0.75	BDL
Co	0.24	0.11	0.19	0.29	0.16
Mn	3.60	1.66	2.72	3.71	4.20
Cr	0.12	BDL	0.14	0.10	BDL

Footnotes:
1 - phosphate determined by Murphy and Riley Method (1962)
2 - fluoride determined by ion selective electrode
BDL - below detection limits

concentrations are an order of magnitude greater than the other anions, with the SO_4^{2-} concentrations being approximately double those of NO_3^-.

The fertilizer evaporation ponds and Triomf Main Drain water is characterised, therefore, by a dominance of the anion SO_4^{2-} and no predominance within the cation suite. A Piper diagram showing the five water samples is given in Figure 4.1. The diagram shows a tight clustering of the five analyses. Pipergrams may be used to categorise water compositions into various hydrochemical facies - distinct zones that have cation and anion concentrations within defined compositional categories (Freeze and Cherry, 1979). These subdivisions are shown in Figure 4.2. Comparing Figure 4.1 with the hydrochemical facies given in Figure 4.2 reveals that the fertilizer evaporation ponds and Triomf Main Drain water is indeed characterised by sulphate dominance in the anion suite. The cation data clusters on the border between 'no dominant type' and the 'sodium/potassium type'.

The Pipergram does not include the anions PO_4^{3-}, NO_3^- or F^-. Although the concentrations of these anions are significantly less than those of SO_4^{2-}, they do contribute significantly to the total anion concentration, with PO_4^{3-} ranging from 318 to 724 mg/l, NO_3^- from 980 to 1990 mg/l and F^- from 76 to 320 mg/l.

Total elemental analysis by ICP-AES reveals elevated concentrations of various metals, notably Al, Fe, Zn, Mn, As and Si. Aluminium concentrations are noteably high, ranging in concentration from 18.9 to 130 mg/l, with the higher concentrations occurring in the Triomf Main Drain samples. Similarly, the concentrations of Mn and Zn are also higher in the Triomf Main Drain samples. Iron does not display this trend, although the highest concentration of Fe (sample K3 - 10.70 mg/l) found in these waters does occur in the Triomf Main Drain. Arsenic was only detected in samples K1 and K3 (0.91 and 0.75 mg/l respectively). However, arsenic concentrations in samples K2, K4 and K5 may also exceed 0.1 mg/l (present irrigation water guideline) but were not detected due to the comparatively high detection limit for arsenic (0.5 mg/l).

4.3.1.1 Chemical Speciation Modelling

It is increasingly realised that the distribution, mobility and biological availability of chemical elements depends not simply on their concentrations but, critically, on the chemical and physical associations which they undergo in natural systems. Changes in environmental conditions, whether natural or anthropogenic, can strongly influence the behaviour of both essential and toxic elements by altering the form in which they occur (Forstner and Wittmann,

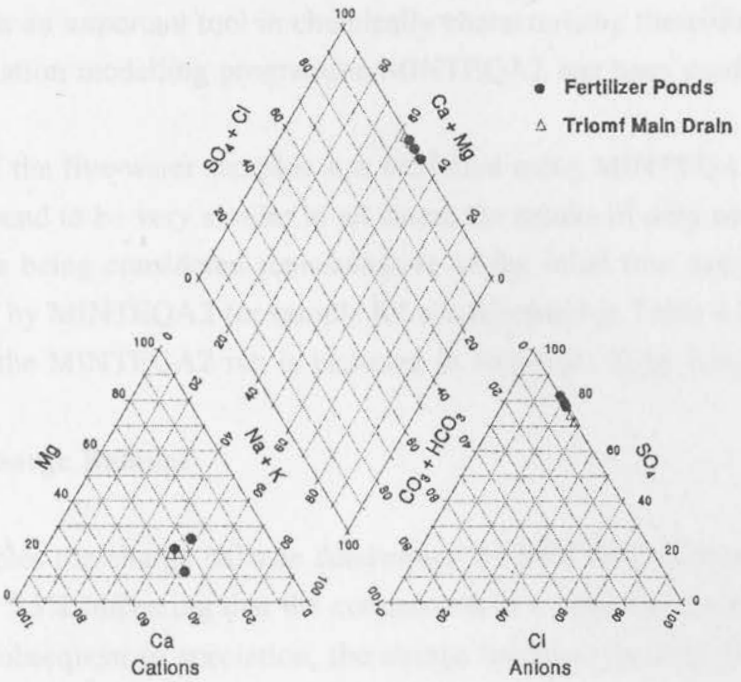

Figure 4.1 Pipergram representing the composition of water samples K1 to K5 from the fertilizer evaporation ponds and Triomf Main Drain. Solid circles represent samples K1, K2 and K5 from the fertilizer ponds, and open triangles represent samples K3 and K4 from the Triomf Main Drain.

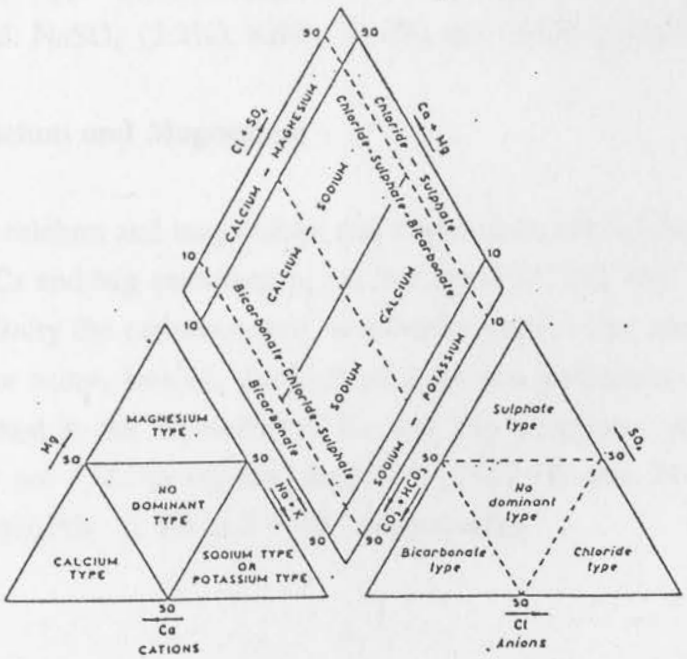

Figure 4.2 Piper trilinear diagram showing hydrochemical facies (Ward, 1975).

1979; Ure and Davidson, 1994). Consequently, chemical speciation modelling of the water sample analyses is an important tool in chemically characterising these waters. The chemical equilibrium speciation modelling programme MINTEQA2 has been used to this end.

The speciation of the five water samples was modelled using MINTEQA2. However, as the speciation was found to be very similar in all cases, the results of only one sample (K1) will be discussed, this being considered representative of the other four samples. The chemical species predicted by MINTEQA2 for sample K1 are tabulated in Table 4.2, and the complete output file from the MINTEQA2 run is included in Appendix D by way of example.

4.3.1.1.1 Charge Balance

For all five samples the charge balance determined by MINTEQA2 prior to speciation was between 0.5 and 5.5% indicating that the concentrations of most of the major ions had been accounted for. Subsequent to speciation, the charge balance typically decreased to between 0.25 and 3%.

4.3.1.1.2 Sodium, Potassium, Ammonium, Chloride and Nitrate

MINTEQA2 predicted that sodium, potassium, ammonium, chloride and nitrate occur predominantly as the free ions Na^+, K^+, NH_4^+, Cl^-, and NO_3^- (96.8%, 95.6%, 92.2%, 99.9% and 100%, respectively). The remaining Na^+, K^+ and NH_4^+ occurs in anionic complexes with the sulphate ligand: $NaSO_4^-$ (3.2%), KSO_4^- (4.4%) and $NH_4SO_4^-$ (7.8%).

4.3.1.1.3 Calcium and Magnesium

The speciation of calcium and magnesium was found to be very similar, with approximately 70% of the total Ca and Mg occurring as the free ions Ca^{2+} and Mg^{2+}. Because these waters contain zero alkalinity the carbonate and bicarbonate species that are typically formed with Ca and Mg do not occur. Instead, the high sulphate and phosphate concentrations in these waters have resulted in the formation of Ca and Mg complexes with these ligands. The species predicted are $CaSO_4^o$(aq) and $MgSO_4^o$(aq) (27.4% and 24.4%, respectively) and $CaH_2PO_4^+$ and $MgH_2PO_4^+$ (2.9% and 3.8%, respectively).

Table 4.2 Chemical species predicted by MINTEQA2 as likely to be present in the Kynoch Fertilizer Limited evaporation ponds and Triomf Main Drain (using sample K1).

Constituent	Percentage Speciation Predicted
Na	Na^+ (96.8%), $NaSO_4^-$ (3.2%)
Ca	Ca^{2+} (69.6%), $CaSO_4$(aq) (27.4%), $CaH_2PO_4^+$ (2.9%)
Mg	Mg^{2+} (71.0%), $MgSO_4$(aq) (24.4%), $MgH_2PO_4^+$ (3.8%)
K	K^+ (95.6%), KSO_4^- (4.4%)
NH_4	NH_4^+ (92.2%), $NH_4SO_4^-$ (7.8%)
Cl	Cl^- (99.9%)
SO_4	$SO4^{2-}$ (57.6%), $CaSO_4$(aq) (11.0%), $NH_4SO_4^-$ (9.2%), $MgSO_4$(aq) (14.3%), $NaSO_4^-$ (1.1%), KSO_4^- (2.2%), HSO_4^- (4.6%)
PO_4	$H_2PO_4^-$ (69.6%), $CaH_2PO_4^+$ (5.6%), $MgH_2PO_4^+$ (10.7%), H_3PO_4 (13.9%)
NO_3	NO_3^- (100.0%)
F	AlF_3(aq) (38.9%), AlF_4^- (14.7%), AlF_2^+ (4.8%), SiF_6^{2-} (25.5%), MgF^+ (1.4%), F^- (4.6%), HF(aq) (9.7%),
Al	AlF_3(aq) (68.0), AlF_2^+ (12.6%), AlF_4^- (19.3%)
Fe	Fe^{2+} (46.1%), $FeH_2PO_4^+$ (38.0%), $FeSO_4$(aq) (15.9%)
Cu	Cu^{2+} (70%), $CuSO_4$(aq) (27.8%), $CuCl^+$ (1.7%)
Ni	Ni^{2+} (71.2%), $NiSO_4$(aq) (26.9%), $NiCl^+$ (1.6%)
Zn	Zn^{2+} (64.0%), $ZnSO_4$(aq) (29.0%), $ZnCl^+$ (1.5%), $Zn(SO_4)_2^{2-}$ (5.2%)
Cd	Cd^{2+} (37.9%), $CdCl^+$ (32.6%), $CdSO_4$(aq) (21.2%), $Cd(SO_4)_2^{2-}$ (5.2%) $CdCl_2$(aq) (2.1%)
Cr	Cr^{2+} (100.0%)
Mn	Mn^{2+} (71.9%), $MnSO_4$(aq) (25.3%), $MnCl^+$ (2.6%)
As	H_3AsO_4 (20.0%), $H_2AsO_4^-$ (80.0%)
H_2O	SiF_6^{2-} (100.0%)
H	$H_2PO_4^-$ (44.6%), $CaH_2PO_4^+$ (3.6%), $MgH_2PO_4^+$ (6.9%), H^+ (11.2%), H_3PO_4 (13.4%), SiF_6^{2-} (8.3%), $H_2SO_4^-$ (7.1%), HF(aq) (4.8%).

4.3.1.1.4 Sulphate and Phosphate

Sulphate complexes with numerous cations forming neutral species with divalent Mg and Ca ions and anionic species with the monovalent Na, K and NH_4 ions. The neutral sulphate species $CaSO_4(aq)$ and $MgSO_4(aq)$ predominate over the anion species $NH_4SO_4^-$, $NaSO_4^-$ and KSO_4^-. MINTEQA2 predicts, however, that these species make up less than 50% of the total sulphate species, with SO_4^{2-} representing 57.6% of the total and HSO_4^- making up the remaining 4.6%.

Phosphate occurs as $H_2PO_4^-$ (69.6%) and H_3PO_4 (13.9%), with the remaining species being the monovalent cations $CaH_2PO_4^+$ (5.6%) and $MgH_2PO_4^+$ (10.7%).

4.3.1.1.5 Fluoride and Aluminium

Fluoride complexes strongly with Al^{3+} and Fe^{3+}. Due to the high concentrations of Al in these waters, the dominant fluoride complexes are those formed with Al. These include $AlF_3(aq)$ (38.9%), AlF_4^- (14.7%) and AlF_2^+ (4.8%). All the aluminium in these waters is predicted by MINTEQA2 to occur in these three fluoride complexes.

The divalent anion SiF_6^{2-} also represents a significant percentage of fluoride speciation (25.5%) with HF(aq) (9.7%), F^- (4.6%) and MgF^+ (1.4%) making up the remaining few percent.

4.3.1.1.6 Iron

Iron exists in solution either as Fe^{2+} or Fe^{3+}. For the purposes of the MINTEQA2 speciation, all iron was assumed to be in the reduced Fe^{2+} state, since ferrous iron constituents tend to be more soluble than ferric iron ones (Wetzel, 1983). MINTEQA2 predicted that 46.1% of Fe would be in the Fe^{2+} form with the remaining being as $FeH_2PO_4^+$ (38.0%) and $FeSO_4(aq)$ (15.9%).

Because iron compounds in water are easily oxidised (Dallas and Day, 1993), it is likely that most of the iron present in the water is in the ferric state. The most common specie of ferric iron, however, is hydrated ferric hydroxide ($Fe[OH]_3$) which has a low solubility and is usually present as suspensions of flocculated $Fe[OH]_3$ (Wetzel, 1983). Because the water samples were filtered through 0.2 µm filters prior to ICP-AES analysis, it is probable that much of the flocculated iron present was removed.

4.3.1.1.7 Manganese

Manganese occurs in several valence states, however Mn^{3+} is thermodynamically unstable in aqueous solutions under normal conditions and Mn^{4+} compounds are insoluble at most pH values. Studies of theoretical thermodynamic redox equilibria of manganese by Stumm and Morgan (1981) show that for pH values less than ±7 and under a wide range of Eh conditions, Mn occurs as the divalent cation Mn^{2+}. Consequently manganese was entered into MINTEQA2 as Mn^{2+}. The model predicts that 71.9% of the total Mn is present as Mn^{2+} with $MnSO_4(aq)$ being the dominant complex formed (25.3%). Some complexation with Cl^- occurs in the form of the cationic complex $MnCl^+$ (2.6%).

4.3.1.1.8 Zinc, Nickel, Cadmium

The three metals zinc, nickel and cadmium occur as three principal species: free ions, sulphate complexes and chloride complexes. In the case of zinc and nickel the free ion forms are the dominant species (64.0% and 71.2%, respectively) with sulphate and chloride complexes representing less than 30% of the total species. The cadmium speciation is quite different, however, with only 37.9% occurring in the free ionic form. The sulphate and chloride complexes formed with cadmium also differ from those of zinc and nickel, in that the situation is reversed for cadmium with chloride complexes dominating over sulphate complexes.

4.3.1.1.8 Arsenic

Arsenic is found to be stable in four oxidation states under the Eh conditions occurring in aquatic systems: As(V), As(III), As(0) and As(-III), although the free element occurs only rarely (Fergusen and Garvis, 1972), and As(-III) is found only at extremely low Eh conditions. In general, inorganic arsenic is either pentavalent (eg. in arsenates) or trivalent (eg. in arsenites) with arsenites predominating in oxic surface waters. Taking these factors into consideration, arsenic was thus entered into MINTEQA2 in the arsenite trivalent form. The results of the modelling reveal that the arsenic remains in the trivalent form subsequent to speciation with 20.0% percent occurring as H_3AsO_4 and 80.0% as $H_2AsO_4^-$. These results are strongly pH dependent with the ratio of H_3AsO_4 to $H_2AsO_4^-$ decreasing with increasing pH. At pH values greater than 2.2, $H_2AsO_4^-$ is the dominant form (under oxic conditions) whereas H_3AsO_4 is the dominant form at pH values less than 2.2 (Alloway, 1995). Sample K1 has a pH of 2.7 and is therefore comparatively close to the thermodynamic boundary between H_3AsO_4 and $H_2AsO_4^-$. The other water samples (K2 to K5) have pH values >2.7 and hence

one may predict that $H_2AsO_4^-$ will represent close to 100% of the arsenic species in these waters.

4.3.1.2 Mineral Solubility Equilibria

MINTEQA2 was used to calculate the saturation indices of minerals likely to occur in the evaporation ponds and Triomf Main Drain waters. The stability of minerals may be predicted from thermochemical data due to the fact that the least soluble minerals are those with the lowest free energy. It important to note, however, that thermochemical considerations show which reactions are possible, but kinetic considerations are necessary to predict the time required for such transformations to occur. For solid phases with rapid precipitation/dissolution kinetics, the equilibrium aqueous concentrations of the element will be solubility-controlled. In the absence of the solubility-controlling solids, adsorption/desorption reactions will control aqueous concentrations (Rai and Kittrick, 1989).

The saturation indices calculated by MINTEQA2 for various minerals possibly occurring in the evaporation ponds, using sample K1 as an example, are illustrated graphically in Figure 4.3 (the numerical results for all five water samples, K1 to K5, are tabulated in Appendix D: Table D1). Only those minerals with saturation indices greater than -0.5 are shown, with values between -0.5 and 0.5 indicating equilibrium between the mineral and aqueous phase and values >0.5 indicating supersaturation.

Three forms of silica are predicted to be supersaturated in these waters, namely quartz, cristobalite (a structurally 'disordered' polymorph) and chalcedony (secondary quartz). Quartz has the highest saturation index (1.16) of the three silica minerals, as would be anticipated from the fact that silica mineral solubility decreases as a function of increasing packing density of the silica tetrahedra and long-range crystal order (Drees *et al.,* 1989). The formation of silica minerals is mediated by high salinities and the presence of metallic ions. Chemisorption of metallic ions, such as Al and Fe, to silica surfaces reduces the dissolution rates of silica due to the formation of relatively insoluble silicate coatings. In this regard, the high Al concentrations found in these waters may be playing an important role. However, these waters are acidic with the consequence that the sorption of Al onto the surface of silica minerals may enhance dissolution rates (Drees *et al.,* 1989). Hence there are conflicting processes affecting the precipitation/dissolution of silica minerals that may be occurring in these waters, and which suggest that the prediction of supersaturated conditions for quartz, chalcedony and cristobalite by MINTEQA2 does not necessarily indicate that net precipitation

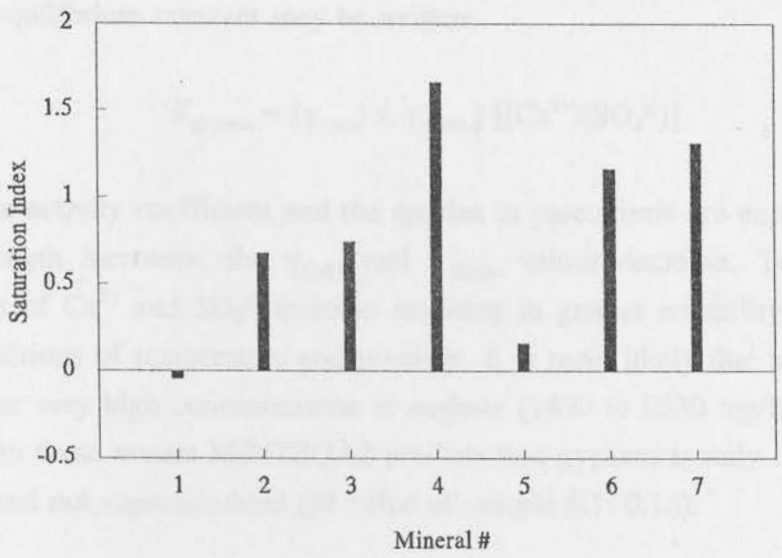

Figure 4.3 Plot of saturation indices for selected minerals possibly occuring in the Kynoch Fertilizer Evaporation Pond sample K1. SI values between -0.5 and 0.5 indicate equilibrium; positive values >0.5 indicate supsersaturation; negative values <-0.5 indicate undersaturation. Minerals are: #1 Anhydrite; #2 Chalcedony, #3 Cristobalite; #4 Fluorite; #5 Gypsum; #6 Quartz; #7 $MnH(PO_4)$. Numerical values for the saturation indices of the above minerals are tabulated in Appendix D:Table D1.

of these minerals is occurring. Quartz in particular is also kinetically unreactive at low temperatures and rarely precipitates or dissolves at a significant rate (Drever, 1988).

MINTEQA2 also predicted that gypsum, fluorite and $MnH(PO_4)$ are saturated to supersaturated (SI values of sample K1 are 0.16, 1.66, and 1.31, respectively) with anhydrite being close to equilibrium (SI value of sample K1: -0.05). Gypsum and anhydrite (anhydrous gypsum) are calcium sulphate minerals and fluorite is a calcium fluoride mineral. Gypsum is the most common form of $CaSO_4$ in soils being approximately 100 times less soluble than most other sulphate minerals found in soils and is most likely the predominant Ca^{2+} and SO_4^{2-} controlling solid phase. The formation of anhydrite is kinetically unfavourable under conditions at the earth's surface and consequently any anhydrite formed is soon hydrated to form gypsum. The high salt content of these waters may be expected to have a marked effect on the solubility of these minerals as salinity increases mineral solubilities. This is known as the *ionic strength effect* because the increased solubility is caused by decreases in activity coefficients as a result of increased ionic strength (Freeze and Cherry, 1979). In the case of

gypsum, the equilibrium constant may be written:

$$K_{gypsum} = [\gamma_{Ca2+} \times \gamma_{SO42-}] [(Ca^{2+})(SO_4^{2-})]$$

where γ is the activity coefficient and the species in parenthesis are expressed in molality. As ionic strength increases, the γ_{Ca2+} and γ_{SO42-} values decrease. To compensate, the concentrations of Ca^{2+} and SO_4^{2-} increase resulting in greater solubility of gypsum at the specified conditions of temperature and pressure. It is most likely due to this phenomenon that despite the very high concentrations of suphate (1400 to 3530 mg/l) and calcium (468 to 589 mg/l) in these waters MINTEQA2 predicts that gypsum is only in equilibrium with these waters and not supersaturated (SI value of sample K1: 0.16).

MINTEQA2 predicted that fluorite is considerably more supersaturated than gypsum, as would be expected given that the solubility of fluorite is significantly less than that of gypsum (the equilibrium constant for fluorite is $10^{-9.8}$ versus $10^{-4.5}$ for gypsum) (Freeze and Cherry, 1979). Lindsay (1979) constructed a unified solubility diagram of the various Ca, Al and Fe phosphates present in soils that includes fluorite. Plotting the log $H_2PO_4^-$ values determined by MINTEQA2 on the unified solubility diagram of Lindsay (1979), however, shows that, except for sample K2, the waters are undersaturated with respect to the fluorapatite-fluorite system (Figure 4.4). This may be due to the fact that Ca^{2+} and F^- activities are strongly affected, if not controlled, by gypsum solubility and complexation with Al^{3+}, respectively.

The lack of any Eh values prohibited the accurate determination of the oxidation state of several of the elements. For the purposes of modelling the speciation and mineral solubility equilibria using MINTEQA2, it was assumed that all Mn was in the Mn^{2+} state. As a consequence, one cannot attach very much significance to the model's prediction of the supersaturation of $MnH(PO_4)$ without first confirming whether manganese is in fact present in the Mn^{2+} state.

4.3.1.3 Water Quality Assessment

The quality of the fertilizer ponds and Triomf Main Drain water will be assessed in terms of the Draft South African Water Quality Guidelines for Industrial Use (Department of Water Affairs and Forestry, 1995). Because this water represents wastewater from the manufacture of phosphate fertilizers it is undoubtedly unsuitable for domestic use, livestock watering or irrigation. The only potential use may lie in the industrial sector, and it is the purpose of this

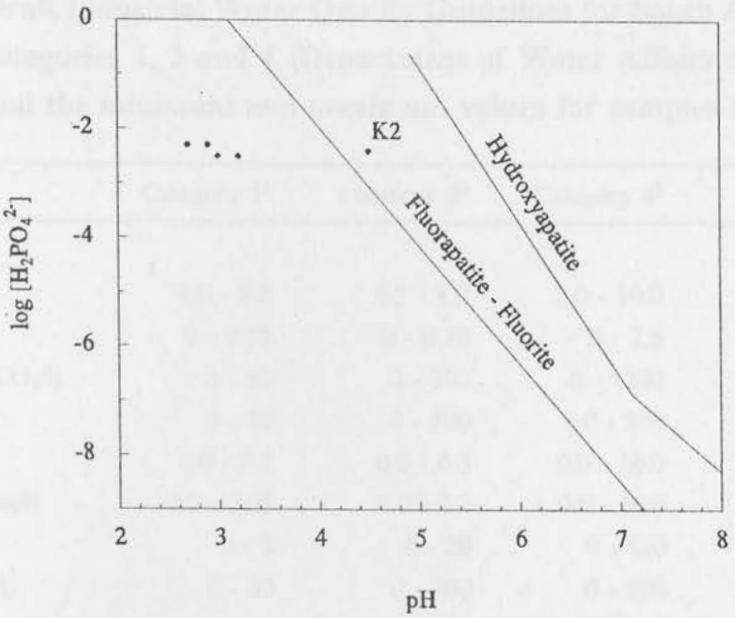

Figure 4.4 A solubility diagram for hydroxyapatite and fluorapatite - fluorite (after Lindsay, 1979) showing the positions of the fertilizer evaporation pond and Triomf Main Drain samples.

assessment, therefore, to determine whether this water meets the industrial water use requirements. The Draft South African Water Quality Quidelines for Industrial Use divide the water quality standards into four catgories, with category 1 being standards for industries requiring a high quality of water and category 4 being industries that can make use of very poor quality water. The standards for categories 1, 3 and 4 are tabulated in Table 4.3, together with the minimum and maximum values for the five water samples.

The low pH (<4.5) and high EC values (>6.3 mS/cm) of this water immediately excludes it for use even by category 4 industries. The sulphate and chloride concentrations also exceed all four category standards. In the case of sulphate, the sulphate concentrations in this water are an order of magnitude greater than the category 4 standard. The silica, manganese and iron concentrations exceed catergory 1 - 3 standards but are, however, within the category 4 standards.

In summary, these wastewaters are highly contaminated and are unsuitable in terms of a number of components for any industrial use.

Table 4.3 Draft Industrial Water Quality Guidelines for South Africa for industrial categories 1, 3 and 4 (Department of Water Affairs and Forestry, 1995) and the minimum and maximum values for samples K1 to K5.

Sample No.	Category 1[1]	Category 3[2]	Category 4[3]	K1 - K5[4]
pH	7.0 - 8.0	6.5 - 8.0	5.0 - 10.0	2.7 - 4.5
EC (mS/cm)	0 - 0.15	0 - 0.70	0 - 2.5	6.3 - 11.7
Alkalinity (mg $CaCO_3$/l)	0 - 50	0 - 300	0 - 1200	-
Chloride (mg Cl/l)	0 - 20	0 - 100	0 - 500	561 - 1030
Iron (mg Fe/l)	0.0 - 0.1	0.0 - 0.3	0.0 - 10.0	0.14 - 3.55
Manganese (mg Mn/l)	0.0 - 0.05	0.0 - 0.2	0.0 - 10.0	1.66 - 4.20
Silica (mg Si/l)	0 - 5	0 - 20	0 - 150	19.2 - 60.34
Sulphate (mg SO_4/l)	0 - 30	0 - 200	0 - 500	1400 - 3530

Footnotes:
1 - category 1 industries are those that require a high quality water with relatively tight to stringent specifications of limits for most of the relevant water quality constituents.
2 - category 3 industries are those industries for which domestic water quality is the baseline minimum.
3 - category 4 industries are those that can use water of more or less any quality.
4 - minimum and maximum values for samples K1 to K5

4.3.2 Sediment

Forstner and Wittman (1979) list the following heavy metals as being used in the fertilizer industry: Cd, Cu, Fe, Hg, Mn, Pb, Ni and Zn. A sediment sample was thus collected from the Triomf Main Drain, the main effluent outlet for Kynoch Fertlizer Limited, to determine if these metals are being released by the factory and to assess the degree of heavy metal contamination of the sediment.

The results of the analyses carried out on the sediment are shown in Tables 4.4 and 4.5. The saturated paste extracts of the sediment were found to be very similar in chemistry and water quality to that of the water samples discussed in section 4.3.1, and will therefore not be discussed further.

The drain sediment was found to be acid with a pH of 3.5 (in water) and 3.4 (in $CaCl_2$). Sediment pH is the dominant factor controlling the chemical behaviour of metals, and the acidity of the sediment is particularly important as heavy metal ions are most mobile under acid conditions. In addition to pH, organic matter content and clay content play an important role in determining the mobility of heavy metals. Clay minerals and organic matter contribute

Table 4.4 Analysis of sediment sample K6 collected in the Triomf Main Drain located adjacent to the Kynoch Fertilizer Limited evaporation ponds.

pH (water)	3.5		
pH ($CaCl_2$)	3.4		
Organic C	11.8%		
	SATURATED PASTE EXTRACT		
pH	3.3		
EC (mS/cm)	8.0		
Acidity (mmol/l)	33.2		
Cations (mg/l)		**Anions (mg/l)**	
Na^+	406	Cl^-	825
Ca^{2+}	836	SO_4^{2-}	770
Mg^{2+}	456	$^1PO_4^{3-}$	386
K^+	441	NO_3^-	247
NH_4^+	489	$^2F^-$	50.1

Footnotes: 1 - phosphate determined by Murphy and Riley Method (1962)
2 - fluoride determined by ion selective electrode
BDL - below detection limits

to the cation exchange capacity (CEC) of the sediment, and hence the ability of the sediment to 'retain' various heavy metals. Although clay content of the sediment was not determined, organic carbon was determined using the Walkley-Black Method (Walkley, 1935). For sediments, the organic matter content may be estimated from the organic carbon values by multiplying by a factor of 1.6 (Alloway, 1995).

The organic carbon content of the sediment was found to be 11.8% and hence the organic matter content may be estimated to be approximately 19%. The sediment thus contains a large proportion of organic matter (approximately 1/5 of the total sediment). In addition to being involved in cation exchange capacity reactions, solid-phase humic substances such as humic acids also adsorb metals by forming chelate complexes (Alloway, 1995). It may be anticipated, therefore, that this sediment has the capacity to complex a significant proportion of any heavy metals that are released in the Kynoch effluent stream.

The bulk sediment XRFS analyses, listed in Table 4.5, reveal that as far as major element

Table 4.5 **Major and trace element concentrations in sediment sample K6 collected in the Triomf Main Drain located adjacent to the Kynoch Fertilizer Limited evaporation ponds (by XRFS using powder briquettes).**

Major Element Concentrations (%) (expressed as oxides)		Trace Element Concentrations (ppm)	
Na_2O	0.31	Zn	247
CaO	14.83	Cu	524
MgO	1.17	Ni	9.8
K_2O	1.42	Co	4.5
P_2O_5	17.49	Mn	45
BaO	0.04	Cr	82
[1]Fe_2O_3	14.63	V	47
Al_2O_3	2.79	Mo	20
TiO_2	0.19	Nb	2.5
SiO_2	11.54	Zr	39
SO_4^{2-}	17.30	Y	12
Cl	0.21	Sr	497
[2]Organic matter	19.0	U	BDL
		Rb	139
TOTAL	100.92	Th	6.0
		Pb	865

Footnotes: 1 - total Fe expressed as Fe_2O_3
2 - calculated as % organic carbon times 1.6
BDL - below detection limits

analysis is concerned the sediment is composed predominantly of the elements Ca, P, S, Fe and Si, with Na, Mg, K, Ba, Al, and Ti making up less than 6%. The trace element data indicates that a number of heavy metals are enriched in this sediment, however, some form of standard or reference concentrations are required to assess this data. To this end, the concentrations of selected heavy metals in three materials and the sediment have been tabulated in Table 4.6 for comparison with the sediment. The materials chosen are a shale standard (from Forstner and Wittmann, 1979), average concentrations of metals in 87 recent lake sediments (from Forstner and Wittmann, 1979) and the average concentrations of metals in phosphate fertilizers (Alloway, 1995). The shale standard was chosen as the site is underlain by argillaceous shales.

Comparison of the sediment metal concentrations with those of the three reference materials

Table 4.6 Heavy Metal Concentrations in Selected Materials (in ppm)

Metal	Shales[1]	Recent lake sediments[2]	Phosphate fertilizers[3]	Sediment (K6)
Zn	95	118	50 - 1450	247
Cu	45	45	1 - 300	524
Ni	68	66	7 - 38	9.8
Co	19	16	1 - 12	4.5
Mn	850	760	40 - 2000	45
Cr	90	62	66 - 245	82
V	-	-	2 - 1600	47
Mo	-	-	0.1 - 60	20
Sr	300	151	-	497
Pb	20	34	7 - 225	865

Footnotes:
1 - from Forstner and Wittmann (1979), pg 136
2 - from Forstner and Wittmann (1979), pg 136
3 - from Alloway (1995),pg 45.

shows that Pb, Zn, Cu and Sr are notably high, exceeding both the shale standard and the lake sediment values. The Cr concentration in the sediment is comparable to that of the shale standard and lake sediments and the Ni, Co and Mn concentrations are significantly lower than those of the two reference standards. Comparing the Pb, Zn and Cu concentrations to those of the phosphate fertilizer, shows that although the Zn value falls well within the range found in phosphate fertilizers, the Pb and Cu values exceed phosphate fertilizer concentrations by 640 ppm and 224 ppm, respectively, indicating that a significant amount of Pb and Cu accumulation has occurred in the sediment.

On the basis of the above comaprison, the sediment may be described as high in Pb, Zn, Cu and Sr, with Pb, Cu and Sr contamination being the most prominent. Given the high PO_4^{3-} concentrations in the drain water, the Pb may well be in the form of insoluble lead phosphate precipitates. Alloway (1995) states that chloropyromorphite ($Pb_5(PO_5)_3Cl$) is the most insoluble of the lead phosphate minerals and is thus the most likely to control the solubility of Pb^{2+}.

Copper on the other hand is most likely to occur either in the adsorbed form or complexed with organic matter (Alloway, 1995).

4.3.3 Fertilizer Evaporation Pond Precipitate

The X-ray diffractogram of a sample of precipitate from the fertilizer evaporation ponds (Ppt1 - refer Figure 3.2) is shown in Figure 4.5. Despite the prediction by MINTEQA2 of the supersaturation of minerals such as gypsum, anhydrite, fluorite, quartz, and cristobalite in the fertilizer pond water, only gypsum is detected in the precipitate. This may be because the lower limit of detection of these minerals is relatively high and hence, although present in the precipitate, they are not detectable or it may be because these minerals are in fact not present. If the latter is true, then this would illustrate that predictions of mineral solubility equilibria based on thermochemical data alone cannot necessarily be used to make inferences concerning the precipitation or dissolution of minerals without also taking kinetic considerations into account.

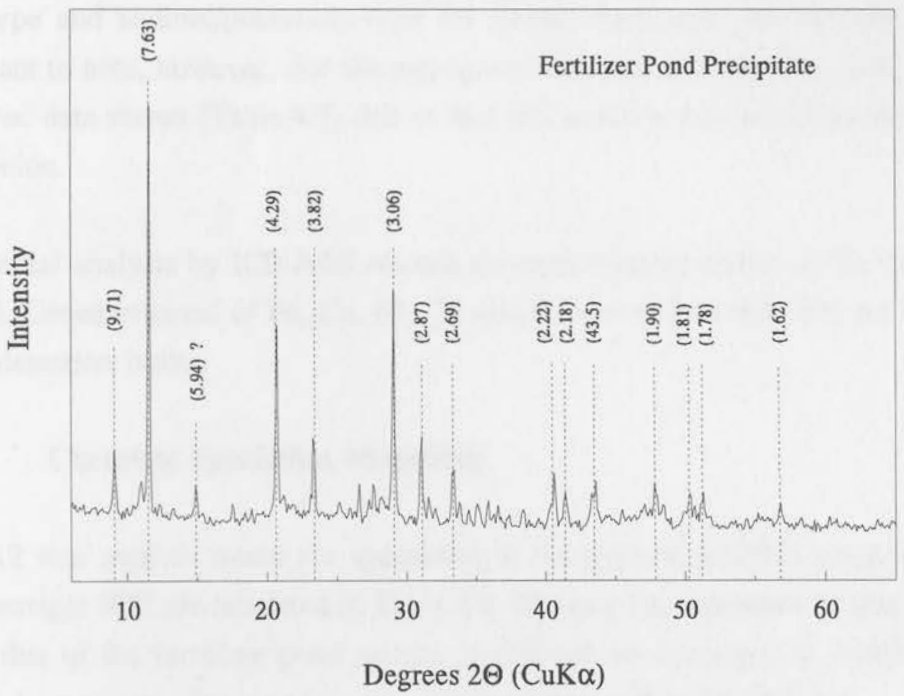

Figure 4.5 XRD plot of intensity versus degrees 2θ for the fertilizer pond precipitate sample Ppt1. Labelled peaks are those of gypsum (except for the peak labelled with a question mark which could not be identified) with the values in parentheses in Å units.

4.4 Results and Discussion of the Gypsum Waste Dumps

4.4.1 Water analyses

The results of the water sample analysis from the gypsum leachate collection pond located south of the gypsum dumps are tabulated in Table 4.7. Similar to the fertilizer pond waters, this water is characterised by very high salinity (9.8 mS/cm), low pH (3.9) and high acidity (20.7 mol/l). The TDS of this water is approximately 6.5 $g.dm^{-3}$.

The cations Na^+, Ca^{2+}, Mg^{2+}, K^+ and NH_4^+ are all present in this water, with NH_4^+ being the most abundant cation and Na^+ and Mg^{2+} the least. Similar to the fertilizer pond waters the anionic suite is dominated by SO_4^{2-} and NO_3^-. The NO_3^- anion is, however, almost double the concentration of the SO_4^{2-} anion. The major cations and anions have been plotted on a pipergram (Figure 4.6) to show that this water falls in the same hydrochemical facies as the fertilizer pond waters, ie. sulphate dominant in the anions and borderline between 'no dominant type' and 'sodium/potassium type' for cations. Particularly in the case of this water it is important to note, however, that the pipergram does not include NH_4^+, PO_4^{3-}, NO_3^- or F^-. The tabulated data shows (Table 4.7) that in fact this water is dominated by the NH_4^+ cation and NO_3^- anion.

Total elemental analysis by ICP-AES reveals elevated concentrations of the metals Al, Zn, Mn, and Si. Concentrations of Fe, Cu, Ni, Cd and Co are all low with Pb, As and Cr being below the detection limits.

4.4.1.1 Chemical Speciation Modelling

MINTEQA2 was used to model the speciation in the gypsum leachate pond water and the results for sample SD5 are tabulated in Table 4.8. Because the speciation of this water is very similar to that of the fertilizer pond waters, it will not be discussed in detail. Instead, the differences in speciation between the two water groups will be highlighted.

4.4.1.1.1 Charge Balance

The charge balance prior to speciation was 7.2% indicating an excess of cations. Subsequent to speciation the charge determined by MINTEQA2 was 1.3%. This suggests that one or more of the free ion cations are in fact present as anionic complexes.

Table 4.7 Analysis of water sample SD5 from the Gypsum leachate collection pond.

pH	3.9		
EC (mS/cm)	9.8		
Acidity (mmol/l)	20.7		
Cations (mg/l)		**Anions (mg/l)**	
Na^+	300	Cl^-	844
Ca^{2+}	671	SO_4^{2-}	1936
Mg^{2+}	239	$^1PO_4^{3-}$	408
K^+	691	NO_3^-	2673
NH_4^+	860	$^2F^-$	49.1
Total Elemental Concentrations (mg/l)			
Si	18.60	Zn	1.94
Al	90.8	Cd	0.10
Fe	0.24	As	BDL
Cu	0.57	Co	0.17
Ni	0.43	Mn	2.09
Pb	BDL	Cr	BDL

Footnotes: 1 - phosphate determined by Murphy and Riley Method (1962)
2 - fluoride determined by ion selective electrode
BDL - below detection limits

4.4.1.1.2 Calcium and Magnesium

Although the species of calcium and magnesium formed in the gypsum water sample are identical to those predicted for the fertilizer pond waters, the proportion of free ions to sulphate complexes is slightly different. Whereas approximately 70% of Ca and Mg occurred as the free ions Ca^{2+} and Mg^{2+} in the fertilizer pond waters, this percentage was approximately 80% in the gypsum pond water. Consequently, the proprotions of $CaSO_4(aq)$ and $MgSO_4(aq)$ species in the gypsum pond water are also less, being 18.8% and 16.7%, respectively.

4.4.1.1.3 Sulphate

Sulphate speciation in the gypsum pond water deviates slightly from that of the fertilizer ponds in that the species HSO_4^- does not occur. Instead the species $AlSO_4^+$ is predicted, representing 1.5% of total suphate.

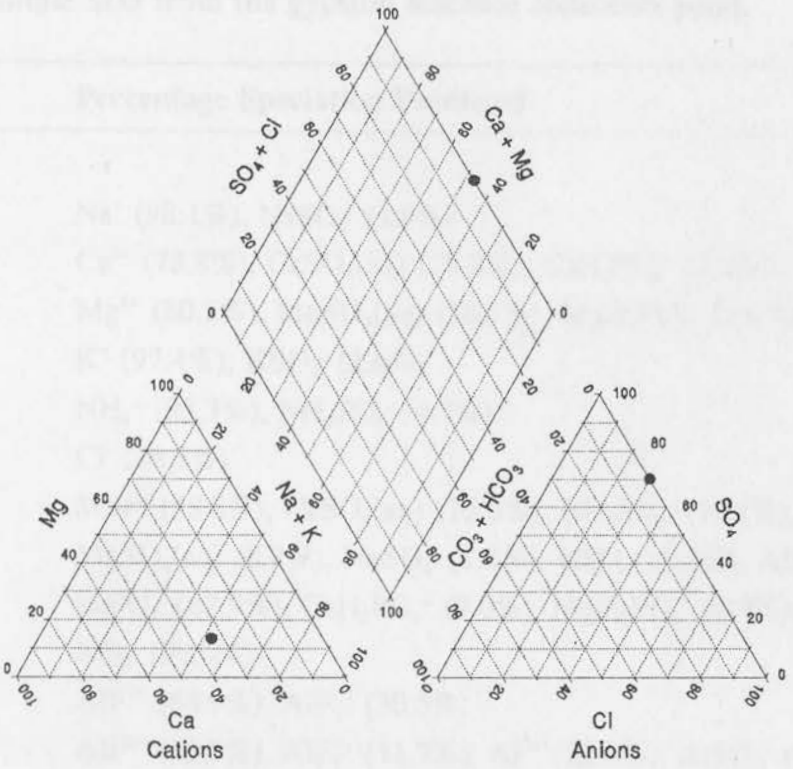

Figure 4.6 Pipergram representing the composition of water sample SD5 from the gypsum leachate collection pond.

4.4.1.1.4 Fluoride and Aluminium

The speciation of F and Al in the gypsum pond water is quite different from that of the fertilizer ponds. Fluoride is predicted to occur in only two species in the gypsum pond water, namely AlF^{2+} (68.9%) and AlF_2^+ (30.5%), whereas in the fertilizer ponds AlF_3(aq) (38.9%) and SiF_6^{2-} (25.5%) represents the dominant species, with AlF_4^- (14.7%), AlF_2^+ (4.8%), MgF^+ (1.4%), F^- (4.6%) and HF(aq) (9.7%) making up the remainder. The speciation of F in the gypsum pond water would thus appear to be much simpler.

In contrast, the Al speciation in the gypsum pond is much more complex than that of the fertilizer ponds. First and foremost, 22.7% of the Al in the gypsum pond is predicted to be in the form of free Al^{3+} ions whereas no free Al^{3+} ions occur in the fertilizer ponds. This is of particular environmental importance due to the bioavailability of Al when in the Al^{3+} form. The mineral solubility controls on the equilibrium aqueous concentrations of this ion are

Table 4.8 Chemical species predicted by MINTEQA2 as likely to be present in sample SD5 from the gypsum leachate collection pond.

Constituent	Percentage Speciation Predicted
Na	Na^+ (98.1%), $NaSO_4^-$ (1.9%)
Ca	Ca^{2+} (78.8%), $CaSO_4$(aq) (18.8%), $CaH_2PO_4^+$ (2.3%)
Mg	Mg^{2+} (80.2%), $MgSO_4$(aq) (16.7%), $MgH_2PO_4^+$ (3.0%)
K	K^+ (97.4%), KSO_4^- (2.6%)
NH_4	NH_4^+ (95.3%), $NH_4SO_4^-$ (4.7%)
Cl	Cl^- (98.9%)
SO_4	$SO4^{2-}$ (58.8%), $CaSO_4$(aq) (15.6%), $NH_4SO_4^-$ (11.1%), $MgSO_4$(aq) (8.2%), $NaSO_4^-$ (1.2%), KSO_4^- (2.3%), $AlSO_4^+$ (1.5%)
PO_4	$H_2PO_4^-$ (82.9%), $CaH_2PO_4^+$ (9.0%), $MgH_2PO_4^+$ (6.8%), H_3PO_4 (1.1%)
NO_3	NO_3^- (99.0%)
F	AlF^{2+} (68.9%), AlF_2^+ (30.5%)
Al	AlF^{2+} (52.9%), AlF_2^+ (11.7%), Al^{3+} (22.8%), $AlSO_4^+$ (9.2%), $Al(SO_4)_2^-$ (2.8%)
Fe	Fe^{2+} (56.1%), $FeH_2PO_4^+$ (32.2%), $FeSO_4$(aq) (11.7%)
Cu	Cu^{2+} (71%), $CuSO_4$(aq) (26%), $CuCl^+$ (1.3%)
Ni	Ni^{2+} (80.1%), $NiSO_4$(aq) (18.3%), $NiCl^+$ (1.5%)
Zn	Zn^{2+} (75.6%), $ZnSO_4$(aq) (20.8%), $ZnCl^+$ (1.6%), $Zn(SO_4)_2^{2-}$ (2.1%)
Cd	Cd^{2+} (45.7%), $CdCl^+$ (33.4%), $CdSO_4$(aq) (15.4%), $Cd(SO_4)_2^{2-}$ (2.1%) $CdCl_2$(aq) (1.8%), $CdNO_3^+$ (1.6%)
Cr	Cr^{2+} (100.0%)
Mn	Mn^{2+} (80.3%), $MnSO_4$(aq) (17.1%), $MnCl^+$ (2.5%)
H_2O	$AlOH^{2+}$ (95.0%), $Al(OH)_2^+$ (5.0%)
H	$H_2PO_4^-$ (80.5%), $CaH_2PO_4^+$ (8.7%), $MgH_2PO_4^+$ (6.7%), H^+ (1.9%), H_3PO_4 (1.5%)

discussed in more detail in section 4.4.1.2 on mineral solubility equilibria.

Aluminium sulphate species are also predicted in the gypsum ponds which are not predicted in the fertilizer ponds. These are $AlSO_4^+$ (9.2%) and $Al(SO_4)_2^-$ (2.8%). The remaining aluminium fluoride species are common to both waters.

4.4.1.1.5 Iron, Nickel, Zinc and Manganese

The species of Fe, Ni, Zn and Mn in the two waters is predicted to be the same. The proportions of the various species is slightly different, however, with the percentage of each metal occurring in the free ion form being approximately 10% greater in the gypsum pond water.

4.4.1.1.6 Cadmium

The speciation of cadmium follows the same trend as that of the metals described above, with the added difference that the species $CdNO_3^+$ (1.6%) is also predicted to occur in the gypsum pond water.

4.4.1.2 Mineral Solubility Equilibria

The saturation indices calculated by MINTEQA2 for various minerals possibly occurring in the gypsum leachate pond are illustrated graphically in Figure 4.7 (the numerical results are tabulated in Appendix D: Table D2).

As is the case for the fertilizer evaporation ponds, three forms of silica (quartz, cristobalite and chalcedony), gypsum and $MnH(PO_4)$ are predicted to be supersaturated and anhydrite is very close to equilibrium. The saturation indices for these minerals in the gypsum pond water are very similar to those of the fertilizer pond water and hence no further discussion of these mineral solubility predictions is necessary. The solubility of fluorite in the gypsum pond water is of interest, however, due to the fact that it is strongly undersaturated whereas in the fertilizer pond water it is supersaturated. The reason for this is most probably due to the differences in speciation of F and Al in the two waters that were discussion in section 4.5.1.1.4. In the fertilizer pond water 4.6% of F is predicted to occur as the free ion F^-, however, in the gypsum pond water all the F occurs in complexation with aluminium as the species AlF^{2+} and AlF_2^+. Hence there is no free ionic F available to form an insoluble CaF_2 precipitate in the gypsum pond water and fluorite remains undersaturated.

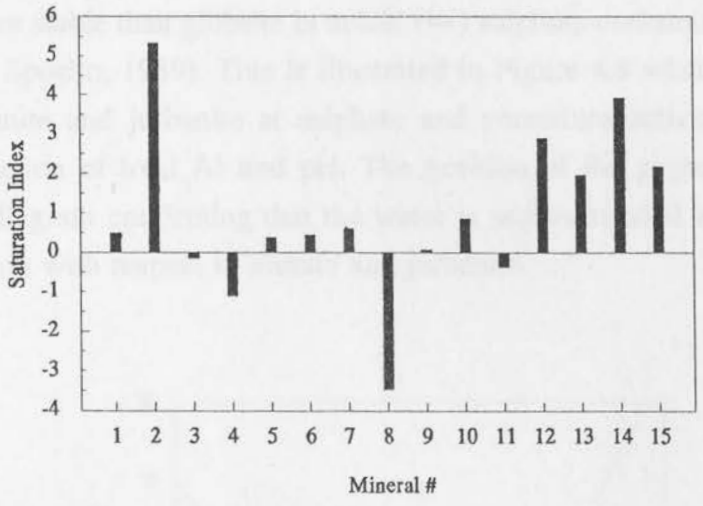

Figure 4.7 Plot of saturation indices for selected minerals possibly occurring in the gypsum leachate pond. Positive values indicate supsersaturation; negative values indicate undersaturation. Minerals are: #1 $AlOH(SO_4)$; #2 Alunite; #3 Anhydrite; #4 Boehmite; #5 Chalcedony, #6 Cristobalite; #7 Diaspore; #8 Fluorite; #9 Gypsum; #10 Quartz; #11 Halloysite; #12 Kaolinite; #13 Muscovite; #14 Pyrophyllite; #15 $MnH(PO_4)$. Numerical values for the saturation indices of the above minerals are tabulated in Appendix D:Table D2.

In addition to the above minerals, MINTEQA2 also predicted the saturation and supersaturation of a variety of Al-containing minerals, namely:

(i) the aluminium hydroxides diaspore (AlO(OH)) and boehmite (AlO(OH)),

(ii) the aluminium sulphates alunite ($KAl_3(SO_4)_2(OH)_6$) and jurbanite (anhydrous) ($Al(SO_4)(OH)$),

(iii) the aluminosilicates kaolinite ($Al_4(Si_4O_{10})(OH)_8$), halloysite ($Al_4(Si_4O_{10})(OH)_8$) muscovite ($KAl_2(AlSi_3O_{10})(OH,F)_2$), and pyrophyllite ($Al_2(Si_4O_{10})(OH)_2$).

Of these minerals, alunite is calculated to be the most supersaturated (SI value of 5.327). This result is in accordance with studies of pore water of phosphogypsum treated soils (Luther and Dudas, 1993; Alva *et al.,* 1990; O'Brien and Sumner, 1988). Pyrophyllite and kaolinite are predicted to be the next most supersaturated minerals after alunite. The supersturation of these minerals is most likely due to the high concentration of Al in this water (90.8 mg/l) coupled with the high acidity and thus presence of Al in the Al^{3+} form.

Gibbsite may have been expected to be supersaturated in this water. However, alunite and jurbanite are more stable than gibbsite in acidic (<4) sulphate-containing waters (>10^{-3} mol/l) (Lindsay, 1979; Sposito, 1989). This is illustrated in Figure 4.8 where the solubility curves for gibbsite, alunite and jurbanite at sulphate and potassium activities of 10^{-4} have been plotted as a function of total Al and pH. The position of the gypsum pond water is also plotted on this diagram confirming that the water is undersaturated with respect to gibbsite and in equilibrium with respect to alunite and jurbanite.

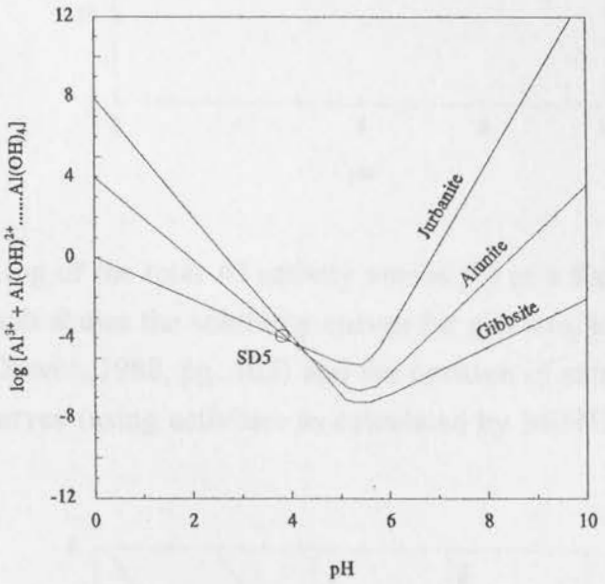

Figure 4.8 A solubility diagram for gibbsite, alunite and jurbanite, at sulphate and potassium activities of 10^{-4} (from Drever, 1988, pg. 220), showing the position of the gypsum leachate pond sample (SD5).

The behaviour of aluminium makes it impossible to present the solubility of aluminum silicates in a simple way. In principle a three-dimensional diagram is needed with aluminium concentration, silica activity and pH as axes. Instead, two different stability diagrams have been plotted in Figure 4.9. Figure 4.9a is plotted at a fixed silica activity of 10^{-3} (which was the order of magnitude for silica activity predicted by MINTEQA2) and shows the solubilities of gibbsite, kolinite and pyrophyllite as a function of total Al and pH. An alternative approach is to assume that aluminium is retained entirely in solid phases and to write reactions between minerals on this basis (Drever, 1988). This approach has been used for the construction of Figure 4.9b, where the stability relationships among selected minerals in the system K_2O - Al_2O_3 - SiO_2 - H_2O (at 25°C) are depicted.

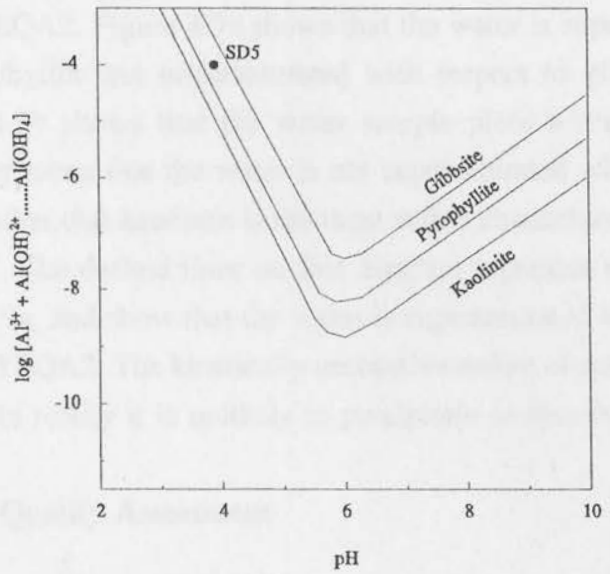

Figure 4.9a Plot of log of the total Al activity versus pH at a fixed silica activity of 10^{-3}. The graph shows the solubility curves for gibbsite, kaolinite and pyrophyllite (from Drever, 1988, pg. 105) and the position of sample SD5 with respect to these curves (using activities as calculated by MINTEQA2).

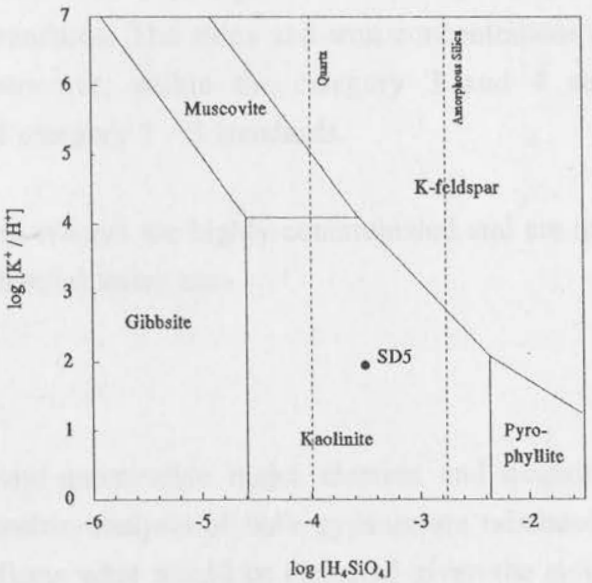

Figure 4.9b Plot of log of the ratio of the activities of K^+ over H^+ versus log of the silica activity. The stability relationships of selected minerals in the system K_2O-Al_2O_3-SiO_2-H_2O (at 25°C) are shown (from Drever, 1988, pg. 108) along with the position of sample SD5 (using activities as calculated by MINTEQA2).

The gypsum pond sample has been plotted on these two diagrams using the relevant activities as predicted by MINTEQA2. Figure 4.9a shows that the water is supersaturated with respect to kaolinite and pyrophyllite but undersaturated with respect to gibbsite, as predicted by MINTEQA2. Figure 4.9b shows that the water sample plots within the stability field of kaolinite. This does not mean that the water is not supersaturated with respect to muscovite and pyrophyllite but rather that kaolinite is the most stable aluminium silicate mineral within the system considered. The dashed lines on this diagram represent solubility lines, like the solid lines in Figure 4.9a, and show that the water is supersaturated with respect to quartz as was predicted by MINTEQA2. The kinetically unreactive nature of quartz at low temperatures means, however, that in reality it is unlikely to precipitate or dissolve at a significant rate.

4.4.1.3 Water Quality Assessment

As with the water from the fertilizer ponds and Triomf Main Drain, the gypsum pond water will be assessed in terms of the Draft South African Water Quality Quidelines for Industrial Use (Department of Water Affairs and Forestry, 1995), the aim being to assess whether this water meets the industrial water use requirements of one or more of the four categories.

The low pH (3.9) and high EC (9.8 mS/cm) of this water immediately excludes it for use even by category 4 industries. The sulphate and chloride concentrations in this water also exceed all category standards. The silica and iron concentrations exceed catergory 1 and 2 standards but are, however, within the category 3 and 4 standards. The manganese concentrations exceed category 1 - 3 standards.

In summary, these wastewaters are highly contaminated and are unacceptable for any of the four categories of industrial water use.

4.4.2 Gypsum

The results of the semi-quantitative major element and quantitative trace element x-ray fluorescence spectrometric analysis of bulk gypsum are tabulated in Table 4.9. The major element analysis confirms what would be expected given the stoichiometric composition of gypsum. That is to say, the sample is largely CaO and SO_4^{2-} (approx. 86%) with SiO_2, P_2O_5 and Al_2O_3 as minor components.

The trace element analysis shows that the majority of the elements analysed for occur either in low concentrations or are below the detection limits. The concentrations of Zn, Cu and Pb

Table 4.9 Major and trace element concentrations in gypsum sample PG1 collected from the gypsum dumps on the Kynoch Fertilizer Limited site (by XRFS using powder briquettes).

Major Element Concentrations (%) (expressed as oxides)		Trace Element Concentrations (ppm)	
Na_2O	0.02	Zn	1.88
CaO	39.46	Cu	8.14
MgO	0.01	Ni	BDL
K_2O	0.01	Co	BDL
P_2O_5	0.45	Mn	BDL
BaO	0.03	Cr	33.9
$^1Fe_2O_3$	0.07	V	BDL
Al_2O_3	0.19	Mo	BDL
TiO_2	0.01	Nb	BDL
SiO_2	0.41	Zr	36.1
SO_4^{2-}	47.01	Y	54.4
Cl	0.01	Sr	2508
		U	BDL
TOTAL	87.66	Rb	BDL
		Th	19.7
		Pb	14.4

Footnotes: 1 - total Fe expressed as Fe_2O_3
BDL - below detection limits

may be compared with those of phosphate fertilizer tabulated in Table 4.6 illustrating that these metals do indeed occur in low concentrations. The only notably high concentration is that of Sr. This is usually the case in gypsum waste, however, as phosphate rock (the primary material used in the manufacture of phosphate fertilizers) typically consists of apatite, a calcium phosphate mineral in which Sr commonly substitutes for Ca^{2+}. The strontium is concentrated into the waste stream during the manufacture of phosphate fertilizer and ultimately ends up in the solid gypsum waste.

4.5 Results and Discussion of the Sulphur Stockpile

4.5.1 Water Analyses

The results of the water sample analysis from the sulphur leachate collection drain located to the south of the sulphur stockpile area are tabulated in Table 4.10. This water is extremely acidic with a pH of 1.5 and acidity of 328 mmol/l, and is also highly saline (EC 20.7 mS/cm). Although acidic leachate may evolve over time from the oxidation of elemental sulphur, rhombic sulphur, as is found on the AECI stockpile, is one of the least active non-metals, being stable at room temperature. The marked acidicty of this water is most likely to have been caused, therefore, by the fire which occurred on the stockpile at end of December 1995. During the fire, elemental sulphur would have reacted with oxygen in the air to form sulphur dioxide according to the reaction:

$$S + O_2 \rightarrow SO_2$$

The spraying of water on the burning stockpile created an ideal environment for the sulphur dioxide to dissolve in water to form sulphurous acid which, when exposed to air, would have oxidised to sulphuric acid:

$$SO_2 + H_2O \rightarrow H_2SO_3$$

$$2H_2SO_3 + O_2 \rightarrow 2H_2SO_4$$

The acidity of this water is thus most probably due to the presence of sulphurous and sulpuric acid.

The proportions of major anions and cations occurring in this water are shown plotted on a pipergram in Figure 4.10. Because this water contains no detectable NH_4^+ and low PO_4^{3-}, NO_3^- and F^- (in comparison to the other anion concentrations) the pipergram may be considered to be an accurate and useful representation of the composition of this water. As would be expected, this water is dominated by SO_4^{2-} in the anion suite, with the SO_4^{2-} concentration two orders of magnitude greater than that of Cl^-. The cations are dominated by Na^+ with Ca^{2+} being the next most significant cation. This water may thus be characterised as falling within the hydrochemical facies 'sulphate/sodium dominant type'.

Table 4.10 Analysis of water sample SD2 from the sulphur stockpile leachate collection drain.

pH	1.5		
EC (mS/cm)	20.7		
Acidity (mmol/l)	328		
Cations (mg/l)		**Anions (mg/l)**	
Na^+	1440	Cl^-	675
Ca^{2+}	824	SO_4^{2-}	13600
Mg^{2+}	437	$^1PO_4^{3-}$	1.5
K^+	130	NO_3^-	88
NH_4^+	0	$^2F^-$	0.2
Total Elemental Concentrations (mg/l)			
Si	49.1	Zn	1.94
Al	845	Cd	0.35
Fe	423	As	1.68
Cu	1.90	Co	1.02
Ni	1.74	Mn	18.1
Pb	BDL	Cr	1.08

Footnotes:
1 - phosphate determined by Murphy and Riley Method (1962)
2 - fluoride determined by ion selective electrode
BDL - below detection limits

Because the water is extremely acidic it could be anticipated that the concentrations of heavy metals would be elevated due to the mobilization of any metals occuring within the surrounding soils. The total element ICP-AES analyses confirm that this is the case, with the concentrations of Al and Fe being extremely high and those of Mn and As also being notably high.

4.5.1.1 Chemical Speciation Modelling

MINTEQA2 was used to model the speciation in this water and the results are tabulated in Table 4.11.

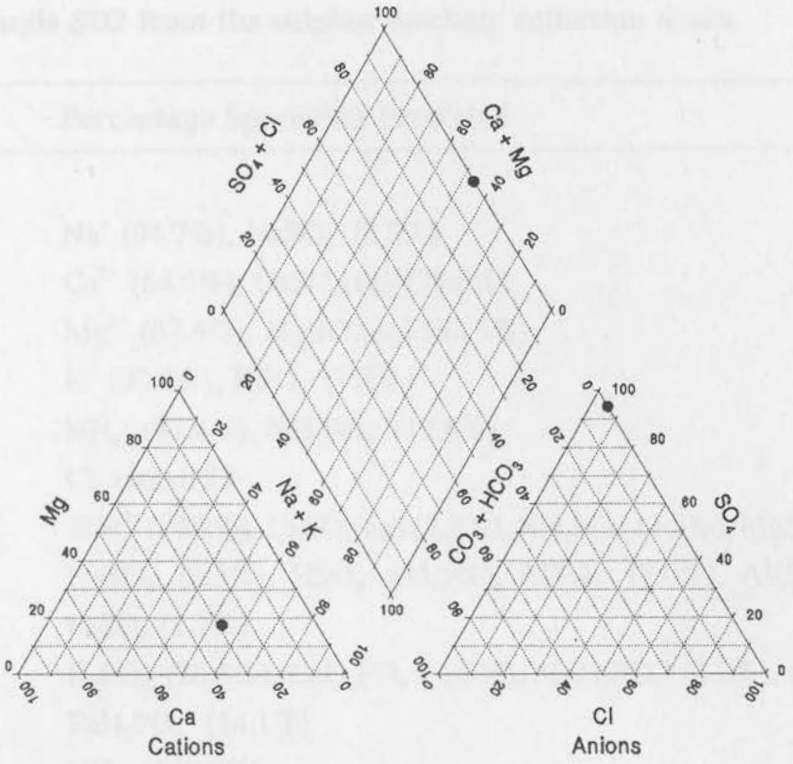

Figure 4.10 Pipergram representing the composition of water sample SD2 from the sulphur leachate collection drain.

4.5.1.1.1 Charge Balance

The charge balance of this water prior and subsequent to speciation by MINTEQA2 is similar at approximately 1.7%.

4.5.1.1.2 Sodium, Calcium, Magnesium, Potassium and Ammonium

These ions are predicted to occur either as free ions or in complexation with sulphate. Approximately 90 - 95% of Na, K and NH_4 is in the form of free monovalent ions with the remainder as anionic sulphate complexes. A lesser percentage of Ca and Mg occur as free ions (64 - 67%) due to the fact that these ions are divalent and thus form strong bonds with the divalent sulphate anion.

Table 4.11 Chemical species predicted by MINTEQA2 as likely to be present in sample SD2 from the sulphur leachate collection drain.

Constituent	Percentage Speciation Predicted
Na	Na^+ (94.7%), $NaSO_4^-$ (5.3%)
Ca	Ca^{2+} (64.4%), $CaSO_4$(aq) (35.6%)
Mg	Mg^{2+} (67.4%), $MgSO_4$(aq) (32.5%)
K	K^+ (92.7%), KSO_4^- (7.3%)
NH_4	NH_4^+ (87.4%), $NH_4SO_4^-$ (12.6%)
Cl	Cl^- (100.0%)
SO_4	$SO4^{2-}$ (29.7%), $CaSO_4$(aq) (5.2%), $NH_4SO_4^-$ (3.9%), $MgSO_4$(aq) (4.1%), $NaSO_4^-$ (2.3%), HSO_4^- (33.3%), $AlSO_4^+$ (7.0%), $Al(SO_4)_2^-$ (12.5%), $FeSO_4$ (1.7%)
PO_4	$H_2PO_4^-$ (20.8%), $CaH_2PO_4^+$ (1.9%), $MgH_2PO_4^+$ (2.2%), H_3PO_4 (61.0%), $FeH_2PO_4^+$ (14.1%)
NO_3	NO_3^- (100.0%)
F	AlF^{2+} (99.8%)%)
Al	Al^{3+} (39.8%), $AlSO_4^+$ (31.8%), $Al(SO_4)^{2-}$ (28.3%)
Fe	Fe^{2+} (67.4%), $FeSO_4$(aq) (32.5%)
Cu	Cu^{2+} (70%), $CuSO_4$(aq) (27%), $CuCl^+$ (1.3%)
Ni	Ni^{2+} (64.8%), $NiSO_4$(aq) (34.3%)
Zn	Zn^{2+} (52.9%), $ZnSO_4$(aq) (33.7%), $Zn(SO_4)_2^{2-}$ (12.7%)
Cd	Cd^{2+} (37.3%), $CdCl^+$ (18.0%), $CdSO_4$(aq) (29.2%), $Cd(SO_4)_2^{2-}$ (14.8%)
Cr	Cr^{2+} (100.0%)
Mn	Mn^{2+} (66.0%), $MnSO_4$(aq) (32.6%), $MnCl^+$ (1.3%)
As	H_3AsO_4 (78.6%), $H_2AsO_4^-$ (21.4%)
H_2O	$AlOH^{2+}$ (100.0%)
H	H^+ (47.9%), HSO_4^- (52.1%)

4.5.1.1.3 Sulphate and Phosphate

Sulphate occurs predominantly as HSO_4^- (33.3%) and as a free ion (SO_4^{2-} 29.7%) The remaining sulphate occurs in complexation with (in order of decreasing abundance): Al^{3+}, Ca^{2+}, Mg^{2+}, NH_4^+, and Na^+. This order is a result of the fact that SO_4^{2-} will form complexes with the higher charge cations in preference to those of lower charge.

Phosphate occurs mainly in the form H_3PO_4 (61.0%) and $H_2PO_4^-$ (20.8%). Some complexation with Fe^{2+}, Ca^{2+} and Mg^{2+} is also predicted.

4.5.1.1.4 Heavy Metals

The speciation of the heavy metals will not be discussed in detail here because the species formed are similar to those found in the gypsum pond and fertilizer ponds water. What is significant about the sulphur leachate water, however, is the fact that because of its acidicty a significantly larger percentage of the heavy metals occur in the free ionic form and are mobile and bioavailable. The approximate proportions of these metals as free ions are:

(i) Al and Cu: 40% in free ionic form,
(ii) Zn and Ni: 50 - 65% in free ionic form,
(iii) Fe and Mn: 66 - 67% in free ionic form,
(iv) Cr: 100% in ionic form.

4.5.1.1.5 Hydrogen

Whereas H was found largely in the $H_2PO_4^-$ anion in the gypsum and fertilizer pond water with very little occurring in the free ionic form, in the sulphur leachate water, 47.9% of H occurs as H^+ with the remaining percent being in the form of HSO_4^-, and hence the extremely high acidity.

4.5.1.2 Mineral Solubility Modelling

The saturation indices calculated by MINTEQA2 for various minerals possibly occurring in the sulphur leachate collection drain have been tabulated in Appendix D: Table D3. As with the waters discussed so far, the minerals gypsum, anhydrite, quartz, cristobalite and chalcedony are predicted to be either close to equilibrium or supersaturated in the sulphur leachate drian water. Despite the high Al and Fe concentrations in this water, however, no

Al or Fe containing minerals were found to be supersaturated or close to equilibrium. The explanation for this lies in the fact that the water is very acidic and consequently the solubility of these metals is very high.

To verify this explanation and also to determine what minerals would be predicted to be supersaturated should the pH of the water increase slightly, MINTEQA2 was used to determine the speciation and mineral solubilities of minerals for this water composition but at pH values of 2 and 3.5. The results for the various minerals that change from an undersaturated state at pH 1.5 (the measured pH of the water) to an increasingly saturated state at pH values 2 and 3.5 are shown graphically in Figure 4.11 (the SI values for the minerals shown are tabulated in Appendix D: Table D4).

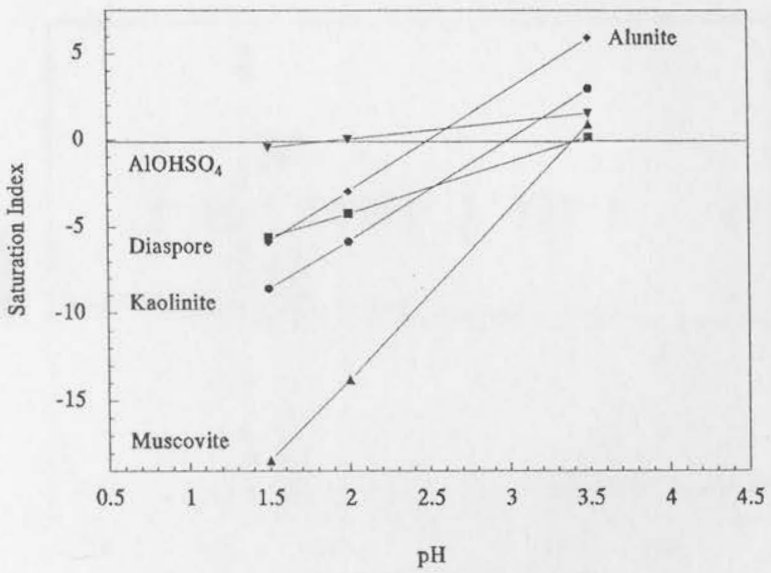

Figure 4.11 Plot of saturation index versus pH for minerals predicted by MINTEQA2 to change from an undersaturated state at pH 1.5 to a supersaturated state at pH 3.5 for the sulphur leachate collection drain water (sample SD2).

As would be predicted based on the above discussion of Al solubility, with increasing pH the saturation indices of a number of Al containing minerals increase markedly. The range of minerals found to be supersaturated at pH values of between 2 and 3.5 is similar to those predicted to be supersaturated in the gypsum pond water. The magnitudes of the SI values at pH 3.5 (pH of the gypsum pond water is 3.9) are also comparable.

4.5.1.3 Water Quality Assessment

The extreme acidity and salinity of this water coupled with the elevated heavy metals concentrations make it unsuitable for any use, industrial or otherwise.

4.5.2 Sulphur

X-ray diffractograms of two sulphur samples collected on the northern and southern portions of the dump are shown in Figure 4.12. No minerals aside from elemental sulphur could be identified in these scans.

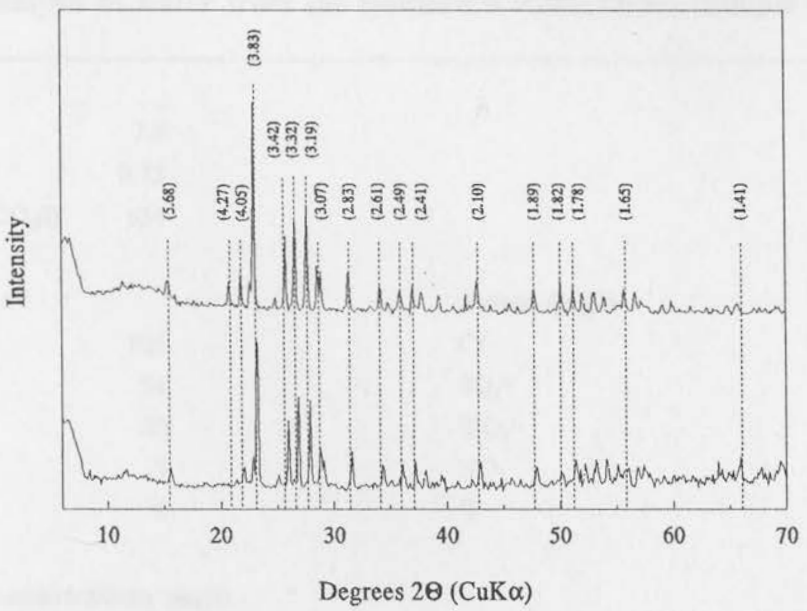

Figure 4.12 XRD plot of intensity versus degrees 2θ for two sulphur samples collected from the sulphur stockpile. The major sulphur peaks are labelled with the d-spacings shown in parentheses in Å units.

4.6 Results and Discussion of Heldeview Drain Water Quality

Water was sampled from the Heldeview Main Drain were it enters the ACEI site north-east of the gypsum dumps. The sample (SD1) was collected so that the quality of water entering the surface water drainage system on the site could be asssessed and to determine whether this water contains any constituents that may adding to the contamination of the site.

The results of the water analysis are shown in Table 4.12. This water is slightly alkaline (pH 7.8) and has a low salinity (EC 0.75 mS/cm). The water contains no detectable (by HPIC) nitrate/nitrite or ammonia and plots within the bicarbonate/sodium hydrochemical facies (Figure 4.13).

Table 4.12 Analysis of water from the Heldeview Main Drain (sample SD1).

pH	7.8		
EC (mS/cm)	0.75		
Alkalinity (mg $CaCO_3$/l)	634		
Cations (mg/l)		**Anions (mg/l)**	
Na^+	101	Cl^-	146
Ca^{2+}	54	SO_4^{2-}	43
Mg^{2+}	20	[1]PO_4^{3-}	0
K^+	5	NO_3^-	0
NH_4^+	0	[2]F^-	0.2
Total Elemental Concentrations (mg/l)			
Si	53.1	Zn	BDL
Al	BDL	Cd	BDL
Fe	0.15	As	BDL
Cu	BDL	Co	BDL
Ni	BDL	Mn	BDL
Pb	BDL	Cr	BDL

Footnotes:
1 - phosphate determined by Murphy and Riley Method (1962)
2 - fluoride determined by ion selective electrode
BDL - below detection limits

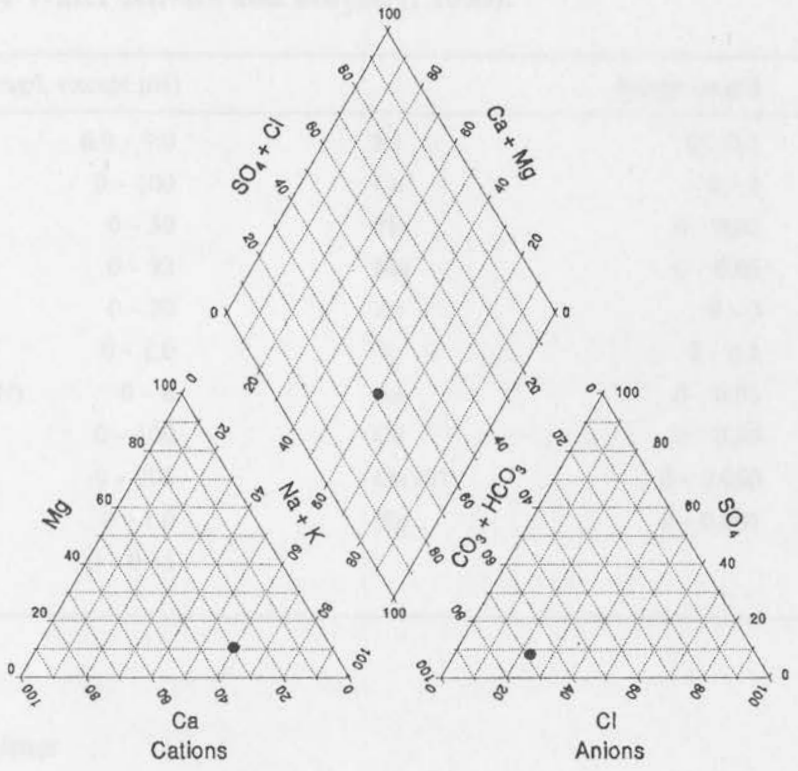

Figure 4.13 Pipergram representing the composition of water sample SD1 from the Heldeview Main Drain.

Comparing this water with the draft domestic guidelines for South African water (Department of Water Affairs and Forestry, 1995), as tabulated in Table 4.13, shows that it meets the requirements for pH, and the major cations and anions Mg^{2+}, K^{+}, SO_4^{2-} and NH_4^{+} but exceeds, albeit only marginally, the standards for Na^{+}, Ca^{2+} and Cl^{-}.

The heavy metal total element concentrations in this water are for the most part below detection limits (ICP-AES). Iron, the only heavy metal detected, exceeds the standards, however, by 0.05 ppm.

In general this water is a very high quality, and although it marginally exceeds a few of the requiments for domestic drinking water it does not contain any constituents that may be seen to have a deleterious effect on the environmental quality of the water and soils on the AECI site.

Table 4.13 Draft Domestic Water Quality Guidelines for South Africa (Department of Water Affairs and Forestry, 1995).

	Range (in mg/l, except pH)		Range (mg/l)
pH	6.0 - 9.0	Fe	0 - 0.1
Na	0 - 100	Cu	0 - 1
K	0 - 50	Pb	0 - 0.01
Ca	0 - 32	Mn	0 - 0.05
Mg	0 - 30	Zn	0 - 3
NH_4	0 - 1.0	V	0 - 0.1
Nitrate/Nitrite (as N)	0 - 6	As	0 - 0.01
Cl	0 - 100	Cd	0 - 0.05
SO_4	0 - 200	Cr(VI)	0 - 0.050
F	0 - 1.0	Hg	0 - 0.001
Al	0 - 0.15		

4.7 Conclusions

The objective of this chapter has been to characterise, chemically, potential sources of contamination that may be impacting on the environmental quality of the Dead Tree Area. Four such potential sources have been discussed, namely the fertilizer evaporation ponds/Triomf Main Drain area, the gypsum waste dumps, the sulphur stockpile, and water entering the site via the Heldeview Main Drain. Brief summations of the charactersitics of each potential contamination source are outlined below.

Fertilizer evaporation pond/Triomf Main Drain

The fertilizer evaporation pond/Triomf Main Drain water was found to be characterised by very high salinity (6.3 - 11.7 mS/cm), low pH (<4.5) and high acidity (12.9 - 34.6 mmol/l). The anionic composition of this water is dominated by sulphate although chloride, phosphate fluoride and nitrate concentrations are also high. There is, however, no dominant cation. The water contains elevated concentrations of numerous metals, the most extreme being Al which ranges in concentration from 18.9 to 130 mg/l.

Although a number of minerals were predicted by MINTEQA2 to be close to equilibrium or supersaturated in this water, only gypsum was found in the precipitate forming in the

evaporation ponds. The sediment analysis revealed a particularly high organic matter content (11.8%) as well as elevated concentrations of the heavy metals Pb, Cu and Zn. It is proposed that the elevated metal concentrations are a consequence of the high organic matter in the sediment which allows for the complexation, and hence accumulation, of a large proportion of any metals released in the Kynoch Fertilizer Limited aqueous effluent stream.

Gypsum leachate collection pond

As in the case of the fertilizer pond water, the water in the gypsum leachate collection pond was also found to be very saline (9.8 mS/cm) and have a low pH (3.9) and high acidity (20.7 mmol/l). Although high in Ca^{+}, K^{+} and SO_4^{2-}, this water is dominated by NH_4^{+} and NO_3^{-}. The heavy metal concentrations in this water are lower than those of the fertilizer pond water, except for Al which is comparable in concentration (90.8 mg/l). MINTEQA2 predicted the supersaturation of numerous Al containing minerals as well as those minerals found to be supersaturated in the fertilizer pond water. The reason for the differences in SI between the two waters is attributed to the fact that 22.8% of Al is predicted to occur as a free ion in the gypsum water whereas in the fertilizer water no free ionic Al is predicted.

Sulphur leachate collection drain

Water from the sulphur leachate collection drain was found to be characterised by extreme acidity (328 mmol/l; pH 1.5) and high salinity (20.7 mS/cm), far in excess of that found in the fertilizer or gypsum water. As was expected, sulphate concentrations in this water were also extreme (13600 mg/l). The acidity of the water is believed to have resulted in the mobilization of heavy metals in the surrounding soils and to be the explanation for the high Al, Fe, Mn, and As concentrations found in this water.

Heldeview Main Drain

The Heldeview Main Drain water was found to be of high quality, meeting the majority of the draft domestic water quality guidelines set by the Department of Water Affairs and Forestry (1995). It does not contain any constituents that could pose a contamination risk to the AECI site.

General

The results show that the fertilizer evaporation ponds/Triomf Main Drain, gypsum waste

dumps and sulphur stockpile sites contain a variety of contaminants that may be impacting on the environmental quality of the Dead Tree Area. This chapter has served as a chemical characterisation of the above sites and will be used in the following chapter to assess the effects of these sites, if any, on the aqueous chemistry of the Dead Tree Area.

5. AQUEOUS CHEMISTRY OF THE DEAD TREE AREA

5.1 Introduction

The objectives of this chapter are twofold: firstly, to characterise the aqueous chemistry of the Dead Tree Area; and secondly, to assess the degree of contamination of the water in the area and to determine what impact the fertilizer evaporation ponds/Triomf Main Drain, gypsum dumps and/or sulphur stockpile have had on the quality of the water. The second objective requires knowledge concerning the chemical characteristics of the fertilizer evaporation ponds/Triomf Main Drain, gypsum dumps and sulphur stockpile, and hence the results presented in chapter 4 will be drawn upon in this regard.

In this chapter the results of the analyses of subsurface water from the Dead Tree Area are discussed, and an explanation for the results is proposed on the basis of the known potential sources of contamination in the immediate area. Chemical modelling has been used to investigate mineral solubility equilibria and the speciation of ionic components in the water, and these results used to further characterise the differences and commonalities present within the various water samples.

The quality of the water in the Dead Tree Area has also been assessed in terms of the draft water quality guidelines for domestic and industrial use.

5.2 Water Sampling and Analysis

The collection and analysis of subsurface water samples from the Dead Tree Area has been described in chapter 3. In total, 13 subsurface samples were collected and analysed following standard methods described in *Standard Methods for the Examination of Water and Waste Water* (Greenberg *et al.,* 1985). Analyses conducted were pH, electrical conductivity (EC), alkalinity/acidity, major cations and anions (HPIC), phosphorus (Murphy and Riley, 1962), fluoride (ion selective electrode method) and total elemental concentrations (ICP-AES).

5.3 Prediction of Chemical Speciation and Saturation Indices (S.I.)

The mathematical model MINTEQA2 (Allison *et al.,* 1991), a geochemical equilibrium speciation model for dilute aqueous systems, has been used to investigate the ionic speciation predicted to occur in the water samples analysed, as well as to calculate saturation indices for minerals likely to occur under the prevailing conditions. Details concerning the theoretical

basis of this model have been discussed in chapter 3.

5.4 Data Presentation

A number of methods of data presentation were explored for graphical representation of the analytical results. Although contouring of the data on a geographical location map of the area was considered to be most visually effective, scientifically this approach is inappropriate due to the paucity of the sampling points. Because of this, the use of scaled bars plotted on a geographical location map was thought more desirable. In most instances this approach was found to be visually ineffective, however, as in a number of cases the range of the data resulted in certain bars obscuring others. Consequently a compromise has been sought whereby two-dimensional histograms are employed in conjunction with an associated geographical location map.

Each group of histograms is presented with a geographical location map placed above the histograms. The five transect lines along which the 13 water sampling points were located are shown on the map (transects were oriented NW-SE, with the transect number increasing from NE to SW). The data presented on the histograms are grouped according to the transect number. The histograms thus allow for the easy comparison of results along and between transects, and hence changes across the Dead Tree Area.

Unlike the major cation and anion data, the presentation of heavy metal concentrations using three-dimensional histograms was found to be quite effective in displaying the spatial trends in the data. Hence three-dimensional histograms have been used in conjunction with a geographical location map for various metals of interest.

5.5 Results and Discussion

5.5.1 General Discussion and Review of Results

The results of the water analyses are tabulated in Tables 5.1 and 5.2, and presented graphically in Figures 5.1 to 5.4.

The pH, EC, alkalinity and acidity data presented in Figure 5.1 reveal that the subsurface water in the Dead Tree Area exhibits marked spatial variability, with certain samples being strongly acidic (pH<2.5; acidity 5.9 to 17.1 mmol/l) and others being close to neutrality with pH values >6 (alkalinity between 100 to 520 mg $CaCO_3$/l). The range in electrical

Table 5.1 Analyses of subsurface water samples from the Dead Tree Area.

Sample No.	pH	EC	Alkalinity/ Acidity		Na^+	Ca^{2+}	Mg^{2+}	K^+	NH_4^+	Cl^-	SO_4^{2-}	$^1PO4^{3-}$	NO_3^-	$^2F^-$
A1	3.4	24.7		13	3850	1010	2860	1900	120	11600	5370	1.8	ND	7.52
A2	6.9	13.0	519		2020	385	956	122	ND	4690	1200	1.2	43.2	10.1
A3	7.1	90.3	529		18100	2370	6980	382	ND	42500	3480	0.6	244	0.54
A4	5.6	1.9	50.8		321	75.1	132	20.1	ND	722	129	0.3	5.22	2.51
a1	2.2	18.1		17	2290	805	1520	182	130	5760	3090	2.8	703	27.5
a2	2.4	19.3		5.9	2390	381	1090	73.5	ND	5370	1360	0.6	449	3.31
a3	2.1	81.4		6.5	23200	2510	6370	195	ND	51500	3090	0.6	973	0.32
B1	6.5	15.8	139		3080	417	1380	66.0	ND	4380	888	0.3	ND	1.52
B2	4.6	3.7		1.2	540	102	200	65.3	23.5	1330	152	ND	ND	0.61
B3	7.2	7.1	160		1120	174	388	48.4	42.4	2430	393	0.3	ND	1.11
C1	5.7	4.6	39.4		605	137	239	32.5	24.2	1440	195	ND	43.4	0.35
C2	5.9	2.0	29.5		285	43.6	63.2	13.9	8.01	491	103	ND	ND	0.14
D1	5.7	1.6	19.7		181	43.3	66.4	11.2	8.06	429	68.5	ND	ND	0.14

Footnotes:
Units - EC in mS/cm; alkalinity as mg $CaCO_3$/l; acidity in mmol/l; all ion concentrations in mg/l
1 - phosphate determined by Murphy and Riley Method (1962)
2 - fluoride determined by ion selective electrode
ND - not detected

Table 5.2 Total elemental analyses of subsurface water samples from the Dead Tree Area.

Sample No.	Si	Al	Cu	Ni	Pb	Zn	Cd	As	Co	Mn	Cr	Fe
A1	38.9	108	BDL	1.34	1.03	0.61	0.12	BDL	0.35	17.8	0.14	1.14
A2	20.5	BDL	BDL	BDL	BDL	0.16	0.08	BDL	BDL	BDL	0.12	0.10
A3	17.2	BDL	BDL	0.49	1.01	0.21	0.16	BDL	0.21	0.06	0.23	0.16
A4	15.4	3.88	BDL	BDL	BDL	0.18	0.06	BDL	BDL	0.23	BDL	10.6
a1	34.5	67.2	BDL	0.97	BDL	0.48	0.11	BDL	0.26	13.2	0.12	2.78
a2	43.5	3.33	BDL	0.29	BDL	0.17	0.09	BDL	BDL	0.96	0.11	1.17
a3	38.9	1.87	BDL	0.36	1.06	0.20	0.14	BDL	0.16	0.09	0.19	0.42
B1	5.11	BDL	BDL	0.20	BDL	0.19	0.10	BDL	0.10	0.05	0.13	0.14
B2	21.4	1.76	BDL	0.19	BDL	0.18	0.08	BDL	BDL	1.24	0.10	3.60
B3	0.76	BDL	BDL	0.16	BDL	0.16	0.08	BDL	BDL	0.06	0.10	0.13
C1	2.92	BDL	BDL	0.16	BDL	0.14	0.08	BDL	BDL	0.05	BDL	0.13
C2	12.0	BDL	BDL	0.15	BDL	0.15	0.07	BDL	BDL	0.11	BDL	0.45
D1	6.59	BDL	BDL	BDL	BDL	0.16	0.07	BDL	BDL	0.19	BDL	0.12

Footnotes: Units - all concentrations in mg/l
BDL - below detection limits

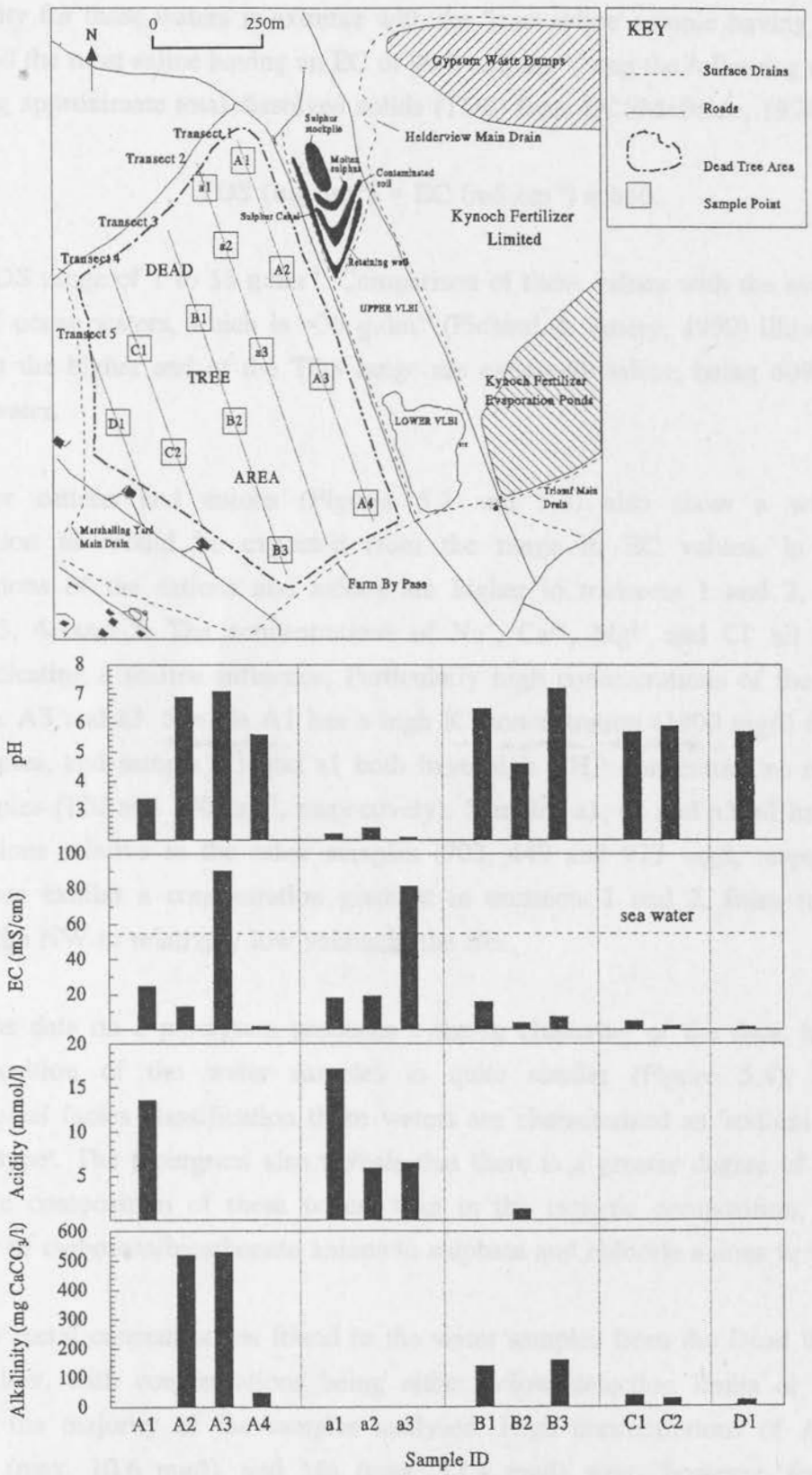

Figure 5.1 Histograms showing pH, electrical conductivity, acidity and alkalinity for subsurface water samples from the Dead Tree Area. The positions of the samples are shown on the map.

conductivity for these waters is extreme with the 'least saline' sample having an EC of 1.6 mS/cm and the most saline having an EC of 90.3 mS/cm. Using the following expression for calculating approximate total dissolved solids (TDS) from EC (McBride, 1994):

$$TDS\ (mg.dm^{-3}) \approx EC\ (mS.cm^{-1}) \times 640,$$

gives a TDS range of 1 to 58 $g.dm^{-3}$. Comparison of these values with the average TDS or salinity of ocean waters, which is $\approx$35 $g.dm^{-3}$ (Pickard & Emery, 1990) illustrates that the samples at the higher end of the TDS range are extremely saline, being 60% more saline than sea water.

The major cations and anions (Figures 5.2 and 5.3) also show a wide range in concentration as would be expected from the range in EC values. In general, the concentrations of the cations and anions are higher in transects 1 and 2, compared to transects 3, 4, and 5. The concentrations of Na^+, Ca^{2+}, Mg^{2+} and Cl^- all show similar trends, indicating a marine influence. Particularly high concentrations of these ions occur in samples A3 and a3. Sample A1 has a high K^+ concentration (1900 mg/l) relative to the other samples, and sample A1 and a1 both have high NH_4^+ concentrations relative to the other samples (120 and 130 mg/l, respectively). Samples a1, a2 and a3 all have high NO_3^- concentrations relative to the other samples (703, 449 and 973 mg/l, respectively). The PO_4^{3-} values exhibit a concentration gradient in transects 1 and 2, from relatively high values in the NW to relatively low values in the SE.

Plotting the data on a pipergram produces a strong clustering of the data, indicating that the composition of the water samples is quite similar (Figure 5.4). Based on a hydrochemical facies classification these waters are characterised as 'sodium and chloride dominant type'. The pipergram also reveals that there is a greater degree of variability in the anionic composition of these waters than in the cationic composition, and that the proportion of carbonate/bicarbonate anions to sulphate and chloride anions is very low.

The heavy metal concentrations found in the water samples from the Dead Tree Area are generally low, with concentrations being either below detection limits or only slightly above for the majority of the samples analysed. High concentrations of Al (max. 108 mg/l), Fe (max. 10.6 mg/l), and Mn (max. 17.8 mg/l) were, however, found in some samples. The spatial trends of selected metals are shown in Figure 5.4 (numerical data in Table 5.2). Figure 5.4 shows that, in general, the highest concentrations of metals occur in the most northern portion of the Dead Tree Area adjacent to the sulphur stockpile (sample

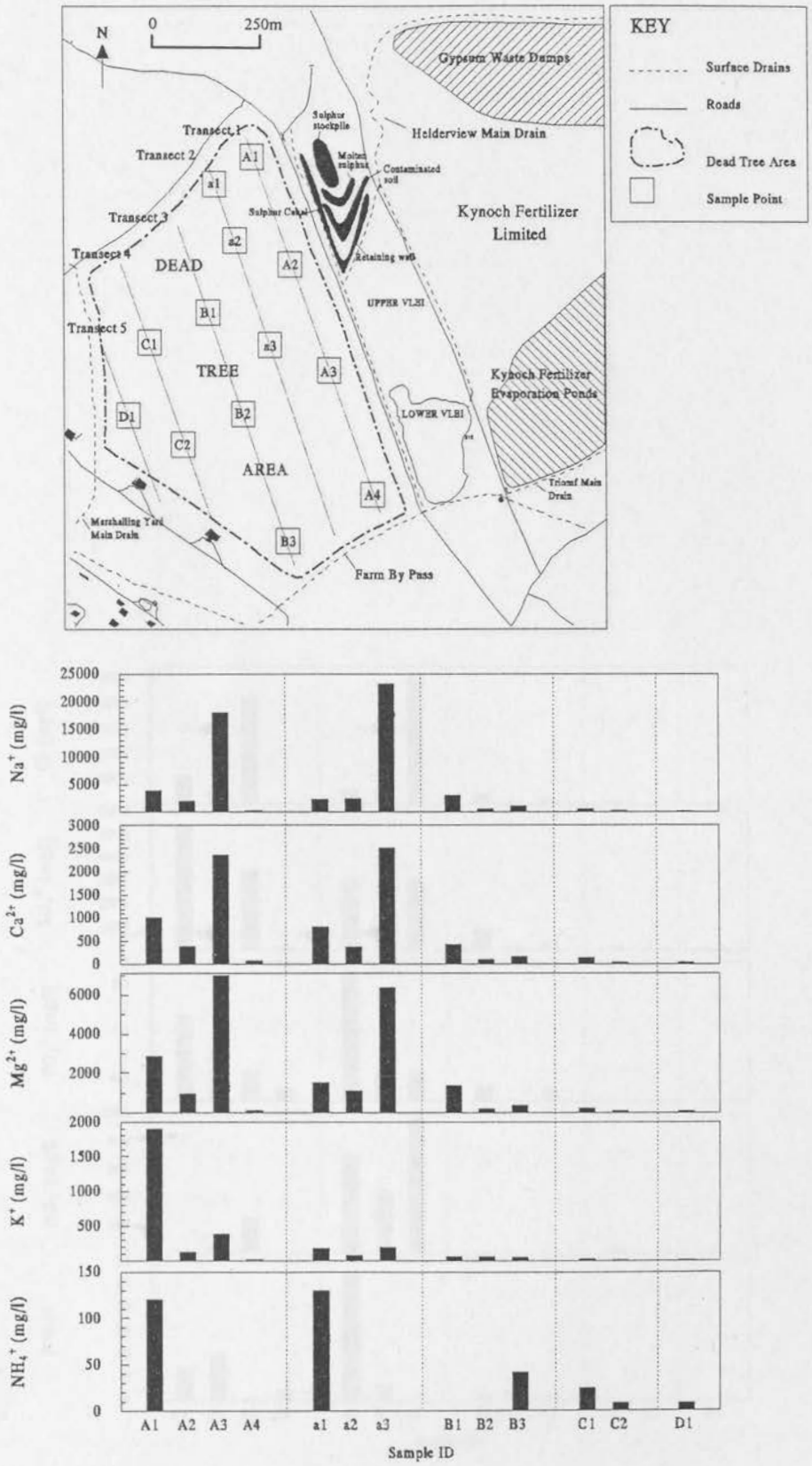

Figure 5.2 Histograms showing the major cation concentrations for subsurface water samples from the Dead Tree Area. The positions of the samples are shown on the map.

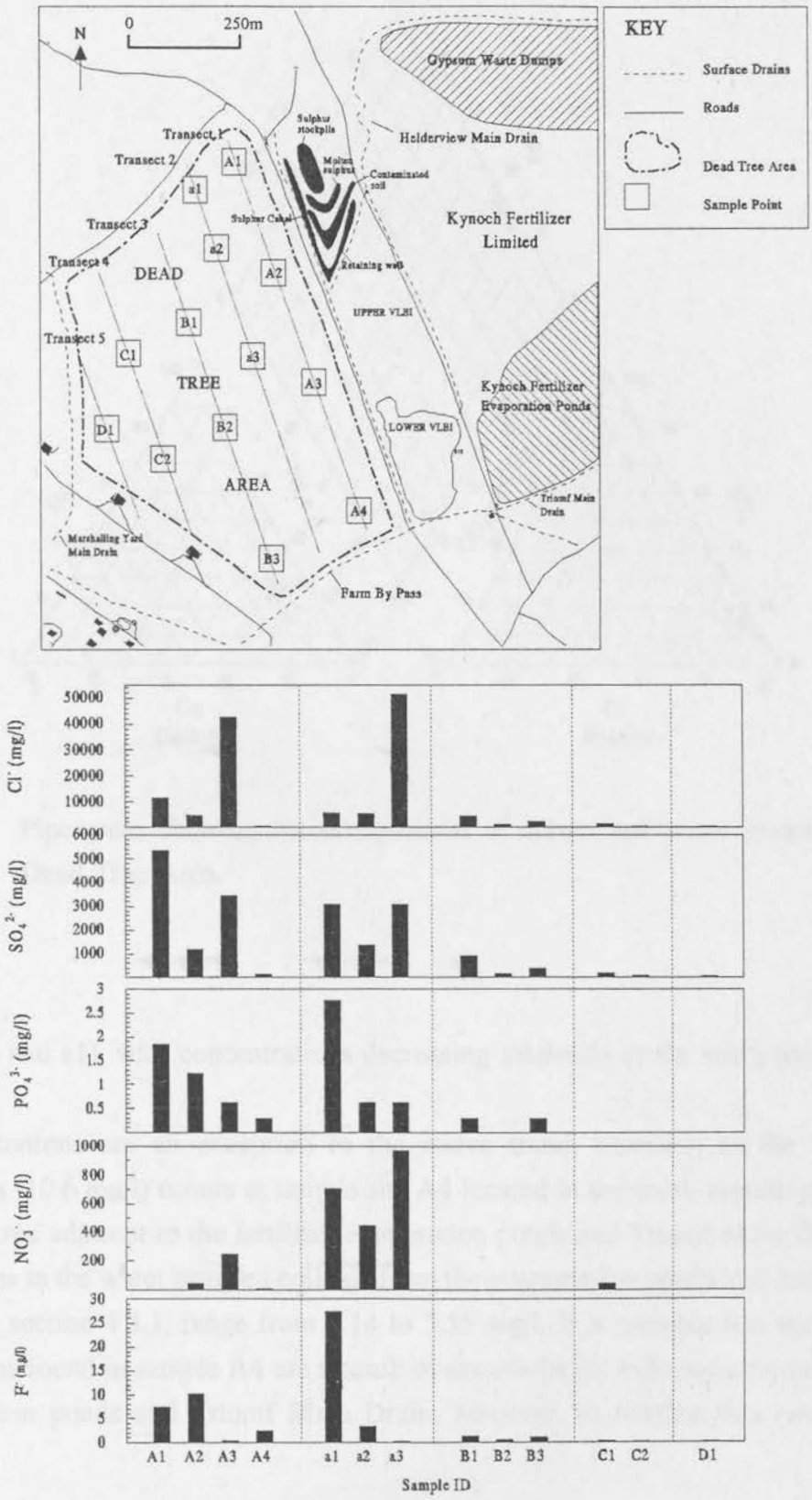

Figure 5.3 Histograms showing the major anion concentrations for subsurface water samples from the Dead Tree Area. The positions of the samples are shown on the map.

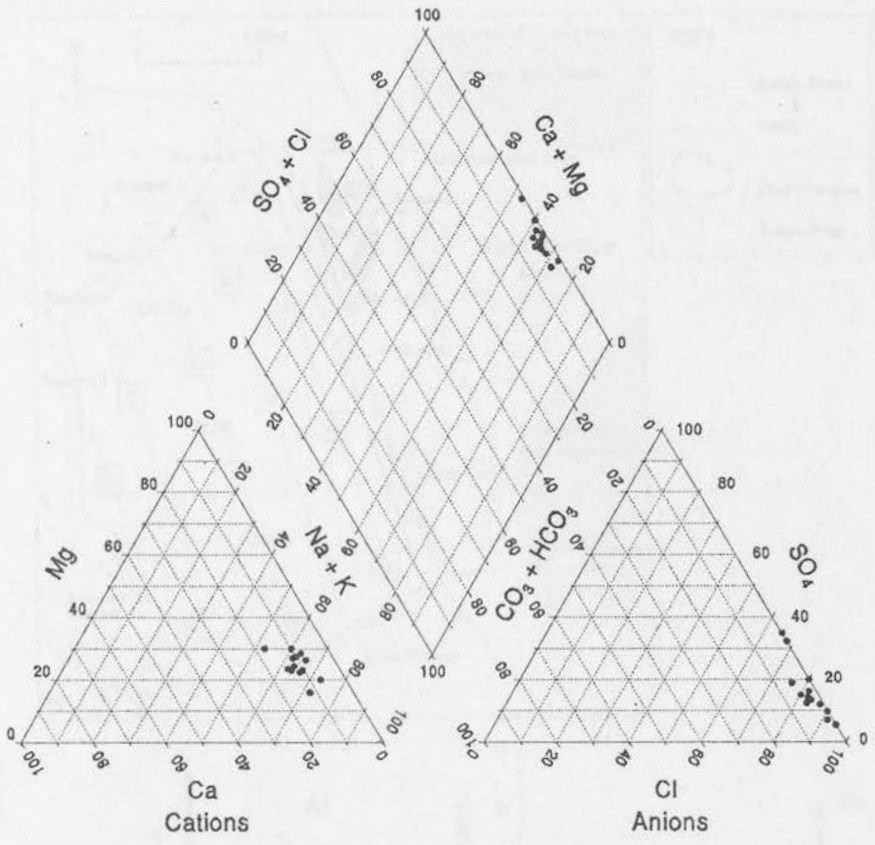

Figure 5.4. Pipergram showing the composition of subsurface water samples from the Dead Tree Area.

positions A1 and a1), with concentrations decreasing markedly to the south and south-east.

Iron concentrations are an exception to the above trend, however, as the highest iron concentration (10.6 mg/l) occurs at sample site A4 located in the south-eastern portion of the Dead Tree Area adjacent to the fertilizer evaporation ponds and Triomf Main Drain. The Fe concentrations in the water samples collcted from the evaportation ponds and drain, discussed in chapter 4, section 4.3.1, range from 0.14 to 3.55 mg/l. It is possible that the elevated Fe concentrations found in sample A4 are a result of accumulation and concentration of Fe from the evaporation ponds and Triomf Main Drain, however, to confirm this further work is required.

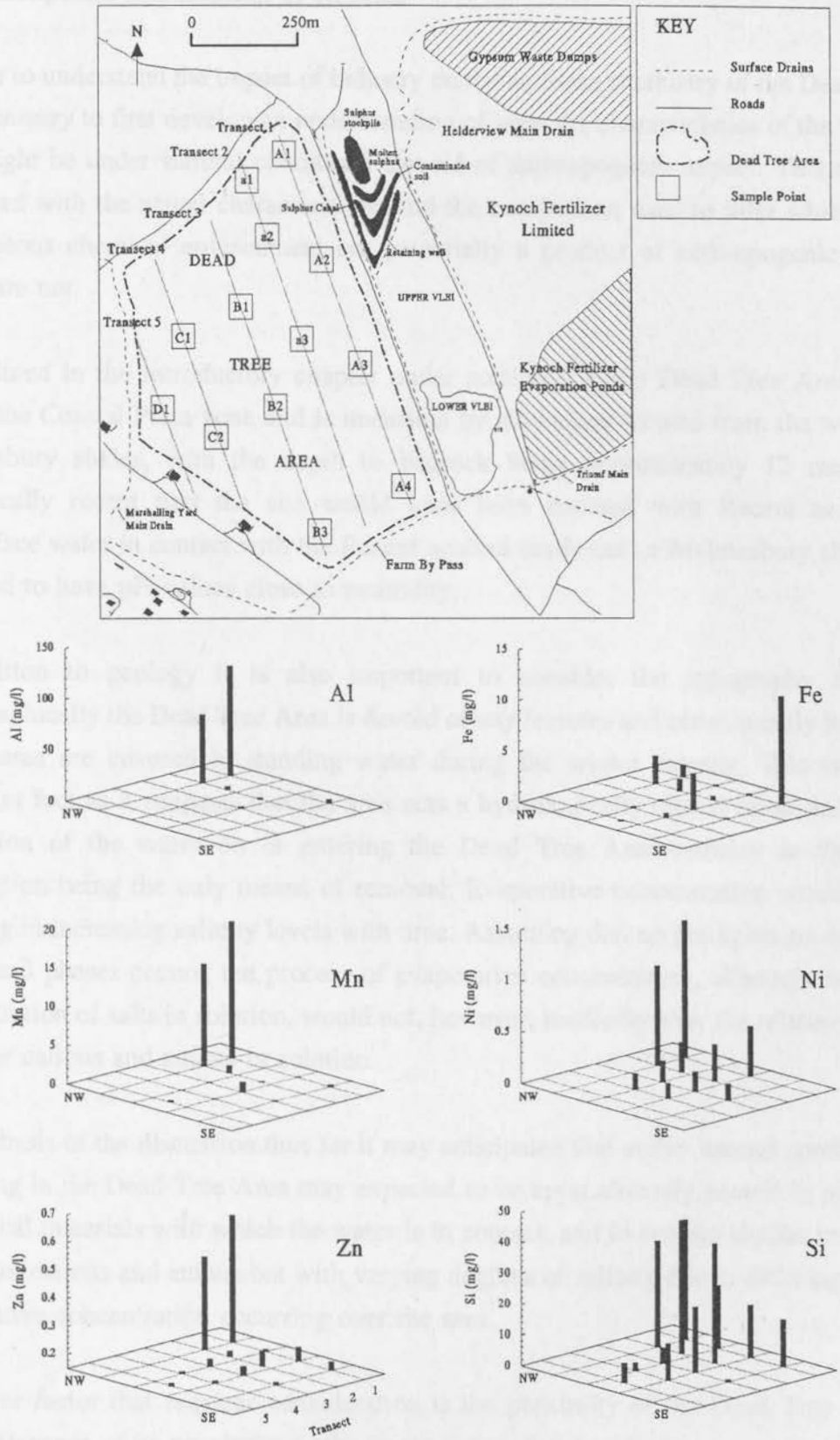

Figure 5.5 3-D Histograms showing Al, Fe, Mn, Ni, Zn and Si concentrations for subsurface water samples from the Dead Tree Area. The positions of the samples are shown on the map.

5.5.2 Proposed Explanation of Results

In order to understand the impact of industry on the aqueous chemistry of the Dead Tree Area it is necessary to first develop an understanding of what the characteristics of the water in this area might be under 'natural conditions' devoid of anthropogenic impact. This may then be compared with the actual characteristics, and the comparison used to infer which aspects of the aqueous chemical environment are potentially a product of anthropogenic impact and which are not.

As outlined in the introductory chapter under section 1.2, the Dead Tree Area is situated within the Coastal Plain zone and is underlain by silty clays formed from the weathering of Malmesbury shales, with the depth to bedrock being approximately 12 metres. In the geologically recent past the site would have been covered with Recent aeolian sands. Subsurface water in contact with the Recent aeolian sands and or Malmesbury shales may be expected to have pH values close to neutrality.

In addition to geology it is also important to consider the topography of the area. Topographically the Dead Tree Area is devoid of any features and consequently large portions of the area are covered in standing water during the winter months. This is a critically important fact as it suggests that the area acts a hydrologically closed basin, ie. that a large proportion of the water on or entering the Dead Tree Area remains in the area with evaporation being the only means of removal. Evaporative concentration would thus occur resulting in increasing salinity levels with time. Assuming that no precipitation or dissolution of mineral phases occurs, the process of evaporative concentration, although increasing the concentration of salts in solution, would not, however, markedly alter the relative proportions of major cations and anions in solution.

On the basis of the discussion thus far it may anticipated that under 'natural conditions' water occurring in the Dead Tree Area may expected to be approximately neutral in pH due to the geological materials with which the water is in contact, and to contain similar proportions of the major cations and anions but with varying degrees of salinity due to differing amounts of evaporative concentration occurring over the area.

A further factor that requires consideration is the proximity of the Dead Tree Area to the ocean. Because of its proximity to the ocean (some few hundred metres or less) the area is likely to receive a substantial input of windblown salts, notably sodium and chloride. Hence it may also be anticipated that, in addition to the above characteristics, the water in the Dead

Tree Area may contain significantly elevated concentrations of the ions Na^+ and Cl^- in relation to the other ions in solution.

In summary, water occurring in the Dead Tree Area may be expected to have a pH close to neutral, contain varying degrees of salinty, but with similar ionic proportions, and contain elevated Na^+ and Cl^- levels. If the high salt content of the subsurface water samples from the Dead Tree Area is a result of a marine influence, the proportions of the major ions in solution should be the same as those found in sea water. If the proportions of major ions in the water samples differ significantly from that of sea water, this may indicate anthropogenic impact.

5.5.2.1 Marine Impact on the Dead Tree Area

In Figures 5.6 and 5.7, the concentrations of Na^+ versus Cl^-, Ca^{2+} versus Mg^{2+}, Cl^- versus SO_4^{2-}, and Na^+ versus K^+ in the subsurface water samples are shown. The lines representing the ratios of these respective ion pairs in sea water are also shown, to illustrate similarities and differences in ion proportions between the subsurface water samples from the Dead Tree Area and sea water.

There is a direct linear relationship betwen Na^+ and Cl^-, and Ca^{2+} and Mg^{2+}, and the ratio of these respective ion pairs is very similar to that of sea water (Figure 5.6). This indicates that there is a strong marine influence on the aqueous chemistry of the Dead Tree Area, and that the high concentrations of Na^+, Cl^-, Ca^{2+}, and Mg^{2+} detected in these waters are a result of the accumulation of marine salts and not the result of anthropogenic contamination.

In contrast to the Na^+ versus Cl^- and Ca^{2+} versus Mg^{2+} values, the Cl^- versus SO_4^{2-} and Na^+ versus K^+ values do not all lie close to the sea water lines for these respective ion pairs. Samples A1 and a1 on the plot of Cl^- versus SO_4^{2-} show the greatest deviation from the sea water line. Because the Cl^- concentrations display a marine signature, as shown by the plot of Na^+ versus Cl^- discussed above, the positions of samples A1 and a1 on the plot of Cl^- versus SO_4^{2-} indicates that the SO_4^{2-} concentrations in these waters are elevated relative to chloride and that this elevation is indicative of either anthropogenic contamination, or non-conservative behaviour during evaporative concentration. A similar argument may be made for sample A1 on the plot of Na^+ versus K^+, to show that deviation of this sample from the sea water line indicates elevated concentrations of K^+ relative to Na^+, and that this elevation is indicative of anthropogenic contamination.

Figures 5.6 and 5.7 show, thus, that a large component of the salinity of the subsurface water

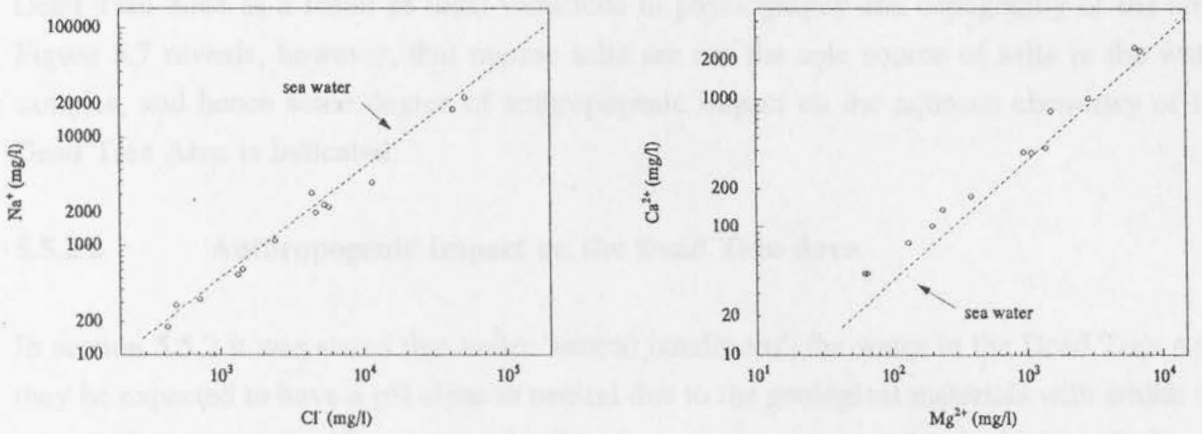

Figure 5.6 Plots of Na^+ versus Cl^- and Ca^{2+} versus Mg^{2+} showing the relationship between these ion pairs. The lines representing the ratios of Na^+/Cl^- and Ca^{2+}/Mg^{2+} in sea water are shown for comparison.

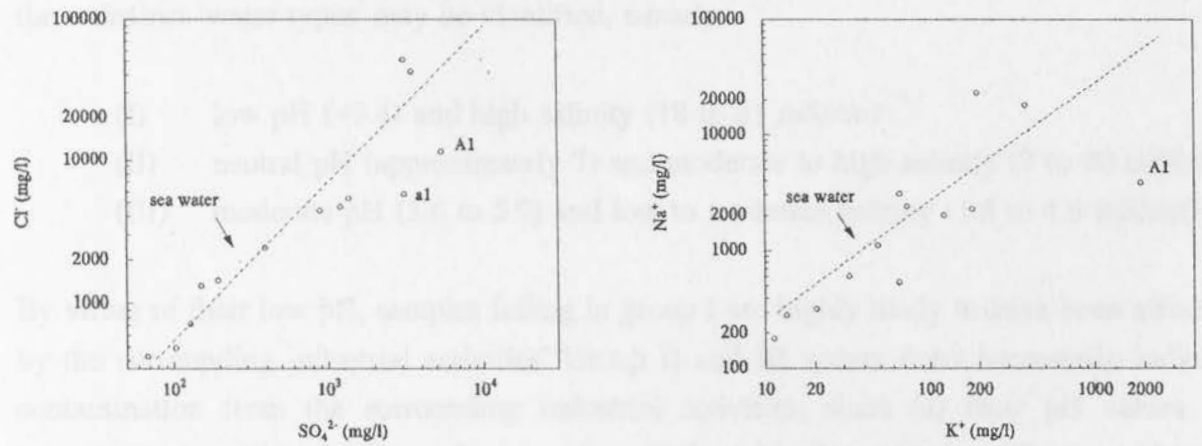

Figure 5.7 Plots of Cl^- versus SO_4^{2-} and Na^+ versus K^+ showing the relationship between these ion pairs. The lines representing the ratios of Cl^-/SO_4^{2-} and Na^+/K^+ in sea water are shown for comparison.

samples from the Dead Tree Area is marine in origin. There is thus a differential distribution of salts in the local environment, with elevated salt concentrations naturally occurring in the Dead Tree Area as a result of local variations in physiography and topography of the area. Figure 5.7 reveals, however, that marine salts are not the sole source of salts in the water samples, and hence some degree of anthropogenic impact on the aqueous chemistry of the Dead Tree Area is indicated.

5.5.2.2 Anthropogenic Impact on the Dead Tree Area

In section 5.5.2 it was stated that under 'natural conditions', the water in the Dead Tree Area may be expected to have a pH close to neutral due to the geological materials with which the water is in contact. As the water would, therefore, not be anticipated to be highly alkaline or acidic, this would seem to be the most logical parameter to investigate first in assessing anthropogenic impact on the site.

In Figure 5.8 the electrical conductivity of the water samples has been plotted against their pH values to investigate whether there is a natural grouping of the data. Based on a visual interpretation of this plot, it is proposed that there is indeed a grouping of the data and that three distinct 'water types' may be identified, namely:

(I) low pH (<3.4) and high salinity (18 to 81 mS/cm)
(II) neutral pH (approximately 7) and moderate to high salinity (7 to 90 mS/cm).
(III) moderate pH (5.6 to 5.9) and low to moderate salinity (1.6 to 4.6 mS/cm)

By virtue of their low pH, samples falling in group I are highly likely to have been affected by the surrounding industrial activities. Group II and III waters don't necessarily indicate contamination from the surrounding industrial activities, since (a) their pH values lie approximately within the range that may be anticipated under natural conditions (although group III waters have a slightly lower pH than would be expected based on known geology) and (b) the range of salinity encountered is most likely attributable to differing degrees of evaporative concentration of salts that are predominantly of marine origin. The 'marine signature' of these waters has been discussed in section 5.5.2.1.

The spatial distribution of the three groups identified is illustrated on the geographical location map associated with the plot of EC versus pH in Figure 5.8. This map is purely schematic and does not reflect contours of any parameter in any way. The map is considered useful, however, as it does show a degree of spatial grouping of the data based on the

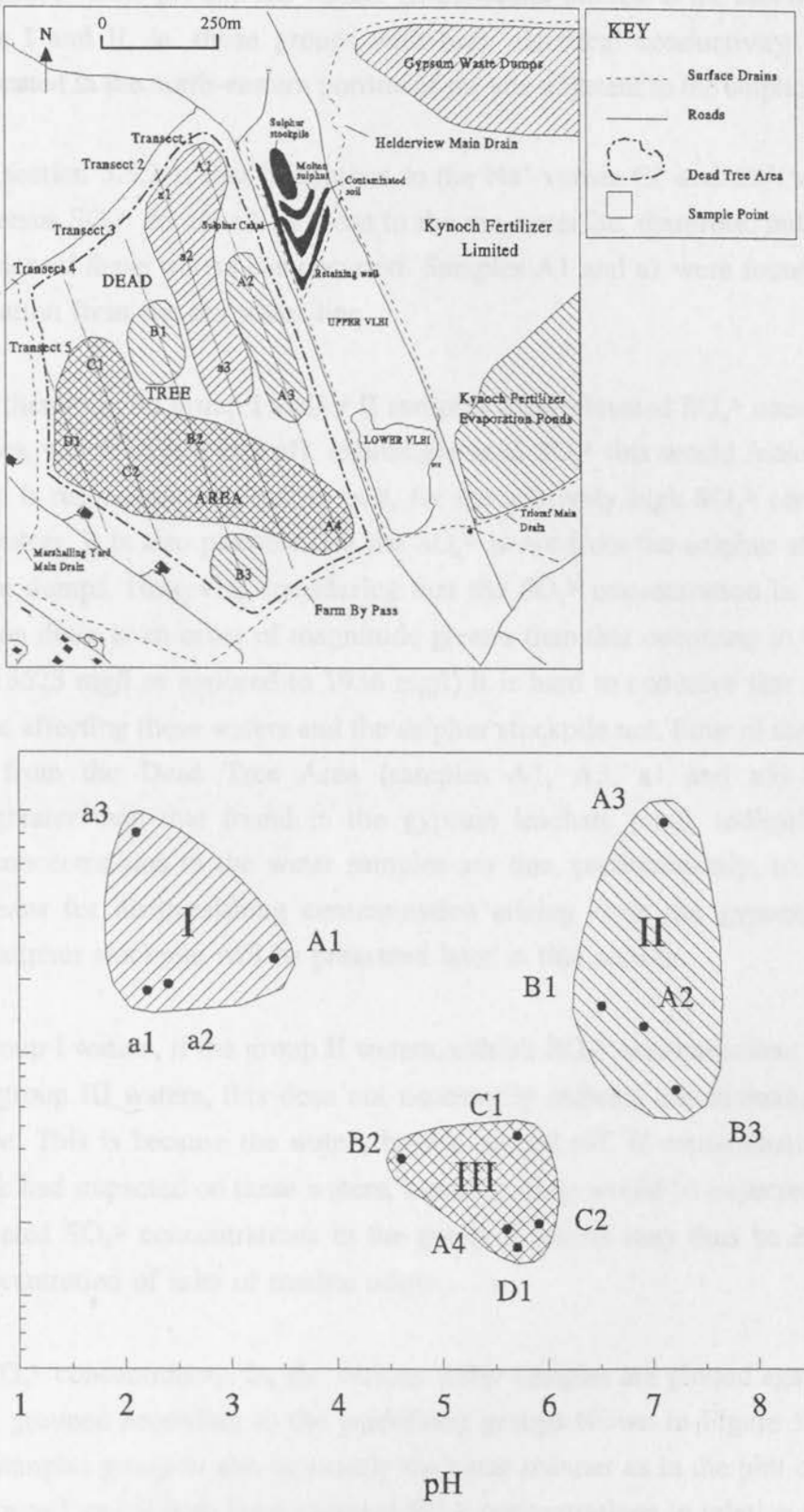

Figure 5.8 Plot of electrical conductivity versus pH for subsurface water samples from the Dead Tree Area. The samples have been grouped into three groups and the spatial distribution of the groups shown on the accompanying map.

identification of groups from pH and EC values. Of particular interest is the fact that samples falling in groups I and II, ie. those groups with high electrical conductivity values, are predominantly located in the north-eastern portion of the site adjacent to the sulphur stockpile.

It was shown is section 5.5.2.1, that in contrast to the Na^+ versus Cl^- and Ca^{2+} versus Mg^{2+} values, the Cl^- versus SO_4^{2-} do not all lie close to the sea water lie, therefore, indicating that SO_4^{2-} contamination of these waters has occurred. Samples A1 and a1 were found to display the greatest deviation from the sea water line.

The question is, therefore, do group I and/or II samples show elevated SO_4^{2-} concentrations? If group I samples, which have a low pH, exhibit elevated SO_4^{2-} this would indicate that the sulphur stockpile is responsible, at least in part, for the relatively high SO_4^{2-} concentrations found in these waters. It is also possible that the SO_4^{2-} is not from the sulphur stockpile but from the gypsum dumps. However, considering that the SO_4^{2-} concentration in the sulphur leachate collection drain is an order of magnitude greater than that occurring in the gypsum leachate pond (13623 mg/l as apposed to 1936 mg/l) it is hard to conceive that the gypsum leachate could be affecting these waters and the sulphur stockpile not. Four of the subsurface water samples from the Dead Tree Area (samples A1, A3, a1 and a3) have SO_4^{2-} concentrations greater than that found in the gypsum leachate pond, indicating that the elevated SO_4^{2-} concentrations in the water samples are due, predominantly, to the sulphur stockpile. A means for distinguishing contamination arising from the gypsum dumps as apposed to the sulphur stockpile will be presented later in this section.

In contrast to group I waters, if the group II waters, exhibit SO_4^{2-} concentrations in excess of those found in group III waters, this does not necessarily indicate contamination from the sulphur stockpile. This is because the waters have a neutral pH. If contamination from the sulphur stockpile had impacted on these waters, however, they would be expected to have an acidic pH. Elevated SO_4^{2-} concentrations in the group II waters may thus be explained by evaporative concentration of salts of marine origin.

In Figure 5.9, SO_4^{2-} concentrations for the various water samples are plotted against pH, and the samples are grouped according to the predefined groups shown in Figure 5.8. The plot shows that the samples group in almost exactly the same manner as in the plot of EC versus pH, and that groups I and II both have elevated SO_4^{2-} concentrations in relation to group III. As discussed above this indicates that (a) group I waters have been affected by contamination from the sulphur stockpile, and (b) that evaporative concentration of salts in the group II waters has occurred, and to a greater degree than that which has occurred in group III waters.

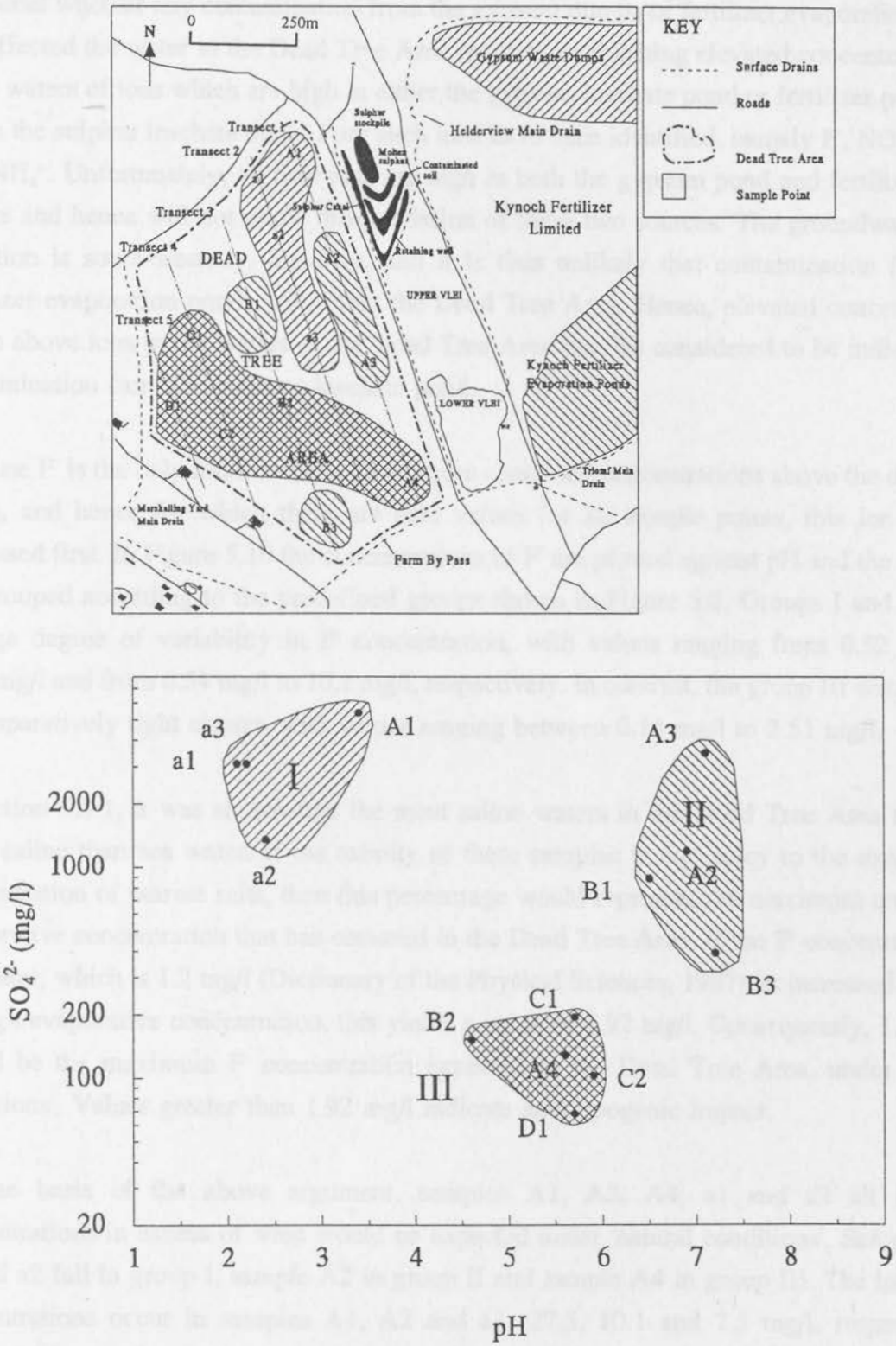

Figure 5.9 Plot of SO_4^{2-} concentration versus pH for subsurface water samples from the Dead Tree Area. The samples have been grouped according to the predefined groups shown in Figure 5.8, and the spatial distribution of these groups shown on the accompanying map.

To assess whether any contamination from the gypsum dumps or fertilizer evaporation ponds has affected the water in the Dead Tree Area requires establishing elevated concentrations in these waters of ions which are high in either the gypsum leachate pond or fertilizer ponds but not in the sulphur leachate drain. Four such ions have been identified, namely F^-, NO_3^-, PO_4^{3-}, and NH_4^+. Unfortunately, all four ions are high in both the gypsum pond and fertilizer pond waters and hence will not allow differentiation of these two sources. The groundwater flow direction is south-westerly, however, and it is thus unlikely that contamination from the fertilizer evaporation ponds will effect the Dead Tree Area. Hence, elevated concentrations of the above ions in the waters of the Dead Tree Area may be considered to be indicative of contamination from the gypsum leachate pond.

Because F^- is the only ion for which all samples contained concentrations above the detection limits, and hence for which there are data values for all sample points, this ion will be discussed first. In Figure 5.10 the concentrations of F^- are plotted against pH and the samples are grouped according to the predefined groups shown in Figure 5.8. Groups I and II show a large degree of variability in F^- concentration, with values ranging from 0.32 mg/l to 27.5 mg/l and from 0.54 mg/l to 10.1 mg/l, respectively. In contrast, the group III waters form a comparatively tight cluster, with values ranging between 0.14 mg/l to 2.51 mg/l.

In section 5.5.1, it was shown that the most saline waters in the Dead Tree Area are 60% more saline than sea water. If the salinity of these samples is due soley to the evaporative concentration of marine salts, then this percentage would represent the maximum amount of evaporative concentration that has occurred in the Dead Tree Area. If the F^- concentration of sea water, which is 1.2 mg/l (Dictionary of the Physical Sciences, 1987), is increased by 60% through evaporative concentration, this yields a value of 1.92 mg/l. Consequently, 1.92 mg/l would be the maximum F^- concentration expected in the Dead Tree Area, under 'natural conditions'. Values greater than 1.92 mg/l indicate anthropogenic impact.

On the basis of the above argument, samples A1, A2, A4, a1 and a2 all have F^- concentrations in excess of what would be expected under 'natural conditions'. Samples A1, a1 and a2 fall in group I, sample A2 in group II and sample A4 in group III. The highest F^- concentrations occur in samples A1, A2 and a1 (27.5, 10.1 and 7.5 mg/l, respectively), whereas those of samples a2 and A4 are significantly lower (3.31 and 2.51 mg/l, respectively). The spatial distribution of the three samples with values >7.5 mg/l, ie. samples A1, A2 and a1, is shown overlaid on the spatial distribution of the three predifined groups on the map in Figure 5.10. The highest concentrations of F^- occur in the most northern portion of the Dead Tree Area, indicating the gypsum dumps as the most probable source of the F^-.

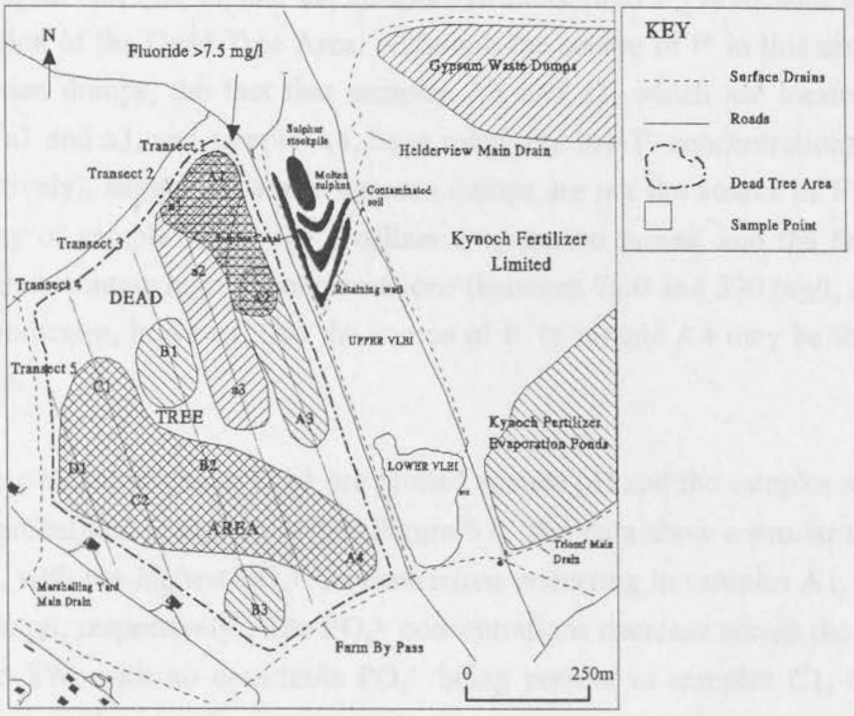

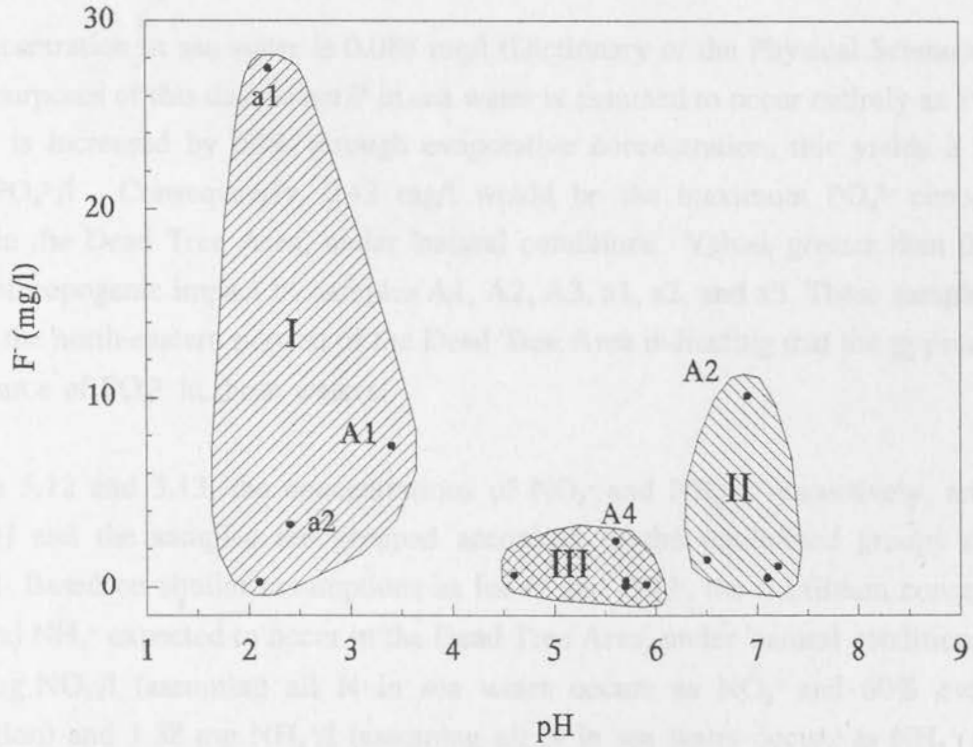

Figure 5.10 Plot of F^- concentration versus pH for subsurface water samples from the Dead Tree Area. The samples have been grouped according to the predefined groups shown in Figure 5.8. The spatial distribution of these groups, as well as that of samples with F^- concentrations >7.5 mg/l, are shown on the accompanying map.

In contrast to samples A1, A2, a1 and a2, sample A4 (2.51 mg/l F^-) is located in the most south-eastern portion of the Dead Tree Area. Although the source of F^- in this sample could be from the gypsum dumps, the fact that samples A3 and a3, which are located between samples A1, A2, a1 and a3, and sample A4, have relatively low F^- concentrations (0.54 and 0.32 mg/l, respectively), suggests that the gypsum dumps are not the source of F^- in sample A4. The proximity of sample A4 to the fertilizer evaporation ponds, and the fact that the fertilizer pond waters contain high F^- concentrations (between 76.0 and 320 mg/l, see chapter 4, section 4.3.1) indicates, however, that the source of F^- in sample A4 may be the fertilizer evaporation ponds.

In Figure 5.11 the concentrations of PO_4^{3-} are plotted against pH and the samples are grouped according to the predefined groups shown in Figure 5.8. The data show a similar trend to the F^- concentrations, with the highest PO_4^{3-} concentrations occurring in samples A1, A2 and a1 (1.8, 1.2 and 2.8 mg/l, respectively). The PO_4^{3-} concentrations decrease across the Dead Tree Area from NE to SW, with no detectable PO_4^{3-} being present in samples C1, C2 and D1 located in the most south-westerly portion of the site.

The P concentration in sea water is 0.088 mg/l (Dictionary of the Physical Sciences, 1987). If for the purposes of this discussion P in sea water is assumed to occur entirely as PO_4^{3-}, and this value is increased by 60% through evaporative concentration, this yields a value of 0.43 mg PO_4^{3-}/l . Consequently, 0.43 mg/l would be the maximum PO_4^{3-} concentration expected in the Dead Tree Area, under 'natural conditions'. Values greater than 0.43 mg/l indicate anthropogenic impact ie. samples A1, A2, A3, a1, a2, and a3. These samples are all located in the north-eastern portion of the Dead Tree Area indicating that the gypsum dumps are the source of PO_4^{3-} in these waters.

In Figures 5.12 and 5.13, the concentrations of NO_3^- and NH_4^+, respectively, are plotted against pH and the samples are grouped according to the predefined groups shown in Figure 5.8. Based on similar assumptions as for F^- and PO_4^{3-}, the maximum concentrations of NO_3^- and NH_4^+ expected to occur in the Dead Tree Area, under 'natural conditions', would be 4.51 mg NO_3^-/l (assuming all N in sea water occurs as NO_3^- and 60% evaporative concentration) and 1.38 mg NH_4^+/l (assuming all N in sea water occurs as NH_4^+ and 60% evaporative concentration). The concentrations of NO_3^- and NH_4^+ detected in the Dead Tree Area subsurface water samples range from 5.22 to 973 mg/l and 8.01 to 130 mg/l, respectively. The spatial distribution of these ions, shown in Figure 5.12 and 5.13, is, however, more complex than that of F^- and PO_4^{3-}. The highest concentrations of NO_3^- occur in samples a1, a2 and a3 (703, 449, and 973 mg/l). Elevated concentrations of NO_3^- also occur

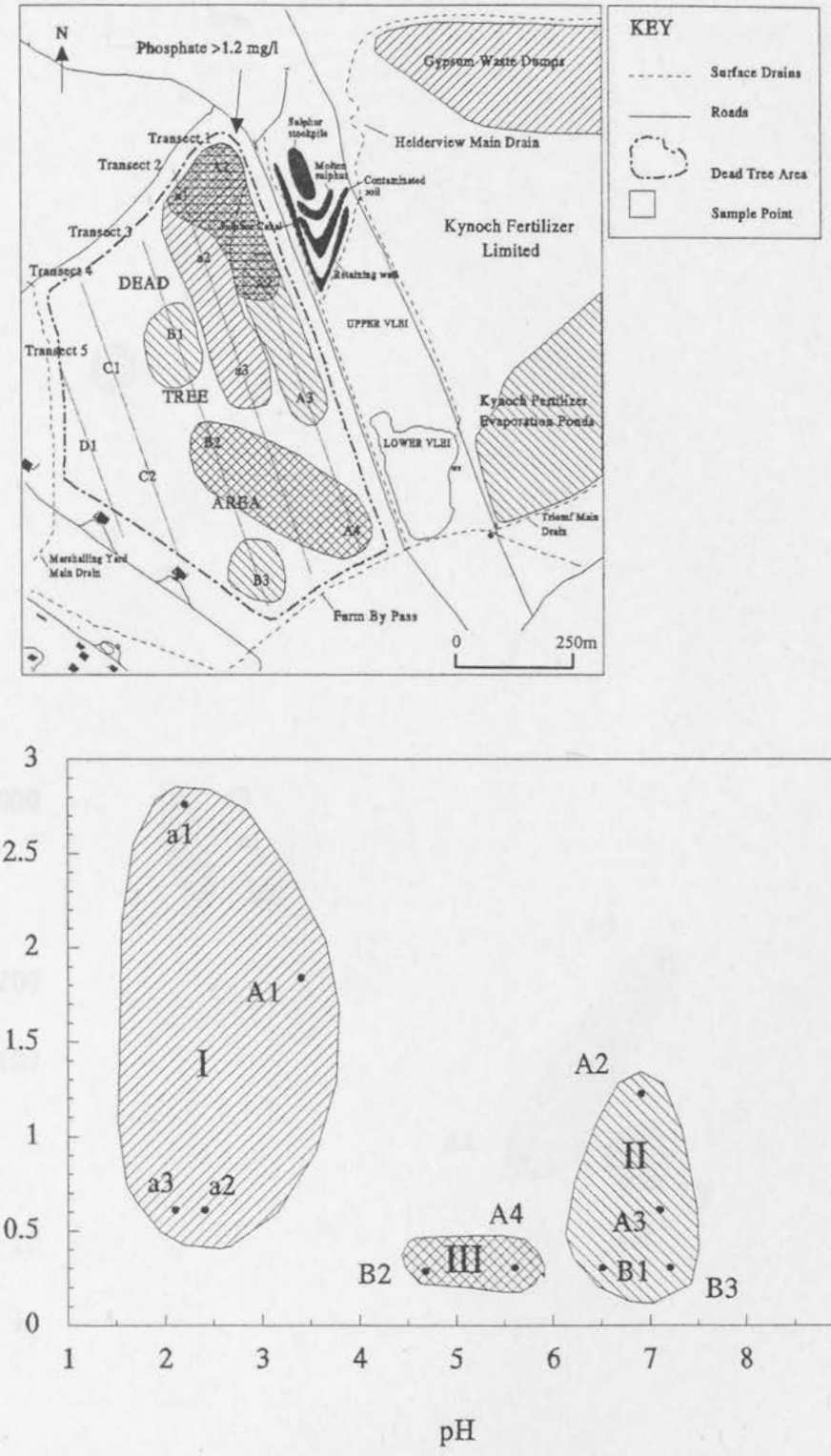

Figure 5.11 Plot of PO_4^{3-} concentration versus pH for subsurface water samples from the Dead Tree Area. The samples have been grouped according to the predefined groups shown in Figure 5.8. The spatial distribution of these groups, as well as that of samples with PO_4^{3-} concentrations >1.2 mg/l, are shown on the accompanying map.

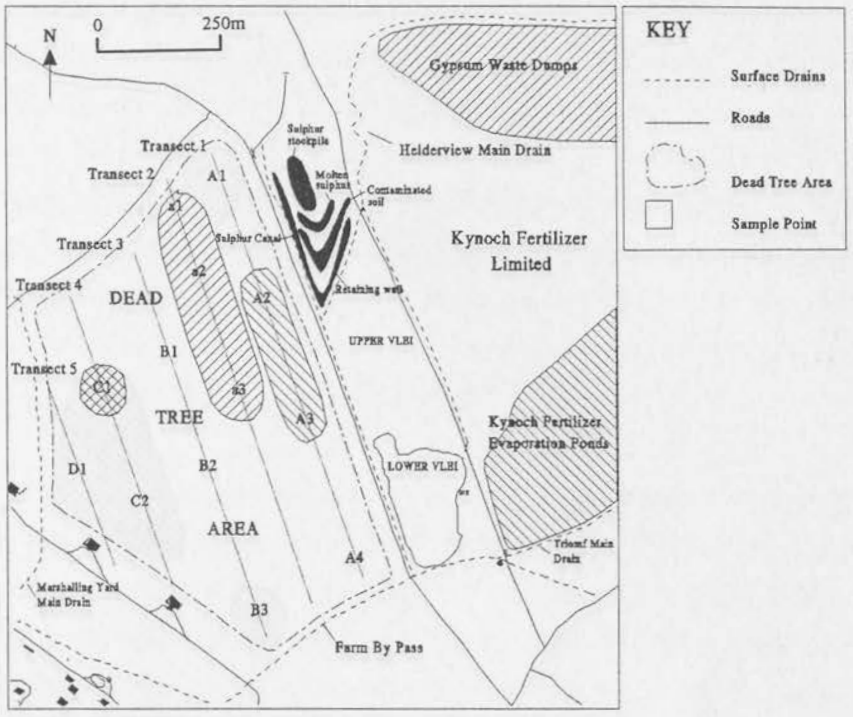

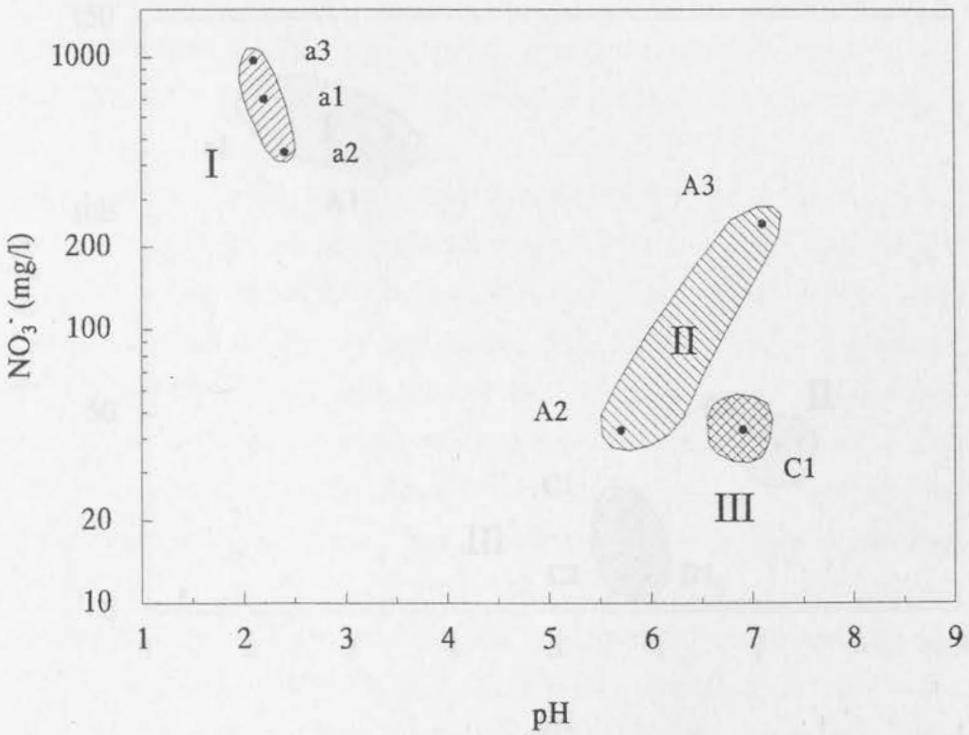

Figure 5.12 Plot of NO_3^- concentration versus pH for subsurface water samples from the Dead Tree Area. The samples have been grouped according to the predefined groups shown in Figure 5.8, and the spatial distribution of these groups shown on the accompanying map.

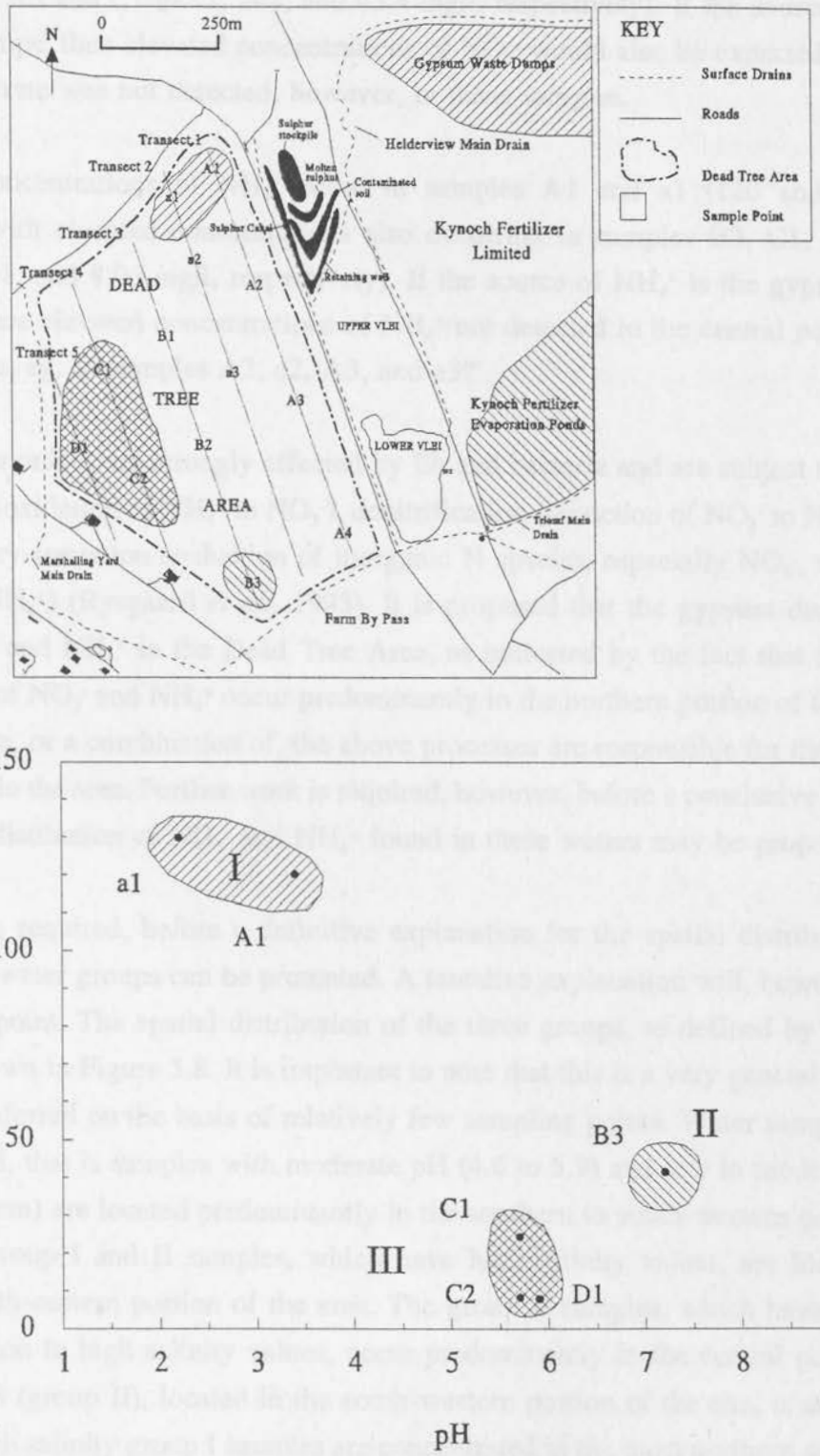

Figure 5.13 Plot of NH_4^+ concentration versus pH for subsurface water samples from the Dead Tree Area. The samples have been grouped according to the predefined groups shown in Figure 5.8, and the spatial distribution of these groups shown on the accompanying map.

in samples A2, A3 and C1 (43.2, 244, and 43.4 mg/l, respectively). If the source of NO_3^- is the gypsum dumps, then elevated concentrations of NO_3^- would also be expected in samples A1 and B1. Nitrate was not detected, however, in these samples.

The highest concentrations of NH_4^+ occur in samples A1 and a1 (120 and 130 mg/l, respectively), with elevated concentrations also occurring in samples B3, C1, C2 and D1 (42.4, 24.2, 8.01, and 8.06 mg/l, respectively). If the source of NH_4^+ is the gypsum dumps, however, why are elevated concentrations of NH_4^+ not detected in the central portion of the Dead Tree Area, eg. in samples A2, a2, A3, and a3?

Nitrate and ammonium are strongly affected by Eh and bacteria and are subject to processes of nitrification (oxidation of NH_4^+ to NO_3^-), denitrification (reduction of NO_3^- to N_2O and N_2), and dissimilatory reduction (reduction of inorganic N species, especially NO_3^-, to inorganic N, especially NH_4^+) (Rysgaard *et al.,* 1993). It is proposed that the gypsum dumps are the source of NO_3^- and NH_4^+ in the Dead Tree Area, as indicated by the fact that the elevated concentrations of NO_3^- and NH_4^+ occur predominantly in the northern portion of the area, and that one or more, or a combination of, the above processes are responsible for distribution of NO_3^- and NH_4^+ in the area. Further work is required, however, before a conclusive explanation for the spatial distibution of NO_3^- and NH_4^+ found in these waters may be proposed.

Further work is required, before a definitive explanation for the spatial distribution of the three proposed water groups can be presented. A tentative explanation will, however, will be offered at this point. The spatial distribution of the three groups, as defined by pH and EC values, was shown in Figure 5.8. It is important to note that this is a very general distribution that has been inferred on the basis of relatively few sampling points. Water samples plotting within group III, that is samples with moderate pH (4.6 to 5.9) and low to moderate salinity (1.6 to 4.6 mS/cm) are located predominantly in the southern to south-western portion of the site, whereas group I and II samples, which have high salinity values, are located in the central and north-eastern portion of the area. The group II samples, which have neutral pH values in addition to high salinity values, occur predominantly in the central portion of the site. Sample B3 (group II), located in the south-western portion of the site, is an exception. The low pH/high salinity group I samples are concentrated in the most northern section of the area but also form a "tongue" of low pH/high salinity water that extends southwards into the central section of the area.

Based on the distribution of sulphate, fluoride, phsophate, nitrate and ammonium in the water samples, it may be proposed that a groundwater contaminant plume has evolved from the

sulphur stockpile and gypsum dumps and that this plume has impacted on the aqueous chemistry of the Dead Tree Area. In Figure 5.14, the proposed movement of contaminants from the sulphur stockpile and gypsum dumps are illustrated schematically. A groundwater plume radiating south-westerly from the sulphur stockpile and gypsum dumps as indicated in this figure would impact first on the north-eastern section of the Dead Tree Area. This groundwater plume is likely to contain elevated concentrations of F^-, NO_3^-, NH_4^+, PO_4^{3-} and SO_4^{2-} and hence be responsible for *concentrations of these ions which exceed that which would be expected from the evaporative concentration of salts of marine origin.* It is important to note, however, that the salinity of the water samples arising from elevated concentrations of Na^{2+}, Cl^-, Ca^{2+}, and Mg^{2+} is natural and may be attributed to the evaporative concentration of marine salts.

The pH values of samples A1, a1, a2, and a3 (3.4, 2.2, 2.4 and 2.1, respectively) are all lower than that of the gypsum leachate collection pond water (pH 3.9), but higher than the leachate from the sulphur stockpile (pH 1.5). This suggests that mixing of subsurface water in the Dead Tree Area with a low pH contaminant plume evolving from the sulphur stockpile has occurred at the above sample points. The pH of samples A2, A3, and B1 is greater than 6.5, howeer, indicating that this plume has not affected these waters. The contaminant plume has thus migrated south-westward from the sulphur stockpile, across sample points A1, and a1, and then formed a "tongue" which extends across sample points a2, and a3 (see Figure 5.14). Some interaction between sample B2 and this low pH plume have occurred, as the pH of this sample (4.6) is lower than that of samples A2, A3, and B1. A possible explanation for the particular movment of this plume, may be that it is following a preferential flow path that has developed along residual structure from the Malmesbury shale still present in the clays of the area.

One further factor that needs consideration is the extreme salinity values found in samples A3 and a3 located in the central section of the area. The salinity of these two samples exceed that of the other samples by some 60 mS/cm or more and hence this would seem to indicate that concentration of contaminants around samples A3 and a3 in excess of other samples is occurring. This may be a consequence of bedrock topography and/or surface topography both or either of which may be resulting in the preferential accumulation and subsequent evaporative concentration of salts in the central portion of the site. A more detailed investigation will be needed, however, to confirm or refute the above explanation.

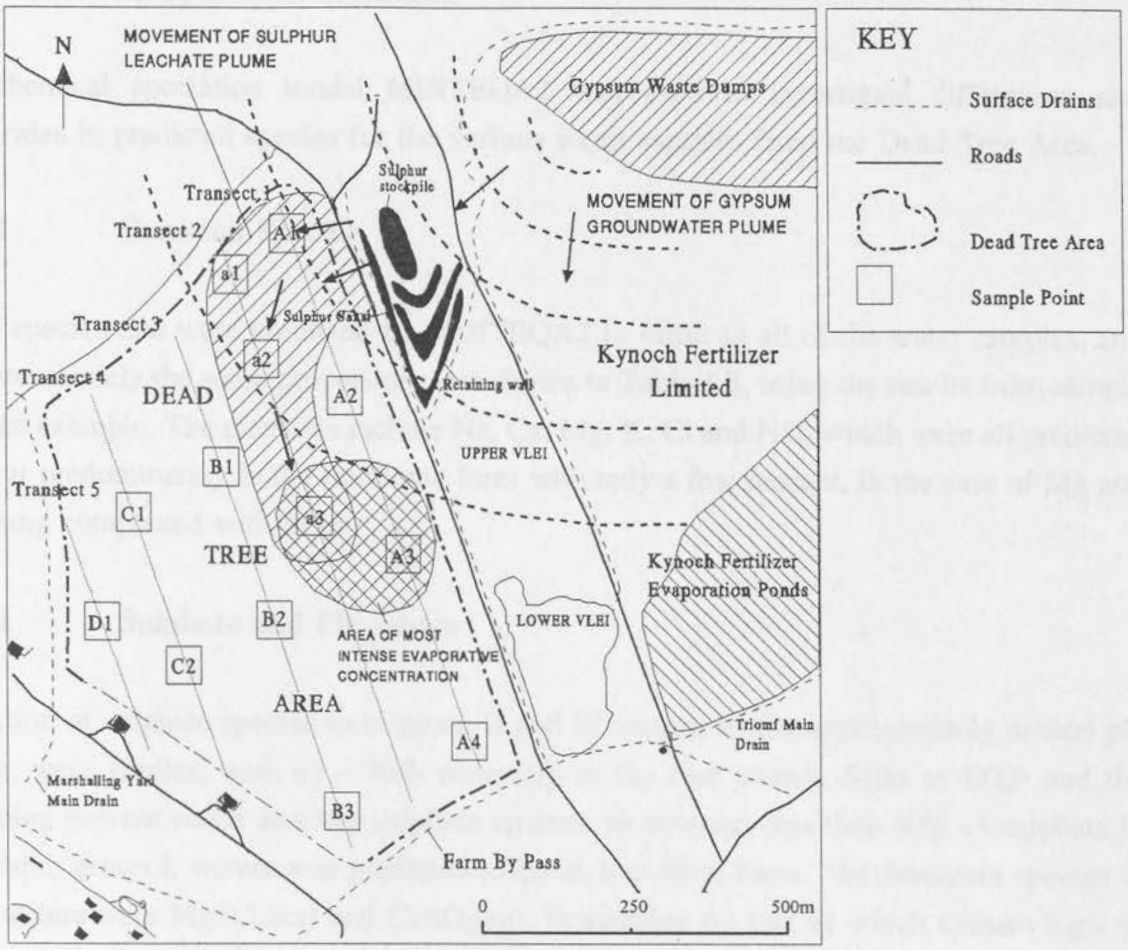

Figure 5.14 Schematic illustration of the proposed movement of groundwater contaminants from the gypsum dumps and sulphur stockpile.

5.5.3 Chemical Speciation Modelling

The chemical speciation model MINTEQA2 was used to investigate differences and similarities in predicted species for the various water samples from the Dead Tree Area.

5.5.3.1 Common Species

Those species that were predicted by MINTEQA2 to occur in all of the water samples, and in approximately the same proportions, are shown in Table 5.3, using the results from sample a3 as an example. The elements include Na, Ca, Mg, K, Cl and NO_3 which were all predicted to occur predominantly in the free ionic form with only a few percent, in the case of Mg and Ca, being complexed with SO_4^{2-}.

5.5.3.2 Sulphate and Phosphate

Prediction of sulphate speciation in group II and III waters, ie. the approximately neutral pH waters, were similar, with 65 - 70% occurring in the free anionic form as SO_4^{2-} and the remaining percent as Ca and Mg sulphate species. In contrast, less than 50% of sulphate in the acidic, group I, waters was predicted to be in free ionic form. The dominant species in these waters were $MgSO_4(aq)$ and $CaSO_4(aq)$. In samples A1 and a1 which contain high Al concentrations, approximately 3% of the total sulphate is complexed with Al in the species $AlSO_4^+$ and $Al(SO_4)^{2-}$.

Similar to sulphate, the speciation of phopshate in group II and III waters differs markedly from that of group I waters. The dominant species in the group II and III waters is $MgHPO_4(aq)$ (approx. 50 to 60%) whereas in the acidic group I waters, as may be anticipated, the more protonated forms $H_2PO_4^-$ and H_3PO_4 are the dominant species. The species $MgH_2PO_4^+$ and $CaH_2PO_4^+$ were predicted to be present in all three water groups.

5.5.3.3 Fluoride

As in the case of sulphate and phosphate, the speciation of F in group II and III samples is predicted to be similar, with F^- and MgF^+ being the only species. In the case of the acidic group I samples, no free ionic F is predicted to occur and less than 5% occurs as MgF^+. Instead F is found predominantly complexed with Al as AlF^{2+} (approx. 80%) and AlF_2^+ (approx. 15%).

Table 5.3 Chemical species predicted by MINTEQA2 as likely to be present in approximately the same proportions in all of the water samples from the Dead Tree Area. Values from sample a3 are used by way of example.

Constituent	Percentage Speciation Predicted
Na	Na^+ (99.4%)
Ca	Ca^{2+} (91.8%), $CaSO_4$(aq) (8.2%)
Mg	Mg^{2+} (92.8%), $MgSO_4$(aq) (7.2%)
K	K^+ (99.2%)
Cl	Cl^- (99.9%)
NO_3	NO_3^- (100.0%)

5.5.3.4 Heavy Metals

In general the heavy metal concentrations in these waters are very low, in many instances being below detection limits. Elevated concentrations of certain metals, notably Al and Mn, were detected, however, in some of the acidic group I water samples and hence the predicted speciation of these metals is of potential interest.

Due to the acidity of these waters the solubility of Al is greatly increased, and it is thus not surprising that Al is predicted to occur largely (35 to 59%) in the free ionic form as Al^{3+}. The remaining species include, in order of decreasing abundance, AlF^{2+}, AlF_2^+, $AlSO_4^+$ and $Al(SO_4)^{2-}$.

As in the case of Al, Mn occurs largely in the free ionic form, with only a few percent (< 20%) occurring in complexation with the anions Cl^- and SO_4^{2-}, as the species $MnCl^+$ and $MnSO_4$(aq).

5.5.4 Mineral Solubility Equilibria

Based on the range in chemical composition of the water samples from the Dead Tree Area, it may be anticipated that:

(i) the range of minerals that are predicted by MINTEAQ2 to be either in equilibrium with or supersaturated with respect to these water samples would also vary significantly, and

(ii) the saturation indices of minerals for water samples falling within the same group (as defined in Figure 5.8) would be similar.

The MINTEQA2 results for samples A2, A3, B1 and B3 are tabulated in Appendix E: Table E5 and for samples B2, A1 and A4 in Appendix E: Table E6. No minerals were predicted to be close to equilibrium (SI between -0.5 and 0.5) or supersaturated with respect to samples a1, a2, a3, C1, C2 and D1. The results show the following general correspondences with the three predefined groups:

(i) *Group I [low pH (<3.4)/high salinity (18 to 81 mS/cm)]:* no minerals with SI values greater than -0.5 were predicted by MINTEQA2 to occur for samples a1, a2 and a3. Although elevated Al concentrations (particularly in sample a1 which contains 67.2 mg/l Al) are present in these waters, the MINTEQA2 results reveal that the solubility of Al in these samples is sufficiently high (due to the low pH values of <2.5) that saturation of Al bearing minerals does not occur. According to MINTEQA2, sample A1, which was also included in group I does, however, show supersaturation for three Al containing minerals, namely alunite, kaolinite and pyrophyllite. The explanation for the differences in SI values between samples a1, a2, and a3 and sample A1 is most likely due to two factors. Firstly, the Al concentration in sample A1 (108 mg/l) is one to two orders of magnitude greater that of the other three samples, and secondly, the pH of sample A1 is significantly higher (pH 3.4) than that of samples a1, a2 and a3 (pH 2.2, 2.4 and 2.1, respectively). This has the consequence that the solubility of Al in sample A1 is significantly less than in the other three samples, and supersaturation of Al containing minerals may be expected.

(ii) *Group II [(neutral pH (≈7)/moderate-high salinity (7 to 90 mS/cm)]:* the MINTEQA2 results for samples A2, A3, B1 and B3 are similar and the range of minerals quite different from those in group I and III samples. These results will be discussed later in this section.

(iii) *Group III [(moderate pH (5.6 to 5.9)/low-moderate salinity (1.6 to 4.6 mS/cm)]:* no minerals with SI values greater than -0.5 were predicted by MINTEQA2 to occur for samples C1, C2 and D1. The proposed explanation for this is that the salt concentrations in these waters are sufficiently low not to result in the saturation of any minerals. Although the salt contents of samples A4 and B2, which were also included in group III, are equivalent to samples C1, C2, and D2, numerous Al containing

minerals were predicted to be supersaturated in these two samples.

The saturation indices of selected minerals for samples B2 and A4 are shown graphically in Figure 5.15. Although the magnitude of the SI values for these two samples are different, the relative values of the different minerals are similar, with alunite, kaolinite, leonhardite, muscovite and pyrophyllite being the most supersaturated minerals in both samples. These minerals are all Al containing minerals and hence the difference in magnitude of SI values between the two samples is a consequence of the Al concentrations in the two samples and its relative solubility. Sample A4 has an Al concentration of 3.88 mg/l and a pH of 5.6. Sample B2, on the other hand, has an Al concentration of 1.76 mg/l and a pH of 4.6. Sample A4, therefore, has a higher Al concentration and a lower Al solubility than sample B2, and it is thus not surprising that the SI values of Al containing minerals are higher for sample A4 than those of sample B2.

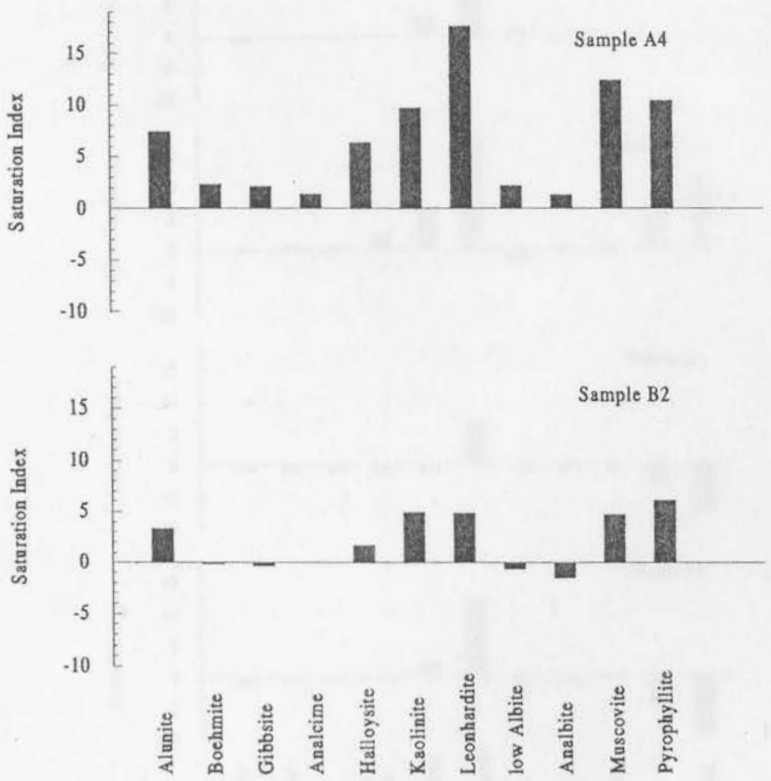

Figure 5.15 Saturation Indices of selected minerals calculated by MINTEQA2 for samples A4 and B2. Data values from Appendix D: Table D6.

In contrast to samples A4 and B2, the samples from group II (A2, A3, B1 and B3) are characterised by being in equilibrium with or supersaturated with respect to a range of Ca and Mg sulphates, carbonates, phosphates, fluorides and silicates. The SI values of these minerals for samples A2, A3, B1 and B3 are shown graphically in Figure 5.16.

The plot shows that the carbonate minerals aragonite, calcite, dolomite and magnesite, are in equilibrium in all four samples. Fluorite, anhydrite and gypsum are also close to equilibrium in all four samples. The major differences in SI values are for the silicate minerals talc and tremolite, which are undersaturated in samples B1 and B3, supersaturated in sample A3, and in equilibrium in sample A2. These differences are most probably due to the fact that (a) in samples B1 and B3, the Si concentrations are comparatively low (5.11 and 0.76 mg/l, respectively) whereas in samples A2 and A3, the concentrations are high (20.5 and 17.2 mg/l,

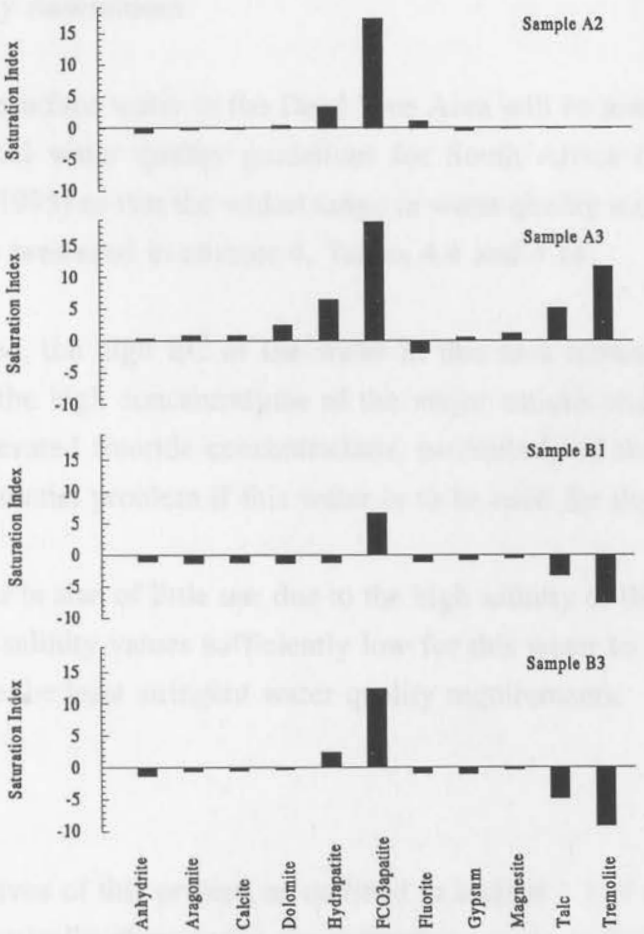

Figure 5.16 Saturation Indices of selected minerals calculated by MINTEQA2 for samples A2, A3, B1 and B3. Data values from Appendix D: Table D5.

respectively), and (b) the Ca^{2+} and Mg^{2+} concentrations in A3 are an order of magnitude greater than those of A2, B1 or B3. Hence it may be anticipated that these minerals are undersaturated in samples B1 and B3, due to the low Si concentrations in these samples, in equilibrium with sample A2 due to the high Si concentration but comparatively low Ca^{2+} and Mg^{2+} concentrations, and supersaturated in sample A3 due to high concentrations of Si, Ca^{2+} and Mg^{2+}.

In summary, MINTEQA2 predicts no minerals with SI values greater than -0.5 for water samples in groups I and III, and predicts that the minerals aragonite, calcite, dolomite, magnesite, fluorite, anhydrite and gypsum are all either close to equilibrium or supersaturated in all four samples in group II. Samples A4 and B2, which were included in group II, are an exception to the above generalizations, as MINTEQA2 predicts that a range of Al containing minerals are supersaturated with respect to these samples.

5.5.5 Water Quality Assessment

The quality of the subsurface water in the Dead Tree Area will be assessed against the draft domestic and industrial water quality guidelines for South Africa (Department of Water Affairs and Forestry, 1995) so that the widest range in water quality standards are considered. These standards were presented in chapter 4, Tables 4.4 and 4.14.

As may be anticipated, the high EC of the water in this area immediately excludes it for domestic use due to the high concentrations of the major cations and anions. Heavy metal contamination and elevated fluoride concentrations, particularly of those samples in groups I and II are also a potential problem if this water is to be used for domestic purposes.

Industrially, this water is also of little use due to the high salinity of the water. Only samples A4, C2 and D1 have salinity values sufficiently low for this water to be used by category 4 industries which have the least stringent water quality requirements.

5.6 Conclusions

In meeting the objectives of this project, as outlined in section 1.1 of chapter 1, this chapter has (a) served to chemically characterise the subsurface water in the Dead Tree Area, and (b) has considered whether contamination from the gypsum dumps, fertilizer evaporation ponds and/or sulphur stockpile has impacted on the water in the Dead Tree Area.

The analyses of subsurface water in the Dead Tree Area revealed marked spatial variability in water charactertistics. On the basis of pH and EC data the water samples were grouped into three groups, namely: low pH/high salinity, neutral pH/moderate to high salinity, and moderate pH/low to moderate salinity.

Based on consideration of the geology, topography and proximity to the ocean of the Dead Tree Area, it was proposed that under 'natural conditions' subsurface water in this area would have an approximately neutral pH and low to high salinity depending on the degree of evaporative concentration. The ratios of Na^+ to Cl^- and Ca^{2+} to Mg^{2+} in all samples were found to be the same as those of sea water. The ratios of Cl^- to SO_4^{2-} and Na^+ to K^+ were not, however, found to be the same as those of sea water for all samples, indicating anthropogenic contamination.

Because the water in the Dead Tree Area would have a neutral pH under 'natural conditions', samples that had low pH values were suspected to have been affected by contamination from one or more of the surrounding industrial activities. These samples were located adjacent to the sulphur stockpile and hence SO_4^{2-} concentrations in these samples were investigated. The low pH/high salinity samples were found to have elevated SO_4^{2-} concentrations. This was considered to indicate that these samples had been impacted by a low pH contaminant plume evolving from the sulphur stockpile.

To assess whether contamination from the gypsum dumps or fertilizer evaporation ponds has also affected the water in the Dead Tree Area, the concentrations of F^-, PO_4^{2-}, NO_3^- and NH_4^+ were investigated, as these were shown in chapter 4 to be elevated in the gypsum leachate ponds and fertilizer evaporation ponds but not in the sulphur leachate drain. Elevated concentrations of these ions were found in water samples located in the north-eastern section of the site. Based on this finding and the fact that the groundwater flow direction is south-west, it was proposed that these ions represent contamination originating from the gypsum dumps. It has thus been concluded that contamination from the gypsum dumps and sulphur stockpile has impacted on the water in the Dead Tree Area.

Chemical speciation modelling revealed that in all water samples, the elements Na, Ca, Mg, K, Cl and NO_3 were predicted to occur predominantly in the free ionic form. The speciation of the remaining elements were similar within the group II and III samples due to the similarity in pH values of these samples, but very different to that of group I samples due to their lower pH. The range and variability in mineral solubility equilibria were predicted by MINTEQA2 to be large due to the large range in chemical composition of the water samples.

However, the suite of minerals found to be close to equilibrium or supersaturated in water samples from any one group were, in general, found to be similar.

The quality of subsurface water in the Dead Tree Area was assessed according to the domestic water use and industrial water use guidelines as these provided the widest range in water quality requirements. The water quality was found to be poor, and did not meet either the domestic or the industrial use guidelines.

6. SOIL CHEMISTRY OF THE DEAD TREE AREA

6.1 Introduction

The objectives of this chapter are twofold: firstly, to chemically characterise the soils of the Dead Tree Area, with emphasis on the effects of industrial contamination on soil salinity and sodicity and consequent effects on the growth of plants; and secondly, to determine the effect of gypsum application, as an amelioration strategy, on the hydraulic conductivity of a composite soil sample from the Dead Tree Area. The first objective requires knowledge concerning 'background levels' of salinity and sodicity of soils in the area. In this regard, the chemistry of soils from the farmland area, located north of the gypsum dumps, will also be considered.

In this chapter the general characteristics of the soils in the Dead Tree Area and farmland area, such as major and trace element composition, soil pH, organic carbon content, clay content and clay mineralogy, are first described and compared. The salinity and sodicity of these soils is then discussed, and the results of foliar analyses of *Eucalyptus* trees growing on the perimeter of the Dead Tree Area interpreted in light of these findings. In conclusion, the results of a leaching trial are used to assess the effect of gypsum application as an amelioration strategy for saline, sodic soils in the Dead Tree Area.

6.2 Soil and Foliar Sampling and Analysis

The collection and analysis of soil samples from the Dead Tree Area and farmland area (located north of the gypsum dumps) has been described in chapter 3. Fourteen soil samples were collected, each comprising a surface and subsurface sample, and analysed following standard methods described in *Methods of Soil Analysis, Part 1: Physical and Mineralogical Methods* (Klute *et al. (ed.)*, 1989) and *Methods of Soil Analysis, Part 2: Chemical and Microbiological Properties* (Page *(ed.)*, 1982). Analyses conducted were pH, soluble salts, organic carbon (Walkley, 1935), exchangeable/extractable cations (ammonium acetate method), clay percentage, mineralogical analysis of clay fraction by XRD, and bulk soil analysis by XRFS. Non-standard methods, details of which are discussed below, included determination of dispersible clay percentage and leaching tests to determine the effect of gypsum amendment on the hydraulic conductivity of a composite soil from the Dead Tree Area.

Sixteen *Eucalyptus* foliar samples were collected along two transects, oriented NE to SW, in the Dead Tree Area (see chapter 3). The samples were analysed for N, P, K, Ca, Mg, Na, Mn, Fe, Zn and Cu in the laboratories of the Institute for Commercial Forestry Research, University of Natal, Pietermaritzburg following standard methods described in Donkin *et al.*, (1993), Heffernan (1985), Kalra and Maynard (1991), and Nicholson (1984).

6.2.1 Dispersible Clay Percentage

Dispersible clay percentage was determined using the method of Levy and Torrento (1995). The soil samples (13 g) were first washed with 30 ml of distilled water (DW) for 30 seconds to remove excess salts. The suspensions were then centrifuged and the electrical conductivity (EC) of the supernatant measured. When the EC of the supernatant was higher than 0.1 dS/m, washing was repeated until an EC < 0.1 dS/m was obtained. The samples were transfered to 250 ml plastic bottles, and the volume brought to 200 ml by adding DW, to obtain a soil:solution ratio of 1:15. The bottles were placed on a horizontal shaker, and shaken at 125 cycles per minute for 30 min. The bottles were then left standing for 4 hours. From each bottle, 20 ml of suspension was siphoned off from a depth of 50 mm and oven dried, and the amount of clay determined gravimetrically. Percent dispersed clay, ie. the ratio of mass of clay dispersed to the mass of clay in the test sample expressed in percent, was then calculated.

6.2.2 Effect of Gypsum Amendment on Soil Hydraulic Conductivity

The effect of gypsum application on the hydraulic properties of a soil composite was studied using leaching columns following methods described by Smith and Fey (1996).

A composite soil sample was created by mixing equal parts, by mass, of six soil samples (A2a, A3a, B1a, B2a, C1a & C2a) from the Dead Tree Area. Samples were dried, crushed and sieved through a 2 mm nylon sieve prior to compositing. Six soil columns were prepared using 5.4 cm diameter and 14 cm long perspex cylinders. The base of each cylinder was fitted with a perforated perspex disc and a rubber stopper with a central glass tube as an outlet. The soil columns were packed on a base of glass wool matting, which was mounted on the perforated perspex disc. Glass wool matting was also placed on top of the soil column to protect the soil surface against disruption and development of preferential flow paths by the influent water. The columns were capped with a rubber stopper with a central glass tube as an inlet, and the inlet tubes connected, by means of plastic pipping, to a single constant head mariotte bottle. The experimental set up is illustrated in Figure 6.1.

The six columns were labelled A to F with columns A and B being controls containing untreated soil composite. In columns C and D, gypsum from the gypsum dumps at Kynoch Fertilizer Limited was applied to the soil surface at a rate equivalent to 10 tons/ha. In columns E and F, the same gypsum source and application rate was used, however, the gypsum was mixed into the soil samples prior to the packing of the columns. The depth of soil in each column was 130 mm.

All columns were leached using distilled water and the time and volume of leachate generated recorded incrementally. At each increment, a sample of leachate was collected and the pH and electrical conductivity of the solution determined.

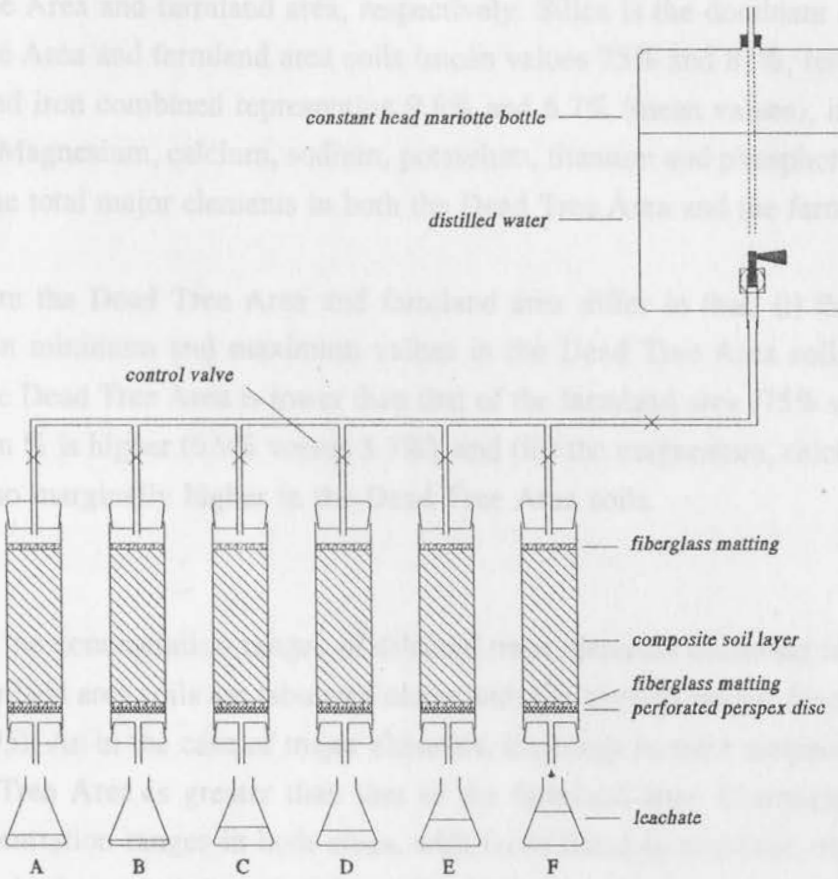

Figure 6.1 Illustration of soil column leaching apparatus. Columns A and B were untreated control samples, C and D had the equivalent of 10 tons/ha of gypsum applied to the soil surface, and E and F had the equivalent of 10 tons/ha gypsum mixed into the soil column. The depth of soil in each column was 130 mm.

6.3 Results and Discussion

6.3.1 Major and Trace Element Composition

The results of the XRFS semi-quantitative major element anlayses and quantitative trace element analyses of soil samples from the Dead Tree Area and farmland area are tabulated in Tables 6.1 and 6.2. Surface soil samples are designated with a lower case 'a' eg. B1a, and subsurface soils with a lower case 'b' eg. B1b. This convention will be followed throughout this chapter.

The major element results have been summarised in Table 6.3, which shows the mean, minimum and maximum values of the major elements, expressed as % oxides, for soils from the Dead Tree Area and farmland area, respectively. Silica is the dominant element in both the Dead Tree Area and farmland area soils (mean values 75% and 82%, respectively), with aluminium and iron combined representing 9.8% and 6.7% (mean values), in the two areas, respectively. Magnesium, calcium, sodium, potassium, titanium and phosphorus make up less than 4% of the total major elements in both the Dead Tree Area and the farmland area soils.

The soils from the Dead Tree Area and farmland area differ in that, (i) there is a greater range between minimum and maximum values in the Dead Tree Area soils, (ii) the mean silica % in the Dead Tree Area is lower than that of the farmland area (75% versus 82%) and the aluminium % is higher (6.9% versus 3.7%), and (iii) the magnesium, calcium and sodium values are also marginally higher in the Dead Tree Area soils.

In Table 6.4, the concentration ranges of selected trace elements occurring in the Dead Tree Area and farmland area soils are tabulated along with the 'normal ranges' found in soils (from Alloway, 1995). As in the case of major elements, the range in trace element concentrations in the Dead Tree Area is greater than that of the farmland area. Comparison of the trace element concentration ranges in both areas, with those listed as normally occurring in soils, shows that, in both cases, these ranges lie well within the concentration ranges found in soils, and that these concentrations are very low. This indicates that either the soils in both areas are poor in silicates composed of transition metal cations, and/or have been highly weathered resulting in the dissolution of such minerals (particularly olivines, pyroxenes and amphiboles) and removal of these metals from the soils.

Table 6.1 **Major element concentrations (semi-quantitative, expressed as % oxides) in soils from the Dead Tree Area and farmland area (using powder briquettes) and organic matter determined by wet digestion.**

Sample No.	Fe_2O_3	TiO_2	BaO	CaO	K_2O	Cl	SO_2	P_2O_5	SiO_2	Al_2O_3	MgO	Na_2O	Organic Matter(%)	Total
Dead Tree Area														
A1a	2.29	0.15	0.02	0.44	0.29	0.66	1.23	0.17	55.3	2.14	0.53	0.38	28	91.62
A1b	1.21	0.14	0.03	0.07	0.27	0.10	0.14	0.05	84.8	1.27	0.27	0.19	0.3	88.82
A2a	1.07	0.15	0.02	0.12	0.31	0.15	0.12	0.02	89.0	1.56	0.46	0.29	0.6	93.89
A2b	2.36	0.25	0.02	0.32	0.76	0.32	0.17	0.03	70.0	8.16	3.94	0.55	0.3	86.99
A3a	1.97	0.23	0.03	0.38	0.49	3.21	0.32	0.07	80.1	3.13	1.23	2.94	1.3	95.37
A3b	4.66	0.36	0.03	0.37	0.83	1.79	0.21	0.02	68.7	11.31	5.95	1.57	0.0	95.84
A4a	1.86	0.26	0.02	0.32	0.65	0.03	0.16	0.11	78.2	3.54	0.35	0.23	5.2	91.05
A4b	1.34	0.23	0.02	0.11	0.68	0.01	0.05	0.04	84.6	3.54	0.35	0.28	0.0	91.28
B1a	2.12	0.30	0.03	0.35	0.61	0.43	0.22	0.08	73.6	3.40	0.96	0.43	1.6	84.18
B1b	3.45	0.39	0.03	0.27	0.89	0.32	0.11	0.02	77.7	9.29	3.81	0.69	0.0	96.96
B2a	3.38	0.26	0.03	0.69	0.62	0.17	0.25	0.10	71.4	5.27	0.99	0.22	0.6	84.10
B2b	4.06	0.36	0.02	0.47	0.88	0.07	0.08	0.03	72.6	12.47	2.35	0.32	0.3	94.06
B3a	4.49	0.49	0.03	0.56	1.02	0.08	0.38	0.33	63.5	8.88	0.97	0.29	2.6	83.66
B3b	4.95	0.57	0.03	0.27	1.35	0.02	0.07	0.04	68.9	14.70	2.37	0.44	0.5	94.22
C1a	3.13	0.32	0.03	0.97	0.68	0.22	0.30	0.13	68.6	5.29	1.23	0.33	4.3	85.57
C1b	3.32	0.36	0.02	0.28	0.77	0.02	0.06	0.03	79.2	9.16	1.49	0.26	0.0	94.99
C2a	2.53	0.31	0.02	0.57	0.72	0.02	0.15	0.09	71.8	6.31	0.77	0.17	2.7	86.19
C2b	3.55	0.35	0.02	0.31	0.88	0.02	0.07	0.03	76.3	11.19	1.53	0.23	0.3	94.76
D1a	3.03	0.29	0.02	0.28	0.63	0.03	0.10	0.06	90.9	6.20	0.87	0.20	1.8	94.37
D1b	3.67	0.35	0.02	0.29	0.76	0.01	0.15	0.03	76.8	11.29	1.53	0.19	0.0	95.04
Farmland Area														
1a	4.58	0.23	0.02	0.13	0.78	0.01	0.05	0.12	79.7	6.13	0.52	0.16	0.0	92.48
1b	4.86	0.21	0.02	0.09	0.74	0.01	0.06	0.06	76.7	6.30	0.05	0.14	0.0	89.72
2a	1.98	0.10	0.01	0.06	0.19	0.01	0.04	0.07	87.2	1.73	0.11	0.06	1.7	93.27
2b	2.58	0.09	0.01	0.05	0.17	0.00	0.03	0.06	89.9	1.56	0.10	0.05	1.7	96.45
3a	2.24	0.11	0.01	0.09	0.26	0.01	0.06	0.10	78.9	2.36	0.22	0.07	13.4	97.97
3b	2.31	0.09	0.01	0.04	0.21	0.00	0.03	0.05	84.7	2.09	0.18	0.06	7.4	97.17
4a	2.61	0.18	0.03	0.45	0.58	0.01	0.11	0.16	83.5	4.10	0.64	0.17	0.0	92.56
4b	3.11	0.18	0.02	0.39	0.57	0.03	0.11	0.06	81.8	6.09	1.22	0.21	0.0	93.81

Table 6.2 Trace element concentrations (quantitative) in soils from the Dead Tree Area and farmland area (using powder briquettes).

Sample No.	Zn	Cu	Ni	Co	Mn	Cr	V	Mo	U	Pb
Dead Tree Area										
A1a	9.3	23	52	3.2	155	64	23	6.2	1.9	16
A1b	5.0	8.2	21	BDL	92	33	12	3.6	0.8	6.0
A2a	4.5	6.1	11	2.2	124	33	11	2.6	BDL	4.5
A2b	9.3	3.8	16	6.9	203	37	36	0.2	0.3	6.7
A3a	13	10	40	BDL	198	53	23	3.8	1.6	11
A3b	17	6.4	64	9.7	365	64	56	2.4	1.0	14
A4a	16	14	16	2.7	169	55	20	4.5	0.5	25
A4b	6.1	5.9	9.2	BDL	89	37	19	2.4	1.7	5.1
B1a	14	11	18	3.7	262	67	24	3.8	1.2	13
B1b	15	7.6	53	6.5	247	60	55	3.1	0.5	13
B2a	20	15	48	5.0	374	70	31	5.7	0.5	24
B2b	16	7.2	26	8.8	143	65	45	2.6	BDL	14
B3a	32	25	26	5.9	250	77	47	5.1	3.4	27
B3b	20	9.9	27	15	365	70	59	2.4	3.0	21
C1a	24	16	25	3.8	246	67	30	5.3	2.4	26
C1b	14	7.1	18	6.2	171	55	38	3.2	1.3	11
C2a	17	8.8	15	5.0	250	51	29	3.1	0.9	20
C2b	1.2	5.6	19	7.1	92	59	41	2.3	0.8	13
D1a	13	12	27	5.5	196	68	35	5.0	1.6	17
D1b	12	5.5	20	11	126	71	52	2.2	1.2	13
Farmland Area										
1a	16	8.1	16	4.6	85	44	52	2.4	0.2	13
1b	13	6.0	19	4.0	65	42	57	1.7	0.1	11
2a	6.1	5.2	7.4	BDL	61	29	33	3.1	1.0	3.9
2b	5.5	10	20	BDL	89	42	35	5.2	1.2	4.7
3a	10	6.4	16	2.6	68	31	36	2.1	0.5	7.5
3b	6.4	6.1	20	2.4	61	32	35	3.0	0.4	3.8
4a	13	10	23	BDL	101	45	33	2.7	0.1	10
4b	11	5.9	14	3.8	77	48	47	2.0	0.3	9.9

Footnotes: Units - all elements expressed in ppm
BDL - below detection limits

Table 6.3 Major element mean, minimum and maximum values in soils[1] from the Dead Tree Area and farmland area (using XRFS semi-quantitative major element analyses on powder briquettes).

Element	Dead Tree Area			Farmland Area		
	Mean	Min.	Max.	Mean	Min.	Max.
SiO_2	75	55.3	90.1	82	76.7	89.9
Al_2O_3	6.9	1.27	14.7	3.7	1.56	6.30
Fe_2O_3	2.9	1.07	4.95	3.0	1.98	4.86
MgO	1.6	0.27	5.95	0.4	0.05	1.22
CaO	0.4	0.07	0.97	0.2	0.09	0.45
Na_2O	0.5	0.17	2.94	0.1	0.07	0.21
K_2O	0.7	0.27	1.35	0.5	0.17	0.57
TiO_2	0.3	0.14	0.57	0.2	0.09	0.23
P_2O_5	0.1	0.02	0.17	0.1	0.05	0.16

Footnotes: 1 - all data in %

Table 6.4 Concentration ranges of selected trace elements in soils[1] and soils from the Dead Tree Area and farmland area.

Element	Normal Range in Soils[1]	Range in Dead Tree Area	Range in farmland area
Zn	1 - 900	1.2 - 32	5.5 - 16
Cu	2 - 250	3.8 - 25	5.2 - 10
Ni	2 - 270	9.2 - 64	7.4 - 23
Co	0.5 - 65	BDL - 15	BDL - 4.6
Mn	20 - 10000	89 - 374	61 - 101
Cr	5 - 1500	33 - 77	31 - 48
V	3 - 500	11 - 59	33 - 57
Mo	0.1 - 40	0.2 - 6.2	1.7 - 5.2
U	0.7 - 9	BDL - 3.4	0.1 - 1.2
Pb	2 - 300	4.5 - 27	3.8 - 13

Footnotes: Units - all elements in ppm
1 - from Alloway, 1995, pg. 354
BDL - below detection limits

6.3.2 Soil pH, organic C% and clay%

The results of the soil pH, organic carbon and clay content analyses for the Dead Tree Area and farmland area are tabulated in Table 6.5. The soil pH values have been illustrated graphically in Figure 6.2.

The soil pH(water) values for the Dead Tree Area and farmland area range from 3.3 to 7.7 with the averages for the two areas being 6.3 and 5.9, respectively. Three samples from the Dead Tree Area, namely A1a, A1b and B2a, may be classified as acid soils because their pH(water) values are less than 5.5 (De Pauw, 1994). Of the three samples, A1a and A1b have pH(water) values significantly less than 5.5, with pH(water) values of 3.3 and 4.0, respectively. The analysis of *soil water sample A1*, sampled at the same location as soil samples A1a and A1b and reported in chapter 5, revealed high acidity (pH 3.4; acidity 13.6 mmol/l) and an elevated Al concentration (1.8 mg/l) in this water. Consequently the low pH(water) values of these two soil samples are expected.

Figure 6.2 shows that, with the exception of samples A4 and D1, the subsurface soils in the Dead Tree Area have higher pH(water) values than the surface samples. Samples 1, 2 and 3 in the farmland area show this same trend. The most extreme difference in pH(water) between surface and subsurface samples occurs in sample B2, in the Dead Tree Area, which has a surface pH(water) of 5.2 and subsurface pH(water) of 7.5.

The pH($CaCl_2$) values in both the surface and subsurface soils of all samples are less than those of the pH(water) values. This is expected as the use of 0.01*M* $CaCl_2$ results in a higher proportion of exchangeable H^+ and Al^{3+} being displaced than when distilled water is used, and consequently a lower pH value is recorded. The measurement of soil pH in $CaCl_2$ is useful, thus, because the difference between pH($CaCl_2$) and pH(water) provides a crude indication of the exchange capacity of the soil (Wild, 1994). The 'ΔpH' values, which are tabulated in Table 6.5, have a range of bewteen 0 and 1.1 pH units in the Dead Tree Area, and a comparatively narrower range of between 0.4 and 1.0 pH units in the farmland area. No trend exists between ΔpH values and surface and subsurface samples.

The organic carbon percentage of the soil samples is shown graphically in Figure 6.3 (see Table 6.5. for numerical data). The soils range in organic carbon % from 0.2% in samples A2b, B2b and C2b, to 17.4% in sample A1a. Alloway (1995) lists the average organic carbon % of 3045 soil samples from the USA as being 4.18% (minimum 0.09%; maximum 63.0%, median 1.05%). Twenty three out of twenty eight of the soil samples from

Table 6.5 **Soil pH(water and $CaCl_2$), organic C% and clay % for surface (eg. A1a) and subsurface (eg. A1b) samples form the Dead Tree Area and farmland area.**

Sample No.	pH (water)	pH ($CaCl_2$)	ΔpH	Organic C (%)	Clay %[1]
Dead Tree Area					
A1a	3.3	3.2	0.1	17.4	ND
A1b	4.0	3.7	0.3	0.2	ND
A2a	7.2	6.7	0.5	0.4	4.60
A2b	7.7	7.4	0.3	0.2	18.1
A3a	7.2	7.1	0.1	0.8	ND
A3b	7.7	7.7	0.0	0.3	ND
A4a	5.8	4.9	0.9	3.3	5.50
A4b	5.6	4.7	0.9	4.5	3.90
B1a	6.5	6.3	0.2	1.0	ND
B1b	7.4	7.2	0.2	0.5	ND
B2a	5.2	4.8	0.4	1.6	15.7
B2b	7.5	6.7	0.8	0.2	ND
B3a	5.8	5.0	0.5	1.6	21.9
B3b	6.9	6.1	0.8	0.3	ND
C1a	6.4	5.9	0.5	2.7	ND
C1b	6.7	5.8	0.9	1.6	27.3
C2a	6.1	5.2	0.9	1.7	ND
C2b	6.6	5.8	0.8	0.2	ND
D1a	6.3	5.5	0.8	1.1	15.9
D1b	6.3	5.2	1.1	1.1	ND
Farmland Area					
1a	5.6	4.8	0.8	1.4	ND
1b	5.7	4.9	0.8	0.8	14.9
2a	5.6	4.8	0.8	1.1	ND
2b	5.8	4.9	0.9	1.1	ND
3a	6.1	5.2	0.9	8.4	ND
3b	6.0	5.0	1.0	4.6	5.20
4a	6.2	5.6	0.6	4.3	ND
4b	6.9	6.5	0.4	1.6	ND

Footnotes: 1 - analyses by the Institute for Soil, Water and Climate
ND - not determined

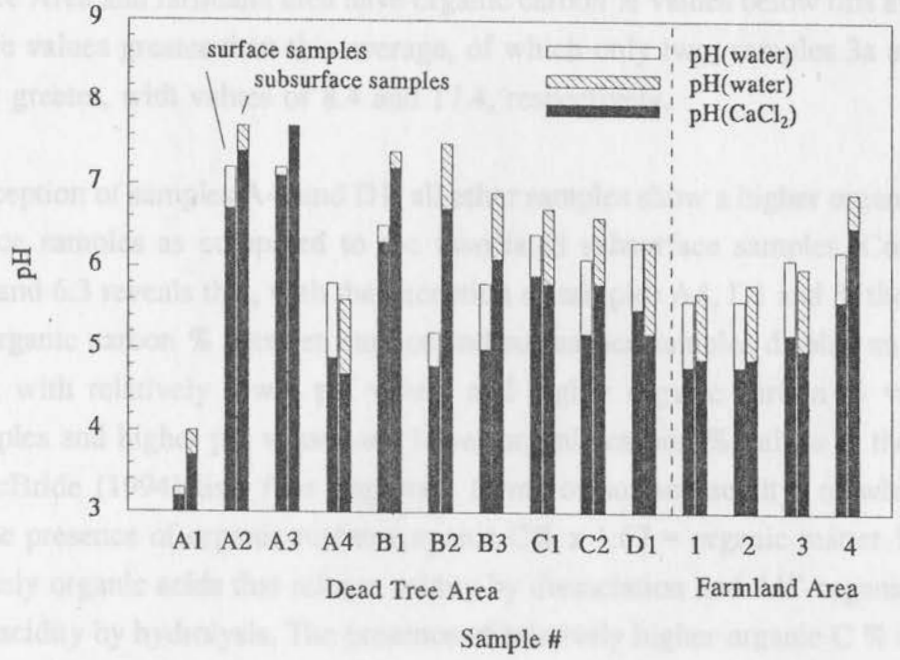

Figure 6.2 Histogram showing pH (water and $CaCl_2$) values for surface and subsurface soil samples from the Dead Tree Area and farmland area.

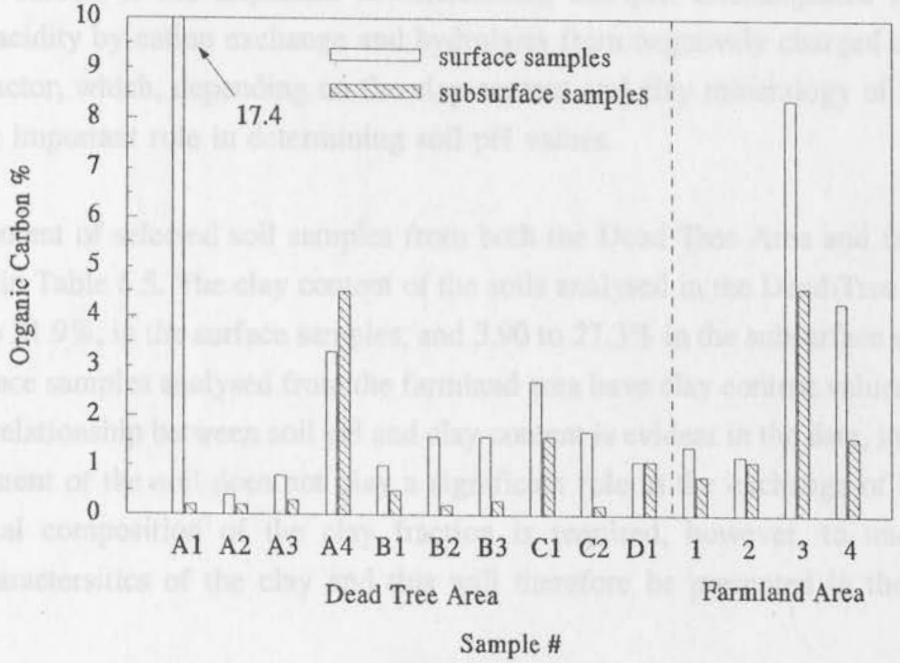

Figure 6.3 Histogram showing organic carbon values for surface and subsurface soil samples from the Dead Tree Area and farmland area.

the Dead Tree Area and farmland area have organic carbon % values below this average. Five samples have values greater than this average, of which only two, samples 3a and A1a, are significantly greater, with values of 8.4 and 17.4, respectively.

With the exception of samples A4, and D1, all other samples show a higher organic carbon % in the surface samples as compared to the associated subsurface samples. Comparison of Figures 6.2 and 6.3 reveals that, with the exception of samples A4, D1 and 3, the differences in pH and organic carbon % between surface and subsurface samples display an antipathetic relationship, with relatively lower pH values and higher organic carbon % values in the surface samples and higher pH values and lower organic carbon % values in the subsurface samples. McBride (1994) lists four important forms of surface acidity, of which, two are related to the presence of organic matter (organic C% x 1.67 = organic matter % (Alloway, 1995)), namely organic acids that release acidity by dissociation and Al^{3+}-organic complexes that release acidity by hydrolysis. The presence of relatively higher organic C % values in the surface soil samples may, therefore, be one cause of the lower pH(water) values for these samples.

That this relationship does not hold for samples A4, D1 and3, suggests that factors other than soil organic carbon % are important in determining soil pH. Exchangeable H^+ and Al^{3+}, released as acidity by cation exchange and hydrolysis from negatively charged clay surfaces is another factor, which, depending on the clay content and clay mineralogy of the soil may also play an important role in determining soil pH values.

The clay content of selected soil samples from both the Dead Tree Area and farmland area is tabulated in Table 6.5. The clay content of the soils analysed in the Dead Tree Area ranges from 4.60 to 21.9%, in the surface samples, and 3.90 to 27.3% in the subsurface samples. The two subsurface samples analysed from the farmland area have clay content values of 5.20 and 14.9%. No relationship between soil pH and clay content is evident in the data, indicating that the clay content of the soil does not play a significant role in the exchange of H^+ and Al^{3+}. Mineralogical composition of the clay fraction is required, however, to understand the exhange charactersitics of the clay and this will therefore be presented in the proceeding section.

6.3.3 Mineralogical Analysis

The X-ray diffractograms of the clay fraction of selected soil samples from the Dead Tree Area and farmland area are shown in Figure 6.4, 6.5 and 6.6.

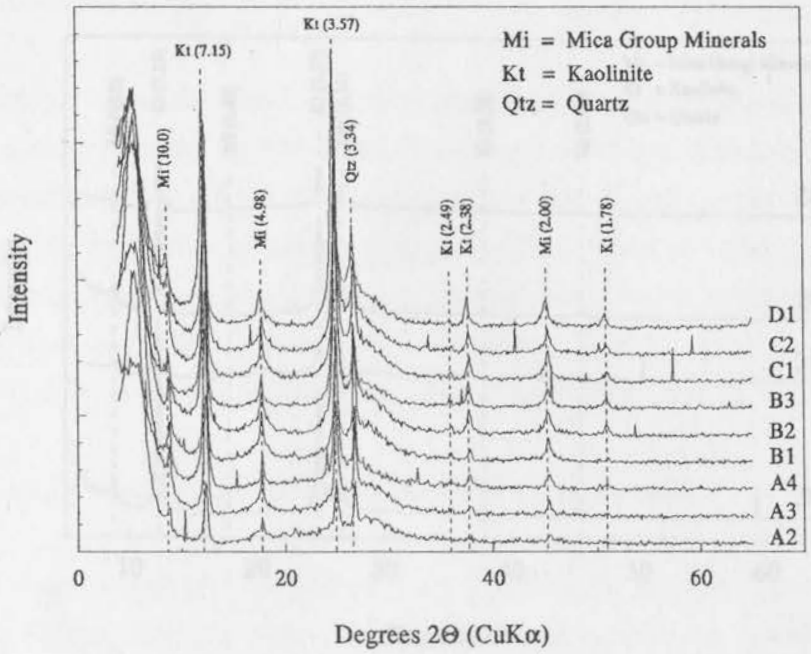

Figure 6.4 XRD plot of intensity versus 2θ for the clay fractions of nine of the surface soil samples from the Dead Tree Area. Peak locations are shown for kaolinite (Kt), quartz (Qtz), and the mica group minerals (Mi) [*d*-spacings in Å units are given in parenthesis].

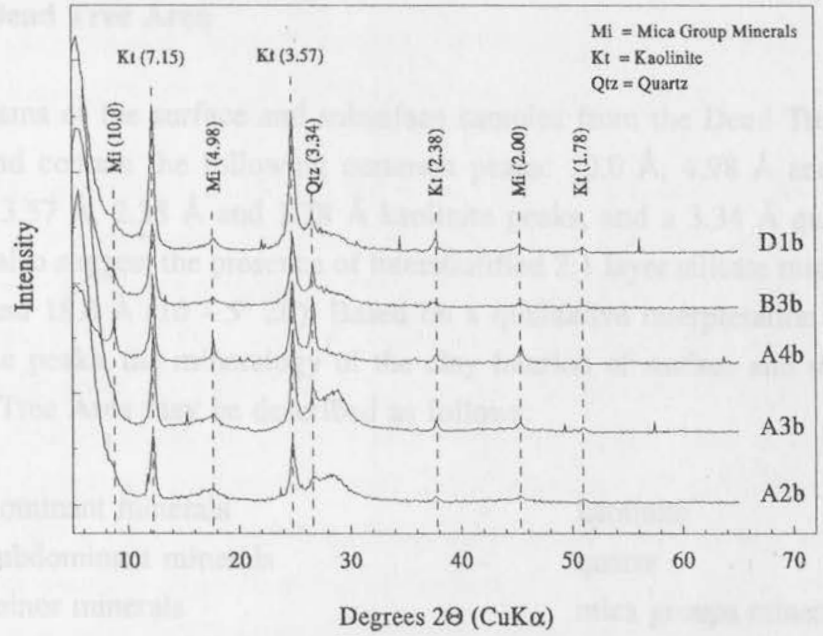

Figure 6.5 XRD plot of intensity versus 2θ for the clay fractions of five of the subsurface soil samples from the Dead Tree Area. Peak locations are shown for kaolinite (Kt), quartz (Qtz), and the mica group minerals (Mi) [*d*-spacings in Å units are given in parenthesis].

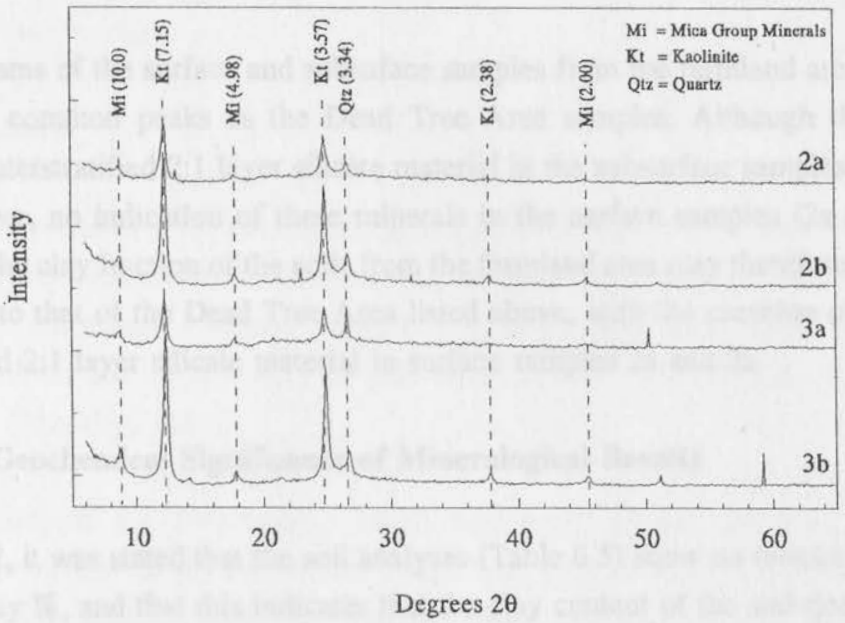

Figure 6.6 XRD plot of intensity versus 2θ for the clay fractions of four of the soil samples from the farmland area (two surface samples and two subsurface samples). Peak locations are shown for kaolinite (Kt), quartz (Qtz), and the mica group minerals (Mi) [*d*-spacings in Å units are given in parenthesis].

6.3.3.1 Dead Tree Area

The diffractograms of the surface and subsuface samples from the Dead Tree Area are all very similar, and contain the following common peaks: 10.0 Å, 4.98 Å and 2.00 Å mica peaks, 7.15 Å, 3.57 Å, 2.38 Å and 1.78 Å kaolinite peaks, and a 3.34 Å quartz peak. The diffractograms also suggest the presence of interstratified 2:1 layer silicate material occurring between 10.0 and 18.0 Å (10 - 5° 2θ). Based on a qualitative interpretation of the relative intensities of the peaks, the mineralogy of the clay fraction of surface and subsurface soils from the Dead Tree Area may be described as follows:

dominant minerals	-	kaolinite
subdominant minerals	-	quartz
minor minerals	-	mica groups minerals (interstratified 2:1 layer silicates?)

The scans of samples C1a, C2a, B2a, A3b and D1b contain peaks which are neither common to these five samples nor found in the other samples and which could not be identified.

6.3.3.2 Farmland Area

The diffractograms of the surface and subsuface samples from the farmland area contain the same range of common peaks as the Dead Tree Area samples. Although there is some suggestion of interstratified 2:1 layer silicate material in the subsurface samples (2b and 3b), there is, however, no indication of these minerals in the surface samples (2a and 3a). The mineralogy of the clay fraction of the soils from the farmland area may therefore be described as comparable to that of the Dead Tree Area listed above, with the exeption of the absence of interstratified 2:1 layer silicate material in surface samples 2a and 2a.

6.3.3.3 Geochemical Significance of Mineralogical Results

In section 6.3.2, it was stated that the soil analyses (Table 6.5) show no relationship between soil pH and clay %, and that this indicates that the clay content of the soil does not play an significant role in the exchange of H^+ and Al^{3+}. On the basis of the clay mineralogical results an explanation for this will be discussed.

Clay minerals have a marked effect on soil chemical properties due to their comparatively large surface area and permanent negative surface charge. The negative surface charge of the clay minerals means that they contribute to the cation exchange (CEC) of the soil. However, the CEC of the clay minerals depends strongly on the mineral structure and hence the type of clay mineral present in the soil is as important as the clay content.

Although the clay content in the Dead Tree Area and farmland area varies from 3.90 % to 27.3 %, the dominant clay mineral in both the Dead Tree Area and farmland area soils is kaolinite, with the mica group minerals representing only a minor component of the clay fraction. Kaolinite is a 1:1 clay mineral, comprising one tetrahedral silica sheet and one octahedral gibbsite sheet, in which the 1:1 units are tightly bonded together by hydrogen bonds between hydrogen and oxygen atoms of adjacent layers. Mica group minerals are, however, 2:1 clay minerals, comprising tetrahedral silica sheets sandwiching a gibbsite sheet, in which the 2:1 units are only weakly bonded. Consequently, the surface area and CEC of the mica group minerals is larger than that of the kaolinite minerals (100 - 200 m^2/g and 10 - 40 $cmol_c/kg$) which have surface areas of between 5 and 40 m^2/g and CEC's of between 3 and 20 $cmol_c/kg$ (Alloway, 1995).

The CEC of the clay fraction of the soils in the Dead Tree Area and farmland area is, therefore, predicted to be very low. Hence the clay content of the soils will not play a

significant role in the exchange of H^+ and Al^{3+}, and a relationship between clay content and pH would not be expected.

6.3.4 Soil Salinity

Soil salinity is a measure of the concentration of soluble salts in the soil. Soluble salts in soils can be determined from measurements made (i) on aqueous extracts of soil samples, (ii) on samples of soil water itself obtained from the soil, (iii) in soil using buried porous salinity sensors that imbibe and equilibrate with soil water, and (iv) in soil using electromagnetic (EM) systems (Rhoades, 1982).

Of the four methods for determining soluble salts listed above, two have been used to characterise the salinity of the soils in the Dead Tree Area as described in chapter 3. They are: (i) samples of soil water itself (the results of which have already been discussed in some detail in chapter 5 in regard to the aqueous chemistry of the Dead Tree Area) and (ii) aqueous extracts of soil samples. Because the soils in the Dead Tree Area are typically saturated, the results of the aqueous extracts, which were prepared using saturated soil pastes, should be comparable. Due to insufficient soil water, soil water samples from the farmland area could not be collected. However, aqueous extracts of these soil samples have been prepared as a means of comparing the salinity conditions of the soils in the Dead Tree Area with those of soils that are considered not to have been impacted by industrial activities in the area. In this section, the general chemical characteristics of the saturated paste extracts will first be discussed and compared with the soil water samples, presented in chapter 5. The significance of these results will then be discussed in terms of soil salinity.

6.3.4.1 Chemical characteristics of soil saturated paste extracts

The results of the saturated paste extract analyses for soils in the Dead Tree Area and farmland area are tabulated in Table 6.6. The pH, electrical conductivity, acidity and alkalinity results are illustrated graphically in Figure 6.7. The soil water analyses for the Dead Tree Area, presented in chapter 5, are also illustrated in Figure 6.7 for comparison with the saturated paste results. Because the soil water samples represent seepage water sampled at a depth of aproximately 40 to 50 cm, the same depth at which the subsurface soil samples were collected, these results have been plotted in conjunction with the subsurface soil saturated paste results. The soil water results are expected to be comparable to the soil subsurface saturated paste results, but may not, however, be comparable to the soil surface saturated paste results, due to the fact that this soil water may not neccesarily have been in contact with

Table 6.6 Analyses of saturated paste extracts of soils from the Dead Tree Area and Farmland Area.

Sample No.	pH	EC	Alkalinity/	Acidity	Na^+	Ca^{2+}	Mg^{2+}	K^+	NH_4^+	Cl^-	SO_4^{2-}	$PO4^{3-}$	NO_3^-	$^1F^-$
Dead Tree Area														
A1a	2.9	19.5		18.4	2760	1100	1780	351	ND	5600	1250	ND	ND	0.4
A1b	3.5	14.5		6.6	2040	502	1100	133	93	4230	518	ND	ND	10.1
A2a	7.5	13.8	470		2090	451	926	241	ND	4310	276	ND	ND	12.4
A2b	8.2	10.7	350		1910	281	592	120	ND	3240	258	ND	ND	13.7
A3a	7.5	47.1	470		11900	2180	5280	805	ND	28700	ND	ND	ND	2.8
A3b	6.5	35.3	208		9080	1150	3090	1310	ND	18300	ND	ND	ND	0.5
A4a	6.5	0.5	75.4		48.2	20.1	31.5	14.7	4.02	69.8	16.4	ND	2.10	0.4
A4b	5.5	0.8	50.8		87.6	23.1	24.4	17.0	ND	153	10.2	ND	ND	2.9
B1a	7.1	13.0	319		1740	429	686	91.4	ND	4190	98.5	ND	ND	1.9
B1b	7.9	14.6	280		2090	335	680	92.5	ND	4370	104	ND	ND	3.9
B2a	5.4	4.2	63.9		451	224	170	148	ND	1240	11.4	ND	ND	0.3
B2b	7.9	4.2	1390		600	168	165	100	ND	1020	22.1	ND	1.02	1.2
B3a	6.4	1.7	150		265	64.2	71.8	36.4	9.50	427	28.4	ND	ND	5.5
B3b	7.5	2.2	190		417	57.3	63.4	15.3	ND	301	146	ND	ND	3.5
C1a	6.9	4.2	170		662	139	215	72.2	ND	1340	33.6	ND	ND	0.8
C1b	7.3	1.8	170		258	55.4	70.6	19.1	ND	476	16.0	ND	ND	0.5
C2a	6.5	0.5	88.4		103	33.4	26.4	47.0	4.01	257	9.20	ND	ND	0.2
C2b	7.3	1.6	139		298	63.0	44.8	40.7	ND	405	24.1	ND	ND	0.2
D1a	7.3	1.6	229		199	66.1	70.1	29.1	ND	679	9.58	ND	9.16	0.8
D1b	6.8	0.8	65.5		155	31.4	39.0	9.02	ND	288	18.4	ND	ND	0.5
Farmland Area														
1a	6.4	0.5	72.7		41.5	58.2	9.22	19.8	7.41	66.8	23.7	ND	ND	2.8
1b	5.3	0.6	54.1		60.4	75.4	14.5	29.4	ND	51.2	48.2	ND	ND	1.9
2a	6.4	0.3	73.7		35.0	17.9	5.78	20.4	ND	46.5	5.02	ND	ND	1.1
2b	6.3	0.2	49.2		21.4	15.1	4.75	16.8	3.45	31.7	4.15	ND	1.04	1.0
3a	6.6	0.3	73.7		36.7	20.6	8.60	15.0	2.01	32.2	10.5	ND	ND	1.3
3b	6.5	0.2	13.11		35.0	12.5	3.04	6.2	ND	24.1	ND	ND	ND	1.3
4a	6.7	1.4	129.5		144	233	63.1	28.5	ND	578	91.0	ND	ND	2.8
4b	7.3	2.9	129.5		474	260	123	12.7	ND	1020	231	ND	ND	5.5

Footnotes Units -EC in mS/cm; alkalinity as mg $CaCO_3$/l; acidity in mmol/l; all ion concentrations in mg/l ND - not detected
1 - fluoride determined by ion selective electrode

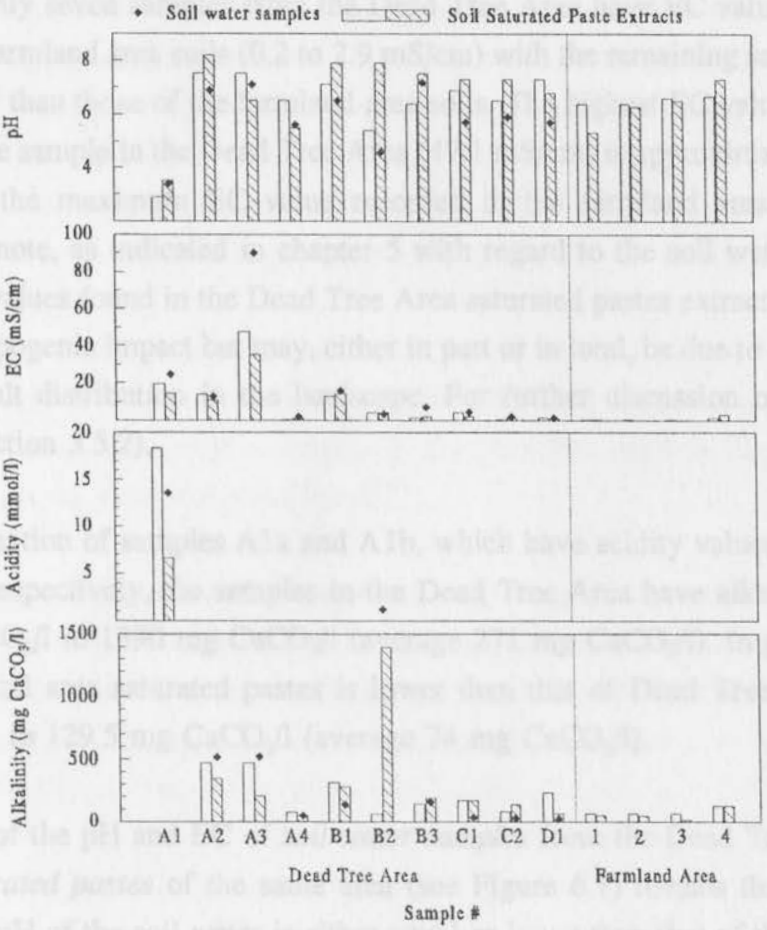

Figure 6.7 Histograms of pH, electrical conductivity, acidity and alkalinity for soil saturated paste extracts and soil water samples from the Dead Tree Area and farmland area.

the surface (0 - 6 cm) soil layer.

The pH and EC values of the saturated paste extracts (Table 6.6) for the Dead Tree Area and farmland area range from 2.9 to 8.2 pH units and 0.5 to 47.1 mS/cm, and 5.3 to 7.3 pH units and 0.2 to 2.9 mS/cm, respectively. The histogram plots of these values (see Figure 6.7) show that both the pH and EC values of the Dead Tree Area exhibit a far greater variability than those of the farmland area. Five of the Dead Tree Area samples (A2a, A2b, A3a, B1b and B2b) have pH values greater than the maximum pH value recorded in the farmland area (pH_{max} 7.3), and two samples (A1a and A1b) have pH values less than the minimum pH recorded in the farmland area (pH_{min} 5.3). The remaining thirteen samples have pH values which fall within the range of pH values found in the farmland area soils (5.3 to 7.3).

In contrast, only seven samples from the Dead Tree Area have EC values falling within the range of the farmland area soils (0.2 to 2.9 mS/cm) with the remaining samples all having EC values greater than those of the farmland area soils. The highest EC value recorded for a soil saturated paste sample in the Dead Tree Area (47.1 mS/cm) is approximately 16 times greater than that of the maximum EC value recorded in the farmland area (2.9 mS/cm). It is important to note, as indicated in chapter 5 with regard to the soil water analyses, that the elevated EC values found in the Dead Tree Area saturated pastes extracts do not neccessarily reflect anthropogenic impact but may, either in part or in total, be due to a naturally occurring differential salt distribution in the landscape. For further discussion of this issue, refer to chapter 5 (section 5.5.2).

With the exception of samples A1a and A1b, which have acidity values of 18.4 mmol/l and 6.6 mmol/l, respectively, the samples in the Dead Tree Area have alkalinities ranging from 50.8 mg $CaCO_3$/l to 1390 mg $CaCO_3$/l (average 271 mg $CaCO_3$/l). In general the alkalinity of the farmland area saturated pastes is lower than that of Dead Tree Area, ranging from 13.1 $CaCO_3$/l to 129.5 mg $CaCO_3$/l (average 74 mg $CaCO_3$/l).

Comparison of the pH and EC of *soil water samples* from the Dead Tree Area with that of the *soil saturated pastes* of the same area (see Figure 6.7) reveals that, for six out of ten samples, the pH of the soil water is either equal or lower than that of the saturated pastes of both surface and subsurface soils. In the case of samples A1, A3, A4 and B3, the pH values of the soil water falls between those of the respective surface and subsurface saturated paste values. For all samples the EC of the soil water is equal or higher than that of the saturated pastes of both surface and subsurface soils. In particular, the EC of soil water sample A3 (90.3 mS/cm) is close to double that of the soil saturated paste extracts (A3a - 47.1 mS/cm; A3b - 35.3 mS/cm).

The consistently higher EC values found in the soil water samples as compared to the saturated paste extracts may be suggestive of a higher soil : water ratio under field conditions than under simulated field conditions using saturated pastes. A lower soil : water ratio would also produce a relatively higher pH value due to increased hydrolytic exchange. This may explain why six of the soil water samples have lower pH values than the corresponding soil saturated paste extracts. The explanation is not valid, however, in the case of soil water samples A1, A3, A4 and B3, pH values of which fall between those of the respective surface and subsurface saturated paste values.

An alternative explanation is that the soil water samples do not actually represent soil water

exisiting in contact with the soil at the level sampled (between 40 to 50 cm for the subsurface soil samples), but represent soil water which has seeped into the sampling pits from some greater depth. Under such circumstances, the soil water sampled would not be expected to be comparable to saturated paste extracts of soil samples sampled at 40 to 50 cm depth, but rather to reflect the soluble salt concetration of the soil at some unknown depth. Further work is required before a conclusive explanation of these results can presented.

The results of the saturated paste extract cation and anion analyses are illustrated graphically in Figures 6.8 and 6.9 (numerical data is tabulated in Table 6.6). The soil water analyses for the Dead Tree Area, presented in chapter 5, are also illustrated in Figures 6.8 and 6.9 for comparison with the saturated paste results.

Figures 6.8 and 6.9 show that the major cation and anion data of the soil saturated paste extracts from the Dead Tree Area follow similar trends to those of the soil water samples from the Dead Tree Area (discussed in Chapter 5). The farmland area saturated paste ion concentrations are low in comparison to the saturated pastes extract ion concentrations of soil samples from the Dead Tree Area, as may be predicted from the EC data already presented in this section.

It is also expected, from the EC values, that the ion concentrations for the saturated pastes are equal to or less than those of the soil water samples. Exceptions to the above generalisation occur, however, for K^+ and F^-. For samples A2, A3 and B2 the saturated paste extract concentrations of K^+ exceed those of the respective soil water samples. In the case of F^-, the saturated paste extract concentrations exceed those of the soil water in all cases except samples A1a, A4a, and B2a. Comparison of F^- concentrations in the saturated paste extracts from the farmland area and Dead Tree Area shows that the F^- concentrations in the farmland area samples exceed those of samples A1a, A3b, A4a, B2a, C1, C2, and D1 in the Dead Tree Area. This suggests that the farmland area is not unaffected by the industrial activities of the surrouding area and that F^- contamination, most likely originating from the adjacent gypsum dumps, has impacted on the farmland soils. Further indication of this impact is found in the fact that the highest F^- concentration recorded in the farmland area occurs in sample 4b (5.5mg F^-/l), the sample located in closest proximity to the the gypsum dumps.

In Figure 6.10 the composition of the soil water samples from the Dead Tree Area, and soil saturated paste samples from the Dead Tree Area and farmland area have been plotted on a pipergram. As has already been discussed in chapter 5, the soil water samples form a relatively tight cluster of points which lie within the 'sodium and chloride dominant'

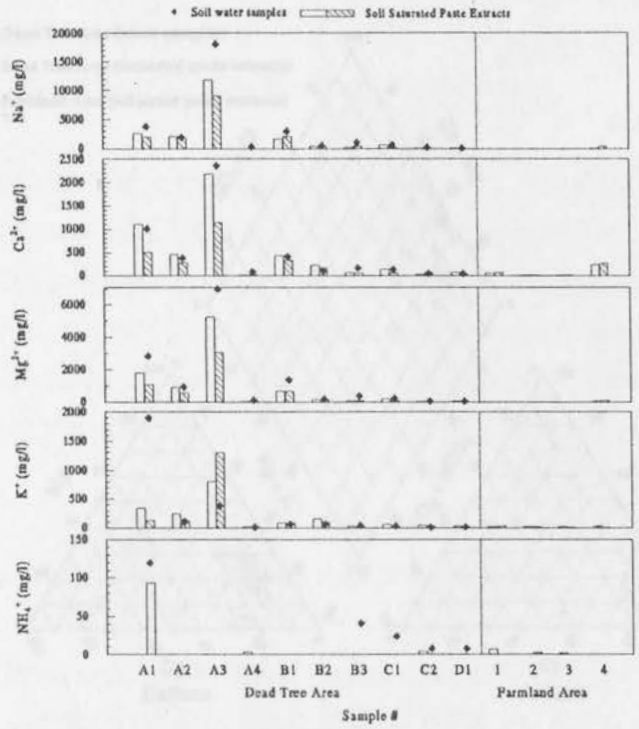

Figure 6.8 Histograms of the major cations for soil saturated paste extracts and soil water samples from the Dead Tree Area and farmland area.

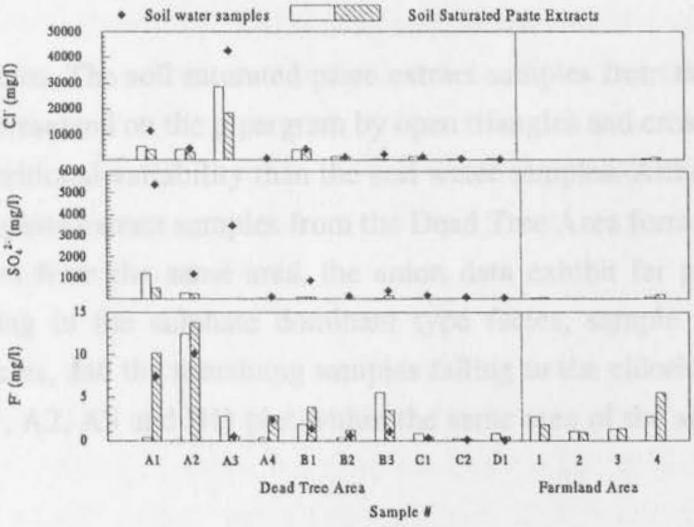

Figure 6.9 Histograms of the major anions for soil saturated paste extracts and soil water samples from the Dead Tree Area and farmland area (phosphate was not detected in the saturated paste extracts and nitrate was only detected in four samples (A4a - 2.10 mg/l, B2b - 1.02 mg/l, D1a - 9.16 and 2b - 1.04 mg/l)).

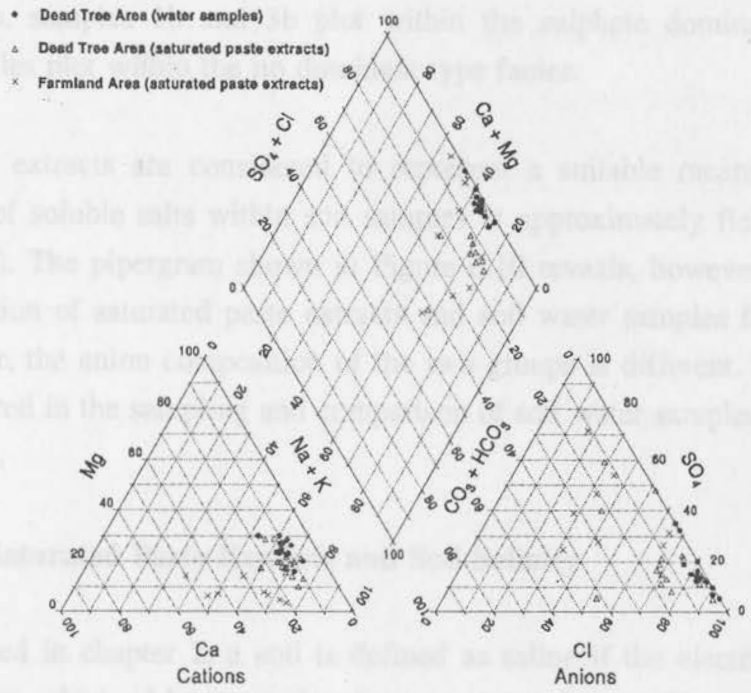

Figure 6.10 Pipergram showing the composition of the soil saturated paste extracts from the Dead Tree Area and farmland area, and soil water samples from the Dead Tree Area.

hydrochemical facies. The soil saturated paste extract samples from the Dead Tree Area and farmland area, represented on the pipergram by open triangles and crosses, respectively, show far greater compositional variability than the soil water samples. Although the cation data of the soil saturated paste extract samples from the Dead Tree Area form a tight cluster with the soil water samples from the same area, the anion data exhibit far greater variability, with sample B3b falling in the sulphate dominant type facies, sample A4a falling in the no dominant type facies, and the remaining samples falling in the chloride dominant type. Only four samples (A1, A2, A3 and B1) plot within the same area of the anion triangle as the soil water samples.

The saturated paste extracts of the farmland area soils exhibit greater variability in Ca^{2+} and $Na^{+} + K^{+}$ composition than the saturated paste extracts and soil water samples from the Dead Tree Area. The farmland area saturated paste extracts also contain less Mg^{2+} in proportion to Ca^{2+} and $Na^{+} + K^{+}$ than the Dead Tree Area samples. The cation data of the farmland area does, however, form a loose cluster lying predominantly in the sodium dominant facies. In

contrast, the anion data does not form a cluster. Samples 4a and 4b plot within the chloride dominant facies, samples 1b and 3b plot within the sulphate dominant facies, and the remaining samples plot within the no dominant type facies.

Saturated paste extracts are considered to represent a suitable means to determine the concentrations of soluble salts within soil samples at approximately field water conditions (Rhoades, 1982). The pipergram shown in Figure 6.10 reveals, however, that although the cation composition of saturated paste extracts and soil water samples from the Dead Tree Area are similar, the anion composition of the two groups is different. This illustrates that caution is required in the sampling and comparison of soil water samples with soil saturated paste extracts.

6.3.4.2 Saturated Paste Extracts and Soil Salinity

As was discussed in chapter 2, a soil is defined as saline if the electrical conductivity of its aqueous phase, obtained by extraction from a saturated paste, has a value >4 mS/cm. In Figure 6.11 an enlarged version of the histogram of EC values presented in Figure 6.7 is shown along with the position of the 4 mS/cm 'cut-off value' above which soils are characterised as saline. The plot shows that for the Dead Tree Area samples A1, A2, A3, B1, B2 and the surface sample of C1 represent saline soils, and samples A4, B3, C2, D1 and the subsurface sample of sample C1 are sub-saline. The farmland area soils are all sub-saline. The most elevated EC values in the farmland area soil saturated pastes occur in the surface and subsurface samples of sample 4 (1.4 mS/cm and 2.9 mS/cm). The relative proximity of this sample to the gypsum dumps (refer Figure 3.2, pg. 3-4, chapter 3) suggests that the slightly elevated EC of the sample, in comparison to the other three samples in the farmland area, is a consequence of gypsum dump leachate interaction with the soil surrounding the gypsum dumps.

The high salinity of the soil water and soil saturated paste extracts from the Dead Tree Area may be affecting plant growth due to the fact that high soil salinity lowers the free energy of water in solution, thereby reducing the osmotic potential of the soil solution and ability of plant roots to extract water from the soil. This osmotic pressure generated by salts in solution may be estimated from the electrical conductivity (EC) of the solution using the empirical equation (McBride, 1994):

$$\text{Osmotic pressure (atmospheres)} = \text{EC (mS/cm)} \times 0.36$$

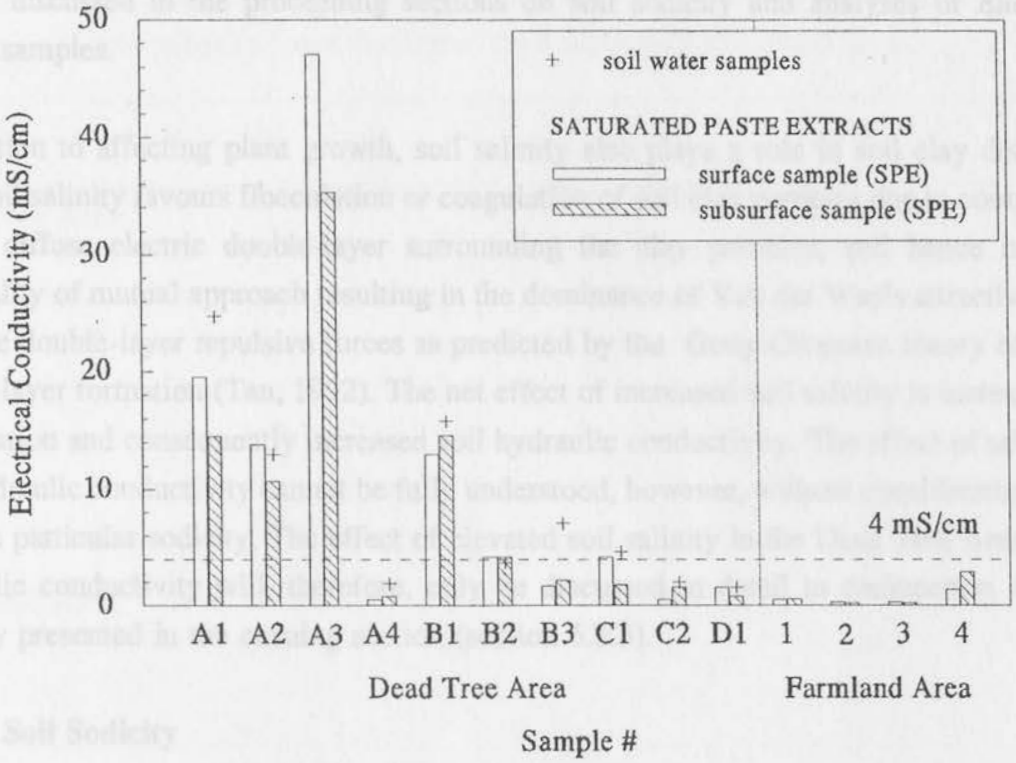

Figure 6.11 Electrical conductivity of the soil water and saturated paste extracts from the Dead Tree Area and farmland area. The 4 mS/cm line indicates the 'cut-off' above which soils are classified as saline.

Using the saturated paste extract and soil water EC values for the Dead Tree Area yields osmotic pressures of between 0.2 and 17 atmospheres and 0.6 and 33 atmospheres, respectively. Hence, in the case of soil sample A3, the soil solution is retained in a lowered free energy state equivalent to a maximum of up to 33 atmospheres of water tension, and is therefore not readily available to plant roots. McBride (1994) states that most plants reach their permanent wilting point at approximately 15 atmospheres of water tension (EC ≈ 42 mS/cm). Hence, it is possible to conclude that soil salinity in the Dead Tree Area is impeding water uptake by plants, and that there is a high probability that the death of *Eucalyptus* trees observed in the Dead Tree Area is a consequence, either in part or total, of salinity-induced osmotic stress. The highest probability of tree mortality resulting from salinity is likely to be associated with trees located in the vicinity of sample A3, due to the markedly elevated salinity of this sample (A3a - 47 mS/cm; A3b - 35.3 mS/cm).

Tree mortality in the Dead Tree Area may also be a consequence, at least in part, of specific ion toxicity effects and/or nutritional imbalances resulting from high salinity. These effects

will be discussed in the proceeding sections on soil sodicity and analyses of *Eucalyptus* foliage samples.

In addition to affecting plant growth, soil salinity also plays a role in soil clay dispersion. High soil salinity favours flocculation or coagulation of soil clay particles due to compression of the diffuse electric double-layer surrounding the clay particles, and hence increased probability of mutual approach resulting in the dominance of Van der Waals attractive forces over the double-layer repulsive forces as predicted by the Gouy-Chapman theory of diffuse double-layer formation (Tan, 1992). The net effect of increased soil salinity is increased clay flocculation and consequently increased soil hydraulic conductivity. The effect of salinity on soil hydraulic conductivity cannot be fully understood, however, without consideration of salt type, in particular sodicity. The effect of elevated soil salinity in the Dead Tree Area on soil hydraulic conductivity will, therefore, only be discussed in detail in conjunction with soil sodicity presented in the ensuing section (section 6.3.5).

6.3.5 Soil Sodicity

The sodium status of soils is characterised by the proportion of Na^+ on the soil exchange sites, termed exchangeable sodium percentage (ESP) and the proportion of Na^+ to divalent cations in the soil solution, termed sodium adsorption ratio (SAR) (Ayers and Westcot, 1985; Sposito, 1989; McBride, 1994). In Table 6.7 the exchangeable cations and exchangeable sodium percentage for selected soil samples from the Dead Tree Area and farmland area are tabulated. The exchangeable cation values listed in Table 6.7 have not been corrected for soil salinity and hence the ESP values calculated do not represent the true *exchangeable* sodium percentage of the soils but rather a 'total potential' exchangeable sodium percentage.

The ESP values tabulated in Table 6.7 are shown graphically in Figure 6.12. The plot shows that samples A2a and A2b have ESP in excess of 20%, samples A4b and B3a have values between 10 and 20%, and the remaining samples have values <10%. Six out of eight samples analysed in the Dead Tree Area have ESP values greater than the maximum value recorded in the farmland area (8.55%).

An ESP value of 15% has traditionally been considered the cut-off value above which soils are considered sodic (Tan, 1992) and above which marked clay swelling and dispersion is likely to occur. More recent literature has shown (eg. Levy and Torrento, 1995), however, that marked clay dispersion may occur at ESP values as low as 0.5%, and that factors such as electrolyte concentration and pH need to be considered in conjuntion with ESP and SAR

Table 6.7 **Exchangeable Cations and Exchangeable Sodium Percentage for selected soil samples from the Dead Tree Area and farmland area.**

Sample No.	Na^+	K^+	Ca^{2+}	Mg^{2+}	ESP[2]
Dead Tree Area					
A2a	1.90	0.10	1.48	2.61	45.3
A2b	3.92	0.32	2.93	12.2	25.3
A4a	0.25	0.15	3.80	1.27	4.81
A4b	0.31	0.17	0.97	0.68	17.0
B2a	1.60	0.81	7.83	7.85	9.70
B3a	1.61	0.29	5.39	5.33	14.4
C1b	1.88	0.40	5.00	15.1	9.18
D1a	0.15	0.40	3.02	0.48	3.85
Farmland Area					
1b	0.10	0.11	0.99	0.59	5.92
3b	0.84	0.32	3.79	5.72	8.55

Footnotes: 1 - analyses performed by the Institute for Soil, Water and Climate

2 - calculated as {exchangeable Na^+}/{$\sum$exchangeable cations} x 100, where all ions are in mmol$_c$/l.

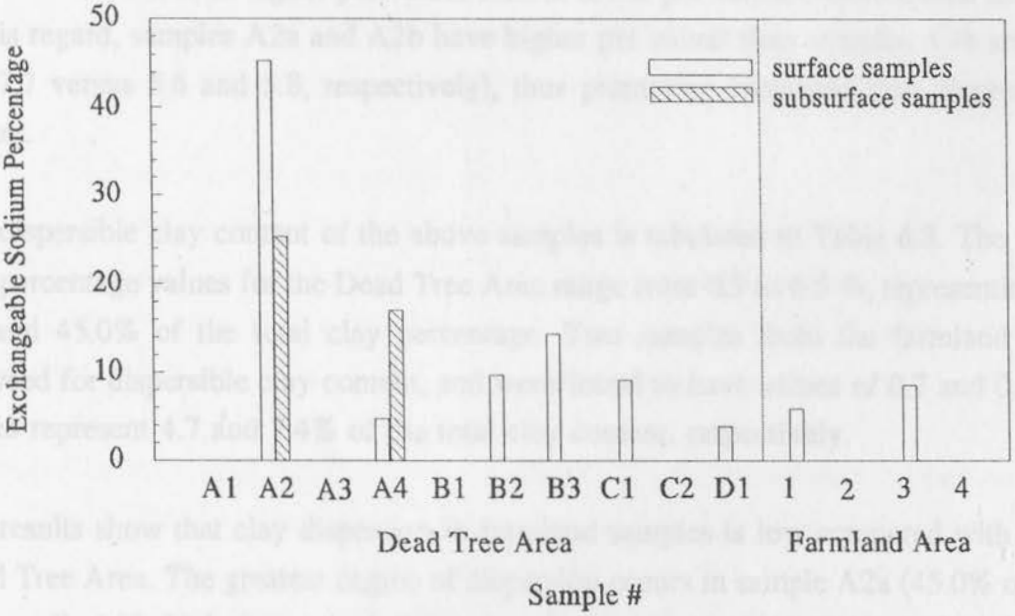

Figure 6.12 The exchangeable sodium percentage (ESP) of selected samples from the Dead Tree Area and farmland area.

values if sodicity effects are to be accurately assessed. The interaction between sodicity, salinity and pH and the resulting effect on clay dispersibility is discussed in detail by Sposito (1989) and McBride (1994), and has been reviewed in chapter 2.

Although samples A2a and A2b have markedly higher ESP values than the other soils for which ESP was determined, this does not necessarily indicate that dispersion in these soils is greater than, for example, samples A4b and B3a which have ESP values of 17.0% and 14.4%, respectively. The electrical conductivity values of the saturated paste extracts of samples A2a and A2b are 13.8 mS/cm and 10.7 mS/cm, respectively, whereas those of samples A4b and B3a are 0.8 mS/cm and 1.7 mS/cm, respectively. Soil samples A2a and A2b would thus be classified as saline-sodic, whereas soil samples A4b and B3a would be classified as sodic (McBride, 1994). Hence, although the ESP values of samples A2a and A2b are high, with the potential to promote clay dispersion, the EC values of these samples are also high, which promotes clay flocculation. In the case of samples A4b and B3a, the ESP values are lower than those of A2a and A2b. The EC values are also lower, however, with the consequence that the degree of clay dispersion in all four samples may in fact be similar.

A further factor which must be taken into consideration, however, is pH because the critical coagulation concentration (CCC) values of clay increase with increasing pH resulting in increased dispersion at higher pH values than at lower pH values (Kretzschmar *et al.,* 1993). In this regard, samples A2a and A2b have higher pH values than samples A4b and B3a (7.2 and 7.7 versus 5.6 and 5.8, respectively), thus promoting increased clay dispersion in the former.

The dispersible clay content of the above samples is tabulated in Table 6.8. The dispersible clay percentage values for the Dead Tree Area range from 0.9 to 6.5 %, representing between 5.6 and 45.0% of the total clay percentage. Two samples from the farmland area were analysed for dispersible clay content, and were found to have values of 0.7 and 0.4%. These values represent 4.7 and 7.4% of the total clay content, respectively.

The results show that clay dispersion in farmland samples is low compared with that of the Dead Tree Area. The greatest degree of dispersion occurs in sample A2a (45.0% of total clay dispersed), with high degrees of dispersion also occurring in samples A4b, A2b and B3a (41.0, 38.9 and 29.8%, respectively). The hydraulic conductivity of these soils may thus be anticipated to be significantly reduced due to clay dispersion. These soil may also, however, be considered to have the greatest potential for remediation through reduction of soil ESP. The remaining samples from the Dead Tree Area have values of <20% total clay dispersed.

Table 6.8 Dispersible clay content for selected soil samples from the Dead Tree Area and farmland area.

Sample No.	Clay %	Dispersible Clay %	Fraction of total clay dispersed (%)
Dead Tree Area			
A2a	4.60	2.1	45.0
A2b	18.1	7.0	38.9
A4a	5.50	0.9	16.4
A4b	3.90	1.6	41.0
B2a	15.7	2.7	17.4
B3a	21.9	6.5	29.8
C1b	27.3	3.3	12.2
D1a	15.9	0.9	5.6
Farmland Area			
1b	14.9	0.7	4.7
3b	5.2	0.4	7.4

The sodium adsorption ratio and electrical conductivity of saturated paste extracts from the Dead Tree Area and farmland area and soil water from the Dead Tree Area are tabulated in Table 6.9. This data is shown graphically in Figure 6.13 along with the potential sodicity hazards of these samples to degrade soil properties as defined by McBride (1994).

The SAR values show a wide range of between 0.1 and 42.1 $mol^{1/2}m^{-3/2}$, and the plots show that, whereas the sodicity hazard of the farmland area samples is in all cases low, the sodicity hazard of the Dead Tree Area samples range from low to very high. Samples A3a and A3b represent the greatest sodicity hazard, with SAR values exceeding 20 $mol^{1/2}m^{-3/2}$.

Samples A1a, A1b, A2a and B1a have a medium sodicity hazard with values between 7 and 13 $mol^{1/2}m^{-3/2}$. The samples located in the south and south-western portion of the Dead Tree Area have a low to medium sodicity hazard rating (samples A4, B2, B3, C1, C2 and D1). Ayers and Westcot (1985) state that sodium toxicity is likely to result in cases where irrigation waters have SAR values >9 $mol^{1/2}m^{-3/2}$. There is thus a high probability that tree mortality in the north-eastern portion of the Dead Tree Area was, at least in part, due to sodium toxicity.

Table 6.9 Electrical Conductivity and Sodium Adsorption Ratio of soil saturated paste extracts from the Dead Tree Area and farmland area, and soil water from the Dead Tree Area.

	Saturated Paste Extracts		Soil Subsurface Water Samples	
Sample No.	EC (mS/cm)	SAR ($mol^{1/2}m^{-3/2}$)[1]	EC (mS/cm)	SAR($mol^{1/2}m^{-3/2}$)[1]
Dead Tree Area				
A1a	19.5	11.9		
A1b	14.5	11.7	24.7	13.9
A2a	13.8	12.9		
A2b	10.7	14.8	13.0	12.5
A3a	47.1	31.4		
A3b	35.3	31.6	90.3	42.1
A4a	0.5	1.6		
A4b	0.8	3.4	1.9	5.1
B1a	13.0	12.1		
B1b	14.6	15.1	15.8	16.3
B2a	4.2	5.5		
B2b	4.2	7.8	3.7	7.1
B3a	1.7	5.4		
B3b	2.2	9.1	7.1	10.7
C1a	4.2	8.2		
C1b	1.8	5.4	4.6	7.2
C2a	0.5	3.2		
C2b	1.6	7.1	2.0	6.4
D1a	1.6	4.1		
D1b	0.8	4.4	1.6	4.1
Farmland Area				
1a	0.5	0.2		
1b	0.6	0.2		
2a	0.3	0.1		
2b	0.2	0.1		
3a	0.3	0.1		
3b	0.2	0.1		
4a	1.4	0.5		
4b	2.9	1.7		

Footnotes: 1 - calculated as $[Na^+]/\{ ([Na^+] + [Mg^{2+}])/2 \}^{0.5}$, where all ions are in $mmol_c/l$.

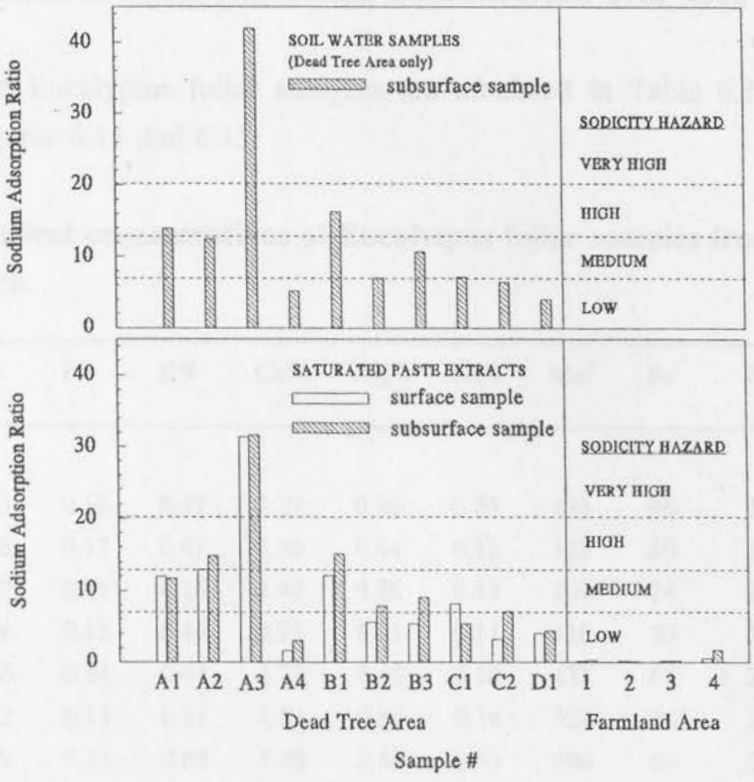

Figure 6.13 Histograms showing the SAR values of saturated paste extracts and soil water from the Dead Tree Area and farmland area along with the relative sodicity hazards of these samples as defined by McBride (1994).

The results presented in the preceeding section on soil salinity and those of ESP, SAR and dispersible clay percentage presented in this section reveal that soil salinity and sodicity is a problem in the Dead Tree Area, and that tree mortality could have been a result of osmotic stress and/or sodium toxicity in addition to waterlogging. In the next section, analyses of *Eucalyptus* foliar samples from the Dead Tree Area will be discussed with the aim of assessing whether the soil salinity and/or sodicity is presently affecting plant growth.

6.3.6 Analysis of *Eucalyptus* foliage from the Dead Tree Area

The results of the Eucalyptus foliar analyses are tabulated in Table 6.10, and illustrated graphically in Figures 6.14 and 6.15.

Table 6.10 Nutrient concentrations of Eucalytpus foliar samples from the Dead Tree Area.

Element	N%	P%	K%	Ca%	Mg%	Na%	Mn[1]	Fe[1]	Zn[1]	Cu[1]	Na/K
Transect A											
A1	1.35	0.18	0.47	1.27	0.36	0.15	494	96	32	4	0.31
A2	1.66	0.17	0.47	1.36	0.44	0.12	728	80	24	5	0.25
A3	1.22	0.15	0.16	1.42	0.38	0.15	1017	74	21	5	0.94
A4	1.39	0.13	0.46	1.25	0.41	0.11	426	70	28	5	0.24
A5	1.46	0.14	0.44	1.29	0.46	0.16	435	63	29	3	0.36
A6	1.62	0.13	0.51	1.34	0.34	0.14	323	763	25	4	0.27
A7	1.99	0.17	0.58	1.60	0.46	0.43	406	66	26	4	0.74
A8	1.18	0.12	0.49	1.10	0.31	0.16	392	81	25	5	0.32
A9	1.38	0.13	0.45	1.50	0.35	0.16	397	87	29	5	0.36
Transect B											
B1	1.31	0.24	0.36	2.16	0.40	0.06	2093	173	36	7	0.17
B2	1.43	0.20	0.46	1.59	0.25	0.15	754	83	22	5	0.32
B3	1.25	0.16	0.38	1.76	0.26	0.15	721	79	25	5	0.39
B4	1.24	0.18	0.38	1.41	0.28	0.17	917	79	15	3	0.45
B5	1.30	0.17	0.45	0.78	0.21	0.17	435	88	15	4	0.38
B6	1.23	0.16	0.33	1.46	0.36	0.11	1196	111	22	5	0.33
B7	1.19	0.13	0.52	1.00	0.25	0.34	345	81	17	4	0.65

Footnotes: 1 - in ppm

The analyses do not show any general trends common to all elements. Within transect A, however, sample A7 has consistently elevated concentrations of N, K, Ca, Mg, and Na, in comparison with the other samples. Within transect B, sample B1 has consistently elevated concentrations of P, Ca, Mn, Fe, Zn and Cu and sample B7 has elevated concentrations of K, Mg and Na, in comparison with the other samples.

It has been shown in chapter 5 and in earlier sections of this chapter, that the greatest degree of salinisation and/or contamination in the Dead Tree Area occurs in the north-eastern

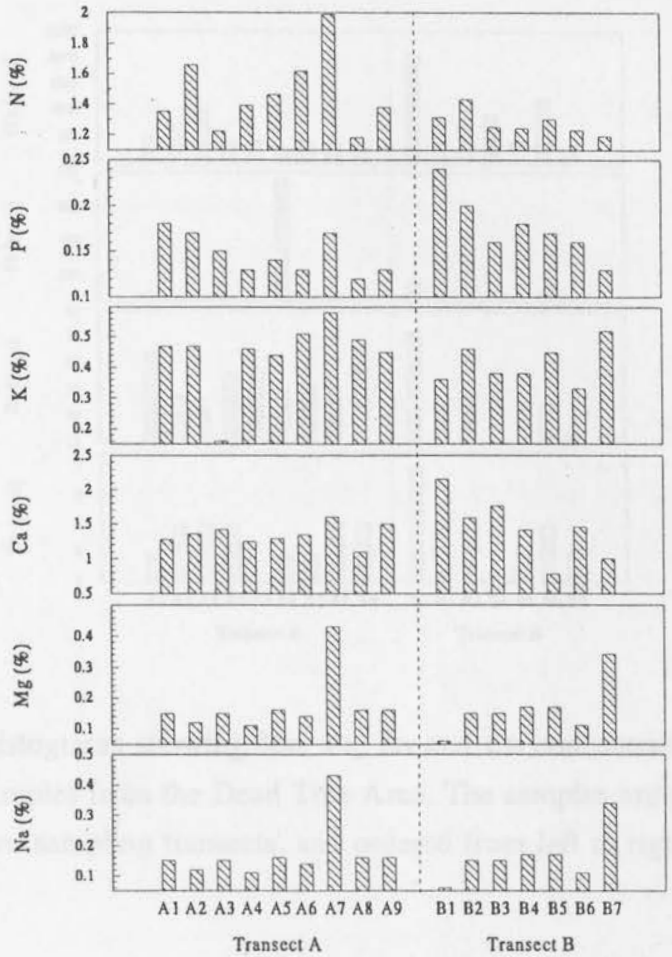

Figure 6.14 Histograms showing N, P, K, Ca, Mg and Na concentrations in Eucalyptus foliar samples from the Dead Tree Area. The samples are grouped according to the two sampling transects, and ordered from left to right, NE to SW.

portion of the area and that the south and south-western portion of the site is relatively less affected. For this reason the foliar samples were collected along transects which traverse from NE to SW to determine whether differences in soil and water quality are reflected in the foliar analyses. Within transect A, only the P concentrations exhibit a general decrease from NE to SW ie. samples A1 to A9. Within transect B, P and Ca exhibit a general decrease from samples B1 to B9 and Mg and Na exhibit a general increase from B1 to B9.

The Mn, Fe, Zn, and Cu concentrations of sample B1 are consistently the highest values within transect B. However, there is no general trend of decreasing values from B1 ro B7 in these elements.

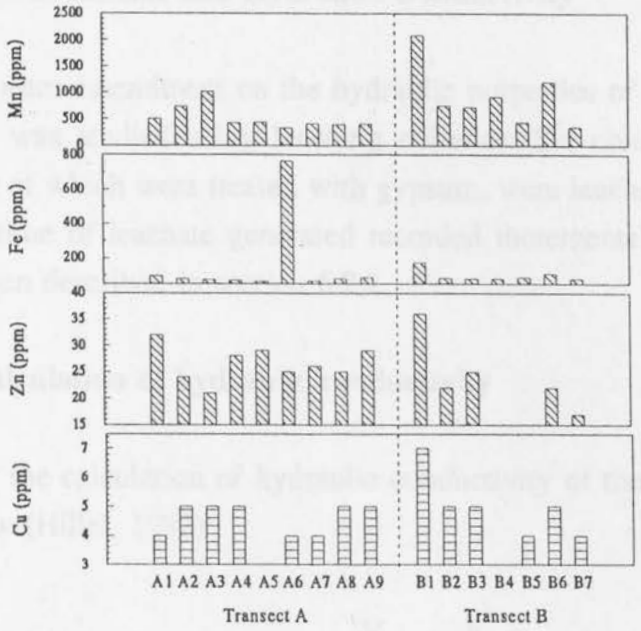

Figure 6.15 Histograms showing Mn, Fe, Zn and Cu concentrations in Eucalyptus foliar samples from the Dead Tree Area. The samples are grouped according to the two sampling transects, and ordered from left to right, NE to SW.

Comparison of the above results with the nutrient concentrations of *Eucalyptus camaldulensis* foliar samples from a waterlogging/salinity stress trial by Farrell *et al.*, (1996) revealed conflicting results. Whereas comparison of the N, Ca, Zn, Cu and Na^+/K^+ results indicated that waterlogging/salinity is affecting the trees, the K and Na results indicated that waterlogging/salinity is not affecting the trees.

Hence although the soil salinity/sodicity results presented in section 6.3.4 and 6.3.5 suggest that plant growth may be affected by high electrolyte concentrations, no conclusive evidence may be drawn from the above results concerning the effects of waterlogging/salinity on the trees in the Dead Tree Area. Further work is thus required to determine the effect, if any, which waterlogging/salinity is having on these trees.

6.3.7 Gypsum Amendment and Hydraulic Conductivity

The effect of gypsum amendment on the hydraulic porperties of a soil composite from the Dead Tree Area was studied using leaching columns. Six columns, two of which were controls and four of which were treated with gypsum, were leached with distilled water and the volume and time of leachate generated recorded incrementally. Details of the method followed have been described in section 6.2.2.

6.3.7.1 Calculation of hydraulic conductivity

The equation for the calculation of hydraulic conductivity of the soil columns was derived from Darcy's Law (Hillel, 1982):

$$K = \frac{V}{At} \times \frac{h}{\Delta H}$$

Experimentally, only volume (V) and (t) need to be measured for the calculation of hydraulic conductivity, since A, ΔH and h are constant. The log K values (y-axis) are plotted against the leachate depth (x-axis, cm) which was calculated by dividing the leachate volume (cm^3) by the cross-sectional area (cm^2) of the column.

6.3.7.2 Results

The results of the leaching trials are shown graphically in Figure 6.16 (the measurements of time, volume, pH, EC and the calculated hydraulic conductivity values are contained in Appendix E).

Figure 6.16 shows that the hydraulic conductivity of the untreated soil columns, A and B, decreased from initial log K values of -2.94 and -3.27, respectively, to final values of -4.49 and -5.28, respectively. These final values are equivalent to hydraulic conductivities of 3.23 x 10^{-5} and 5.22 x 10^{-6}, respectively. Although the results of column A indicate that the rate of decrease of the hydraulic conductivity of the soil columns is decreasing with further leaching, column B shows no indication of such a decrease.

Columns C, D, E, and F, which were all treated with 10 tons/ha gypsum, do not show a decrease in hydraulic conductivity with leaching. Instead the log K values of these columns

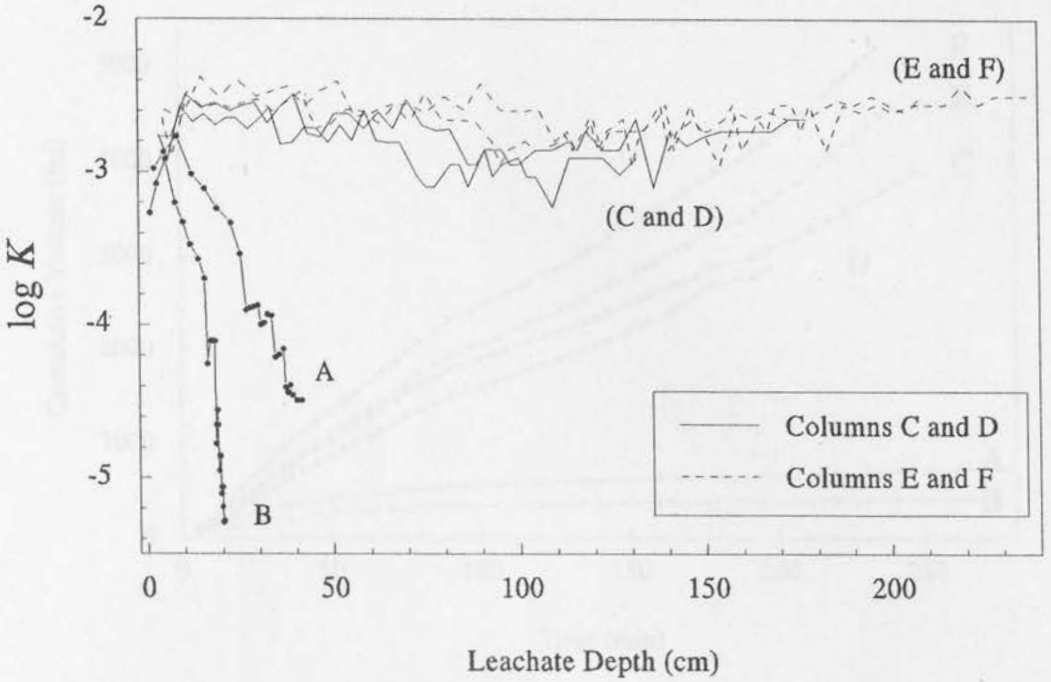

Figure 6.16 Plot of log K versus leachate depth showing the change in hydraulic conductivity for untreated soil columns (A and B), columns with 10 tons/ha gypsum applied to the soil surface (C and D) and 10 tons/ha gypsum mixed into the soil column (E and F).

remained relatively constant for the duration of the trial, with log K values ranging from between -2.43 and -3.23. Figure 6.16 shows that the log K values of columns E and F, which had gypsum mixed into the soil column as opposed to surface application in columns C and D, are generally marginally higher than those of columns C and D. This difference is further highlighted in Figure 6.17 which shows cumulative leachate volume versus time. The plot shows that the graph slopes for columns E and F are greater than those of columns C and D, indicating that the hydraulic conductivity of the former columns is in fact greater than that of the latter.

The results of the EC and pH analyses of the leachate are shown in Figures 6.18 and 6.19, in which they are plotted as a function of time. The electrical conductivity values of the leachate solutions from all six columns decrease exponentially, as would be expected from the dissolution of salts from the soil columns. The pH values of the columns increased from comparatively acidic values to more neutral values. After approximately 30 minutes the pH values of the leachate from columns C, D, E and F remained relatively stable within the pH

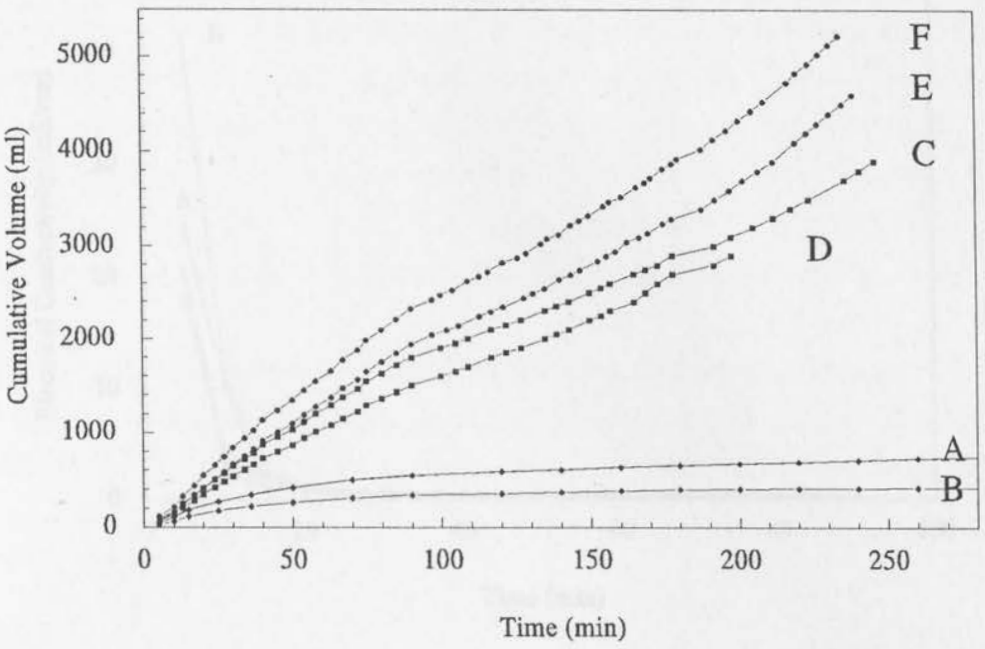

Figure 6.17 Plot of cumulative leachate volume versus time for untreated soil columns (A and B), columns with 10 tons/ha gypsum applied to the soil surface (C and D) and 10 tons/ha gypsum mixed into the soil column (E and F).

range 6.2 to 6.4. The pH values of columns A and B increased considerably more than those of the other columns, however, reaching about pH 7 after 90 minutes.

6.3.7.3 Discussion

Due to the high sodicity of the soils from the Dead Tree Area, reported in section 6.3.5 of this chapter, a significant proportion of the colloidal surfaces in the soil columns will be occupied by Na^+, resulting in a relatively diffuse electric double layer around the colloidal surfaces, and hence dominance of the double-layer repulsive forces over the van der Waals attractive forces. The net result of this is clay dispersion and thus lowered hydraulic conductivity. Leaching of the soil columns with distilled water results in the dissolution and removal of salts from the soil columns. This will further increase the degree of colloidal dispersion as dispersion behaviour is favoured at relatively lower electrolyte concentrations.

In the case of soil columns A and B, which were untreated soil samples, the sodicity of the soil would account for the rapid decrease in hydraulic conductivity as a result of clay

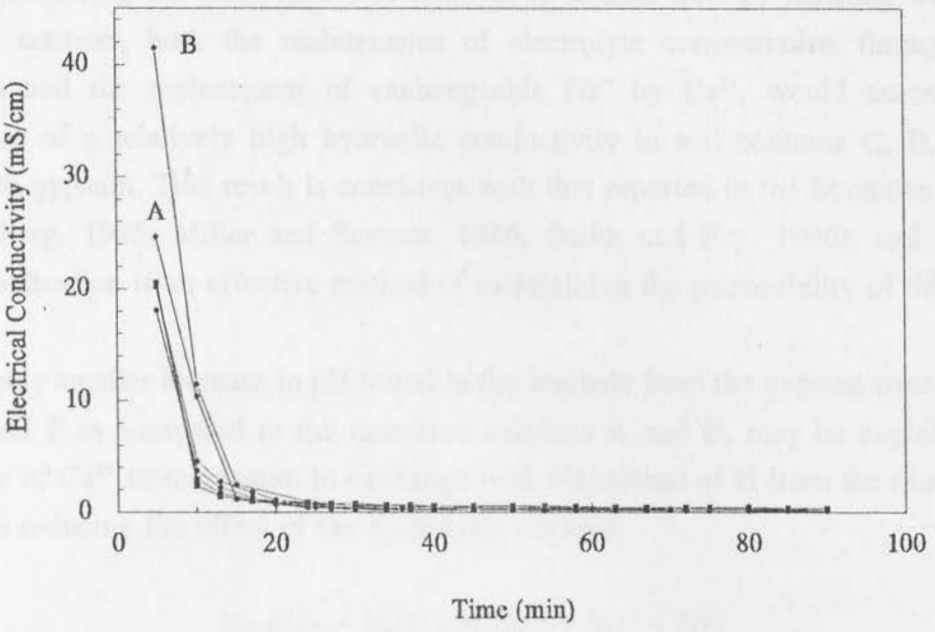

Figure 6.18 Plot of electrical conductivity (EC) versus time for untreated soil columns (A and B), columns with 10 tons/ha gypsum applied to the soil surface (C and D) and 10 tons/ha gypsum mixed into the soil column (E and F).

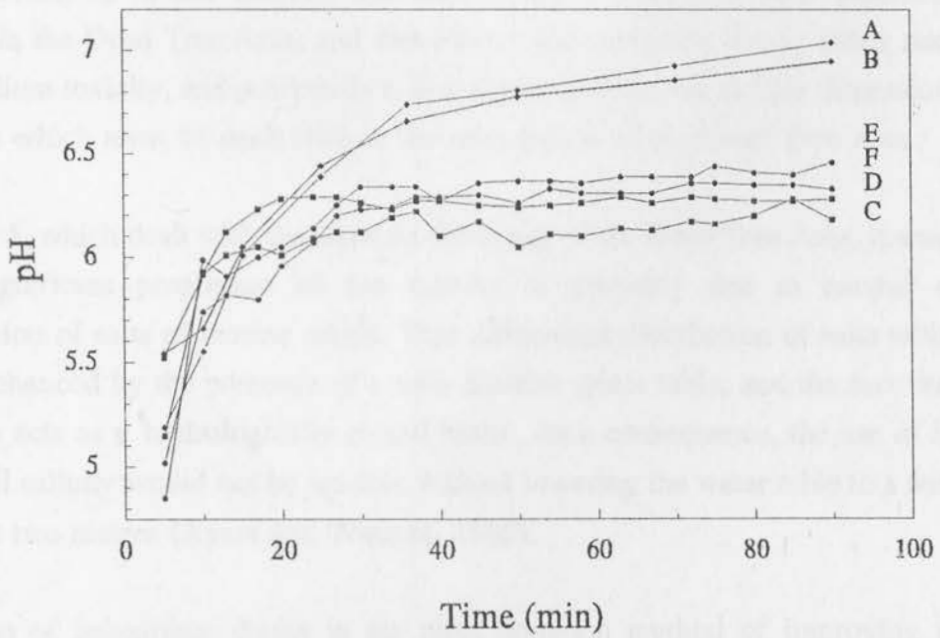

Figure 6.19 Plot of pH versus time for untreated soil columns (A and B), columns with 10 tons/ha gypsum applied to the soil surface (C and D) and 10 tons/ha gypsum mixed into the soil column (E and F).

dispersion following the dissolution and removal of soluble salts by leaching with distilled water. By contrast, both the maintenance of electrolyte concentration through gypsum dissolution and the replacement of exchangeable Na^+ by Ca^{2+}, would account for the maintenance of a relatively high hydraulic conductivity in soil columns C, D, E, and F, treated with gypsum. This result is consistent with that reported in the literature (du Plessis and Shainberg, 1985; Miller and Sumner, 1986; Smith and Fey, 1996), and shows that gypsum application is an effective method of maintaining the permeability of this soil.

The relatively smaller increase in pH found in the leachate from the gypsum treated columns C, D, E and F as compared to the untreated columns A and B, may be explained by the availability of Ca^{2+} from gypsum to exchange with Na instead of H from the dissociation of water, thus reducing the effect of the hydrolysis reaction:

$$\text{Na-clay} + H_2O \leftrightarrow \text{H-clay} + Na^+ + OH^-$$

during leaching.

6.3.7.4 Proposed Remediation for the Dead Tree Area

It has been shown in this chapter, that soil salinity and sodicity both constitute potential problems in the Dead Tree Area, and that *Eucalyptus* mortality, due to either osmotic stress and/or sodium toxicity, and potentially low soil permability, due to clay dispersion represent, key issues which must be dealt with in the remediation of the Dead Tree Area.

In chapter 5, which dealt with the aqueous chemistry of the Dead Tree Area, it was concluded that a significant proportion of the salinity is probably due to natural evaporative concentration of salts of marine origin. This differential distribution of salts within the area may be enhanced by the presence of a very shallow water table, and the fact that the Dead Tree Area acts as a 'hydrologically closed basin'. As a consequence, the use of irrigation to reduce soil salinity would not be feasible without lowering the water table to a suitable depth of at least two metres (Ayers and Westcot, 1985).

Installation of subsurface drains is the most common method of improving the internal drainage rate of a soil. However, as has been shown in this chapter, soil sodicity will result in reduced hydraulic conductivity unless a suitable chemical conditioner, such as gypsum, is applied.

The following remediation strategy is thus proposed:

Step I - *application of gypsum to the soil surface, so at to increase soil hydraulic conductivity (due to the proximity of the gypsum dumps, further trials to determine the optimum application rate so as to minimise transport costs are not imperative; methods to calculate the gypsum requirement of the soil are given in the literature (Shainberg et al., 1989));*

monitoring: tri-axial tests to monitor and assess the effect of the gypsum on soil conductivity.

Step II - *installation of subsurface drains, so at to stabilise and maintain the water table at a minimum of at least two metres below the soil surface;*

monitoring: soil sampling to monitor changes in soil salinity and sodicity (ESP and SAR), and to assess whether the application of a leaching fraction is required or not.

Step III - *irrigation, to flush salts from the soil profile;*

monitoring: as for step II. The use of water from the Heldeview Main Drain would be suitable for 'flushing' salts from the soil profile due to the comparatively low salinity of this water (0.75 mS/cm).

6.4 Conclusions

In this chapter, it has been shown that the soils in the Dead Tree Area are characterised by being slightly acidic to neutral in pH, having generally low organic carbon % and a clay mineralogy dominated by kaolinite, with subdominant quartz.

The saturated paste extracts revealed that the salinity of the soils in the Dead Tree Area is generally greater than that of the farmland area, particularly in the north-eastern portion of the Dead Tree Area. Soil samples A1, A2, A3, B1, B2 and the surface sample of C1 were classified as being saline as a result of the EC of their respective saturated paste extracts being greater than 4 mS/cm. The calculated osmotic pressure of these samples was up to 33 atmospheres, sufficient pressure to significantly impede water uptake by plants. Osmotic

stress may, therefore, have been responsible, at least in part, for the death of trees in the Dead Tree Area.

The ESP values of the soils from the Dead Tree Area were found to range from between 4.81 and 45.3%, indicating that sodicity is potentially a problem in these soils. Following the criterion of McBride (1994), samples A2a and A2b were classified as saline-sodic and samples A4b and B3a as sodic. Although an ESP value of >15% has been reported as the cut-off value above which significant clay dispersion occurs (Tan, 1992), the dispersible clay percentage of selected samples showed that dispersion occurs in these samples at ESP values as low as 4.81%. This is consistent with findings reported in more recent literature (Levy and Torrento, 1995). Calculation of SAR values from the saturated paste extracts and soil water samples, showed that, as with the ESP values, the highest SAR values are found in the north-eastern portion of the Dead Tree Area. The sodicity hazard of these waters, as defined on the basis of SAR values, was found to range from low to very high (1.6 to 42.1 $mol^{1/2}m^{-3/2}$). As in the case of soil salinity and osmotic stress, sodium toxicity resulting from soil sodicity may have been responsible, at least in part, for the death of trees in the Dead Tree Area.

Analyses of *Eucalyptus* foliage samples from the Dead Tree Area were used to assess whether waterlogging/salinity effects could be detected by comparing the results with nutrient concentrations of *Eucalyptus camaldulensis* foliar samples from a waterlogging/salinity stress trial reported in the literature by Farrell *et al.,* (1996). The results were inconclusive, however, and no direct statement could be made concerning the effect of waterlogging/salinity on the *Eucalyptus* trees in the Dead Tree Area.

Gypsum application was found to be an effective means to increase soil hydraulic conductivity by reducing soil sodicity and hence colloidal dispersion, and is considered to represent an important component of any future remediation of the Dead Tree Area.

On the basis of the results presented in this and preceding chapters a three part remediation strategy has been proposed, involving (i) application of gypsum to the soil surface to increase hydraulic conductivity; (ii) installation of subsurface drains to stabilise and maintain the water table at a minimum of at least two metres; and (iii) if neccesary, irrigation to flush salts from the soil profile.

7. DISCUSSION AND RECOMMENDATIONS

7.1 Conclusions

The aim of this study was to conduct an investigation of the water and soils of the Dead Tree Area by addressing a number of key objectives and questions outlined in chapter 1. These objectives and questions together with the answers obtained from this study are discussed below.

1. What are the 'background levels' for water and soils quality in the study area?

1.1 Water

The Heldeview Drain represents the main source of surface water entering the north-eastern potion of the AECI site, and was considered to be an appropriate measure of 'background' water quality levels for the site. The quality of this water was found to be high, meeting the majority of the draft domestic water quality guidelines set by the Department of Water Affairs and Forestry (1995). Due to the differential distribution of salts within the landscape, revealed by the analyses of soil water from the Dead Tree Area, however, the water from the Heldeview Drain was not an appropriate measure of 'background' water quality against which contamination of the water from the Dead Tree Area could be assessed. Instead, the 'background levels' or natural quality of the water in the study area was assessed by determining the 'marine signiature' of the water from the Dead Tree Area, and considering deviations from this signature as indicative of anthropogenic contamination.

1.2 Soils

The 'background levels' for soil quality in the study area were assessed by analysing eight soil samples (4 surface and 4 subsurface) from the farmland area located north of the gypsum dumps. The soils were characterised by being slightly acidic to neutral in pH, having generally low organic carbon and a clay mineralogy dominated by kaolinite, with subdominant quartz. The salinity of the farmland soils was low, with the EC values of the saturated paste extracts ranging from 0.2 to 2.9 mS/cm. The sodicity of the soils was also low, with ESP values of 5.92 and 8.55, and SAR values ranging from 0.1 to 1.7 $mol^{1/2}m^{-3/2}$. Samples 1b and 3b were analysed for dispersible clay, which showed that 4.7 and 7.4 % of the total clay content in these soils was dispersed.

2. *Three key potential sources of contamination may be identified in the site, namely the sulphur stockpile, the fertilizer evaporation ponds and the gypsum dumps. What are the chemical characteristics of these three potential sources of contamination?*

The waste water/leachate associated with all three potential sources of contamination was characterised by being *acidic*, with pH values ranging from 1.5 to 4.5, and acidities of 12.9 mmol/l to 328 mmol/l, and *saline*, with electrical conductivity values ranging from 6.3 mS/cm to 20.7 mS/cm.

2.1 Sulphur stockpile

The chemical characteristics of the sulphur stockpile were assessed by analysing leachate that had evolved from the stockpile. The leachate was found to be characterised by extreme acidity (328 mmol/l; pH 1.5) and sulphate concentrations (13600 mg/l), and high salinity (20.7 mS/cm). The acidity of the leachate is believed to have resulted in the mobilization of heavy metals in the surrounding soils and to be the explanation for the high concentrations of Al (845 mg/l), Fe (423 mg/l), Mn (18.1 mg/l) and As (1.68 mg/l) detected in the leachate. Despite the high Al and Fe concentrations in the leachate, no Al or Fe containing minerals were predicted by MINTEQA2 to be supersaturated or close to equilibrium. This was explained by the fact that the leachate is highly acidic and hence the solubility of these metals is very high. MINTEQA2 predicted that if the pH of the leachate were to increase to 3.5 pH units, the minerals $AlOHSO_4$, kaolinite and muscovite would become supersaturated.

2.2 Fertilizer evaporation ponds

The fertilizer evaporation pond/Triomf Main Drain waters had a higher pH (2.7 to 4.5), lower acidity (13.4 to 34.5 mmol/l), and lower salinity (6.3 to 11.7 mS/cm) than the leachate from the sulphur stockpile. The anionic composition of the water was dominated by sulphate, although chloride, phosphate, fluoride and nitrate concnetrations were also high. There was, however, no dominant cation species. The water contained elevated concentrations of various metals, notably Al, Fe, Zn, Mn, As and Si. Aluminium concentrations were particularly high ranging in concentration from 18.9 to 130 mg/l. Although a number of minerals were predicted by MINTEQA2 to be close to equilibrium or supersaturated in these waters (eg. gypsum, anhydrite, quartz and cristobalite), only gypsum was detected, by XRD analysis, in the precipitate forming in the evaporation ponds. This may have been because the lower limit of detection of these minerals is relatively high and hence, although present in the precipitate, they were not detectable, or it may because these minerals were in fact not present. If the latter is true, then this would illustrate that predictions of mineral solubility equilibria based on thermochemical data alone cannot necessarily be used to make inferences

concerning the precipitation or dissolution of minerals without also taking kinetic considerations into account.

The sediment analysis revealed a particularly high organic matter content (11.8%) as well as elevated concentrations of the heavy metals Pb, Cu and Zn (865, 524 and 247 ppm, respectively). It was proposed that the elevated metal concentrations were a consequence of the high organic matter content, which allowed for the complexation, and hence accumulation, of a large proportion of metals released in the Kynoch Fertilizer Limited aqueous effluent stream.

2.3 Gypsum dumps

The water in the gypsum leachate collection pond had a pH (3.9), acidity (20.7 mmol/l) and salinity (9.8 mS/cm) comparable to that of the fertilizer evaporation pond waters. Although high in Ca^{+}, K^{+} and SO_4^{2-}, the water was dominated by NH_4^{+} and NO_3^{-}. The metal concentrations were low, except for Al (90.8 mg/l), Zn (1.94 mg/l) and Mn (2.09 mg/l). MINTEQA2 predicted the supersaturation of numerous Al containing minerals as well as those minerals found to be supersaturated in the fertilizer pond water.

3. What are the chemical characteristics of the water and soils in the Dead Tree Area?

3.1 Water

The analyses of subsurface water in the Dead Tree Area revealed marked spatial variability in water charactertistics, with certain samples being strongly acidic (pH $<$ 2.5; acidity 5.9 to 17.1 mmol/l) and other being close to neutral with pH values $>$ 6 (alkalinity between 100 and 520 mg $CaCO_3$/l). The range in EC for these waters was extreme, with the 'least saline' sample having an EC of 1.6 mS/cm and the most saline having an EC value 60% more saline than sea water (90.3 mS/cm).

Plotting the major cation and anion data on a pipergram produced a strong clustering, indicating that the composition of the water samples was quite similar. Based on a hydrochemical facies classification these waters were characterised as 'sodium and chloride dominant type'. The pipergram also revealed that there was a greater degree of variability in the anionic composition of these waters than in the cationic composition, and that the proportion of carbonate/bicarbonate anions to sulphate and chloride anions was very low.

The metal concentrations found in the water samples from the Dead Tree Area were generally low, with concentrations being either below detection limits or only slightly above

for the majority of the samples analysed. High concentrations of Al (max. 108 mg/l), Fe (max. 10.6 mg/l), and Mn (max. 17.8 mg/l) were, however, found in some samples.

3.2 Soils

The soils in the Dead Tree Area were characterised by being slightly acidic to neutral in pH, having generally low organic carbon % and a clay mineralogy dominated by kaolinite, with subdominant quartz. The saturated paste extracts revealed that the salinity of the soils in the Dead Tree Area, however, is generally greater than that of the farmland area, particularly in the north-eastern portion of the Dead Tree Area. Soil samples A1, A2, A3, B1, B2 and the surface sample of C1 were classified as being saline as a result of the EC of their respective saturated paste extracts being greater than 4 mS/cm. The calculated osmotic pressure of these samples was up to 33 atmospheres, sufficient pressure to significantly impede water uptake by plants. Osmotic stress may, therefore, have been responsible, at least in part, for the death of trees in the Dead Tree Area.

The ESP values of the soils from the Dead Tree Area were found to range from between 4.81 and 45.3%, indicating that sodicity is potentially a problem in these soils. Following the criteria of McBride (1994), samples A2a and A2b were classified as saline-sodic and samples A4b and B3a as sodic. Although an ESP value of $>15\%$ has been reported as the cut-off value above which significant clay dispersion occurs (Tan, 1992), the dispersible clay percentage of selected samples showed that dispersion occurs in these samples at ESP values as low as 4.81%. This is consistent with findings reported in more recent literature (Levy and Torrento, 1995). Calculation of SAR values from the saturated paste extracts and soil water samples, showed that, as with the ESP values, the highest SAR values are found in the north-eastern portion of the Dead Tree Area. The sodicity hazard of these waters, as defined on the basis of SAR values, was found to range from low to very high (1.6 to 42.1 $mol^{1/2}m^{-3/2}$). As in the case of soil salinity and osmotic stress, sodium toxicity resulting from soil sodicity may have been responsible, at least in part, for the death of trees in the dead Tree Area.

4. What is the degree of contamination of the water and soils in the Dead Tree Area, and has contamination from the gypsum dumps, fertilizer ponds and/or sulphur stockpile impacted on the water and soils quality in the Dead Tree Area?

4.1 Water

On the basis of pH and EC data, the subsurface water samples from the Dead Tree Area were grouped into three groups, namely: low pH/high salinity, neutral pH/moderate to high

salinity, and moderate pH/low to moderate salinity. Based on consideration of the geology, topography and proximity to the ocean of the Dead Tree Area, it was proposed that under 'natural conditions' subsurface water in this area would have an approximately neutral pH and low to high salinity depending on the degree of evaporative concentration. The ratios of Na^+ to Cl^- and Ca^{2+} to Mg^{2+} in all samples were found to be the same as those of sea water indicating that these ions were of marine origin. The ratios of Cl^- to SO_4^{2-} and Na^+ to K^+ were not, however, found to be the same as those of sea water for all samples, indicating either anthropogenic contamination, or non-conservative behaviour during evaporative concentration.

Because the water in the Dead Tree Area would have a neutral pH under 'natural conditions', samples that had low pH values were suspected to have been affected by contamination from one or more of the surrounding industrial activities. These samples were located adjacent to the sulphur stockpile and hence SO_4^{2-} concentrations in these samples were investigated. The low pH/high salinity samples were found to have elevated SO_4^{2-} concentrations. This was considered to indicate that these samples had been impacted by a low-pH contaminant plume emanating from the sulphur stockpile.

To assess whether contamination from the gypsum dumps or fertilizer evaporation ponds has also affected the water in the Dead Tree Area, the concentrations of F^-, PO_4^{2-}, NO_3^- and NH_4^+ were investigated, as these were found to be elevated in the gypsum leachate ponds and fertilizer evaporation ponds but not in the sulphur leachate drain. Elevated concentrations of these ions were found in water samples located in the north-eastern section of the site. Based on this finding and the fact that the groundwater flow direction is south-west, it was proposed that these ions represent contamination originating from the gypsum dumps. It was thus concluded that contamination from the gypsum dumps and sulphur stockpile has impacted on the water in the Dead Tree Area.

The quality of subsurface water in the Dead Tree Area was also assessed according to the domestic water use and industrial water use guidelines as these provided the widest range in water quality requirements. The water quality was found to be poor, and did not meet either the domestic or the industrial use guidelines.

4.2 Soils

The soil saturated paste extracts revealed similar trends in chemical composition to the subsurface water samples form the Dead Tree Area. Hence, the above discussion on water contamination in the Dead Tree Area is equally applicable for the soils of the area.

As in the case of the subsurface water samples, it is important to note that a significant proportion of the salts in the Dead Tree Area are probably of marine origin. The problems of soil salinity and sodicity encountered in the area are, therefore, a 'natural phenomenon' that would probably have occurred in the abscence of AECI's industrial activities.

5. *Do concentrations of various elements in foliar samples from Eucalyptus trees in the Dead Tree Area exceed reported values, and could tree mortality in the area have resulted from toxicity or deficiency effects?*

Analyses of *Eucalyptus* foliage samples from the Dead Tree Area were compared to values reported for *Eucalyptus camaldulensis* foliar samples from a waterlogging/salinity stress trial reported in the literature by Farrell *et al.,* (1996).

The results were inconclusive, however, and no direct statement could be made concerning the effect of waterlogging/salinity on the eucalypts in the Dead Tree Area. The high soil salinity and sodicity (ESP and SAR) in the Dead Tree Area suggested, however, that tree mortality could have been a result of either osmotic stress (a salinity effect) and/or sodium toxicity (a sodicity effect), in addition to waterlogging.

6. *What is the potential of gypsum application as a means of remediating dispersed, sodic soils?*

The leaching trial showed that gypsum application (10 tons/ha) was an effective means to increase soil hydraulic conductivity by reducing soil sodicity and hence colloidal dispersion. Gypsum application is, thus, considered to represent an important component of any future remediation strategy for the Dead Tree Area.

On the basis of the findings of this study, a three part remediation strategy was proposed, involving (i) application of gypsum to the soil surface to increase hydraulic conductivity; (ii) installation of subsurface drains to stabilise and maintain the water table at a minimum of at least two metres; and (iii) if neccesary, irrigation to flush salts from the soil profile.

7.2 Recommendations for further work

Areas of future work which are recommended as a follow up to this study include:

- modelling the water balance of the Dead Tree Area to gain a quantitative understanding of the degree of evaporative concentration occurring in the area;
- a detailed topographic survey of the Dead Tree Area would aid in the identification and understanding of areas of most intense evaporative concentration;
- additional soils and subsurface water samples, particularly in the north-eastern portion of the Dead Tree Area, to further delineate movement of the groundwater contaminant plume; and
- further work is required to understand the effects of soil salinity and sodicity on the *Eucalyptus* trees in the Dead Tree Area. The trees may be accummulating certain salts in the roots as a coping mechanism, and hence, both roots and foliage samples should be analysed, if causal links between elevated constituents in the plants and possibe causes of mortality are to be made.

8. REFERENCES

Allison, J.D., Brown, D.S. and K.J. Novo-Gradac. (1991) *MINTEQA2/PRODEFA2, A Geochemical Assessment Model for Environmental Systems.* EPA/600/3-91/021. Environmental Protection Agency, Athens, GA.

Alloway, B.J. (1995) *Heavy Metals in Soils*, (2nd ed.), Chapman and Hall.

Alva, A.K., Sumner, M.E. and W.P. Miller. (1990) Reaction of gypsum or phosphogypsum in highly weathered acid subsoils. *Soil Sci. Soc. Am. J.,* Vol 54: pp. 993-998.

Ayers, R.S. and D.W. Westcot. (1985) Water quality for agriculture. *FAO Irrigation & Drainage Papers 29,* Food and Agricultural Organisation of the United Nations, Rome, Italy.

Bredenhann, L. and D.D. Airey. (1991) The outlook for waste legislation. *Resource,* Jan-Feb 1991, pp. 19-20.

Cerda, A. and V. Martinez. (1988) Nitrogen fertilization under saline conditions in tomato and cucumber plants. *J. Hort. Sci.* Vol 63: pp. 451-458.

Curtin, D., Stepphun, H and F. Selles. (1993) Plant responses to sulphate and chloride salinity: Growth and ionic relations. *Soil Sci. Soc. Am. J.* Vol 57: pp. 1304-1310.

Dalls, H.F. and J.A. Day. (1993) *The Effect of Water Quality on Riverine Ecosystems: A Review,* Water Research Commission, Pretoria.

Del Moral, R. and C.H. Muller. (1970) The allelopathic effects of *Eucalyptus camaldulensis. American Midlan Naturalist,* Vol 83: pp. 254-282.

Del Moral, Willis, R.J. and D.H. Ashton. (1970) Supression of coastal heath vegetation by *Eucalyptus baxteri. Austr. J. Bot.,* Vol 38, pp. 245-254.

Department of Water Affairs and Forestry. (1995) *Draft of South African Water Quality Guidelines,* (2nd ed.), Vol 3: Industrial Use and Vol 1: Domestic Use.

De Pauw, E.F. (1994) The Management of Acid Soils in Africa. *Outlook on Agriculture*, Vol 23(1): pp. 11-16.

Donkin, M.J., Pearce, J. and P.M. Chetty. (1993) Methods of Routine Plant and Soil Analysis in the ICFR Laboratories. *ICFR Bulletin Series*, No. 6/93, Institute of Commercial Forestry.

Drees, L.R. Wilding, L.P., Smeck, N.E. and A.L. Senkayi. (1989) Silica in Soils: Quartz and Disordered Silica Polymorphs. In Dixon, J.B. and S.B. Weed. (Eds), *Minerals in Soils Environments,* (2nd ed.), Soil Science Society of America, Wisconsin.

Drever, J.I. (1988) *The Geochemistry of Natural Waters,* (2nd ed.), Prentice Hall, Englewood Cliffs, New Jersey.

du Plessis, H. M., and Shainberg, I. (1985) Effect of exchangeable sodium and phosphogypsum on the hydraulic properties of several South African soils. *S. Afr. J. Plant Soil.,* Vol 2: pp. 179-185.

Farooq, S., Niazi, M.L.K., Iqbal, N., and T.M. Shah. (1989) Salt tolerance potential of wild resources of the tribe Triticeae. *Plant Soil,* Vol 19: pp. 255-260.

Farrell, R.C.C., Bell, D.T., Akilan, K., and Marshall, J.K. (1996) Morphological and Physiological Comparisons of Clonal Lines of *Eucalyptus camaldulensis*. II. Responses to Waterlogging/Salinity and Alkalinity. *Aust. J. Plant Physiol.,* Vol 23: pp. 509-518.

Fergusen, J.F. and J. Gavis. (1972) A Review of the As cycle in natural waters. *Water Researh,* Col 6: pp. 1259-1274.

Fey, M.V. (1986) Improving Soil with Gypsum. *Report on a 9 month research visit to the University of Georgia (Unpublished).*

Forstner, U. and G.T.W. Wittmann. (1979) *Metal Pollution in the Aquatic Envionment,* Springer-Verlag, Berlin.

Freeze, R.A. and J.A. Cherry. (1979) *Groundwater,* Prentice-Hall, Inc., Englewood Cliffs, New Jersey.

Greenberg, A.E., Trussel, R.R. and L.S. Clesceri. (1985) *Standard Methods for the Examination of Water and Waste Water.* Sixteenth ed., American Public Health Association, Washington, DC, pp. 513-515.

Greub, L.J., Drolson, P.N., and D.A. Rohweder. (1985) Salt tolerance of grasses and legumes for roadside use. *Agron. J.,* Vol 77: pp. 76-80.

Gupta, R.K. and I.P. Abrol. (1989) Salt-affected soils: Their reclamation and management for crop production. *Adv. Soil. Sci.,* Vol 11: pp. 223-288.

Harraway, T.J. (1996) Chemical characterisation of landfill leachate and its potential mobility through the Cape Flats Sand. *Unpublished M.Sc Thesis, University of Cape Town, RSA.*

Heffernan, B. (1985). *A Handbook of methods of inorganic chemical analysis for forest soil, foliage and water.* CSIR Division of Forest Research, Canberra.

Hillel, D. (1982) *Introduction to Soil Physics.* Academic Press, Chapter 7.

Kalra, Y.P., and Maynard, D.G. (1991) Methods manual for forest soil and plant analysis. Forestry Canada, Northwest Region, Northern Forestry Centre, Edmonton, Alberta. *INF. Rep. NOR-X-319.*

Kirkham, M.B. (1986) Porblems of using wastewater on vegetable crops. *Hort. Science* Vol 21: pp. 24-27.

Klute, A. and C. Dirksen. (1986) Hydraulic conductivity and diffusivity: laboratory methods. In: Klute, A., Campbell, G.S., Jackson, R.D., Martland, M.M., and Nielson, D.R. (Eds.), *Methods of Soil Analysis Part I, Physical and Mineralogical Methods,* Second Edition (Chapter 28), SSSA Book Series, no. 5, Soil Sci. Soc. Am., Madison, WI.

Klute, A., Campbell, G.S., Jackson, R.D., Martland, M.M., and Nielson, D.R. (Eds.), *Methods of Soil Analysis Part I, Physical and Mineralogical Methods,* Second Edition (Chapter 28), SSSA Book Series, no. 5, Soil Sci. Soc. Am., Madison, WI.

Korentajer, L. (1992) Waste production and pollution in South Africa: An overview. *17^{the} Congress Soil Science Society of South Africa* Stellenbosch pp. 1 2.1-2.5.

Kretzschmar, R., Robarge,W.P, and S.B. Weed. (1993) Flocculation of kaolinitic clays: effects of humic substances and iron oxides. *Soil Sci. Soc. Am. J.,* Vol 57: pp. 1277-1283.

Larson, S. and A.E. Widdowson. (1971) Soil fluorine. *J. Soil Sci.,* Vol 22: pp. 210-221.

Levy, R., Fine, P., and A. Feigin. (1986) Sodicity levels of soils equilibrated with wastewaters. *Soil Sci. Soc. Am. J.,* Vol 50: pp. 35-39.

Levy, G.J. and J.R. Torrento. (1995) Clay Dispersion and Macroaggregate Stability as Affected by Exchangeable Potassium and Sodium. *Soil Science,* Vol. 160: No. 5, pp. 352-358.

Lindsay, W.L. (1979) *Chemical equilibria in soils*. John Wiley & Sons, New York.

Lumsdon, D.G. and L.J. Evans. (1995) Predicting chemical speciation and computer simulation. In: Ure, A.M. and Davidson, C.M. (eds) *Chemical Speciation in the Environment.* Blackie Academic and Professional, London.

Luther, S.M. and M.J. Dudas. (1993) Pore Water Chemistry of Phosphogypsum-Treated Soil. *J. Environmental Quality,* Vol 22: p.103-108.

Maas, E.V. and G.J. Hofmann. (1977) Crop salt tolerance - Current assessment. *J. Irrigation and Drainage Division,* ASCE 103(IRZ): 115-134. Proceeding Paper 12993.

Malkin, E. and Y. Waisel. (1986) Mass selection for salt resistance in Rhodes grass (Chloris gayana). *Physiol. Plant.,* Vol 66: pp. 443-446.

Marcum, K.B. and C.L. Murdoch. (1990) Growth responses, ion relations and osmotic adaptions of eleven C_4 turfgrasses to salinity. *Agron. J.,* Vol 82: pp. 892-896.

McBride, M.B. (1994) Environmental Chemistry of Soils. *Oxford University Press.*

McDowell, L.R. (1992) *Minerals in animals and human nutrition.* Academic Press.

Mengel, K. and E.A. Kirkby. (1978) *Principles of plant nutrition.* Internation Potach Institute, Berne, Switzerland.

Miller, W.P. and Sumner, M.E. (1986) Effect of surface-applied gypsum on soil losss and infiltration of highly weathered soils. Presented at *Am. Soc. Agron. Annual Mtg.,* Dec. 1-4, New Orleans, LA.

Mills, A. (1994) Response of Kikuyu grass (*Pennisetum clandestinum*) to irrigation with saline, sodic wastes and nitrogenous, manganiferous effluent. *Unpublished M.Sc Thesis, University of Cape Town, South Africa.*

MLH Architect and Planners Report 96 904. (November 1996) *AECI Helderberg Conceptual Development Framework Draft Report.*

Murphy,J. and J.P. Riley. (1962) A modified single solution method forthe determination of phosphate in natural waters. *Anal. Chim. Acta.,* Vol. 27: pg 31.

Nelson, D.W. and Sommers, L.F. (1982) Total carbon, organic carbon, and organic matter. In *Methods of Soil Analysis, Part 2, 570-571. Am. Soc. Agron., Madison WI.*

Nicholson, G. (1984) Methods of soil, plant and water analysis. *FRI Bulletin* No. 70, Forest Research Institute, New Zealand Forest Service, Rotorua, New Zealand.

Non-affiliated soil advisory working committee (NSAWC). (1990) *Handbook of standard soil testing methods for advisory purposes.* Pretoria: Soil Science Society of South Africa.

Oster, J.D., Shainberg, I. and J.D. Wood. (1980) Flocculation value and gel structure of Na/Ca montmorillonite and illite suspension. *Soil Sci. Soc. Am. J.,* Vol 44: pp. 955-959.

O'Brien, L.D. and M.E. Sumner. (1988) Effects of phosphogypsum leachate on soil chemical composition. *Commun. Soil Sci. Plant Anal.,* Vol 19: pp. 1319-1329.

Paek, K.Y., Chandler, S.F. and T.A Thorpe. (1988) Physiological effects of Na_2SO_4 and NaCl on callus cultures of *Brassica campestri* (Chinese cabbage). *Physiol. Plant.,* Vol 72: pp. 160-166.

Page A.L. (Ed.). (1982) *Methods of Soil Analysis, Part 2: Chemical and Microbiological Properties.* Agronomy Monograph no. 9 (2nd edition), ASAA-SSSA, 667 S. Segoe Road, Madison, WI 53711, USA.

Papadopoulos, I. (1986) Effect of high sulphate irrigation water on soil salinity and yields. *Agron. J.,* Vol 78: pp. 429-432.

Pickard, G.L, and W.J. Emery. (1990) *Descriptive Physical Oceanography: An Introduction.* (5th ed.), Pergamon Press, Oxford, England, pg 14.

Quirk, J.P. & R.K. Schoefield, 1955. The effect of electrolyte concentration on soil permeability. *J. Soil Sci.,* Vol 6: pp. 163-178.

Rai, D. and J.A. Kittrick. (1989) Mineral Equilibria and the Soil System. In Dixon, J.B. and S.B. Weed. (Eds), *Minerals in Soils Environments,* (2nd ed.), Soil Science Society of America, Wisconsin.

Rhoades, J.D. and S.D. Merrill. (1976) Assessing the suitability of water for irrigation: Theoretical and empirical approaches. In: *Prognosis of Salinity and Alkalinity,* FAO Soils Bulletin 31, FAO, Rome.

Rhoades, J.D. (1982) Soluble Salts. In *Methods of Soil Analysis Part 2: Chemical and Microbiological Properties*, Chapter 10. Agronomy Monograph no. 9 (2nd edition), ASAA-SSSA, 667 S. Segoe Road, Madison, WI 53711, USA, (1982).

Rysgaard, S., Risgaard-Petersen, N., Nielsen, L.P., and Revsbech, N.P. (1993) Nitrification and denitrification in lake and estuarine sediments measured by the ^{15}N dilution technique and isotope pairing. *Applied and Environmental Microbiology.,* Vol 59: pp 2093-2098.

Shainberg, I., Summer, M.E., Miller, W.P., Farina, M.P.W., Pavan, M.A. and M.V. Fey. (1989) Use of gypsum on soils; A review. *Adv. Soil Sci.,* Vol 9: pp. 1-11.

Shone, M.G.T. and J. Gale. (1983) Effect of sodium chloride stress and nitrogen source on respiration, growth, and photosynthesis in lucerne (Medicago sativa L.). *J. Exper. Bot.,* Vol 34: pp. 1117-1125.

Simon, Z. and M. Tedesco. (1987) Agronomic requirements for soil utilization in liquid waste disposal systems - the case of Sitel. *Wat. Sci. Tech.,* Vol 19(8): pp. 177-194.

Smith, D.C. and M.V.Fey. (1996) Chemical manipulation of soil for sealing landfills. *Applied Geochemistry*, Vol 11, pp. 325-329.

Sposito, G. (1989) *The Chemistry of Soils.* Oxford University Press.

Steffen, Robertson and Kirsten, Report 180429/1. (June 1992) *Somerset West Factory Site Rehabilitation.*

Steffen, Robertson and Kirsten, Phase I Report 213268/1. (December 1995) *Subsurface Assessment and Remediation at the AECI Somerset West Factory Site.*

Stumm, W. and J.J. Morgan. (1981) *Aquatic Chemistry. An Introduction Emphasizing Chemical Equilibria in Natural Waters,* (2nd ed.), J. Wiley and Sons, New York.

Tan, K.H. (1992) *Principles of Soil Chemistry,* Second Edition, Marcel Dekker Inc., Chapter 9, p. 273.

Thompson, J.G. (1983) The role of the ammonium ion in aiding the disposal of alkaline sodium-rich effluents by irrigation. *Proc. 10th Nat. Congr. Soil Sci. S. Afr.*, Tech. Commun. Dept. Agric. Repub. S. Afr. No. 180, pp. 44-47.

Underwood, E.J. (1971) Trace metals in soils and their environmental significance. *Adv. Soil Sci.* Vol 9: pp. 113-137.

Ure, A.M. and C.M. Davidson. (1994) *Chemical Speciation in the Environment,* Blackie Academic and Professional.

Walkley, A. (1935) An examination of methods for determining organic carbon and nitrogen in soils. *J. Agr. Sci.,* No.25: pp. 598-609.

Ward, R.C. (1975) *Principles of Hydrology,* MacGraw-Hill, London.

Wetzel, R.G. (1983) *Limnology,* (2nd ed.), Saunders College Publishing, Fort Worth.

Wild, A. (1994) *Soils and the Environment: An Introdution.* Cambridge.

9. APPENDICES

APPENDIX A - Description of Standard Analytical Methods

A:A.1 - A.6 WATER ANALYSES

A:A.1 pH (Glass Electrode - Calomel Electrode ph Meter Method)

A glass electrode paired with a calomel (reference) electrode, standardised with buffers of known pH, may be used to indicate the pH of a solution from the millivolts of potential generated when the two electrodes are placed in the solution. The glass electrode is the H^+-sensing electrode and develops potential (voltage) proportional to the logarithm of changes in activity of H^+. It is thus termed the indicating electrode. The calomel electrode (i) contains a saturated KCl bridge that contacts the solution and (ii) has a characteristic potential (voltage) relatively independent of the H^+ activity, and is termed the reference electrode. A temperature probe is used in conjunction with the above paired electrodes to provide for temperature correction.

Procedure

A glass electrode-calomel electrode *Crison microp*H *2001* microprocessor-controlled pH meter with automatic temperature compensation was used for pH measurements, and was calibrated with pH 4 and 7 standard buffer solutions so as to adjust the instrument to the response of the glass electrode. Equilibrium was first established between the electrode and sample by stirring the sample gently to insure homogeneity. Triplicate readings were taken for each sample, rinsing the electrodes with distilled water, and blotting them dry between each measurement.

A:A.2 Electrical Conductivity (EC)

A *Crison microCM 2201* electrical conductivity meter was used for EC measurements. The specific cell constant keyed into the meter was checked to be the same as that listed for the cell in use. The calibration of the meter was assessed by measuring the EC of a standard 0.01 *M* KCl solution and comparing this to the tabulated EC value for that standard at a specific temperature. Triplicate readings were taken for each sample, rinsing the electrode with distilled water and blotting dry between each measurement.

A:A.3 Alkalinity/Acidity

Alkalinity was measured on samples with pH values > 4.5 using a method of potentiometric

titration to an end-point of pH 4.5. Acidity was measured on samples with pH values < 4.5 again using a potentiometric titration to an end-point pH of 8.3. In both instances an automated *TTT 85 Titrator* with *ABU 80 Burette* was used.

A:A.4 Major Cation and Anion Analysis (High Pressure Ion Chromatography)

High Pressure Ion Chromatgraphy (HPIC) was used to determine major cations (K^+, Na^+, Ca^{2+}, and Mg^{2+}) and anions (Cl^-, NO_3^- and SO_4^{2-}) in water samples. HPIC is based on the principle that ions in a solution may be separated using a stationary phase ion exchange resin contained in a column. Detection of the ions of interest is done by conductivity with chemical suppression of the eluant.

Samples were prepared for analysis by filtration through 0.2 µm Millipore filter paper and dilution with Milli-Q de-ionised water to obtain EC values between 50 and 100 µS/cm. Immediately prior to analysis the samples were filtered through Dionex On-Guard P filters to remove organics and particulates. Analyses were carried out by means of a Dionex DX300 series suppressed IC system, which was coupled to an AI-450 chromatography software package.

Anions

An HPIC-AG4A column was used as a guard column, with an HPIC-AS4A-SC separator column. The eluant flow rate was 2.0 ml/min and suppression was achieved by an anion micromembrane suppressor. A mixed sodium carbonate/sodium bicarbonate (1.80 mM Na_2CO_3; 1.70 mM $NaHCO_3$) eluent was used. The run time per sample was 8 minutes.

Cations

An HPIC CG12 guard column was used with a CS12 separator column. A 20 mM methane sulfonic acid eluant was used. The flow rate was 1.0 ml/min and suppression was achieved by a cation micromembrane suppressor. A 20 mM Methyl-sulphonic acid eluant was used. The run time per sample was 15 minutes.

A:A.5 Murphy and Riley Phosphorus Determination (Ascorbic Acid Method)

Phosphorus was determined using the Murphy and Riley (1962) ascorbic acid method as described by Greenberg *et al.* (1985). The method is based on the principle that ammonium molybdate and potassium antimonyl tartrate react in an acid medium with orthophosphate to

form a heteropoly acid - phosphomolybdic acid - that may reduced to an intensely coloured molybdenum blue by ascorbic acid, and that the intensity of the colour is proportional to the amount of phosphate in solution.

Reagents

i. Sulphuric acid *5N*: dilute 70 ml conc. H_2SO_4 to 500 ml with distilled water.

ii. Potassium antimonyl tartrate solution: dissolve 1.3715 g $K(SbO)C_4H_4O.1/2H_2O$ in 400 ml distilled water in a 500 ml volumetric flask and dilute to volume.

iii. Ammonium molybdate solution: dissolve 20 g $(NH_4)_6Mo_7O_{24}.4H_2O$ in 500 ml distilled water.

iv. Ascorbic acid 0.01*M*: dissolve 1.76 g ascorbic acid in 100 ml distilled water. The solution is stable for about 1 week at 4°C.

v. Combined reagent: mix the above reagents in the following proportions for 100 ml of combined reagent: 50 ml *5N* H_2SO_4, 5 ml potassium antimonyl tartrate solution, 15 ml ammonium molybdate solution, and 30 ml ascorbic acid solution. Mix after addition of each reagent. If turbidity forms in the combined reagent, before proceeding, shake and let stand for a few minutes until turbidity disappears. The reagent is stable for 4 hours.

vi. Standard phosphate solution: dilute 50.0 ml stock phosphate solution to 1000 ml with distilled water; 1.00 ml = 2.50 µg P.

Procedure

An aliquot of sample (25 ml) was pipetted into a 125 ml Erlenmeyer flask to which 0.05 ml phenolphthalein indicator was added. If a red colour developed *5N* H_2SO_4 was added dropwise to just discharge the colour. To this 4.0 ml combined reagent was added and mixed thoroughly. After 10 minutes but no more than 30 minutes, the absorbance of the sample at 880 nm was measured using a *Turner 340 spectrophotometer.*

A calibration curve was prepared from a series of six standards with phosphate values ranging from 0 mg P/L to 1.2 mg P/L. Absorbance for the standards was plotted against phosphate concentration to give a straight line passing through the origin (Figure B2.1). A regression equation was calculated for the plot and used to determine mg P/L from the absorbance values of samples.

Calculation

The mg P/L in the original samples was calculated from the equation:

$$mg\ P/L = \frac{mg\ P\ (\approx 29\ mL\ final volume) \times 1000}{mL\ sample}$$

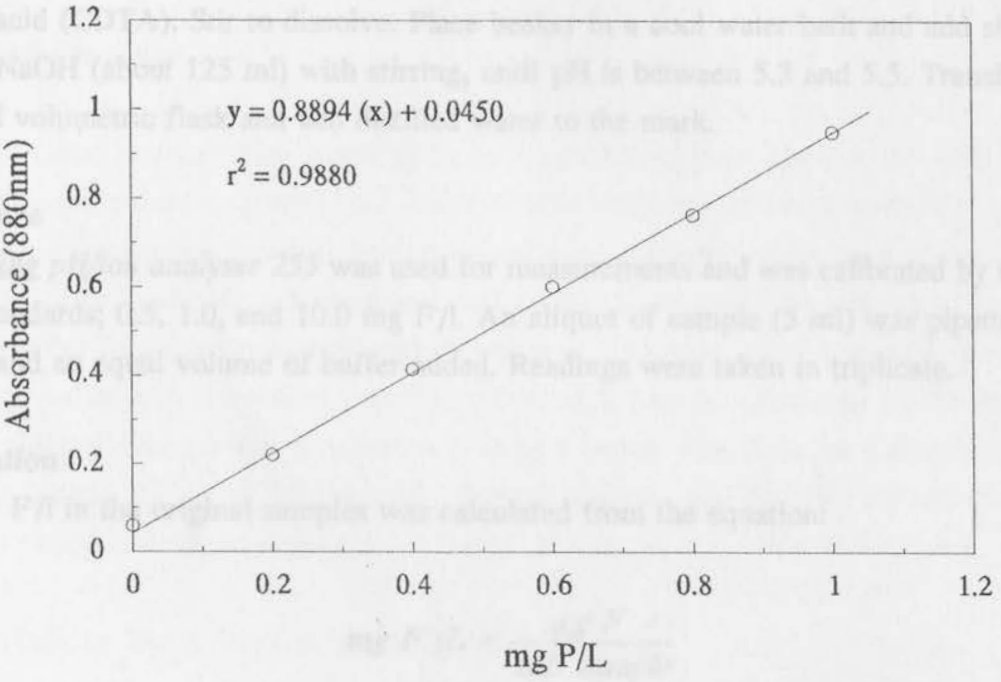

Figure B2.1: Phosphorus calibration curve derived for the standard solutions using the method of Murphy and Riley (1962).

A:A.6 Fluoride (Ion Selective Electrode Method)

Fluoride was determined using a fluoride ion selective electrode. The key element in the fluoride electrode is the laser-type doped lanthanum fluoride crystal across which a potential is established by fluoride solutions of different concentrations. The electrode measures the ion activity of fluoride in solution, however, rather than concentration. Fluoride ion activity depends on the solution total ionic strength and pH, and on fluoride complexing species (notably aluminum and iron). Adding an appropriate buffer provides a uniform ionic strength background, adjusts pH, and breaks up complexes so that, in effect, the electrode measures concentration.

Reagents

i. Stock fluoride solution: dissolve 221.0 mg anhydrous sodium fluoride, NaF, in distilled water and dilute to 1000 ml; 1.00 ml = 100 μg F^-.

ii. Standard fluoride solution: dilute 100 ml stock fluoride solution to 1000 ml with distilled water; 1.00 ml = 10.0 μg F^-.

iii. Fluoride buffer: place approximately 500 ml distilled water in a 1 l beaker and add 57 ml glacial acetic acid, 58 g NaCl, and 4.0 g 1,2 cyclohexylenediaminetetraacetic acid (CDTA). Stir to dissolve. Place beaker in a cool water bath and add slowly *6N* NaOH (about 125 ml) with stirring, until pH is between 5.3 and 5.5. Transfer to a 1 l volumetric flask and add distilled water to the mark.

Procedure

A *Corning pH/ion analyser 255* was used for measurements and was calibrated by means of three standards; 0.5, 1.0, and 10.0 mg F^-/l. An aliquot of sample (5 ml) was pipetted into a beaker and an equal volume of buffer added. Readings were taken in triplicate.

Calculation

The mg F^-/l in the original samples was calculated from the equation:

$$mg\ F^-/L = \frac{\mu g\ F^-}{mL\ sample}$$

A:B.1 - B.7 SOIL ANALYSES

A:B.1 pH (Glass Electrode - Calomel Electrode pH Meter Method)

A glass electrode paired with a calomel (reference) electrode, standardised with buffers of known pH, may be used to indicate the pH of a solution from the millivolts of potential generated when the two electrodes are placed in the solution. The glass electrode is the H^+-sensing electrode and develops potential (voltage) proportional to the logarithm of changes in activity of H^+. It is thus termed the indicating electrode. The calomel electrode (i) contains a saturated KCl bridge that contacts the solution and (ii) has a characteristic potential (voltage) relatively independent of the H^+ activity, and is termed the reference electrode. A temperature probe is used in conjunction with the above paired electrodes to provide for temperature correction.

Procedure

The pH of soil samples was measured both in water and in $CaCl_2$. Ten gram samples of sieved (<2 mm) soils were diluted in 25 ml distilled de-ionised water and 25 ml 0.01*M* $CaCl_2$, respectively, to obtain a 1:2.5 soil : water ratio. The solutions were shaken in centrifuge tubes by a horizontal mechanical shaker for 10 minutes and then allowed to settle for ± 30 minutes after which the solutions' pH were determined as described in Appendicx A:A1 for water samples.

A:B.2 Soluble Salts

Saturated paste extracts were prepared by mixing Milli-Q de-ionised water with 250 g of gently ground, sieved (<2 mm) and air-dried soil until the soil was uniformly saturated. Saturation was considered to have been achieved when the samples glistened as they reflected light, flowed only slightly when tipped, and consolidated easily by tapping or jarring the container after forming a trench through the mixture with the side of a spatula. The samples were then sealed and allowed to equilibrate overnight prior to extraction of the supernatant using a Buchner filter funnel attached to a vacuum pump. The saturated paste extracts were analysed for pH, EC, Alkalinity/Acidity, Cations, Anions, and Fluoride following the same standard methods as those described for water samples in Appendix A:A.1 - A.6.

A:B.3 Walkley-Black Organic Carbon Determination

The method followed was that of Walkley (1935) as described in NSAWC (1990). The method utilises a potassium dichromate ($K_2Cr_2O_7$) and sulphuric acid mixture to oxidise organic matter present;

$$2Cr_2O_7^{2-} + 3C + 16H^{+} = 4Cr_3^{+} + 3CO_2 + 8H_2O.$$

The excess dichromate remaining from this reaction is titrated with iron (II) ammonium sulphate hexahydrate and compared to the titration on a blank. The reduced dichromate is assumed to be equivalent to the organic carbon present in the sample. It is also assumed that soil organic matter has an average valence of zero.

Reagents

i. Potassium dichromate 0.167 mol/l: dissolve 49.04 g potassium dichromate (AR), dried at 105°C, in de-ionised water and make up to 1 l in a volumetric flask.

ii. Sulphuric acid: concentrated AR grade

iii. Ortho-phosphoric acid: concentrated

iv. Iron(II) ammonium sulphate 0.5 mol/l: dissolve 196g iron(II) ammonium sulphate hexahydrate in 500 ml de-ionised water, add 5 ml concentrated H_2SO_4, cool and make up to 1 l with de-ionised water.

v. Barium diphenylamine sulphonate indicator: dissolve 0.4 g indicator in 100 ml de-ionised water.

Procedure

A measured quantity of air-dried and ground (<0.35 mm) sample was transferred to a 500 cm^3 Erlenmeyer flask. A 10 ml aliquot of $K_2Cr_2O_7$ was added to the sample using a pipette and the flask gently swirled to disperse the sample in the solution. Concentrated sulphuric acid, 20 ml, was rapidly added to the solution and the flask swirled for approximately 1 minute. The flask was allowed to cool for 30 minutes. De-ionised water (150 ml) and orthophosphoric acid (10 ml) were added to the flask. Indicator (1 ml) was added and the contents of the flask titrated to a green endpoint with iron(II) ammonium sulphate solution.

Calculation

The carbon content of each determination was calculated using the following equations:

$$Organic\ C\ \% = \frac{[\ cm^3 Fe(NH_4)_2(SO_4)_2\ blank - cm^3 Fe(NH_4)_2(SO_4)_2\ sample\ ] \times M \times 0.3 \times f}{soil\ mass}$$

where M = concentration of $Fe(NH_4)_2(SO_4)_2$ in $mol.dm^{-3}$

f = recovery factor of 1.3 to allow for incomplete oxidation of organic matter

$$conc.\ of\ Fe(NH_4)_2(SO_4)_2\ mol.dm^{-3} = \frac{10cm^3\ K_2Cr_2O_7 \times 0.167 \times 6}{cm^3\ Fe(NH_4)_2(SO_4)_2}$$

A:B.4 Exchangeable/Extractable Cations

The ammonium acetate method was used to determine extractable cations Ca^{2+}, Mg^{2+}, K^+, and Na^+.

Reagents

i. NH_4OAc solution, 1 mol/l, pH 7: dilute 57 ml glacial acetic acid (99.5% AR) with de-

ionised water to a volume of 500 ml. Add 69 ml concentrated ammonia solution to the diluted solution of acetic acid. Mix well and dilute to about 900 ml. Adjust pH to 7 by adding acetic acid or ammonia solution. Make up to 1 l with de-ionised water.

ii. Standard solution (1 000 mg/l): prepare K, Ca, Mg and Na standards with NH_4OAc solution.

Procedure

Place 5 +/- 0.05 g air-dry, < 2mm soil in a 100 cm^3 extraction bottle. Add 50 cm^3 NH_4OAc solution cooled to 20°C to the soil in the extraction bottle and shake horizontally on a reciprocating shaker at 180 oscillations per minute for 30 minutes. Rapidly filter extract through a Buchner funnel and collect filtrate, but discard first few drops. Refilter if extract is not clear. The filtrate should not be stored for longer than 24 hours unless refrigerated. The elements K, Ca, Mg and Na may be determined by either flame emission or atomic absorption spectroscopy.

Calculation

Ammonium acetate extractable cations = (b x 50)/ 5 $mg.kg^{-1}$

where b = mg/l of Ca, Mg, Na and K in extract.

A:B.5 Clay Percentage

Clay percentage was determined using the pipette method. Samples were air dried and gently crushed and a mass of sample passed through a 2 mm sieve. A representative mass of < 2 mm soil was then treated for carbonates, siliceous cementing agents, organic matter and iron oxides where necessary according to the methods described in NSAWC (1990). Dispersion was achieved by treating with 10 ml Calgon dispersing solution, making up the volume with de-ionised water to 250 ml and shaking on a horizontal shaker overnight. The dispersed sample was then washed through a 0.053 mm sieve, passing the silt and clay through the sieve via a funnel into a 1 l cylinder. The cylinder was filled to the 1 l mark and covered with a watch glass. After the appropriate time interval, and depending on temperature, a closed Lowy pipette was lowered to a depth of 7 cm and a 25 ml sample extracted. The clay content of this sample was then determined gravimetrically.

Calculation

$$Percent\ clay = \frac{(D \times E) \times 1000 \times 100}{F \times 25}$$

where D = mass (g) of pipetted clay
E = mass correction of dispersing agent (0.01 g)
F = mass (g) of pretreated oven dry total sample

A:B.6 Mineralogical Analysis of Clay Fraction (XRD)

Mineralogical analysis of the clay fraction (<2 μm particles) of soil samples was performed using a method of dispersion and fractionation to separate out the clay fraction and subsequent analysis of this fraction by means of X-ray diffractometry (XRD).

Separation of Clay Fraction

Depending on the estimated clay content of the soil sample, a subsample of gently ground, sieved (<2 mm) and air-dried soil from each sample was weighed out and placed in a 500 ml beaker and water added to give a 1:1 soil ratio. Hydrogen peroxide was then added incrementally until the sample ceased to froth. The reaction was considered to be complete when the soil sample had lost its dark color or when conspicuous effervescence had ceased. The sample was then centrifuged at 2000 rpm for 10 minutes and the supernatant discarded.

Subsequent to digestion of organic matter, the remaining sample was washed into a 250 ml plastic bottle which was then three-quarters filled with distilled water and shaken, by hand, to form a slurry. A few drops of *1M* NaOH was added to the slurry and it was shaken by hand again. pH was measured and the procedure repeated until the pH stabilized at approximately pH 9. The sample was then shaken mechanically for three hours prior to transfer into a 3 l plastic jar which was filled with tap water, stirred and left covered overnight at room temperature (22°C) After 16 hours the supernatant was siphoned off to a depth of 18 cm based on the calculation (using Stoke's Law) that all particles >2 μm would have settled below the 20 cm mark after this settling period. Depending on the length of time that the slurry actually remained untouched, the depth of siphoning was calculated as:

cm supernatant to be siphoned = (time slurry left standing/16) x 18

The 3 l jar containing the original soil slurry was refilled with pH 9.8 to 10.2 Na_2CO_3 solution and stirred before being left again to settle prior to siphoning. To the decantate

was then added *1M* HCl to restore the pH to < 7 but greater than 5. In order to flocculate the clay within the decanted suspension, solid NaCl crystals were added and the suspension left to settle overnight. The clear supernatant was then siphoned off and discarded. The clay concentrate was transferred into a number of centrifuge tubes for centrifugation at 1000 rpm for 2 minutes, with the supernatant again being discarded. The clay was then dialysed by adding a limited volume of water to it, shaking thoroughly, and pouring it into dialysis tubing. The clay was equilibrated with tap water overnight and then with de-ionised water for two nights. The washing procedure was stopped once it was determined that all chloride had been removed (using silver nitrate). The clay fraction was then stored in a stoppered bottle after a 5 ml aliquot had been pipetted into a porcelain crucible for drying and gravimetric determination of the suspension concentration.

Based on the results of the gravimetric determination described above, the suspension concentration was adjusted so as not to exceed approximately 20 mg/ml. A 2 ml aliquot was then withdrawn and put dropwise onto a level glass slide. The slide was placed in a stable, aerated place to dry, with a cover approximately 1 cm above the slide so as to protect it from dust and other particulate matter in the air. Once dry, the slides were ready for XRD analysis.

XRD Mineralogical Analysis

X-ray diffractometry was performed on each of the clay slides prepared using an automatic *Philips PW 1390* diffractometer, with a PW1316/9 Goniometer, PW 1771/00 Tube Tower, PW 1050/80 radiation shield, PW1390 channel control, PW 1394 motor control, and a PW 1386/55 automatic divergence slit. The diffractometer was fitted with a Cu X-ray tube and operated at an accelerating voltage of 40 kV and a beam current of 20 mA. CuKα radiation was measured at the following settings:

i. NaI scintillation counter and pulse height selector
ii. Step scan with counting time 1 second and step-size of 0.1° 2-theta
ii. Scans from 6 to 75° 2-theta

Results were recorded by computer and the intensity versus two theta plots interpreted manually to yield qualitative estimates of clay mineralogy.

A:B.7 X-Ray Spectrometry (XRFS)

Samples were analysed for major and trace elements using a *Philips PW X'Unique II* X-ray spectrometer. The analytical conditions are given in Appendix B and the sample preparation described below.

Briquette preparation

Soil samples were air-dried, sieved through a 2 mm nylon sieve and then crushed to a particle size of approximately 40 µm in a carbon-steel vessel, using a Siebtechnik swingmill. Undiluted pressed powder briquettes were prepared using 6 g of the dried and crushed sample. The briquettes were pressed in a 30 mm die under 7 - 10 tons of pressure using one drop of Mowiol solution (2% Hoechst Mowiol N 70-80 in distilled water) per gram of sample as a binding agent and boric acid as backing.

APPENDIX B - Instrumental Parameters and Data Quality for Routine Major and Trace Element Determinations by WDXRFS.

DEPARTMENT OF GEOLOGICAL SCIENCES

UNIVERSITY OF CAPE TOWN

INSTRUMENTAL PARAMETERS AND DATA QUALITY FOR ROUTINE MAJOR AND TRACE ELEMENT DETERMINATIONS BY WDXRFS

J P WILLIS

INFORMATION CIRCULAR No. 14

1996

MAJOR ELEMENTS

Nine major elements, Fe, Mn, Ti, Ca, K, P, Si, Al and Mg (with Ni and Cr when Ni and Cr concentrations exceed ~2000 ppm or 0.2 %) are determined using fusion disks prepared according to the method of Norrish and Hutton (1969). The disks are analyzed on a Philips PW1480 wavelength dispersive XRF spectrometer with a dual target Mo/Sc x-ray tube. Fe, Mn and Ti are measured with the tube at 100 kV, 25 mA. The other elements are determined with the tube at 40 kV, 65 mA. Peak only measurements are made on the elements Fe through Mg. Sodium is determined using powder briquettes, the x-ray tube at 40 kV, 65 mA, and with backgrounds measured at -2.00 and +2.00°2θ from the peak position. Analytical conditions are given in Table 1.

Fusion disks made up with 100% Johnson Matthey Specpure SiO_2 are used as blanks for all elements except Si. Fusion disks made up from mixtures of Johnson Matthey Specpure Fe_2O_3 and $CaCO_3$ are used as blanks for Si. Intensity data are collected using the Philips X40 software. Matrix corrections are made on the elements Fe through Mg using the de Jongh model in the X40 software. Theoretical alpha coefficients used in the de Jongh model for all other elements on the analyte element are calculated using the Philips on-line ALPHAS programme. Na_2O is not included in the matrix corrections in de Jongh model, and no matrix corrections are made to the sodium intensities.

Table 1. Analytical conditions for determination of major elements using a Philips PW1480 WDXRF spectrometer.

Element/line	Collimator	Crystal	Detector	PHS LWL	PHS UPL	Counting time (s)	Concentration range *	RMS	No. of standards
FeKα	F	LiF(220)	FL	16	70	150	0 - 17	0.118	14
MnKα	F	LiF(220)	FL	15	70	150	0 - 0.22	0.005	14
TiKα	F	LiF(200)	FL	28	70	150	0 - 2.75	0.020	14
CaKα	F	LiF(200)	FL	36	70	20	0 - 12.5	0.037	14
K Kα	F	LiF(200)	FL	36	70	50	0 - 15.5	0.057	14
P Kα	C	GE(111)	FL	25	75	100	0 - 0.36	0.008	14
SiKα	C	PE(002)	FL	32	74	100	0 - 100	0.408	14
AlKα	C	PE(002)	FL	25	75	80	0 - 17.5	0.136	14
MgKα	F	PX-1	FL	30	74	150	0 - 46	0.095	14
NaKα	F	PX-1	FL	30	78	200	0 - 9	0.189	15

* = all concentrations expressed as wt% oxide

$$RMS = \sqrt{\frac{1}{n-k}\sum\left(Conc_{given} - Conc_{calc}\right)}$$

where

n = no. of standards
k = no. of calibration coefficients, *i.e.* 2, the slope and intercept of the calibration line.
$Conc_{given}$ = recommended concentration for an element in a standard
$Conc_{calc}$ = concentration of an element calculated from the best-fit calibration line

First order calibration lines, with intercept, are calculated using all data points, including blanks. Calibration plots for Fe_2O_3, CaO, SiO_2 and MgO are given in Figures 1 - 4.

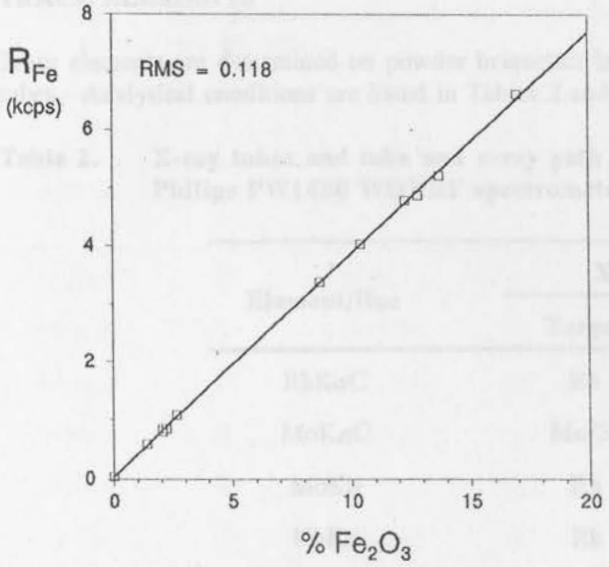

Figure 2. Calibration plot for Fe_2O_3 using "Norrish" fusion disks.

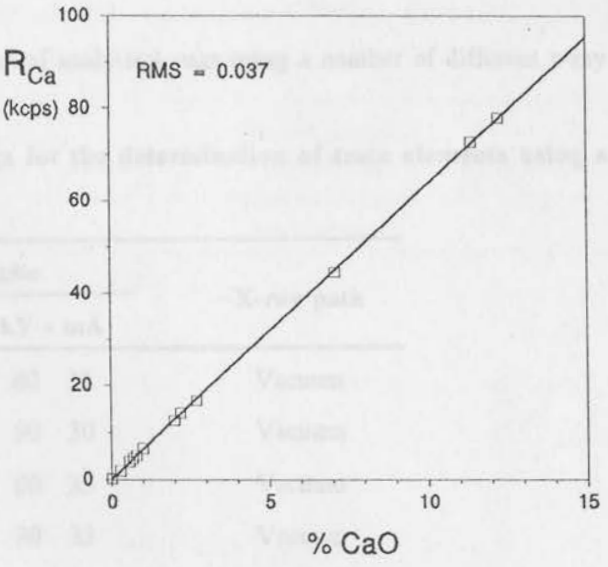

Figure 3. Calibration plot for CaO using "Norrish" fusion disks.

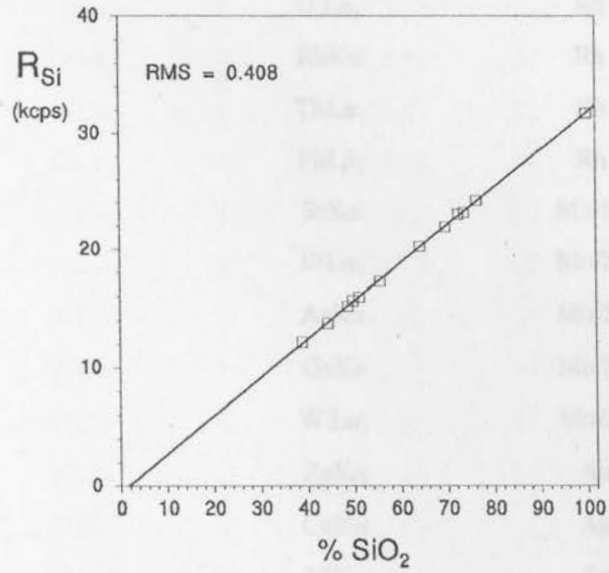

Figure 4. Calibration plot for SiO_2 using "Norrish" fusion disks.

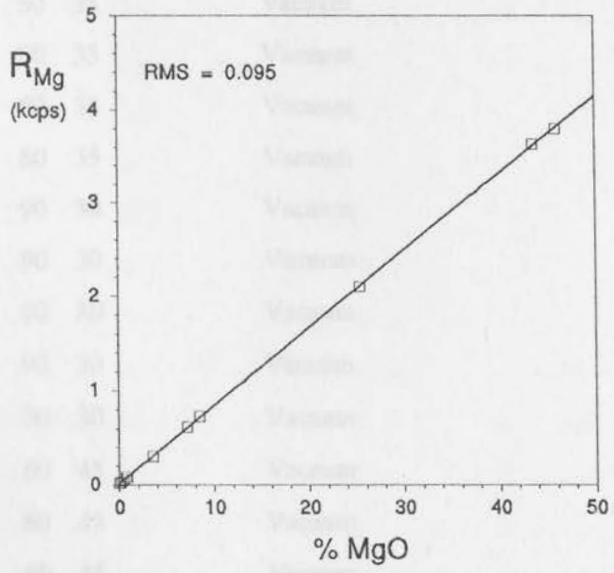

Figure 5. Calibration plot for MgO using "Norrish" fusion disks.

TRACE ELEMENTS

Trace elements are determined on powder briquettes in a series of analytical runs using a number of different x-ray tubes. Analytical conditions are listed in Tables 2 and 3.

Table 2. X-ray tubes and tube and x-ray path settings for the determination of trace elements using a Philips PW1480 WDXRF spectrometer.

Element/line	X-ray tube		X-ray path
	Target	kV - mA	
RhKαC	Rh	80 35	Vacuum
MoKαC	Mo/Sc	90 30	Vacuum
MoKα	Rh	80 35	Vacuum
NbKα	Rh	80 35	Vacuum
ZrKα	Rh	80 35	Vacuum
Y Kα	Rh	80 35	Vacuum
SrKα	Rh	80 35	Vacuum
U Lα_1	Rh	80 35	Vacuum
RbKα	Rh	80 35	Vacuum
ThLα_1	Rh	80 35	Vacuum
PbIβ_1	Rh	80 35	Vacuum
ScKα	Mo/Sc	90 30	Vacuum
BiLα_1	Mo/Sc	90 30	Vacuum
AsKα	Mo/Sc	90 30	Vacuum
GaKa	Mo/Sc	90 30	Vacuum
W Lα_1	Mo/Sc	90 30	Vacuum
ZnKα	Au	60 45	Vacuum
CuKα	Au	60 45	Vacuum
NiKα	Au	60 45	Vacuum
CoKα	Au	50 55	Vacuum
MnKα	Au	50 55	Vacuum
CrKα	Au	50 55	Vacuum
V Kα	Au	50 55	Vacuum
LaLα_1	Au	50 55	Vacuum
CeIβ_1	Au	50 55	Vacuum
NdLα_1	Au	50 55	Vacuum
BaLα_1	Cr	50 55	Vacuum
ScKα	Cr	50 55	Vacuum
S Kα	Mo/Sc	40 65	Vacuum
F Kα	Mo/Sc	40 70	Vacuum

Table 3. Instrumental conditions for determination of trace elements using a Philips PW1480 WDXRF spectrometer.

Element/line	Collimator	Crystal	Detector	PHS LWL	PHS UPL	Counting time (s)	Background position(s) relative to peak position	Concentration range *
RhKαC	F	LiF(220)	SC	34	75	200		
MoKαC	F	LiF(220)	SC	32	74	200		
MoKα	F	LiF(200)	SC	30	74	200	-1.28 +0.54	0 - 280
NbKα	F	LiF(200)	SC	30	74	200		0 - 268
ZrKα	F	LiF(200)	SC	30	74	200		0 - 1210
Y Kα	F	LiF(200)	SC	30	74	200	-0.86 +0.74	0 - 143
SrKα	F	LiF(200)	SC	30	74	200	+0.78	0 - 440
U Lα_1	F	LiF(200)	SC	30	74	200		0 - 15
RbKα	F	LiF(200)	SC	30	74	200	+0.60	0 - 530
ThLα_1	F	LiF(200)	SC	30	74	200		0 - 51
PbIβ_1	F	LiF(200)	SC	30	74	200	+1.52	0 - 40
SeKα	F	LiF(220)	FS	25	75	200	-3.42	
BiLα_1	F	LiF(220)	FS	25	75	200		
AsKα	F	LiF(220)	FS	25	75	200	+1.80	
GaKα	F	LiF(200)	FS	26	74	200	-0.50 +0.70	
W Lα_1	F	LiF(220)	FL	25	67	200	-1.00 +2.10	
ZnKα	F	LiF(220)	FS	20	80	200	-1.08 +4.24	0 - 235
CuKα	F	LiF(220)	FS	20	80	200	+4.44	0 - 227
NiKα	F	LiF(220)	FS	20	80	200	+2.52	0 - 630
CoKα	F	LiF(220)	FL	15	75	200	+1.00	0 - 116
MnKα	F	LiF(220)	FL	15	75	200	-2.30 +4.70	0 - 1700
CrKα	F	LiF(220)	FL	15	75	200	-4.10 +2.90	0 - 465
V Kα	F	LiF(220)	FL	13	67	200	+3.40	0 - 640
LaLα_1	F	LiF(220)	FL	38	68	400	-2.78 +4.22	
CeIβ_1	F	LiF(220)	FL	40	68	400	-1.64	
NdLα_1	F	LiF(220)	FL	40	68	400	+4.82	
BaLα_1	F	LiF(200)	FL	25	75	200	-5.20	0 - 2680
ScKα	F	LiF(200)	FL	25	75	200	-2.78	0 - 54
S Kα	C	Ge(111)	FL	32	72	100	-5.00 +5.00	
F Kα	C	PX-1	FL	25	80	400	+1.82	

* = all concentrations expressed as part per million (ppm or $mg.kg^{-1}$)

The RhKα Compton or the MoKα Compton peak is used to determine the mass absorption coefficients of the specimens at the RhKαC wavelength (Figure 5) or the MoKαC wavelength, and the Compton peak mass absorption coefficient values are used to correct for absorption effects on the Mo, Nb, Zr, Y, Sr, U, Rb, Th, Pb, Br, Se, Bi, As, W, Zn, Cu and Ni analyte wavelengths. Primary and secondary mass absorption coefficients for the Co, Mn, Cr, V, La, Ce, Nd, Ba, Sc, S and F analyte wavelengths are calculated from major element compositions using the tables of Heinrich (1986). Mass absorption coefficient corrections are made to the net peak intensities, (gross peak intensities corrected for dead time losses, background and spectral overlap), to correct for absorption differences between standards and specimens. No corrections are made for enhancement, which could be small but significant ($<\sim 5\%$ relative) for the elements Cr, V, Ba and Sc in certain specimens, depending on their concentrations of Fe, Mn and Ti.

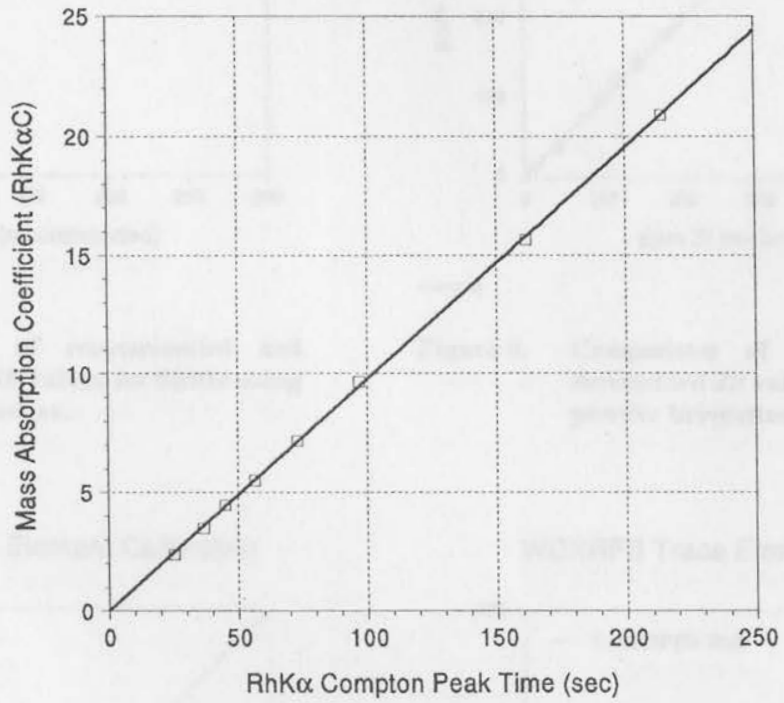

Figure 5. Calibration line for determination of mass absorption coefficients at the RhKαC wavelength. RhKαC peak time is the time required to accumulate 400 000 counts on the RhKαC peak using the fixed count method.

Measured intensity data are processed through the computer program TRACE to correct gross peak intensities for background and spectral overlap and to make mass absorption coefficient corrections according to the methods outlined in Duncan *et al.* (1984). First order calibration lines with zero intercept are calculated using six or more international rock standard reference materials (SRMs) for each element (Figs 7-14). The one standard deviation ($1\,\sigma$) error due to counting statistics and the lower limit of detection is calculated for each element in each specimen.

Table 4 lists the given and calculated concentrations for selected elements in a number of rock SRMs, which give an indication of the accuracy of the trace element data. Table 5 lists the one standard deviation counting error and lower limit of detection for each of the elements in an acidic (low Fe, Ca and Mg, high Si) rock and in a mafic (high Fe, Ca and Mg, low Si) rock. Because of the difference in mass absorption coefficients between the two types of specimen the counting error and lower limit of detection will be slightly higher in mafic rock specimens. The two examples given cover the range of mass absorption coefficients found in the majority of geological rock, soil and sediment specimens.

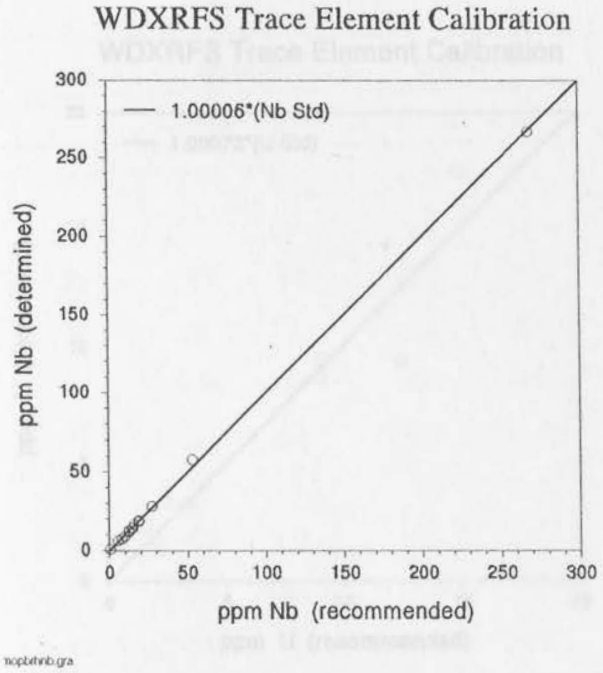

Figure 7. Comparison of recommended and determined Nb values for SRMs using powder briquettes.

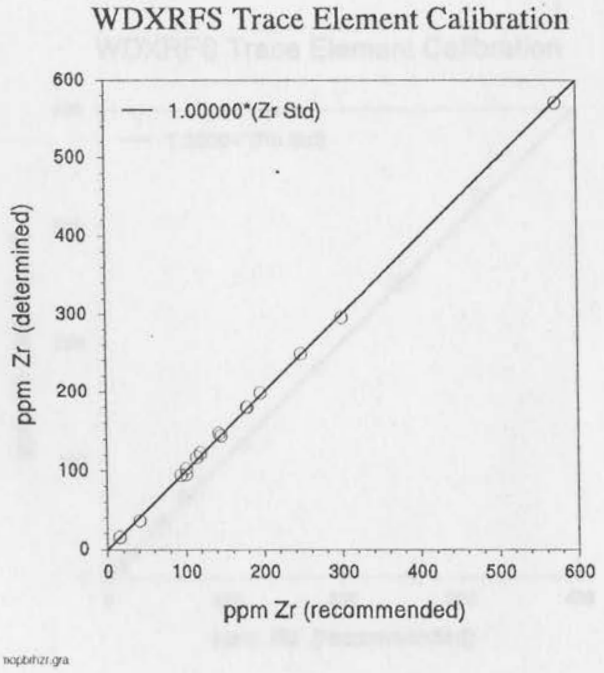

Figure 8. Comparison of recommended and determined Zr values for SRMs using powder briquettes.

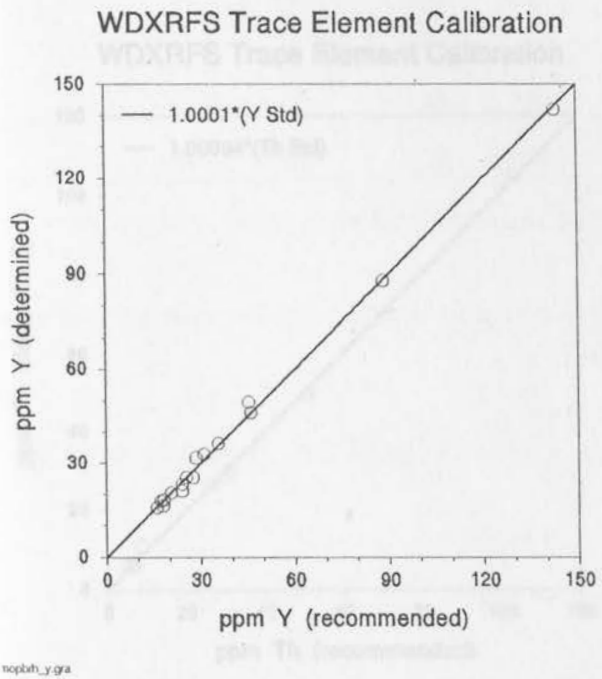

Figure 9. Comparison of recommended and determined Y values for SRMs using powder briquettes.

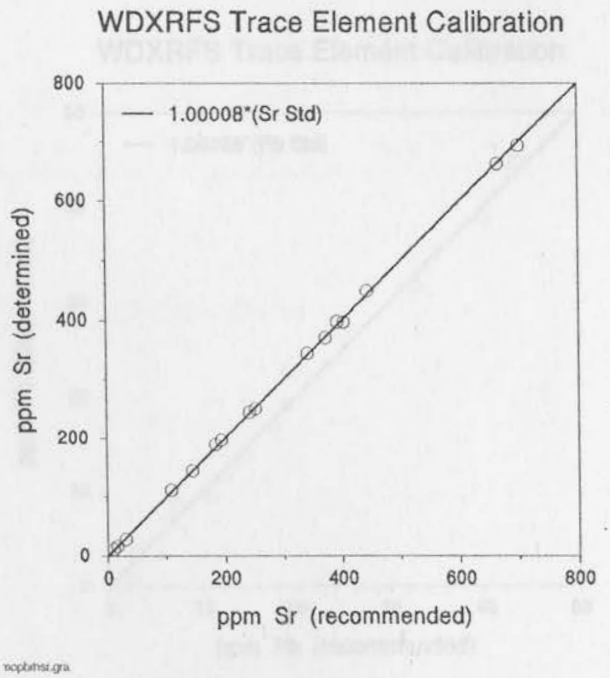

Figure 10. Comparison of recommended and determined Sr values for SRMs using powder briquettes.

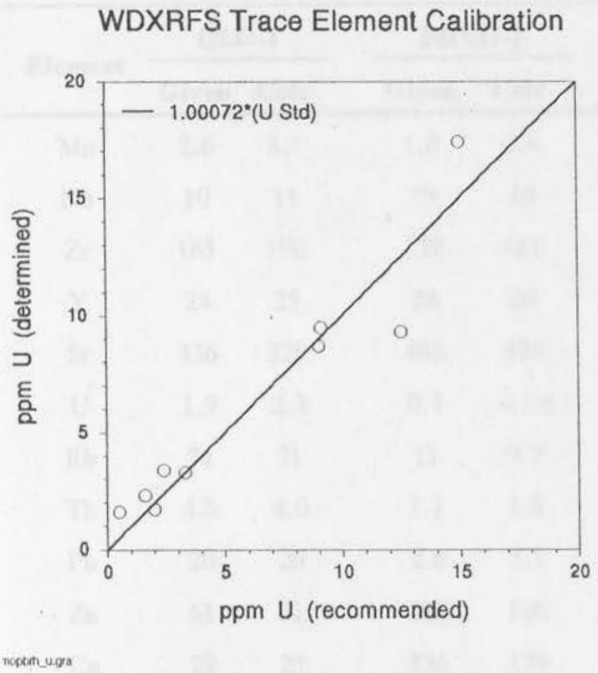

Figure 11. Comparison of recommended and determined U values for SRMs using powder briquettes.

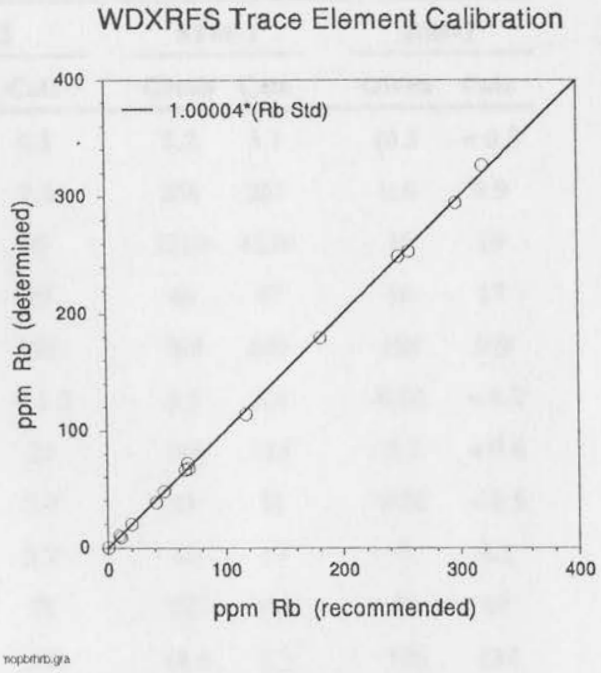

Figure 12. Comparison of recommended and determined Rb values for SRMs using powder briquettes.

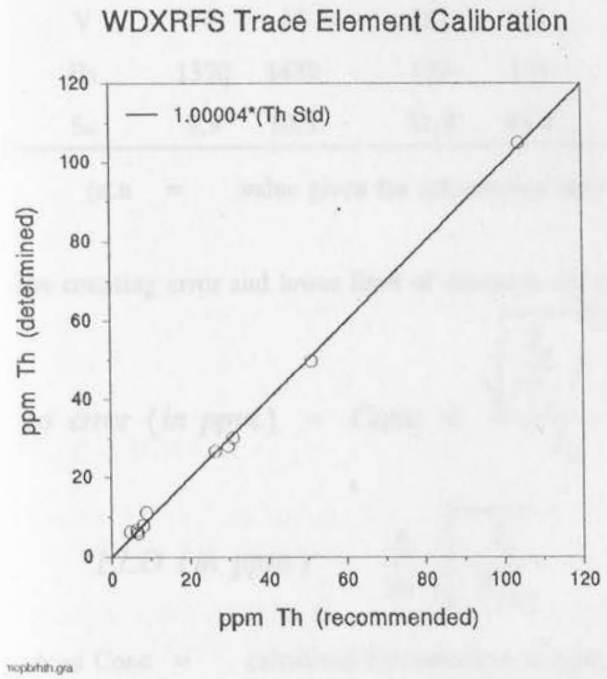

Figure 13. Comparison of recommended and determined Th values for SRMs using powder briquettes.

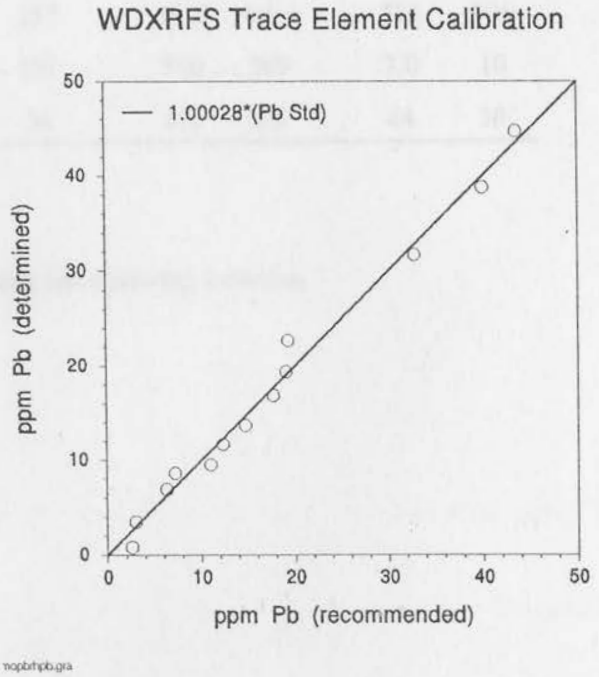

Figure 14. Comparison of recommended and determined Pb values for SRMs using powder briquettes.

Table 4. Given and calculated trace element data (all values in ppm) for some rock SRMs.

Element	QLO-1		BHVO-1		W-2		STM-1		BIR-1	
	Given	Calc	Given	Calc	Given	Calc	Given	Calc	Given	Calc
Mo	2.6	3.5	1.0	0.8	(0.6	0.5	5.2	3.1	(0.5	<0.8
Nb	10	11	19	19	7.9	7.4	268	267	0.6	0.9
Zr	185	190	179	181	94	95	1210	1220	16	19
Y	24	25	28	28	24	23	46	47	16	17
Sr	336	329	403	395	194	195	700	689	108	109
U	1.9	2.3	0.4	<1.6	0.5	<1.2	9.1	8.8	0.01	<1.2
Rb	74	71	11	9.7	20	20	118	114	0.3	<0.6
Th	4.5	4.0	1.1	1.8	2.2	2.7	31	31	0.03	<1.5
Pb	20	20	2.6	3.1	9.3	8.5	18	17	3	3.1
Zn	61	61	105	106	77	79	235	242	71	69
Cu	29	25	136	139	103	108	(4.6	2.1	126	132
Ni	(5.8	1.8	121	127	70	72	(3	1.7	166	170
Co	7.2	7.6	45	44	44	43	0.9	<1.9	51	52
Mn	720	690	1300	1290	1260	1240	1700	1600	1320	1280
Cr	(3.2	3.6	289	312	93	100	(4.3	3.2	382	404
V	54	44	317	314	262	257	(8.7	<1.6	313	306
Ba	1370	1430	139	138	182	191	560	589	7.0	10
Sc	8.9	10.3	31.8	33.9	35	36	0.6	0.5	44	39

(n.n = value given for information only

The counting error and lower limit of detection are calculated using the following formulae:

$$1\sigma \ error \ (in \ ppm) = Conc \times \frac{\sqrt{\frac{I_p}{T_p} + \frac{I_b}{T_b}}}{I_n}$$

and

$$LLD \ (in \ ppm) = \frac{6}{m}\sqrt{\frac{I_b}{T_{total}}}$$

where Conc = calculated concentration in ppm
m = net peak / concentration
I_p = gross peak count rate in cps
I_b = background count rate under the peak in cps
I_n = $I_p - I_b$ = true **net** peak count rate in cps
T_p = counting time for peak in seconds
T_b = total counting time for background in seconds
T_{total} = $T_p + T_b$

N.B. I_b is the calculated background *plus* any corrections for spectral interference, *i.e.* $I_b = I_p - I_n$.

Table 5. Calculated trace element data, 1 σ counting error and lower limit of detection (all values in ppm) for two rock specimens having different mass absorption coefficients.

Element	JR-2			JB-1a		
	Calc	1 σ	LLD	Calc	1 σ	LLD
Mo	4.1	0.2	0.6	1.8	0.3	0.7
Nb	19	0.1	0.4	28	0.2	0.5
Zr	87	0.1	0.3	152	0.2	0.4
Y	51	0.2	0.6	24	0.2	0.6
Sr	8.2	0.1	0.4	444	0.3	0.5
U	11	0.3	0.9	2.3	0.4	1.2
Rb	303	0.2	0.4	39	0.2	0.6
Th	34	0.4	1.1	9.8	0.5	1.4
Pb	24	0.5	1.3	7.5	0.6	1.8
Zn	28	0.2	0.6	84	0.4	0.9
Cu	1.1	0.3	0.8	55	0.5	1.1
Ni	1.3	0.3	0.8	139	0.7	1.3
Co	<1.2	0.4	1.2	37	0.9	2.3
Mn	878	1.7	1.2	1100	2.0	1.8
Cr	1.6	0.4	1.3	406	1.5	2.0
V	1.7	0.4	1.2	193	1.4	3.0
Ba	28	0.6	1.5	523	1.8	3.3
Sc	6.0	0.2	0.5	26	0.4	0.9

REFERENCES

Duncan, A R, Erlank, A J and Betton, P J (1984) Analytical techniques and database descriptions. *Spec. Publ. geol. Soc. S. Afr.*, **13**, Appendix 1, 389-395.

Heinrich, K F J (1986) Mass absorption coefficients for electron probe microanalysis. In: *Proc. 11th Int. Congress on X-ray Optics and Microanalysis, London, Canada*, J B Brown and R H Packwood (Eds).

Norrish, K. and Hutton, J.T. (1969) An accurate X-ray spectrographic method for the analysis of a wide range of geological samples. *Geochim. Cosmochim. Acta*, **33**, 431-453.

APPENDIX C - An example of a MINTEQA2 print out.

PART 1 of OUTPUT FILE

PC MINTEQA2 v3.10 DATE OF CALCULATIONS: 8-MAR-96 TIME: 10:31

Temperature (Celsius): 25.00
Units of concentration: MG/L
Ionic strength to be computed.
If specified, carbonate concentration represents total inorganic carbon.
Do not automatically terminate if charge imbalance exceeds 30%
Precipitation is allowed only for those solids specified as ALLOWED
in the input file (if any).
The maximum number of iterations is: 40
The method used to compute activity coefficients is: Davies equation
Intermediate output file

330	0.000E-01	-2.70 y
500	2.820E+02	-1.91 y
150	5.890E+02	-1.83 y
460	5.230E+02	-1.67 y
410	7.190E+02	-1.74 y
490	7.810E+02	-1.36 y
180	1.030E+03	-1.54 y
732	3.530E+03	-1.43 y
580	7.240E+02	-2.12 y
492	1.990E+03	-1.49 y
270	2.220E+02	-1.93 y
30	6.020E+01	-2.65 y
280	1.640E+00	-4.53 y
230	8.600E-01	-4.87 y
540	5.700E-01	-5.01 y
950	2.070E+00	-4.50 y
160	9.000E-02	-6.10 y
210	1.200E-01	-5.64 y
470	3.600E+00	-4.18 y
770	1.779E+02	-2.73 y
61	1.750E+00	-4.91

H2O has been inserted as a COMPONENT
3 1
330 2.7000 0.0000

INPUT DATA BEFORE TYPE MODIFICATIONS

ID	NAME	ACTIVITY GUESS	LOG GUESS	ANAL TOTAL
330	H+1	1.995E-03	-2.700	0.000E-01
500	Na+1	1.230E-02	-1.910	2.820E+02
150	Ca+2	1.479E-02	-1.830	5.890E+02
460	Mg+2	2.138E-02	-1.670	5.230E+02
410	K+1	1.820E-02	-1.740	7.190E+02
490	NH4+1	4.365E-02	-1.360	7.810E+02
180	Cl-1	2.884E-02	-1.540	1.030E+03
732	SO4-2	3.715E-02	-1.430	3.530E+03
580	PO4-3	586E-03	-2.120	7.240E+02
492	NO3-1	3.236E-02	-1.490	1.990E+03
270	F-1	1.175E-02	-1.930	2.220E+02
30	Al+3	2.239E-03	-2.650	6.020E+01
280	Fe+2	2.951E-05	-4.530	1.640E+00

230	Cu+1	1.349E-05	-4.870	8.600E-01
540	Ni+2	9.772E-06	-5.010	5.700E-01
950	Zn+2	3.162E-05	-4.500	2.070E+00
160	Cd+2	7.943E-07	-6.100	9.000E-02
210	Cr+2	2.291E-06	-5.640	1.200E-01
470	Mn+2	6.607E-05	-4.180	3.600E+00
770	H4SiO4	1.862E-03	-2.730	1.779E+02
61	H3AsO4	1.330E-05	-4.910	1.750E+00
2	H2O	1.000E+00	0.000	0.000E-01

Charge Balance: UNSPECIATED
Sum of CATIONS= 1.550E-01 Sum of ANIONS = 1.710E-01
PERCENT DIFFERENCE = 4.913E+00 (ANIONS - CATIONS)/(ANIONS + CATIONS)

PART 4 of OUTPUT FILE

PC MINTEQA2 v3.10 DATE OF CALCULATIONS: 8-MAR-96 TIME: 21:49:48

PERCENTAGE DISTRIBUTION OF COMPONENTS AMONG
TYPE I and TYPE II (dissolved and adsorbed) species

H3AsO4
- 20.0 PERCENT BOUND IN SPECIES # 61 H3AsO4
- 80.0 PERCENT BOUND IN SPECIES #3300611 H2AsO4 -

Na+1
- 96.8 PERCENT BOUND IN SPECIES # 500 Na+1
- 3.2 PERCENT BOUND IN SPECIES #5007320 NaSO4 -

Ca+2
- 69.6 PERCENT BOUND IN SPECIES # 150 Ca+2
- 27.4 PERCENT BOUND IN SPECIES #1507320 CaSO4 AQ
- 2.9 PERCENT BOUND IN SPECIES #1505802 CaH2PO4 +

Mg+2
- 71.0 PERCENT BOUND IN SPECIES # 460 Mg+2
- 24.4 PERCENT BOUND IN SPECIES #4607320 MgSO4 AQ
- 3.8 PERCENT BOUND IN SPECIES #4605801 MgH2PO4 +

K+1
- 95.6 PERCENT BOUND IN SPECIES # 410 K+1
- 4.4 PERCENT BOUND IN SPECIES #4107320 KSO4 -

NH4+1
- 92.2 PERCENT BOUND IN SPECIES # 490 NH4+1
- 7.8 PERCENT BOUND IN SPECIES #4907320 NH4SO4 -

Cl-1
- 99.9 PERCENT BOUND IN SPECIES # 180 Cl-1

SO4-2
- 57.6 PERCENT BOUND IN SPECIES # 732 SO4-2
- 9.2 PERCENT BOUND IN SPECIES #4907320 NH4SO4 -
- 14.3 PERCENT BOUND IN SPECIES #4607320 MgSO4 AQ
- 11.0 PERCENT BOUND IN SPECIES #1507320 CaSO4 AQ
- 1.1 PERCENT BOUND IN SPECIES #5007320 NaSO4 -
- 2.2 PERCENT BOUND IN SPECIES #4107320 KSO4 -
- 4.6 PERCENT BOUND IN SPECIES #3307320 HSO4 -

PO4-3
- 69.6 PERCENT BOUND IN SPECIES #3305801 H2PO4 -
- 13.9 PERCENT BOUND IN SPECIES #3305802 H3PO4
- 10.7 PERCENT BOUND IN SPECIES #4605801 MgH2PO4 +
- 5.6 PERCENT BOUND IN SPECIES #1505802 CaH2PO4 +

NO3-1
- 100.0 PERCENT BOUND IN SPECIES # 492 NO3-1

F-1
- 4.6 PERCENT BOUND IN SPECIES # 270 F-1

	25.5	PERCENT BOUND IN SPECIES #7702700 SiF6 -2
	1.4	PERCENT BOUND IN SPECIES #4602700 MgF +
	4.8	PERCENT BOUND IN SPECIES # 302701 AlF2 +
	38.9	PERCENT BOUND IN SPECIES # 302702 AlF3 AQ
	14.7	PERCENT BOUND IN SPECIES # 302703 AlF4 -
	9.7	PERCENT BOUND IN SPECIES #3302700 HF AQ
Al+3		
	12.6	PERCENT BOUND IN SPECIES # 302701 AlF2 +
	68.0	PERCENT BOUND IN SPECIES # 302702 AlF3 AQ
	19.3	PERCENT BOUND IN SPECIES # 302703 AlF4 -
Fe+2		
	46.1	PERCENT BOUND IN SPECIES # 280 Fe+2
	15.9	PERCENT BOUND IN SPECIES #2807320 FeSO4 AQ
	38.0	PERCENT BOUND IN SPECIES #2805800 FeH2PO4 +
Cu+1		
	91.7	PERCENT BOUND IN SPECIES #2301800 CuCl2 -
	7.7	PERCENT BOUND IN SPECIES #2301801 CuCl3 -2
Ni+2		
	71.2	PERCENT BOUND IN SPECIES # 540 Ni+2
	1.6	PERCENT BOUND IN SPECIES #5401800 NiCl +
	26.9	PERCENT BOUND IN SPECIES #5407320 NiSO4 AQ
Zn+2		
	64.0	PERCENT BOUND IN SPECIES # 950 Zn+2
	1.5	PERCENT BOUND IN SPECIES #9501800 ZnCl +
	29.0	PERCENT BOUND IN SPECIES #9507320 ZnSO4 AQ
	5.2	PERCENT BOUND IN SPECIES #9507321 Zn(SO4)2-2
Cd+2		
	37.9	PERCENT BOUND IN SPECIES # 160 Cd+2
	32.6	PERCENT BOUND IN SPECIES #1601800 CdCl +
	2.1	PERCENT BOUND IN SPECIES #1601801 CdCl2 AQ
	21.2	PERCENT BOUND IN SPECIES #1607320 CdSO4 AQ
	5.2	PERCENT BOUND IN SPECIES #1607321 Cd(SO4)2-2
Cr+2		
	100.0	PERCENT BOUND IN SPECIES # 210 Cr+2
Mn+2		
	71.9	PERCENT BOUND IN SPECIES # 470 Mn+2
	2.6	PERCENT BOUND IN SPECIES #4701800 MnCl +
	25.3	PERCENT BOUND IN SPECIES #4707320 MnSO4 AQ
H4SiO4		
	73.2	PERCENT BOUND IN SPECIES # 770 H4SiO4
	26.8	PERCENT BOUND IN SPECIES #7702700 SiF6 -2
H2O		
	100.0	PERCENT BOUND IN SPECIES #7702700 SiF6 -2
H+1		
	11.2	PERCENT BOUND IN SPECIES # 330 H+1
	44.6	PERCENT BOUND IN SPECIES #3305801 H2PO4 -
	13.4	PERCENT BOUND IN SPECIES #3305802 H3PO4
	8.4	PERCENT BOUND IN SPECIES #7702700 SiF6 -2
	6.9	PERCENT BOUND IN SPECIES #4605801 MgH2PO4 +
	3.6	PERCENT BOUND IN SPECIES #1505802 CaH2PO4 +
	7.1	PERCENT BOUND IN SPECIES #3307320 HSO4 -
	4.8	PERCENT BOUND IN SPECIES #3302700 HF AQ

PART 5 of OUTPUT FILE

PC MINTEQA2 v3.10 DATE OF CALCULATIONS: 8-MAR-96 TIME: 21:49:48

--------- EQUILIBRATED MASS DISTRIBUTION ----------

IDX	NAME	DISSOLVED		SORBED		PRECIPITATED	
		MOL/KG	PERCENT	MOL/KG	PERCENT	MOL/KG	PERCENT
61	H3AsO4	1.246E-05	100.0	0.000E-01	0.0	0.000E-01	0.0
500	Na+1	1.240E-02	100.0	0.000E-01	0.0	0.000E-01	0.0
150	Ca+2	1.485E-02	100.0	0.000E-01	0.0	0.000E-01	0.0
460	Mg+2	2.174E-02	100.0	0.000E-01	0.0	0.000E-01	0.0
410	K+1	1.859E-02	100.0	0.000E-01	0.0	0.000E-01	0.0
490	NH4+1	4.376E-02	100.0	0.000E-01	0.0	0.000E-01	0.0
180	Cl-1	2.936E-02	100.0	0.000E-01	0.0	0.000E-01	0.0
732	SO4-2	3.714E-02	100.0	0.000E-01	0.0	0.000E-01	0.0
580	PO4-3	7.705E-03	100.0	0.000E-01	0.0	0.000E-01	0.0
492	NO3-1	3.244E-02	100.0	0.000E-01	0.0	0.000E-01	0.0
270	F-1	1.181E-02	100.0	0.000E-01	0.0	0.000E-01	0.0
30	Al+3	2.255E-03	100.0	0.000E-01	0.0	0.000E-01	0.0
280	Fe+2	2.968E-05	100.0	0.000E-01	0.0	0.000E-01	0.0
230	Cu+1	1.368E-05	100.0	0.000E-01	0.0	0.000E-01	0.0
540	Ni+2	9.813E-06	100.0	0.000E-01	0.0	0.000E-01	0.0
950	Zn+2	3.200E-05	100.0	0.000E-01	0.0	0.000E-01	0.0
160	Cd+2	8.093E-07	100.0	0.000E-01	0.0	0.000E-01	0.0
210	Cr+2	2.332E-06	100.0	0.000E-01	0.0	0.000E-01	0.0
470	Mn+2	6.623E-05	100.0	0.000E-01	0.0	0.000E-01	0.0
770	H4SiO4	1.871E-03	100.0	0.000E-01	0.0	0.000E-01	0.0
2	H2O	-2.006E-03	100.0	0.000E-01	0.0	0.000E-01	0.0
330	H+1	2.402E-02	100.0	0.000E-01	0.0	0.000E-01	0.0

Charge Balance: SPECIATED
Sum of CATIONS = 1.263E-01 Sum of ANIONS 1.183E-01
PERCENT DIFFERENCE = 3.276E+00 (ANIONS - CATIONS)/(ANIONS + CATIONS)
EQUILIBRIUM IONIC STRENGTH (m) = 1.700E-01
EQUILIBRIUM pH = 2.700
DATE ID NUMBER: 960308
TIME ID NUMBER: 21494838

PART 6 of OUTPUT FILE

PC MINTEQA2 v3.10 DATE OF CALCULATIONS: 8-MAR-96 TIME: 21:49:48

Saturation indices and stoichiometry of all minerals

ID #	NAME	Sat. Index	Stoichiometry in [brackets]
2003000	ALOH3(A)	-11.926	[1.000] 30 [3.000] 2 [-3.000] 330
6003000	ALOHSO4	-5.896	[-1.000] 330 [1.000] 30 [1.000] 732 [1.000] 2
6003001	AL4(OH)10SO4	-36.464	[-10.000] 330 [4.000] 30 [1.000] 732 [10.000] 2
6041000	ALUM K	-10.737	[1.000] 410 [1.000] 30 [2.000] 732 [12.000] 2
6041001	ALUNITE	-17.632	[1.000] 410 [3.000] 30 [2.000] 732 [6.000] 2 [-6.000] 330
6015000	ANHYDRITE	-0.045	[1.000] 150 [1.000] 732
2003001	BOEHMITE	-10.122	[-3.000] 330 [1.000] 30 [2.000] 2
2046000	BRUCITE	-13.720	[1.000] 460 [2.000] 2 [-2.000] 330
2077000	CHALCEDONY	0.680	[-2.000] 2 [1.000] 770
8646000	CHRYSOTILE	-28.657	[-6.000] 330 [3.000] 460 [2.000] 770 [1.000] 2
8246000	CLINOENSTITE	-11.108	[-1.000] 2 [1.000] 460 [1.000] 770 [-2.000] 330
2077001	CRISTOBALITE	0.744	[-2.000] 2 [1.000] 770
2003002	DIASPORE	-8.417	[-3.000] 330 [1.000] 30 [2.000] 2

8215000 DIOPSIDE -19.599 [-2.000] 2 [1.000] 150 [1.000] 460 [2.000] 770 [-4.000] 330
6046000 EPSOMITE -2.380 [1.000] 460 [1.000] 732 [7.000] 2
8646003 SEPIOLITE(C) -18.301 [-0.500] 2 [2.000] 460 [3.000] 770 [-4.000] 330
7015003 HYDRAPATITE -15.255 [5.000] 150 [3.000] 580 [1.000] 2 [-1.000] 330
4215000 FLUORITE 1.665 [1.000] 150 [2.000] 270
8046000 FORSTERITE -24.994 [-4.000] 330 [2.000] 460 [1.000] 770
2003003 GIBBSITE (C) -10.316 [-3.000] 330 [1.000] 30 [3.000] 2
3003000 Al2O3 -26.067 [2.000] 30 [3.000] 2 [-6.000] 330
8628000 GREENALITE -26.435 [-6.000] 330 [3.000] 280 [2.000] 770 [1.000] 2
6015001 GYPSUM 0.162 [1.000] 150 [1.000] 732 [2.000] 2
4150000 HALITE -5.292 [1.000] 500 [1.000] 180
8450000 MAGADIITE -4.959 [-1.000] 330 [-9.000] 2 [1.000] 500 [7.000] 770
6028000 MELANTERITE -5.102 [1.000] 280 [1.000] 732 [7.000] 2
6050001 MIRABILITE -5.185 [2.000] 500 [1.000] 732 [10.000] 2
8646001 PHLOGOPITE -66.333 [-10.000] 330 [1.000] 410 [3.000] 460 [1.000] 30 [3.000] 770
2077002 QUARTZ 1.163 [-2.000] 2 [1.000] 770
8646004 SEPIOLITE(A) -21.168 [-0.500] 2 [2.000] 460 [3.000] 770 [-4.000] 330
2077003 SIO2(A,GL) 0.175 [-2.000] 2 [1.000] 770
2077004 SIO2(A,PT) -0.133 [-2.000] 2 [1.000] 770
8646002 TALC -25.208 [-4.000] 2 [3.000] 460 [4.000] 770 [-6.000] 330
6050002 THENARDITE -6.102 [2.000] 500 [1.000] 732
8215001 TREMOLITE -58.126 [-8.000] 2 [2.000] 150 [5.000] 460 [8.000] 770 [-14.000] 330
7028001 VIVIANITE -13.249 [3.000] 280 [2.000] 580 [8.000] 2
2047003 PYROCROITE -14.527 [-2.000] 330 [1.000] 470 [2.000] 2
4147000 MNCL2, 4H2O -10.874 [1.000] 470 [2.000] 180 [4.000] 2
6047000 MNSO4 -9.687 [1.000] 470 [1.000] 732
7047000 MN3(PO4)2 -23.783 [3.000] 470 [2.000] 580
4123000 NANTOKITE -2.109 [1.000] 230 [1.000] 180
4223000 CUF -17.680 [1.000] 230 [1.000] 270
2023000 CUPRITE -7.468 [-2.000] 330 [2.000] 230 [1.000] 2
6023000 CU2SO4 -14.649 [2.000] 230 [1.000] 732
4195000 ZNCL2 -15.554 [1.000] 950 [2.000] 180
4295000 ZNF2 -10.466 [1.000] 950 [2.000] 270
2095000 ZN(OH)2 (A) -12.255 [-2.000] 330 [1.000] 950 [2.000] 2
2095001 ZN(OH)2 (C) -12.005 [-2.000] 330 [1.000] 950 [2.000] 2
2095002 ZN(OH)2 (B) -11.555 [-2.000] 330 [1.000] 950 [2.000] 2
2095003 ZN(OH)2 (G) -11.515 [-2.000] 330 [1.000] 950 [2.000] 2
2095004 ZN(OH)2 (E) -11.305 [-2.000] 330 [1.000] 950 [2.000] 2
4195001 ZN2(OH)3CL -19.170 [-3.000] 330 [2.000] 950 [3.000] 2 [1.000] 180
4195002 ZN5(OH)8CL2 -46.245 [-8.000] 330 [5.000] 950 [8.000] 2 [2.000] 180
6095000 ZN2(OH)2SO4 -14.690 [-2.000] 330 [2.000] 950 [2.000] 2 [1.000] 732
6095001 ZN4(OH)6SO4 -35.201 [-6.000] 330 [4.000] 950 [6.000] 2 [1.000] 732
5195000 ZNNO3)2,6H2O -11.887 [1.000] 950 [2.000] 492 [6.000] 2
2095005 ZNO(ACTIVE) -11.114 [-2.000] 330 [1.000] 950 [1.000] 2
2095006 ZINCITE -10.944 [-2.000] 330 [1.000] 950 [1.000] 2
6095002 ZN3O(SO4)2 -33.593 [-2.000] 330 [3.000] 950 [2.000] 732 [1.000] 2
7095000 ZN3(PO4),4W -16.677 [3.000] 950 [2.000] 580 [4.000] 2

8295000 ZNSIO3 -5.577 [-2.000] 330 [-1.000] 2 [1.000] 950 [1.000] 770
8095000 WILLEMITE -17.780 [-4.000] 330 [2.000] 950 [1.000] 770
6095003 ZINCOSITE -10.395 [1.000] 950 [1.000] 732
6095004 ZNSO4, 1H2O -6.817 [1.000] 950 [1.000] 732 [1.000] 2
6095005 BIANCHITE -5.630 [1.000] 950 [1.000] 732 [6.000] 2
6095006 GOSLARITE -5.437 [1.000] 950 [1.000] 732 [7.000] 2
4116000 CDCL2 -9.668 [1.000] 160 [2.000] 180
4116001 CDCL2, 1H2O -8.640 [1.000] 160 [2.000] 180 [1.000] 2
4116002 CDCL2,2.5H2O -8.413 [1.000] 160 [2.000] 180 [2.500] 2
4216000 CDF2 -10.831 [1.000] 160 [2.000] 270
2016000 CD(OH)2 (A) -15.360 [-2.000] 330 [1.000] 160 [2.000] 2
2016001 CD(OH)2 (C) -15.280 [-2.000] 330 [1.000] 160 [2.000] 2
4116003 CDOHCL -9.509 [-1.000] 330 [1.000] 160 [1.000] 2 [1.000] 180
6016000 CD3(OH)4SO4 -35.029 [-4.000] 330 [3.000] 160 [4.000] 2 [1.000] 732
6016001 CD3OH2(SO4)2 -26.758 [-2.000] 330 [3.000] 160 [2.000] 2 [2.000] 732
6016002 CD4(OH)6SO4 -42.499 [-6.000] 330 [4.000] 160 [6.000] 2 [1.000] 732
2016002 MONTEPONITE -16.748 [-2.000] 330 [1.000] 160 [1.000] 2
7016000 CD3(PO4)2 -21.583 [3.000] 160 [2.000] 580
8216000 CDSIO3 -13.531 [-1.000] 2 [1.000] 160 [1.000] 770 [-2.000] 330
6016003 CDSO4 -9.109 [1.000] 160 [1.000] 732
6016004 CDSO4, 1H2O -7.554 [1.000] 160 [1.000] 732 [1.000] 2
6016005 CDSO4,2.7H2O -7.341 [1.000] 160 [1.000] 732 [2.670] 2
2054000 NI(OH)2 -11.073 [-2.000] 330 [1.000] 540 [2.000] 2
6054000 NI4(OH)6SO4 -40.670 [-6.000] 330 [4.000] 540 [1.000] 732 [6.000] 2
2054001 BUNSENITE -12.721 [-2.000] 330 [1.000] 540 [1.000] 2
7054000 NI3(PO4)2 -18.812 [3.000] 540 [2.000] 580
6054001 RETGERSITE -5.823 [1.000] 540 [1.000] 732 [6.000] 2
6054002 MORENOSITE -5.504 [1.000] 540 [1.000] 732 [7.000] 2
8054000 NI2SIO4 -17.925 [-4.000] 330 [2.000] 540 [1.000] 770
8450001 ANALCIME -13.300 [1.000] 500 [1.000] 30 [2.000] 770 [-1.000] 2 [-4.000] 330
8603000 HALLOYSITE -17.770 [2.000] 30 [2.000] 770 [1.000] 2 [-6.000] 330
8603001 KAOLINITE -14.502 [2.000] 30 [2.000] 770 [1.000] 2 [-6.000] 330
8415000 LEONHARDITE -39.622 [-1.000] 2 [-16.000] 330 [2.000] 150 [8.000] 770 [4.000] 30
8450002 LOW ALBITE -12.014 [1.000] 500 [1.000] 30 [3.000] 770 [-4.000] 330 [-4.000] 2
8450003 ANALBITE -12.928 [1.000] 500 [1.000] 30 [3.000] 770 [-4.000] 330 [-4.000] 2
8641000 MUSCOVITE -25.331 [1.000] 410 [3.000] 30 [3.000] 770 [-10.000] 330
8641001 ANNITE -32.480 [1.000] 410 [3.000] 280 [1.000] 30 [3.000] 770 [-10.000] 330
8415001 ANORTHITE -31.304 [1.000] 150 [2.000] 30 [2.000] 770 [-8.000] 330
8603002 PYROPHYLLITE -12.863 [2.000] 30 [4.000] 770 [-4.000] 2 [-6.000] 330
8415002 LAUMONTITE -26.027 [1.000] 150 [2.000] 30 [4.000] 770 [-8.000] 330
8415003 WAIRAKITE -30.433 [1.000] 150 [2.000] 30 [4.000] 770 [-8.000] 330 [-2.000] 2
3006100 AS2O5 -17.867 [2.000] 61 [-3.000] 2

7047001 MNHPO4(C) 1.312 [1.000] 470 [1.000] 580 [1.000] 330
7203000 ALASO4.2W -11.931 [1.000] 30 [1.000] 61 [2.000] 2
[-3.000] 330
7215000 CA3(ASO4)26W -24.777 [3.000] 150 [2.000] 61 [4.000] 2
[-6.000] 330
7247000 MN3ASO428W -21.993 [3.000] 470 [2.000] 61 [8.000] 2
[-6.000] 330
7254000 NI3(ASO4)28W -27.695 [3.000] 540 [2.000] 61 [8.000] 2
[-6.000] 330
7295000 ZN3ASO422.5W -24.233 [3.000] 950 [2.000] 61 [2.500] 2
[-6.000] 330
2015000 LIME -29.898 [-2.000] 330 [1.000] 150 [1.000] 2
2015001 PORTLANDITE -19.778 [-2.000] 330 [1.000] 150 [2.000] 2
2028000 WUSTITE -11.381 [-2.000] 330 [0.947] 280 [1.000] 2
2046001 PERICLASE -18.436 [-2.000] 330 [1.000] 460 [1.000] 2
3028001 HERCYNITE -30.227 [-8.000] 330 [1.000] 280 [2.000] 30
[4.000] 2
3046000 SPINEL -36.346 [-8.000] 330 [1.000] 460 [2.000] 30
[4.000] 2
4250000 CRYOLITE -4.651 [1.000] 30 [3.000] 500 [6.000] 270
8215002 WOLLASTONITE -12.940 [-1.000] 2 [-2.000] 330 [1.000] 770
[1.000] 150
8215003 P-WOLLSTANIT -13.790 [-1.000] 2 [-2.000] 330 [1.000] 770
[1.000] 150
8015001 CA-OLIVINE -34.694 [-4.000] 330 [1.000] 770 [2.000] 150
8015002 LARNITE -36.186 [-4.000] 330 [1.000] 770 [2.000] 150
8015007 CA3SIO5 -68.012 [-6.000] 330 [1.000] 770 [3.000] 150
[1.000] 2
8015003 MONTICELLITE -27.142 [-4.000] 330 [1.000] 770 [1.000] 150
[1.000] 460
8015005 AKERMINITE -44.286 [-1.000] 2 [-6.000] 330 [2.000] 770
[2.000] 150 [1.000] 460
8015004 MERWINITE -62.458 [-8.000] 330 [2.000] 770 [1.000] 460
[3.000] 150
8441000 KALSILITE -16.404 [-4.000] 330 [1.000] 770 [1.000] 30
[1.000] 410
8441001 LEUCITE -12.832 [-2.000] 2 [-4.000] 330 [2.000] 770
[1.000] 30 [1.000] 410
8441002 MICROCLINE -9.868 [-4.000] 2 [-4.000] 330 [3.000] 770
[1.000] 30 [1.000] 410
8441003 H SANIDINE -10.314 [-4.000] 2 [-4.000] 330 [3.000] 770
[1.000] 30 [1.000] 410
8450004 NEPHELINE -17.954 [-4.000] 330 [1.000] 770 [1.000] 30
[1.000] 500
8015006 GEHLENITE -56.953 [-10.000] 330 [2.000] 30 [1.000] 770
[2.000] 150 [3.000] 2
2021100 CR(OH)2 -11.568 [1.000] 210 [2.000] 2 [-2.000] 330
4121000 CRCL2 -25.335 [1.000] 210 [2.000] 180

APPENDIX D - Saturation Indices predicted by MINTEQA2.

Table D1 **Saturation Indices of selected minerals predicted by MINTEQA2 for water samples K1 - K5 from the fertilizer evaporation ponds and Triomf Main Drain.**

Mineral Name	Saturation Index				
	Fertilizer Evaporation Pond			Triomf Main Drain	
	K1	K2	K5	K3	K4
Anhydrite	-0.05	-0.07	-0.09	-0.097	-0.275
Chalcedony	0.68	0.37	-0.14	0.612	0.847
Cristobalite	0.74	0.44	-0.08	0.676	0.911
Fluorite	1.66	2.44	2.52	-0.560	1.742
Gypsum	0.16	0.13	0.12	0.111	-0.066
Quartz	1.16	0.86	0.33	1.095	1.330
$MnH(PO_4)$	1.31	2.59	1.26	1.704	1.411

Table D2 **Saturation Indices of selected minerals predicted by MINTEQA2 for water sample SD5 from the gypsum leachate collection pond.**

Mineral Name	Saturation Index
$AlOH(SO_4)$	0.48
Alunite	5.33
Anhydrite	-0.15
Boehmite	-1.11
Chalcedony	0.37
Cristobalite	0.43
Diaspore	0.59
Fluorite	-3.47
Gypsum	0.05
Quartz	0.85
Halloysite	-0.36
Kaolinite	2.90
Muscovite	1.96
Pyrophyllite	3.91
$MnH(PO_4)$	2.17

Table D3 Saturation Indices of selected minerals predicted by MINTEQA2 for water sample SD2 from the sulphur leachate collection drain.

Mineral Name	Saturation Index
$AlOH(SO_4)$	-0.43
Anhydrite	0.23
Chalcedony	0.82
Cristobalite	0.88
Gypsum	0.44
Quartz	1.29

Table D4 Saturation Indices of selected minerals predicted by MINTEQA2 for water sample SD2 from the sulphur stockpile leachate collection drain at pH values of 1.5, 2.0 and 3.5.

Mineral Name	Saturation Index		
	pH = 1.5	pH = 2.0	pH = 3.5
$AlOH(SO_4)$	-0.43	0.07	1.56
Alunite	-5.84	-2.96	5.91
Diaspore	-5.58	-4.21	0.19
Kaolinite	-8.57	-5.82	2.98
Muscovite	-18.4	-13.8	0.91

Table D5 **Saturation Indices of selected minerals predicted by MINTEQA2 for water samples A2, A3, B1 and B3 from the Dead Tree Area.**

Mineral Name	Saturation Index			
	Sample A2	Sample A3	Sample B1	Sample B3
Anhydrite	-0.66	0.25	-0.99	-1.22
Aragonite	-0.25	0.73	-1.35	-0.61
Calcite	-0.11	0.87	-1.21	-0.47
Dolomite	0.45	2.48	-1.28	-0.32
Hydrapatite	3.39	6.36	-1.19	2.34
FCO3apatite	17.3	18.7	6.62	12.37
Fluorite	1.06	-1.89	-1.13	-0.86
Gypsum	-0.45	0.43	-0.79	-1.01
Magnesite	0.06	1.11	-0.56	-0.35
Talc	-0.05	5.08	-3.28	-4.87
Tremolite	0.03	11.6	-7.69	-9.19

Table D6 **Saturation Indices of selected minerals predicted by MINTEQA2 for water samples B2, A4, and A1 from the Dead Tree Area.**

Mineral Name	Saturation Index		
	Sample B2	Sample A4	Sample A1
Alunite	3.36	7.47	3.83
Boehmite	-0.13	2.39	-2.35
Gibbsite	-0.33	2.19	-2.55
Analcime	-	1.41	-3.57
Halloysite	1.67	6.43	-2.09
Kaolinite	4.94	9.70	1.17
Leonhardite	4.87	17.6	-4.78
low Albite	-0.58	2.28	-2.21
Analbite	-1.50	1.37	-3.12
Muscovite	4.74	12.3	-0.70
Pyrophyllite	6.05	10.5	2.95

APPENDIX E - Leaching Column Data

Recorded measurements and calculated hydraulic conductivity values from leaching column tests. Dashed lines indicate where leaching was interrupted and the columns allowed to stand for a period of 48 hours.

Column A - Untreated soil

Time (min)	Cum. Vol. (ml)	Leachate Depth (cm)	K (cm/s)	log K	pH	EC (mS/cm)
0	0					
5	47	2.1	1.05E-03	-2.98	5.5	24.70
10	107	4.8	1.34E-03	-2.87	5.7	10.40
15	183	8.3	1.70E-03	-2.77	6.1	1.17
25	269	12.2	9.62E-04	-3.02	6.4	0.45
36	345	15.7	7.73E-04	-3.11	6.7	0.28
50	417	18.9	5.76E-04	-3.24	6.8	0.22
70	500	22.7	4.64E-04	-3.33	6.9	0.18
90	552	25.1	2.91E-04	-3.54	7.0	0.15
120	586	26.6	1.25E-04	-3.90		
140	608	27.6	1.29E-04	-3.89		
160	632	28.7	1.31E-04	-3.88		
180	656	29.8	1.34E-04	-3.87		
200	674	30.6	1.01E-04	-3.99		
220	693	31.5	1.04E-04	-3.98		
240	714	32.4	1.18E-04	-3.93		
260	734	33.4	1.15E-04	-3.94		
300	756	34.4	6.16E-05	-4.21		
340	779	35.4	6.44E-05	-4.19		
380	804	36.5	6.99E-05	-4.16		
420	818	37.2	3.92E-05	-4.41		
460	831	37.8	3.64E-05	-4.44		
500	846	38.4	4.06E-05	-4.39		
540	858	39.0	3.50E-05	-4.45		
630	884	40.2	3.23E-05	-4.49		
720	910	41.4	3.23E-05	-4.49		

Column B - Untreated soil (replicate)

Time (min)	Cum. Vol. (ml)	Leachate Depth (cm)	K (cm/s)	log K	pH	EC (mS/cm)
0	0					
5	24	1.1	5.37E-04	-3.27	5.2	41.50
10	61	2.8	8.28E-04	-3.08	5.6	11.47
15	115	5.2	5.21E-03	-2.91	6.0	2.47
25	171	7.8	6.27E-04	-3.20	6.4	0.79
36	217	9.9	4.68E-04	-3.33	6.7	0.46
50	259	11.8	3.36E-04	-3.47	6.8	0.38
70	307	13.9	2.69E-04	-3.57	6.9	0.32
90	343	15.6	2.01E-04	-3.70	7.0	0.29
120	358	16.3	5.60E-05	-4.25		
140	372	16.9	7.83E-05	-4.11		
160	386	17.5	7.83E-05	-4.11		
180	400	18.2	7.83E-05	-4.11		
200	403	18.3	1.68E-05	-4.78		
220	407	18.5	2.24E-05	-4.65		
240	412	18.7	2.80E-05	-4.55		
260	416	18.9	2.24E-05	-4.65		
300	420	19.1	1.12E-05	-4.95		
340	425	19.3	1.40E-05	-4.85		
380	430	19.5	1.40E-05	-4.85		
420	433	19.7	7.83E-06	-5.11		
460	436	19.8	8.67E-06	-5.06		
500	439	19.9	8.67E-06	-5.06		
540	441	20.1	6.44E-06	-5.19		
630	445	20.2	5.10E-06	-5.29		
720	450	20.4	5.22E-06	-5.28		

Column C - Gypsum treated soil
[10 tons/ha applied to soil surface]

Time (min)	Cum. Vol. (ml)	Leachate Depth (cm)	K (cm/s)	log K	pH	EC (mS/cm)
0	0					
5	76	3.5	1.70E-03	-2.77	5.5	20.20
10	152	6.9	1.70E-03	-2.77	5.9	2.94
13	238	10.8	3.21E-03	-2.49	6.0	1.67
17	332	15.1	2.63E-03	-2.58	6.1	1.20
20	408	18.5	2.84E-03	-2.55	6.0	1.02
24	498	22.6	2.52E-03	-2.59	6.1	0.92
27	570	25.9	2.69E-03	-2.57	6.1	0.83
30	646	29.4	2.84E-03	-2.55	6.1	0.77
34	720	32.7	2.07E-03	-2.68	6.2	0.70
37	790	35.9	2.61E-03	-2.58	6.2	0.65
40	876	39.8	3.21E-03	-2.49	6.1	0.60
45	956	43.5	1.79E-03	-2.75	6.2	0.60
50	1032	46.9	1.70E-03	-2.77	6.1	0.57
54	1118	50.8	2.41E-03	-2.62	6.1	0.54
58	1204	54.7	2.41E-03	-2.62	6.1	0.51
63	1290	58.6	1.92E-03	-2.72	6.1	0.49
67	1378	62.6	2.46E-03	-2.61	6.1	0.47
72	1464	66.5	1.92E-03	-2.71	6.2	0.45
75	1544	70.2	2.98E-03	-2.53	6.2	0.43
80	1634	74.3	2.01E-03	-2.70	6.2	0.42
85	1718	78.1	1.88E-03	-2.73	6.3	0.39
90	1803	81.9	1.90E-03	-2.72	6.2	0.38
100	1903	86.5	1.12E-03	-2.95		
105	1953	88.8	1.12E-03	-2.95		
109	2003	91.1	1.40E-03	-2.85		
117	2103	95.6	1.40E-03	-2.85		
122	2153	97.9	1.12E-03	-2.95		
127	2203	100.1	1.12E-03	-2.95		
135	2303	104.7	1.40E-03	-2.85		
139	2353	106.7	1.40E-03	-2.85		
143	2403	109.2	1.40E-03	-2.85		
150	2503	113.8	1.60E-03	-2.79		
154	2553	116.0	1.40E-03	-2.85		

157	2603	118.3	1.87E-03	-2.73
165	2703	122.9	1.40E-03	-2.85
169	2753	125.1	1.40E-03	-2.85
173	2803	127.4	1.40E-03	-2.85
178	2903	131.9	2.24E-03	-2.65
192	3003	136.5	7.99E-04	-3.10
198	3103	141.0	1.87E-03	-2.73
206	3203	145.6	1.49E-03	-2.83
212	3303	150.1	1.72E-03	-2.76
218	3403	154.7	1.87E-03	-2.73
224	3503	159.3	1.87E-03	-2.73
236	3703	168.3	1.87E-03	-2.73
241	3803	172.9	2.24E-03	-2.65
246	3903	177.4	2.24E-03	-2.65

Column D - Gypsum treated soil (replicate)
[10 tons/ha applied to soil surface]

Time (min)	Cum. Vol. (ml)	Leachate Depth (cm)	K (cm/s)	log K	pH	EC (mS/cm)
0	0					
5	78	3.5	1.75E-03	-2.75	6.3	20.6
10	132	6.0	1.21E-03	-2.92	6.3	2.37
13	204	9.3	2.69E-03	-2.57	6.3	1.46
17	280	12.7	2.13E-03	-2.67	6.2	0.99
20	344	15.6	2.39E-03	-2.62	6.3	0.84
24	416	18.9	2.01E-03	-2.69	6.3	0.74
27	476	21.6	2.24E-03	-2.65	6.3	0.68
30	536	24.4	2.24E-03	-2.65	6.2	0.64
34	604	27.5	1.90E-03	-2.72	6.3	0.61
37	662	30.1	2.16E-03	-2.66	6.3	0.57
40	732	33.3	2.61E-03	-2.58	6.3	0.55
45	800	36.4	1.52E-03	-2.81	6.3	0.52
50	870	39.5	1.57E-03	-2.80	6.3	0.51
54	940	42.7	1.96E-03	-2.71	6.3	0.49
58	1009	45.9	1.93E-03	-2.71	6.3	0.47
63	1079	49.0	1.57E-03	-2.80	6.3	0.45

67	1151	52.3	2.01E-03	-2.69	6.3	0.44
72	1223	55.6	1.61E-03	-2.79	6.3	0.42
75	1291	58.7	2.54E-03	-2.59	6.3	0.41
80	1363	61.9	1.61E-03	-2.79	6.3	0.41
85	1433	65.1	1.57E-03	-2.80	6.3	0.31
90	1503	68.3	1.57E-03	-2.80	6.3	0.38
102	1603	72.9	9.33E-04	-3.03		
109	1653	75.1	7.99E-04	-3.10		
116	1703	77.4	7.99E-04	-3.10		
126	1803	81.9	1.12E-03	-2.95		
131	1853	84.2	1.12E-03	-2.95		
138	1903	86.5	7.99E-04	-3.10		
146	2003	91.0	1.40E-03	-2.85		
152	2053	93.3	9.33E-04	-3.03		
157	2103	95.6	1.12E-03	-2.95		
166	2203	100.1	1.24E-03	-2.90		
172	2253	102.4	9.33E-04	-3.03		
178	2303	104.7	9.33E-04	-3.03		
197	2403	109.2	5.89E-04	-3.23		
206	2503	113.8	1.24E-03	-2.90		
215	2603	118.3	1.24E-03	-2.90		
224	2703	122.9	1.24E-03	-2.90		
236	2803	127.4	9.73E-04	-3.01		
245	2903	131.9	1.24E-03	-2.91		

Column E - Gypsum treated soil
[10 tons/ha mixed throughout soil column]

Time (min)	Cum. Vol. (ml)	Leachate Depth (cm)	K (cm/s)	log K	pH	EC (mS/cm)
0	0					
5	100	4.5	2.24E-03	-2.65	5.0	18.10
10	156	7.1	1.25E-03	-2.90	5.7	3.70
13	246	11.2	3.36E-03	-2.47	5.8	2.20
17	340	15.5	2.63E-03	-2.58	5.8	1.33

20	414	18.8	2.76E-03	-2.56	6.0	0.74
24	508	23.1	2.63E-03	-2.58	6.1	0.46
27	584	26.5	2.84E-03	-2.55	6.2	0.35
30	664	30.2	2.98E-03	-2.52	6.2	0.29
34	754	34.3	2.52E-03	-2.59	6.2	0.26
37	830	37.7	2.84E-03	-2.54	6.3	0.24
40	920	41.8	3.36E-03	-2.47	6.3	0.22
45	1006	45.7	1.92E-03	-2.71	6.3	0.21
50	1098	49.9	2.06E-03	-2.68	6.3	0.20
54	1190	54.1	2.57E-03	-2.58	6.3	0.19
58	1280	58.2	2.52E-03	-2.59	6.3	0.19
63	1373	62.4	2.08E-03	-2.68	6.3	0.18
67	1469	66.8	2.69E-03	-2.57	6.3	0.17
72	1565	71.1	2.15E-03	-2.67	6.4	0.17
75	1653	75.1	3.28E-03	-2.48	6.4	0.16
80	1751	79.6	2.19E-03	-2.65	6.4	0.16
85	1849	84.0	2.19E-03	-2.65	6.4	0.15
90	1945	88.4	2.15E-03	-2.66	6.3	0.15
97	2045	92.9	1.60E-03	-2.79		
102	2095	95.2	1.12E-03	-2.95		
106	2145	97.5	1.40E-03	-2.85		
113	2245	102.0	1.60E-03	-2.79		
117	2295	104.3	1.40E-03	-2.85		
121	2345	106.6	1.40E-03	-2.85		
128	2445	111.1	1.60E-03	-2.79		
131	2495	113.4	1.87E-03	-2.73		
135	2545	115.7	1.40E-03	-2.85		
140	2645	120.2	2.24E-03	-2.65		
144	2695	122.5	1.40E-03	-2.85		
147	2745	124.8	1.87E-03	-2.73		
153	2845	129.3	1.87E-03	-2.73		
156	2895	131.6	1.87E-03	-2.73		
159	2945	133.9	1.87E-03	-2.73		
163	3045	138.4	2.80E-03	-2.55		
167	3095	140.7	1.40E-03	-2.85		
170	3145	142.9	1.87E-03	-2.73		
175	3245	147.5	2.24E-03	-2.65		
178	3295	149.8	1.87E-03	-2.73		
188	3395	154.3	1.12E-03	-2.95		

193	3495	158.9	2.49E-03	-2.60
198	3595	163.4	2.24E-03	-2.65
202	3695	167.9	2.49E-03	-2.60
207	3795	172.5	2.24E-03	-2.65
212	3895	177.0	2.24E-03	-2.65
219	4095	186.1	2.98E-03	-2.52
224	4195	190.7	2.80E-03	-2.55
227	4295	195.2	3.20E-03	-2.49
231	4395	199.8	2.80E-03	-2.55
236	4495	204.3	2.49E-03	-2.60
239	4595	208.9	3.20E-03	-2.49

Column F - Ggypsum treated soil (replicate)
[10 tons/ha mixed throughout soil column]

Time (min)	Cum. Vol. (ml)	Leachate Depth (cm)	K (cm/s)	log K	pH	EC (mS/cm)
0	0					
5	114	5.2	2.55E-03	-2.59	5.0	18.10
10	214	9.7	2.24E-03	-2.65	5.7	3.70
13	327	14.9	4.22E-03	-2.37	5.8	2.20
17	437	19.9	3.08E-03	-2.51	5.8	1.33
20	545	24.8	4.03E-03	-2.39	6.0	0.74
24	657	29.9	3.13E-03	-2.50	6.1	0.46
27	747	33.9	3.36E-03	-2.47	6.2	0.35
30	845	38.4	3.66E-03	-2.43	6.2	0.29
34	941	42.8	2.69E-03	-2.57	6.2	0.26
37	1031	46.9	3.36E-03	-2.47	6.3	0.24
40	1137	51.7	3.95E-03	-2.40	6.3	0.22
45	1239	56.3	2.28E-03	-2.64	6.3	0.21
50	1349	61.3	2.46E-03	-2.61	6.3	0.20
54	1447	65.8	2.74E-03	-2.56	6.3	0.19
58	1547	70.3	2.80E-03	-2.55	6.3	0.19
63	1657	75.3	2.46E-03	-2.61	6.3	0.18
67	1769	80.4	3.13E-03	-2.50	6.3	0.17
72	1883	85.6	2.55E-03	-2.59	6.3	0.17
75	1985	90.2	3.81E-03	-2.42	6.4	0.16
80	2099	95.4	2.55E-03	-2.59	6.4	0.16

85	2212	100.5	2.53E-03	-2.59	6.4	0.15
90	2326	105.7	2.55E-03	-2.59	6.3	0.15
97	2426	110.3	1.60E-03	-2.79		
100	2476	112.5	1.87E-03	-2.73		
104	2526	114.8	1.40E-03	-2.85		
109	2626	119.4	2.24E-03	-2.65		
113	2676	121.6	1.40E-03	-2.85		
116	2726	123.9	1.87E-03	-2.73		
121	2826	128.4	2.24E-03	-2.65		
126	2876	130.7	1.12E-03	-2.95		
129	2926	133.0	1.87E-03	-2.73		
134	3026	137.5	2.24E-03	-2.65		
136	3076	139.8	2.80E-03	-2.55		
140	3126	142.1	1.40E-03	-2.85		
144	3226	146.6	2.80E-03	-2.55		
147	3276	148.9	1.87E-03	-2.73		
150	3326	151.2	1.87E-03	-2.73		
155	3426	155.7	2.24E-03	-2.65		
157	3476	158.0	2.80E-03	-2.55		
161	3526	160.3	1.40E-03	-2.85		
166	3626	164.8	2.24E-03	-2.65		
169	3676	167.1	1.87E-03	-2.72		
171	3726	169.4	2.80E-03	-2.55		
175	3826	173.9	2.80E-03	-2.55		
178	3876	176.2	1.87E-03	-2.73		
180	3926	178.5	2.80E-03	-2.55		
188	4026	183.0	1.40E-03	-2.85		
192	4126	187.5	2.80E-03	-2.55		
197	4226	192.1	2.49E-03	-2.60		
201	4326	196.6	2.80E-03	-2.55		
205	4426	201.2	2.49E-03	-2.60		
209	4526	205.7	2.80E-03	-2.55		
217	4726	214.8	2.80E-03	-2.55		
220	4826	219.4	3.73E-03	-2.43		
224	4926	223.9	2.80E-03	-2.55		